iScience

CellPress

Article

Nickel-Catalyzed Asymmetric Domino Ring Opening/Cross-Coupling Reaction of Cyclobutanones via a Reductive Strategy

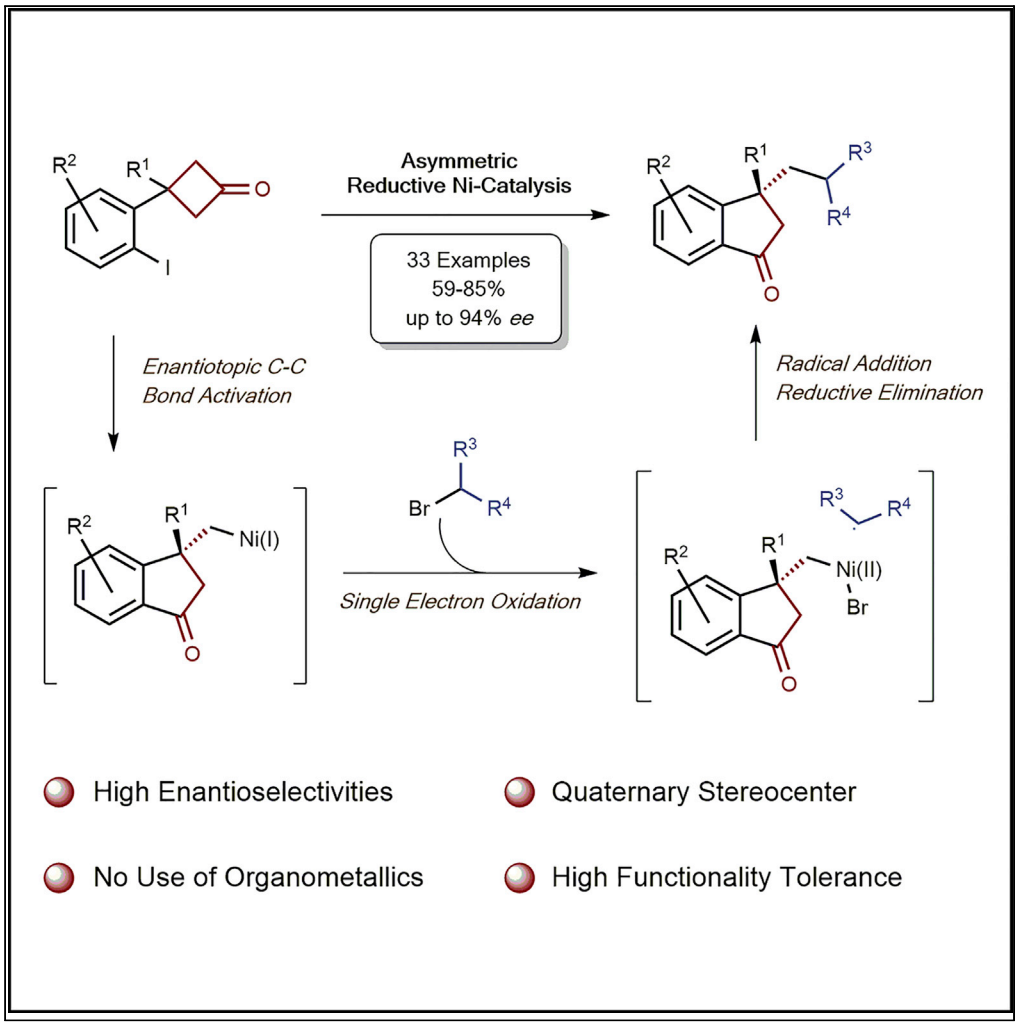

Decai Ding,
Haiyan Dong,
Chuan Wang

chuanw@ustc.edu.cn

HIGHLIGHTS

Asymmetric ring opening of prochiralcyclobutanones via reductive Nickel-catalysis

Merger of electrophilic ring opening and cross-electrophile coupling

Chiral indanones were synthesized in highly enantioselective manner

Ding et al., iScience 23, 101017
April 24, 2020
https://doi.org/10.1016/j.isci.2020.101017

iScience

CellPress

Article

Nickel-Catalyzed Asymmetric Domino Ring Opening/Cross-Coupling Reaction of Cyclobutanones via a Reductive Strategy

Decai Ding,[1] Haiyan Dong,[1] and Chuan Wang[1,2,*]

SUMMARY

Herein we demonstrate the successful application of reductive strategy in the asymmetric domino ring opening/cross-coupling reaction of prochiral cyclobutanones. Under the catalysis of a chiral nickel complex, various aryl iodide-tethered cyclobutanones were reacted with alkyl bromides as the electrophilic coupling partner, providing a variety of chiral indanones bearing a quaternary stereogenic center in highly enantioselective manner, which can be further converted to diverse benzene-fused cyclic compounds including indane, indene, dihydrocoumarin, and dihydroquinolinone. The preliminary mechanistic investigations support a mechanism involving Ni(I)-mediated enantiotopic C–C σ-bond activation of cyclobutanones as key elementary step in the catalytic cycle.

INTRODUCTION

Enantioselective ring opening of small strained molecules is one of the cornerstone reactions in organic synthesis, providing a convenient access to diverse chiral compounds. However, the main progresses in this domain are limited to small heterocyles, eg, epoxides and aziridines (Jacobsen, 2000; Meninno and Lattanzi, 2016; Pastor and Yus, 2005; Schneider, 2006; Wang et al., 2016a, 2016b). Furthermore, significant advances have been made in the Ti-mediated radical-type regiodivergent ring opening of epoxides in recent years (Funken et al., 2016, 2017; Mühlhaus et al., 2019). In contrast, the development of asymmetric ring opening of small carbocycles (Schneider et al., 2014; Grover et al., 2015; Fumagalli et al., 2017) lags behind due to the challenging C-C σ-bond cleavage (Dong, 2014; Marek et al., 2015; Souillart and Cramer, 2015; Nairoukh et al., 2017). Cyclobutanones have proved to be versatile precursors for ring opening or ring expansion reaction involving C-C σ-bond activation (Murakami et al., 1994, 2002,2005a,2005b;Matsuda et al., 2008; Xu and Dong, 2012; Ishida et al., 2012, 2014; Ko and Dong, 2014; Chen et al., 2014; Zhou and Dong, 2015; Juliá-Hernández et al., 2015), but only a few transition-metal-catalyzed asymmetric variants were reported in the last two decades, which are constrained to the following three strategies (Sietmann and Wiest, 2019): (1) In the pioneering work of Murakami, a method with an Rh-promoted enantioselectivenucleophilic ring opening of prochiralcyclobutanones as key step followed by protonation was accomplished, in which a tethered aryl boronate or phenol can serve as the nucleophile (Scheme 1A) (Matsuda et al., 2006,2007); (2) Dong, Cramer, and Murakami developed a variety of Rh- or Ni-catalyzed enantioselective intramolecular cycloadditions of cyclobutanones with various pendant unsaturated units, such as alkenes (Liu et al., 2012; Xu et al., 2012; Souillart et al., 2014; Deng et al., 2019), allenes (Zhou and Dong, 2016), aldehydes (Souillart and Cramer, 2014; Parker and Cramer, 2014), and oximes (Deng et al., 2016), affording an array of bridged bicyclic compounds with high enantiocontrol (Scheme 1B); (3) Cao, Xu, and coworkers achieved Pd-catalyzed enantioselective electrophilic ring opening of cyclobutanones with the appended aryl halide, and the resultant chiral alkyl Pd(II) species containing an indanone scaffold can be successfully trapped by different nucleophiles including aryl boronic acids, iodide, and alkynes (Scheme 1C) (Cao et al., 2019; Sun et al., 2019a,2019b). Moreover, metallic Lewis-acid- or organo-catalyzed asymmetric Baeyer-Villiger oxidation of prochiral cyclobutanones has also been established by Bolm (Bolm and Beckmann, 2000), Imada (Murahashi et al., 2002), Feng (Zhou et al., 2012), and Miller (Featherston et al., 2019). To expand the scope of asymmetric ring opening of cyclobutanones, a conceptionally new reaction pathway is still highly desired.

On the other side, Ni-catalyzed reductive cross-electrophile coupling has emerged as a powerful tool for step-economical C-C bond formation with high functionality tolerance through bypassing the use of organometallics as the coupling partner (Everson and Weix, 2014; Gu et al., 2015; Moragas et al., 2014; Richmond and Moran, 2018; Wang et al., 2016a, 2016; Weix, 2015). Herein we envisaged a Ni-catalyzed cascade

[1]Hefei National Laboratory for Physical Science at the Microscale, Department of Chemistry, Center for Excellence in Molecular Synthesis, University of Science and Technology of China, Hefei, Anhui 230026, P. R. China

[2]Lead Contact

*Correspondence: chuanw@ustc.edu.cn

https://doi.org/10.1016/j.isci.2020.101017

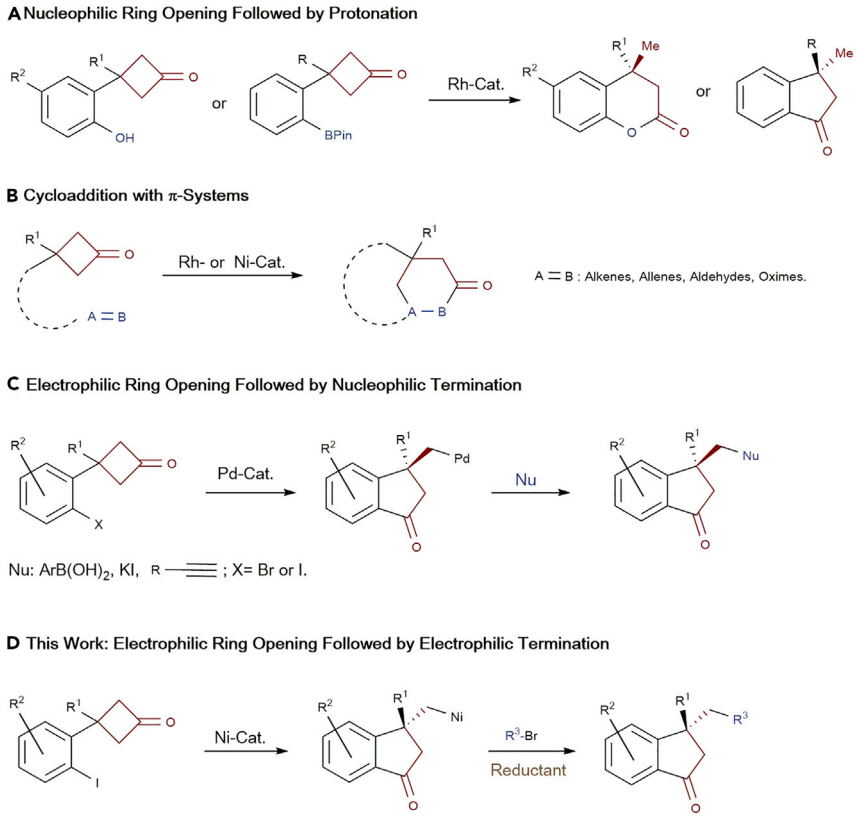

Scheme 1. Strategies for Enantioselective Ring Opening of Cyclobutanones

(A) Nucleophilic Ring Opening Followed by Protonation.

(B) Cycloaddition with π-Systems.

(C) Electrophilic Ring Opening Followed by Nucleophilic Termination.

(D) Electrophilic Ring Opening Followed by Electrophilic Termination.

consisting of enantioselective electrophilic ring opening of aryl-iodide-tethered cyclobutanones and the following termination of the generated alkyl Ni intermediate using electrophilic alkyl bromides via reductive strategy, providing a new entry to chiral indanones in asymmetric fashion, which is featured as a characteristic motif in numerous compounds of pharmaceutical interest (DeSolms et al., 1978; Li, et al., 1995; Inoue et al., 1996; Ito et al., 2004; Huang et al., 2012; Peauger et al., 2017) (Scheme 1D).

RESULTS AND DISCUSSION

Optimization of the Reaction Conditions

For optimization of the reaction conditions, we chose the prochiral cyclobutanone **1a** incorporating an aryl iodide unit and *n*-octyl bromide (**2a**) as model substrates (Table 1). Initially, various types of chiral ligands including BOX, Pyrox, PHOX, BINAP, DIOP, DuPhos, phosphoamidates etc. were investigated in this Ni-catalyzed reaction. However, all these reactions failed to deliver the desired product. To our delight, the reaction employing the Trost ligand **L1** with chiral 1,2-cyclohexanediamine scaffold provided a promising result in terms of both efficiency and enantioselectivity (entry 1). Encouraged by this result, two additional Trost ligands with different backbones (**L2** and **L3**) were tested for our reaction, giving only inferior results (entries 2 and 3). Moreover, the Trost ligand with naphthyl as linker (**L4**) turned out to be unsuitable for the studied reaction (entry 4). Tuning the substitution on the phenyl ring of **L1** revealed that introduction of the bulky and electron-donating *tert*-butyl could improve the performance of the ligand (**L5**) concerning both reactivity and selectivity (entry 5). In sharp contrast, the desired reaction was completely shut down when the electron-withdrawing CF_3 was installed on the phenyl substituent of the phosphine ligand (**L6**, entry 6). Next, a brief solvent screening was undertaken (entries 7–11). In general, moderate to good results were obtained in polar solvents (entries 7–9) wherein the best outcome was achieved in the case of

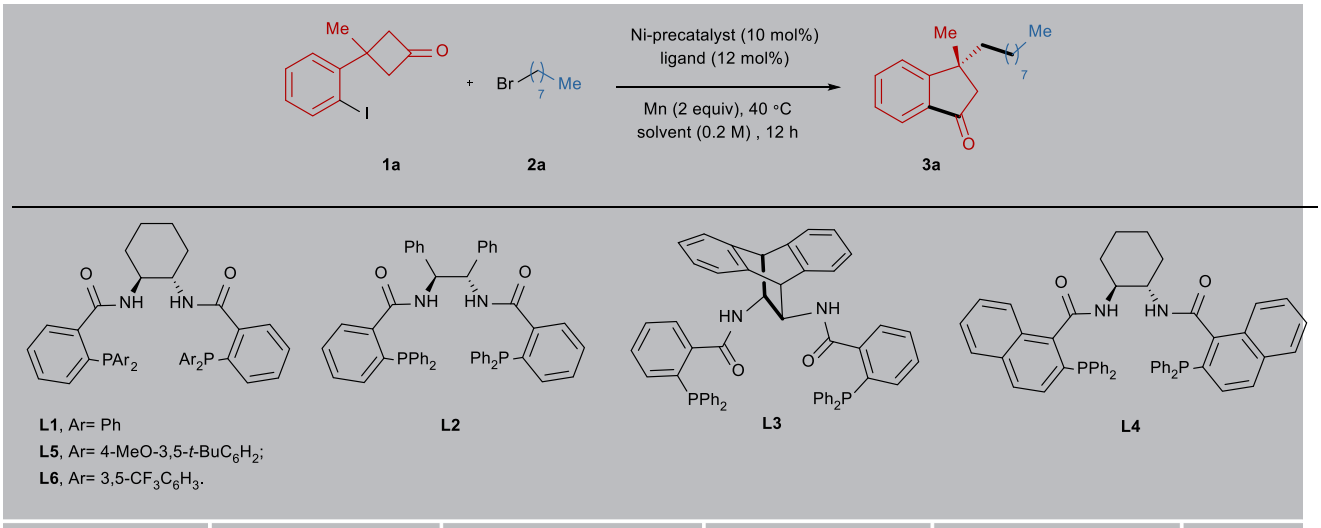

Entry	Ligands	Ni-Salts	Solvent	Yield (%)[a]	*ee* (%)[b]
1	L1	$NiBr_2$·glyme	DMA	66	54
2	L2	$NiBr_2$·glyme	DMA	15	13
3	L3	$NiBr_2$·glyme	DMA	21	19
4	L4	$NiBr_2$·glyme	DMA	0	–
5	L5	$NiBr_2$·glyme	DMA	69	76
6	L6	$NiBr_2$·glyme	DMA	0	–
7	L5	$NiBr_2$·glyme	DMSO	81	34
8	L5	$NiBr_2$·glyme	DMF	53	73
9	L5	$NiBr_2$·glyme	DMI	76	87
10	L5	$NiBr_2$·glyme	THF	0	–
11	L5	$NiBr_2$·glyme	MeCN	0	–
12	L5	$NiBr_2$	DMI	trace	ND[c]
13	L5	NiI_2	DMI	56	85
14	L5	$Ni(acac)_2$	DMI	0	–
15	L5	$Ni(COD)_2$	DMI	73	89
16	**L5**	**$NiCl_2$·glyme**	**DMI**	**83**	**94**
17[d]	L5	$NiCl_2$·glyme	DMI	23	70
18[e]	L5	$NiCl_2$·glyme	DMI	0	–

Table 1. Optimization of the Reaction Conditions

Unless otherwise specified, reactions were performed on a 0.2 mmol scale of the cyclobutanone**1a** using 2.0 equiv of *n*-octyl bromide (**2a**), 10 mol % Ni-precatalyst, 12 mol% ligand and 2 equiv of Mn in 1.0 mL solvent at 40 °C for 12 h.

[a]Yields of the isolated product after column chromatography.

[b]Determined by HPLC-analysis on chiral stationary phase.

[c]Not determined.

[d]Zn was used as reductant instead of Mn.

[e]The bromo analogue of **1a** was used instead of **1a**.

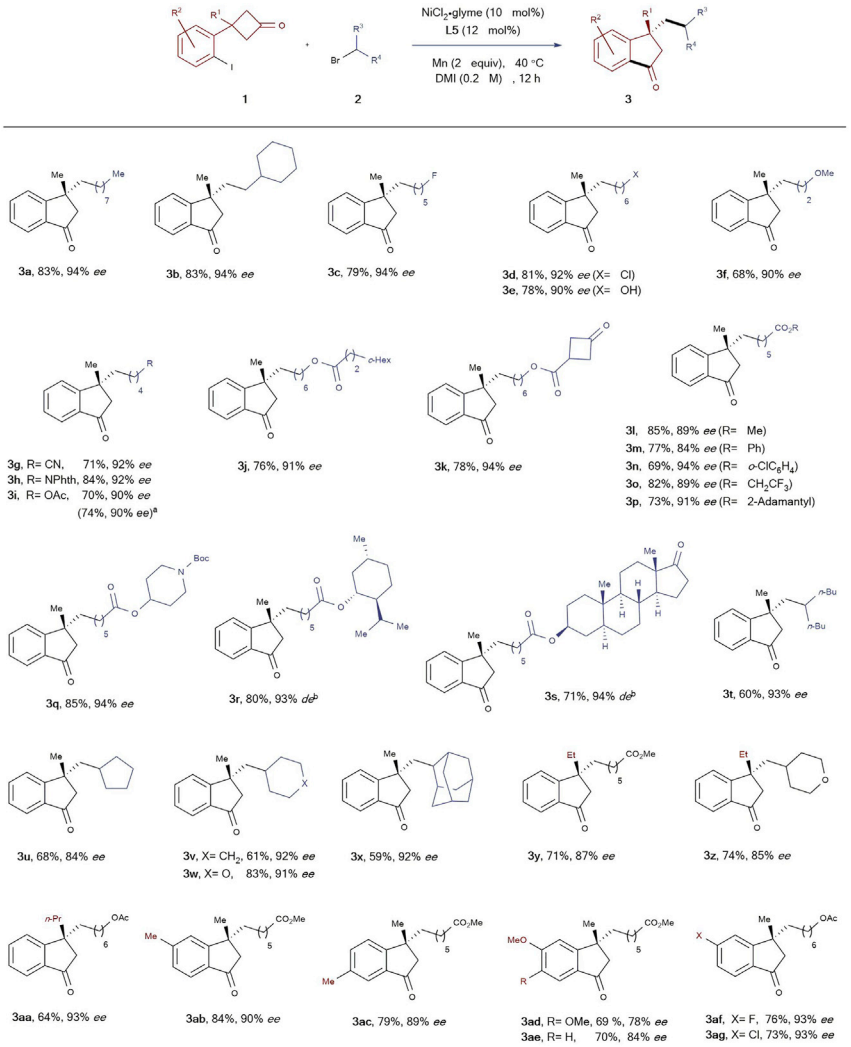

Scheme 2. Evaluation of the Substrate Scope

Unless otherwise specified, reactions were performed on a 0.2 mmol scale of the cyclobutanones **1** using 2.0 equiv of alkyl bromides **2**, 10 mol% $NiCl_2$·glyme, 12 mol% ligand L5, and 2 equiv of Mn in 1.0 mL DMI at 40 ° C for 12 h. Yields of the isolated products after column chromatography. The ee or de were determined by HPLC-analysis on chiral stationary phase. [d]The reaction was performed on a 10 mmol scale. [e]Enantiopure precursors were employed.

1,3-dimethyl-2-imidazolidinone (DMI, entry 9). In less polar solvents such as THF and MeCN, the formation of the product **3a** was not observed (entries 10 and 11). Subsequently, a series of Ni-precatalysts were examined for this reaction (entries 12–16). Gratifyingly, both efficiency and asymmetric induction could be elevated to a high level when $NiCl_2$•glyme was utilized (entry 16). Replacing Mn by Zn as the reducing agent gave rise to a diminished yield and enantiocontrol (entry 17). In addition, we also employed the bromo analogue of **1a** as precursor in this domino ring opening/cross-coupling reaction, but the conversion of **1a** was not observed in this case (entry 18).

Substrate Scope

After establishing the optimal reaction conditions, we started to evaluate the substrate spectrum of this Ni-catalyzed reaction (Scheme 2). First, an array of primary alkyl bromides reacted with the cyclobutanone**1a**. All these reactions proceeded smoothly under the standard conditions, furnishing the product **3a-q** in moderate to good yields and good to excellent enantioselectivities. It is noteworthy that a wide range of functional moieties including chloride (**3d**), alcohol (**3e**), nitrile (**3g**), imide (**3h**), ester (**3i-q**), ketone

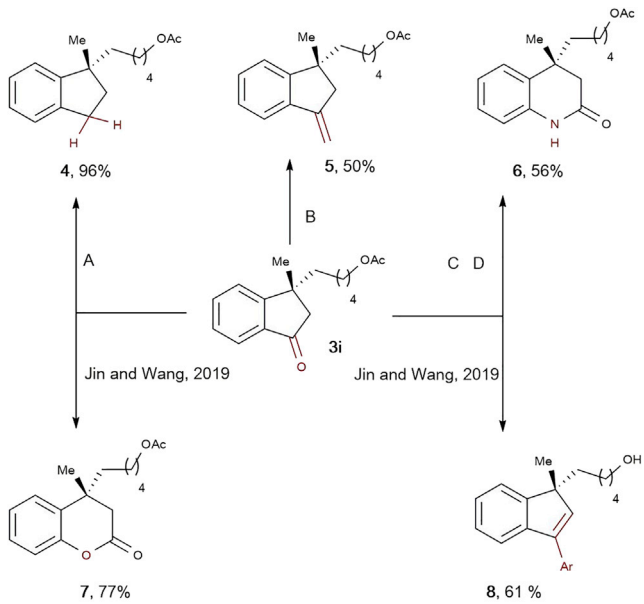

Scheme 3. Derivatizations of the Cross-Coupling Product

(A) Zn-Hg, 6 M HCl, toluene/H_2O, RT, overnight.

(B) $Ph_3P^+CH_2Br^-$ (1.1 equiv), *t*-BuOK (1.5 equiv), MeOH, 0°C to RT, overnight.

(C) $NH_2OH{\cdot}HCl$ (1.1 equiv), NaOAc (2.0 equiv), MeOH, 60°C, 2 h.

(D) PCl_5 (1.0 equiv), THF, 60°C, 1.5 h.

(**3k**), and carbamate (**3q**) were well tolerated. Furthermore, the alkyl bromides containing a menthol or epiandrosterone subunit posed no problem, providing the products **3r** and **3s** in good efficiency and high diastereomeric excesses. Moreover, sterically more demanding secondary alkyl bromides also turned out to be competitive substrates for this reaction, and the corresponding products **3t**-**x** were obtained in moderate to good yields and good to high enantiocontrol. Unfortunately, no desired product was formed when tertiary alkyl and benzyl halides were employed as precursors. Next, the impact of geminal substitution on the β-position of the prochiralcyclobutanones was examined. In the case of ethyl and *n*-propyl substituent comparable results were achieved (**3y**-**aa**), whereas no desired reaction occurred in the case of phenyl substitution. The use of mono-substituted cyclobutanone (R^1= H) as a precursor also failed to deliver the cross-coupling product. Subsequently, we continued to study the scope of this reaction through introduction of either electron-donating or withdrawing groups to the tethered phenyl ring (**3ab**-**ag**), and in all these cases the products were afforded in good yields and good to high enantiomeric excesses. Notably, a 10-mmol-scale reaction for synthesis of **3i** was carried out providing a similar result.

Derivatization of the Products

In order to demonstrate synthetic value of this method, some derivatizations of the cross-coupling product **3i** were conducted (Scheme 3). First, Clemmensen reduction of the keto-moiety afforded a chiral indane **4** in an excellent yield. Compound **3i** was also successfully subjected to Wittig olefination, providing a geminal disubstituted alkene **5** in a moderate yield. Moreover, the conversion of the indanone **3i** into the corresponding oxime using hydroxyl amine followed by PCl_5-mediated Beckmann rearrangement delivered a dihydroquinolinone **6** in 56% yield over two steps. In addition, the framework of dihydrocoumarin (**7**) or 3-aryl indene (**8**) can be constructed starting from the indanone **3i** according to the known procedure in the literature (Jin and Wang, 2017).

Mechanistic Studies

A series of control experiments were designed to uncover the mechanism of this Ni-catalyzed reaction (Scheme 4). First, we performed the stoichiometric reaction between the cyclobutanone**1a** and $Ni(COD)_2$ in the presence of the ligand **L5**. After quenching with water, the formation of the indanone **9** was not observed, whereas the deiodinated product **10** was obtained in 89% yield (Scheme 4A). Considering that MnI_2 is present in the catalytic reaction and can serve as Lewis acid to activate the carbonyl group,

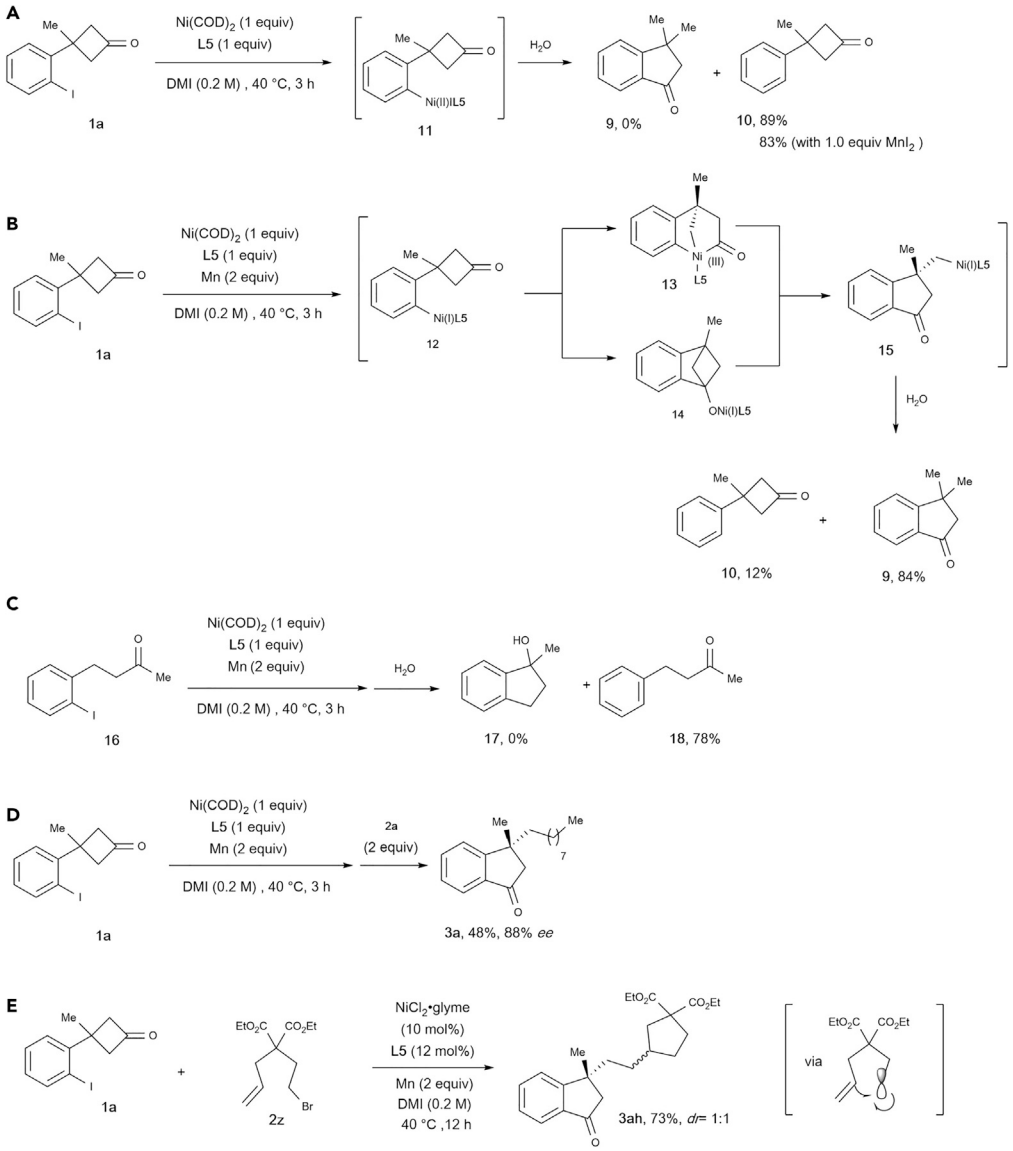

Scheme 4. Control Experiments

(A) Stoichiometric Reaction of **1a** with $Ni(COD)_2$.

(B) Stoichiometric Reaction of **1a** with $Ni(COD)_2$ in the Presence of Mn.

(C) Stoichiometric Reaction of **16** with $Ni(COD)_2$.

(D) Sequential Stoichiometric Reaction.

(E) Radical Clock Experiment.

we performed this stoichiometric reaction with 1 equiv of MnI_2. Again, only the deiodinated product **10** was generated (83% yield). This result confirms the feasibility of oxidative addition of the incorporated aryl iodide to the Ni(0) species, but the generated Ni(II) complex **11** is not able to further react with the Cyclobutanone to approach the indanone motif. When the reductant Mn (2 equiv) was added to the stoichiometric reaction mentioned earlier, the indanone **9** was furnished in 84% yield (Scheme 4B). In this case, the aryl Ni(II) intermediate **11** is probably reduced to the corresponding Ni(I) species **12**, which can subsequently undergo two possible reaction pathways: (1) oxidative addition with the cyclobutanone moiety followed by facile reductive elimination from the bridged bicyclic Ni(III) species **13**; (2) migratory insertion into the carbonyl moiety followed by β-carbon-elimination from the Ni(I) complex **14**. In both cases, the Ni(I) intermediate **15** with the indanone scaffold could be approached, which upon protonation leads to the compound **9**. Moreover, the stoichiometric reaction employing the aryl

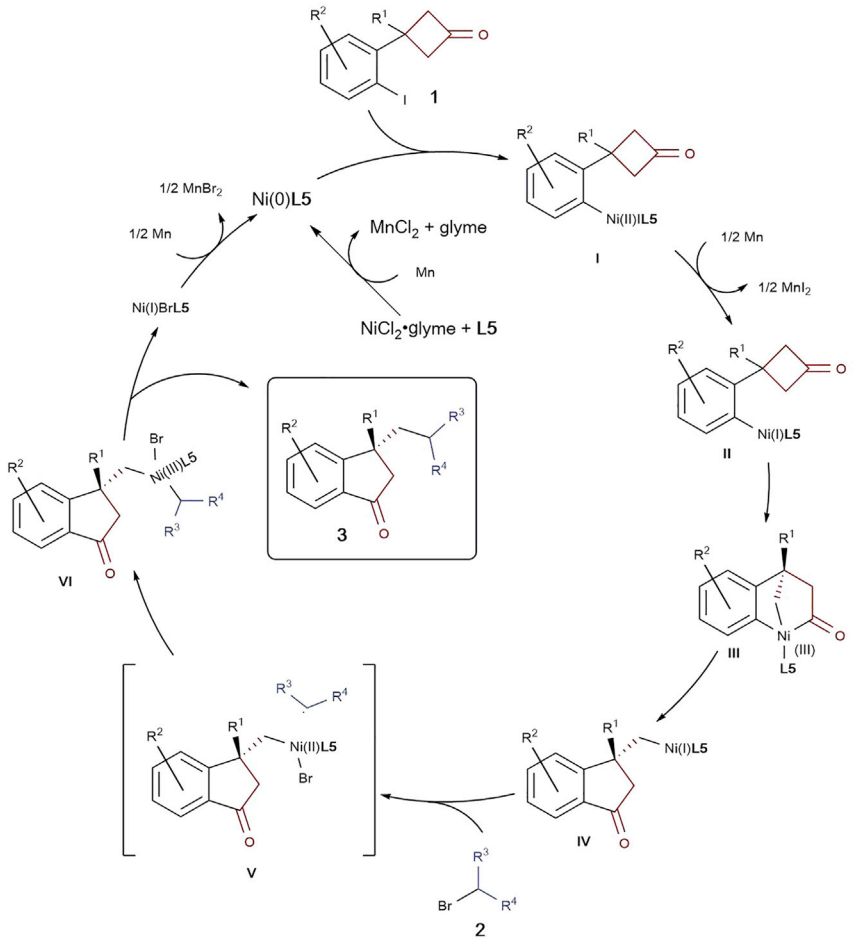

Scheme 5. Proposed Reaction Mechanism

iodide **16** tethering a linear ketone failed to deliver the addition product **17**, arguing against the mechanism involving a Ni(I)-mediated migratory insertion step (Scheme 4C). Next, the sequential stoichiometric reaction with the addition of *n*-octyl bromide (**2a**) in the second stage provided the coupling product **3a** in 88% *ee*, which is similar to one of the catalytic reactions (Scheme 4D). This result suggests that the enantiotopic C-C bond activation is probably the enantiodeterming step with generation of the Ni-complex **15**, which can further react with *n*-octyl bromide to reach the product **3a**. Moreover, an alkyl bromide with a pendant olefinic unit (**2z**) was employed as a precursor in the Ni-catalyzed reaction with cyclobutanone**1a** under the standard conditions, which resulted in cyclization of the alkyl bromide prior to the cross-coupling reaction (Scheme 4E). The corresponding product **3ah** was yielded in a diastereomeric ratio of 1:1, which indicates a free-radical-mediated ring closure for the formation of the cyclopentane ring.

Proposed Catalytic Cycle

On the basis of the results of the control experiments, we proposed a plausible reaction mechanism for this Ni-catalyzed ring opening/cross-coupling reaction (Scheme 5). Initially, a Ni(0) species is generated under the reductive condition, which undergoes oxidative addition with the tethered aryl iodide **1**. Next, the resultant Ni(II) complex **I** is reduced by Mn to the Ni(I) intermediate **II**, which in turn performs enantioselective insertion into one of the two $C(sp^2)$-$C(sp^3)$ σ-bonds of the cyclobutanone to give the bicyclic Ni(III) complex **III**. The subsequent $C(sp^2)$-$C(sp^2)$ reductive elimination affords the alkyl Ni(I) species **IV** with the indanone scaffold. In the next step, alkyl bromides **3** conduct oxidative addition to the complex **IV** via the formation of a cage **V** consisting of an alkyl radical and a Ni(II) species. Upon reductive elimination

from the intermediate **VI**, the indanone products **3** are furnished. Finally, the Ni(0) species is regenerated for the next catalytic cycle via the Mn-mediated reduction of Ni(I)Br.

Conclusion

In summary, we developed a reductive strategy for ring opening of prochiral cyclobutanones via sequential C−C bond cleavage and electrophilic trapping. Under the catalysis of a chiral Ni-complex in assistance of Mn as reducing agent, various cyclobutanones tethering an aryl iodide were reacted with both primary and secondary alkyl bromides, furnishing a variety of chiral indanones containing a quaternary stereogenic center in good to high enantioselectivities. According to the preliminary mechanistic studies, this tandem reaction proceeds with selective insertion of Ni(I) into the C−C σ-bond of cyclobutaonones as the enantio-determining step, and the subsequent cage-bound oxidative addition with alkyl bromides and reductive elimination can afford the ring opening/cross-coupling products.

Limitation of the Study

Tertiary alkyl and benzyl bromides are not applicable in this methodology.

METHODS

All methods can be found in the accompanying Transparent Methods supplemental file.

DATA AND CODE AVAILABILITY

All data and methods can be found in the Supplemental Information.

SUPPLEMENTAL INFORMATION

Supplemental Information can be found online at https://doi.org/10.1016/j.isci.2020.101017.

ACKNOWLEDGMENTS

This work is supported by National Natural Science Foundation of China (Grant No. 21772183), Fundamental Research Funds for the Central Universities (WK2060190086), "1000-Youth Talents Plan" start-up funding as well as University of Science and Technology of China.

AUTHOR CONTRIBUTIONS

C.W. and D.D. conceived and designed the experiments. D.D. and H.D. performed experiments and prepared the Supplementary Information. C.W. directed the project and wrote the paper. All authors discussed the results and commented on the manuscript.

DECLARATION OF INTERESTS

The authors declare no competing financial interests.

Received: February 10, 2020
Revised: March 6, 2020
Accepted: March 23, 2020
Published: April 24, 2020

REFERENCES

Bolm, C., and Beckmann, O. (2000). Zirconium-mediated asymmetric baeyer-villiger oxidation. Chirality *12*, 523–525.

Cao, J., Chen, L., Sun, F.-N., Sun, Y.-L., Jiang, K.-Z., Yang, K.-F., Xu, Z., and Xu, L.-W. (2019). Pd-catalyzed enantioselective ring opening/cross-coupling and cyclopropanation of cyclobutanones. Angew. Chem. Int. Ed. *58*, 897–901.

Chen, P.-h., Xu, T., and Dong, G. (2014). Divergent syntheses of fused β-naphthol and indene scaffolds by rhodium-catalyzed direct and decarbonylative alkyne-benzocyclobutenone couplings. Angew.Chem. Int. Ed. *53*, 1674–1678.

Deng, L., Xu, T., Li, H., and Dong, G. (2016). Enantioselective Rh-catalyzed carboacylationof C=N bonds via C–C activation of benzocyclobutenones. J. Am. Chem. Soc. *138*, 369–374.

Deng, L., Fu, Y., Lee, S.Y., Wang, C., Liu, P., and Dong, G. (2019). Kinetic resolution via Rh-catalyzed C–C activation of cyclobutanones at room temperature. J. Am. Chem. Soc. *141*, 16260–16265.

DeSolms, S.J., Woltersdorf, O.W., Jr., Cragoe, E.J., Jr., Watson, L.S., and Fanelli, G.M., Jr. (1978). (Acylaryloxy)acetic acid diuretics. 2. (2-Alkyl-2-aryl-1-oxo-5-indanyloxy)acetic acids. J. Med. Chem. *21*, 437–443.

G. Dong, ed. (2014). Top.Curr. Chem (Springer-Verlag), p. 346.

Everson, D.A., and Weix, D.J. (2014). Cross-electrophile coupling: Principles of reactivity and selectivity. J. Org. Chem. *79*, 4793–4798.

Featherston, A.L., Shugrue, C.R., Mercado, B.Q., and Miller, S.J. (2019). Asymmetric Baeyer–Villigerreaction with hydrogen peroxide catalyzed by a novel planar-chiral bisflavin. ACS Catal. *9*, 242–252.

Fumagalli, G., Stanton, S., and Bower, J.-F. (2017). Recent methodologies that exploit C–C single-bond cleavage of strained ring systems by transition metal complexes. Chem. Rev. *117*, 9404–9432.

Funken, N., Mühlhaus, F., and Gansäuer, A. (2016). General, highly selective synthesis of 1,3- and 1,4-difunctionalized building blocks by regiodivergent epoxide opening. Angew. Chem. Int. Ed. *55*, 12030–12034.

Funken, N., Zhang, Y.-Q., and Gansäuer, A. (2017). Regiodivergentcatalysis: a powerful tool for selective catalysis. Chem. Eur. J. *23*, 19–32.

Grover, H.K., Emmett, M.R., and Kerr, M.A. (2015). Carbocycles from donor–acceptor cyclopropanes. Org. Biomol. Chem. *13*, 655–671.

Gu, J., Wang, X., Xue, W., and Gong, H. (2015). Nickel-catalyzed reductive coupling of alkyl halides with other electrophiles: concept and mechanistic considerations. Org. Chem. Front. *2*, 1411–1421.

Huang, L., Lu, C., Sun, Y., Mao, F., Luo, Z., Su, T., Jiang, H., Shan, W., and Li, X. (2012). Multitarget-directed benzylideneindanone derivatives: anti-β-amyloid (Aβ) aggregation, antioxidant, metal chelation, and monoamine oxidase B (MAO-B) inhibition properties against Alzheimer's disease. J. Med. Chem. *55*, 8483–8492.

Inoue, A., Kawai, T., Wakita, M., Iimura, Y., Sugimoto, H., and Kawakami, Y. (1996). The simulated binding of (±)-2,3-dihydro-5,6-dimethoxy-2-[[1-(phenylmethyl)-4-piperidinyl] methyl]-1H-inden-1-one hydrochloride (E2020) and related inhibitors to free and acylatedacetylcholinesterases and corresponding structure-activity analyses. J. Med. Chem. *39*, 4460–4470.

Ishida, N., Ikemoto, W., and Murakami, M. (2012). Intramolecularσ-bond metathesis between carbon–carbon and silicon–silicon bonds. Org. Lett. *14*, 3230–3232.

Ishida, N., Ikemoto, W., and Mukarami, M. (2014). Cleavage of C–C and C–Si σ-bonds and their intramolecular exchange. J. Am. Chem. Soc. *136*, 5912–5915.

Ito, T., Tanaka, T., Iinuma, M., Nakaya, K.-i., Takahashi, Y., Sawa, R., Murata, J., and Darnaedi, D. (2004). Three new resveratrol oligomers from the stem bark of vaticapauciflora. J. Nat. Prod. *67*, 932–937.

Jacobsen, E.N. (2000). Asymmetric catalysis of epoxide ring-opening reactions. Acc. Chem. Res. *33*, 421–431.

Jin, Y., and Wang, C. (2017). Nickel-catalyzed asymmetric reductive arylalkylation of unactivated alkenes. Angew. Chem. Int. Ed. *58*, 6722–6726.

Juliá-Hernández, F., Ziadi, A., Nishimura, A., and Martin, R. (2015). Nickel-catalyzed chemo-, regio- and diastereoselective bond formation through proximal C−C cleavage of benzocyclobutenones. Angew.Chem. Int. Ed. *54*, 9537–9541.

Ko, H.M., and Dong, G. (2014). Cooperative activation of cyclobutanones and olefins leads to bridged ring systems by a catalytic [4 + 2] coupling. Nat. Chem *6*, 739–744.

Li, C.S., Black, W.C., Chan, C.-C., Ford-Hutchinson, A.W., Gauthier, J.Y., Gordon, R., Guay, D., Kargman, S., Lau, C.K., Mancini, J., et al. (1995). Cyclooxygenase-2 inhibitors.synthesis and pharmacological activities of 5-methanesulfonamido-1-indanone derivatives. J. Med. Chem. *38*, 4897–4905.

Liu, L., Ishida, N., and Murakami, M. (2012). Atom- and step-economical pathway to chiral benzobicyclo[2.2.2]octenones through carbon-carbon bond cleavage. Angew. Chem. Int. Ed. *51*, 2485–2488.

Marek, I., Masarwa, A., Delaye, P.-O., and Leibeling, M. (2015). Selective carbon–carbon bond cleavage for the stereoselective synthesis of acyclic systems. Angew. Chem. Int. Ed. *54*, 414–429.

Matsuda, T., Shigeno, M., and Murakami, M. (2006). Enantioselective C−C bond cleavage creating chiral quaternary carbon centers. Org. Lett. *8*, 3379–3381.

Matsuda, T., Shigeno, M., and Murakami, M. (2007). Asymmetric synthesis of 3,4-dihydrocoumarins by rhodium-catalyzed reaction of 3-(2-hydroxyphenyl)cyclobutanones. J. Am. Chem. Soc. *129*, 12086–12087.

Matsuda, T., Shigeno, M., and Murakami, M. (2008). Palladium-catalyzed sequential carbon−carbon bond cleavage/formation producing arylatedbenzolactones. Org. Lett. *10*, 5219–5222.

Meninno, S., and Lattanzi, A. (2016). Organocatalyticasymmetric reactions of epoxides: recent progress. Chem. Eur. J. *22*, 3632–3642.

Moragas, T., Correa, A., and Martin, R. (2014). Metal-catalyzed reductive coupling reactions of organic halides with carbonyl-type compounds. Chem. Eur. J. *20*, 8242–8258.

Mühlhaus, F., Weiβbarth, H., Dahmen, T., Schnakenburg, G., and Gansäuer, A. (2019). Merging regiodivergent catalysis with atom-economical radical arylation. Angew. Chem. Int. Ed. *58*, 14208–14212.

Murahashi, S.-I., Ono, S., and Imada, Y. (2002). Asymmetric baeyer–villigerreaction with hydrogen peroxide catalyzed by a novel planar-chiral bisflavin. Angew. Chem. Int. Ed. *41*, 2366–2368.

Murakami, M., Amii, H., and Ito, Y. (1994). Selective activation of carbon-carbon bonds next to a carbonylgroup. Nature *370*, 540–541.

Murakami, M., Itahashi, T., and Ito, Y. (2002). Catalyzed intramolecular olefin insertion into a carbon−carbon single bond. J. Am. Chem. Soc. *124*, 13976–13977.

Murakami, M., Kadowaki, S., Fujimoto, A., Ishibashi, M., and Matsuda, T. (2005a). Acids direct 2-styrylcyclobutanone into two distinctly different reaction pathways. Org. Lett. *7*, 2059–2061.

Murakami, M., Ashida, S., and Matsuda, T. (2005b). Nickel-catalyzed intermolecular alkyne insertion into cyclobutanones. J. Am. Chem. Soc. *127*, 6932–6933.

Nairoukh, Z., Cormier, M., and Marek, I. (2017). Merging C–H and C–C bond cleavage in organic synthesis. Nat. Chem. Rev. *1*, 35.

Parker, E., and Cramer, N. (2014). Asymmetric rhodium(I)-catalyzed C–C activations with zwitterionicbis-phospholane ligands. Organometallics *33*, 780–787.

Pastor, M.I., and Yus, M. (2005). Asymmetric ring opening of epoxides. Curr.Org. Chem. *9*, 1–29.

Peauger, L., Azzouz, R., Gembus, V., Ţînţaş, M.-L., Santos, J.S.O., Bohn, P., Papamicaël, C., and Levacher, V. (2017). Donepezil-based central acetylcholinesterase inhibitors by means of a "bio-oxidizable"prodrug strategy: design, synthesis, and in vitro biological evaluation. J. Med. Chem. *60*, 5909–5926.

Richmond, E., and Moran, J. (2018). Recent advances in nickel catalysis enabled by stoichiometric metallic reducing agents. Synthesis *50*, 499–513.

Schneider, C. (2006). Synthesis of 1,2-difunctionalized fine chemicals through catalytic, enantioselective ring-opening reactions of epoxides. Synthesis *38*, 3919–3944.

Schneider, T.F., Kaschel, J., and Werz, D.B. (2014). A new golden age for donor–acceptor cyclopropanes. Angew. Chem. Int. Ed. *53*, 5504–5523.

Sietmann, J., and Wiest, J.M. (2019). Enantioselectivedesymmetrization of cyclobutanones: a speedway to molecular complexity. Angew. Chem. Int. Ed. *58*, https://doi.org/10.1002/anie.201910767.

Souillart, L., and Cramer, N. (2014). Highly enantioselectiverhodium(I)-catalyzed carbonyl carboacylations initiated by C−C bond activation. Angew.Chem. Int. Ed. *53*, 9640–9644.

Souillart, L., and Cramer, N. (2015). Catalytic C–C bond activations via oxidative addition to transition metals. Chem. Rev. *115*, 9410–9464.

Souillart, L., Parker, E., and Cramer, N. (2014). Highly enantioselectiverhodium(I)-catalyzed activation of enantiotopiccyclobutanoneC−C bonds. Angew.Chem. Int. Ed. *53*, 3001–3005.

Sun, Y.-L., Wang, X.-B., Sun, F.-N., Chen, Q.-Q., Cao, J., Xu, Z., and Xu, L.-W. (2019a). Enantioselectivecross-exchange between C−I and C−C σ bonds. Angew.Chem. Int. Ed. *58*, 6747–6751.

Sun, F.-N., Yang, W.-C., Chen, X.-B., Sun, Y.-L., Cao, J., Xu, Z., and Xu, L.-W. (2019b). Enantioselectivepalladium/copper-catalyzed C–C σ-bond activation synergized with sonogashira-

type C(sp3)–C(sp) cross-coupling alkynylation. Chem. Sci. *10*, 7579–7583.

Wang, C., Luo, L., and Yamamoto, H. (2016a). Metal-catalyzed directed regio- and enantioselective ring-opening of epoxides. Acc. Chem. Res. *49*, 193–204.

Wang, X., Dai, Y., and Gong, H. (2016b). Nickel-catalyzed reductive couplings. Top.Curr. Chem. *374*, 43.

Weix, D.J. (2015). Methods and mechanisms for cross-electrophile coupling of Csp2 halides with alkyl electrophiles. Acc. Chem. Res. *48*, 1767–1775.

Xu, T., and Dong, G. (2012). Rhodium-catalyzed regioselectivecarboacylation of olefins: a C−C bond activation approach for accessing fused-ring systems. Angew.Chem. Int. Ed. *51*, 7567–7571.

Xu, T., Ko, H.M., Savage, N.A., and Dong, G. (2012). Highly enantioselectiverh-catalyzed carboacylation of olefins: efficient syntheses of chiral poly-fused rings. J. Am. Chem. Soc. *134*, 20005–20008.

Zhou, X., and Dong, G. (2015). (4+1) vs (4+2): catalytic intramolecular coupling between cyclobutanones and trisubstitutedallenesvia C–C activation. J. Am. Chem. Soc. *137*, 13715–13721.

Zhou, X., and Dong, G. (2016). Nickel-catalyzed chemo- and enantioselective coupling between cyclobutanones and allenes: rapid synthesis of [3.2.2] bicycles. Angew.Chem. Int. Ed. *55*, 15091–15095.

Zhou, L., Liu, X., Li, J., Zhang, Y., Hu, X., Lin, L., and Feng, X. (2012). Kinetic resolution via Rh-catalyzed C–C activation of cyclobutanones at room temperature. J. Am. Chem. Soc. *134*, 17023–17026.

iScience, Volume *23*

Supplemental Information

Nickel-Catalyzed Asymmetric Domino Ring Opening/Cross-Coupling Reaction of Cyclobutanones via a Reductive Strategy

Decai Ding, Haiyan Dong, and Chuan Wang

Figure S1 ^{1}H NMR Spectrum of 1c, related to Scheme 2

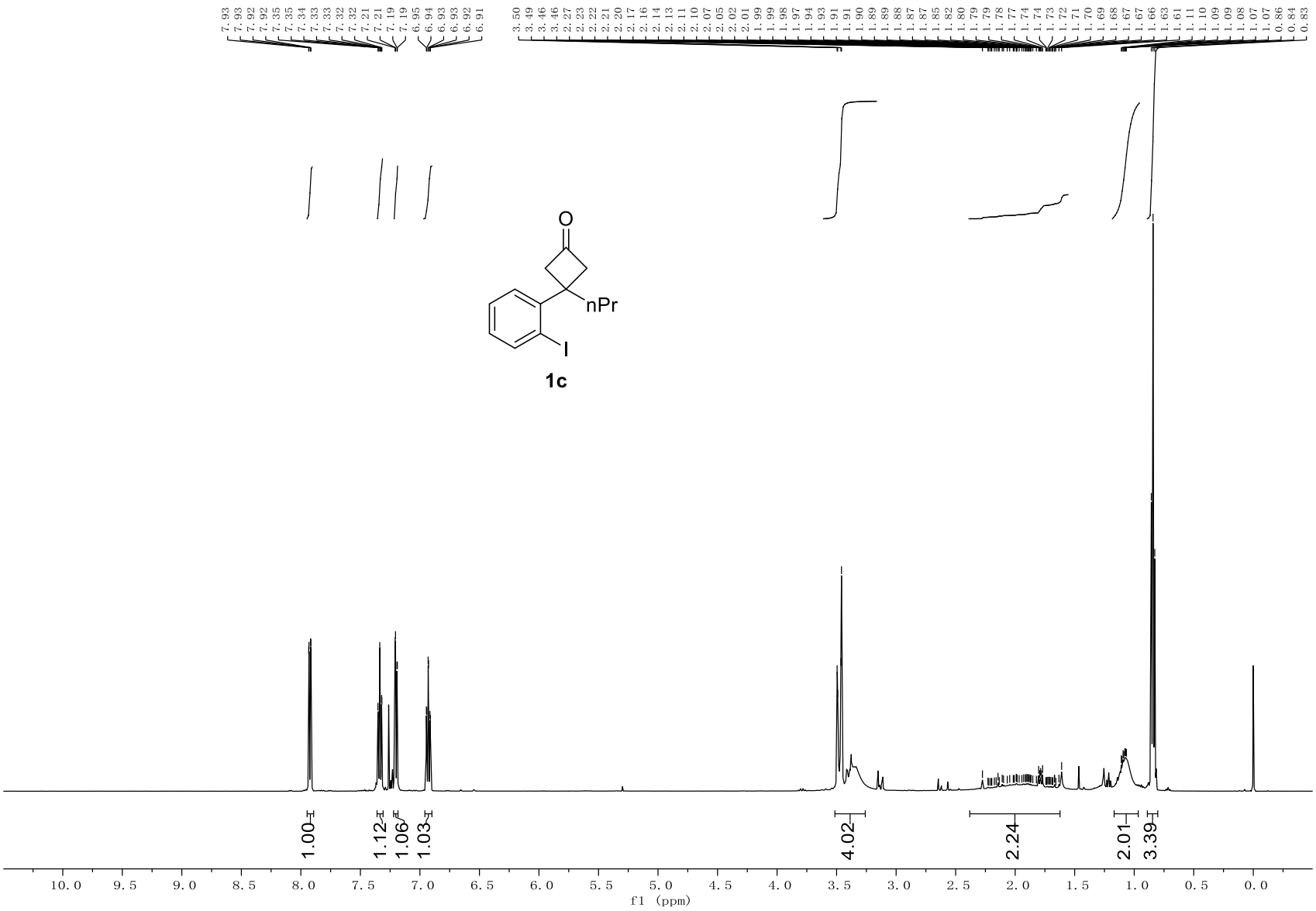

Figure S2 ^{13}C NMR Spectrum of 1c, related to Scheme 2

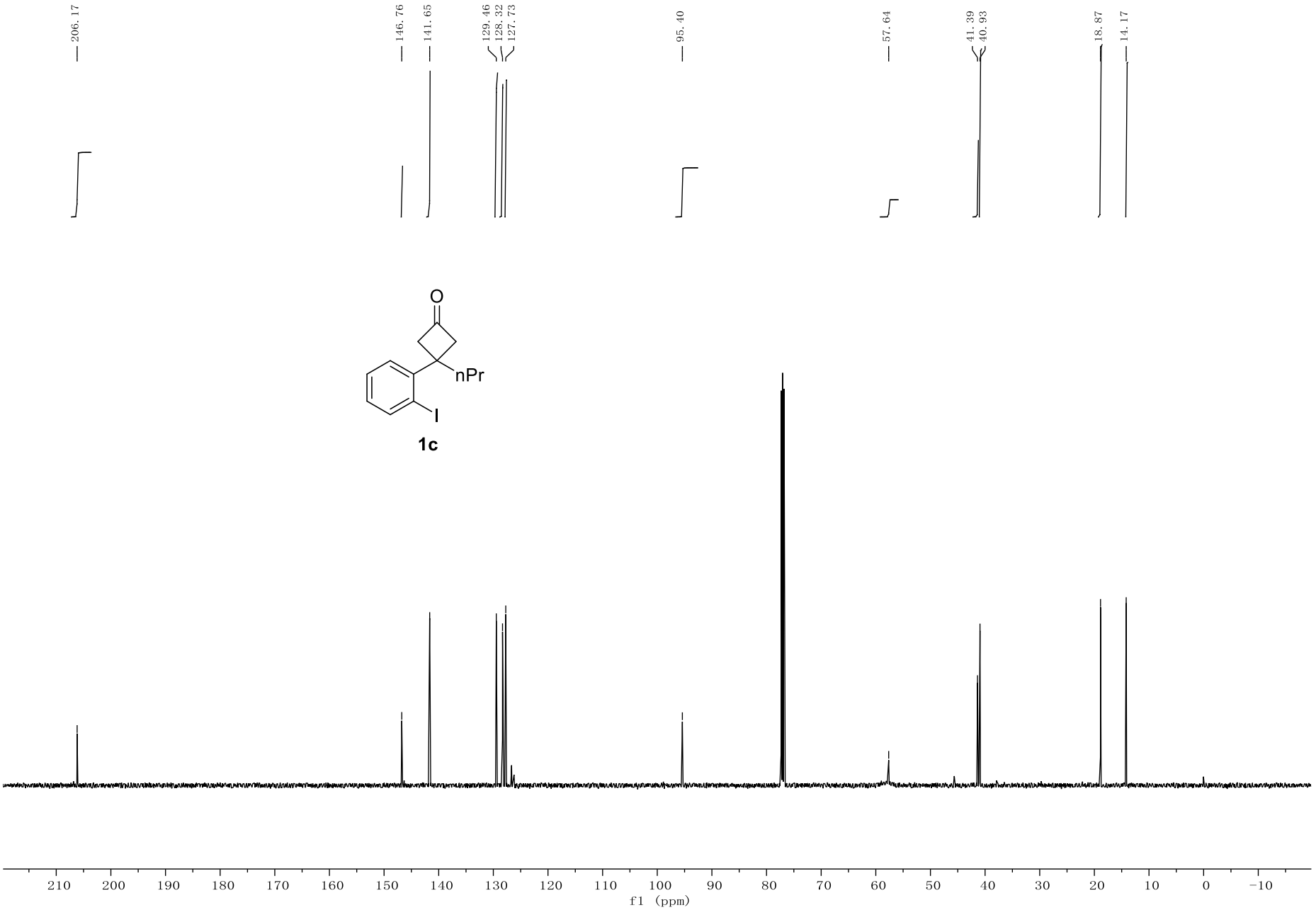

Figure S3 ^{1}H NMR Spectrum of 2k, related to Scheme 2

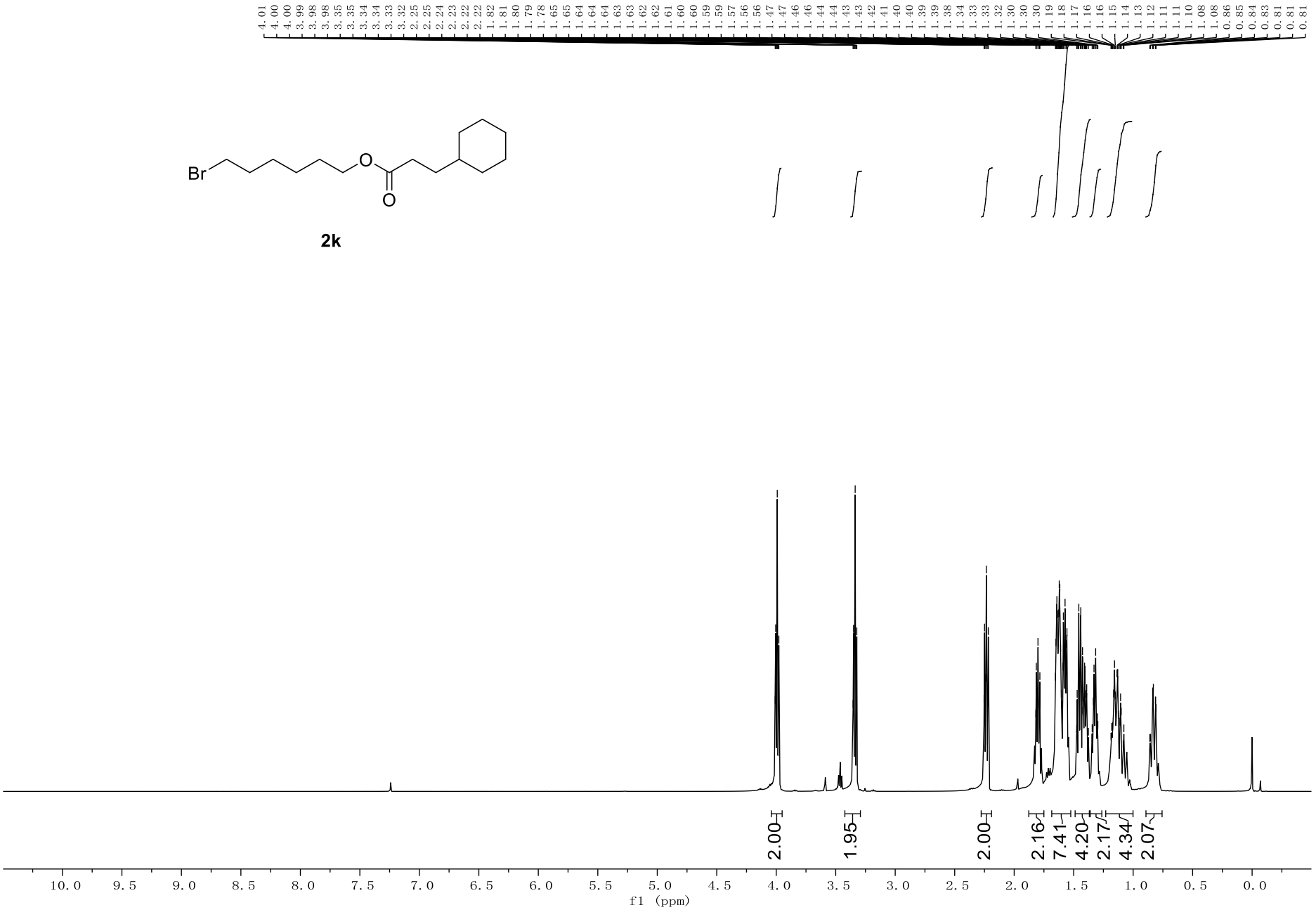

Figure S4 ^{13}C NMR Spectrum of 2k, related to Scheme 2

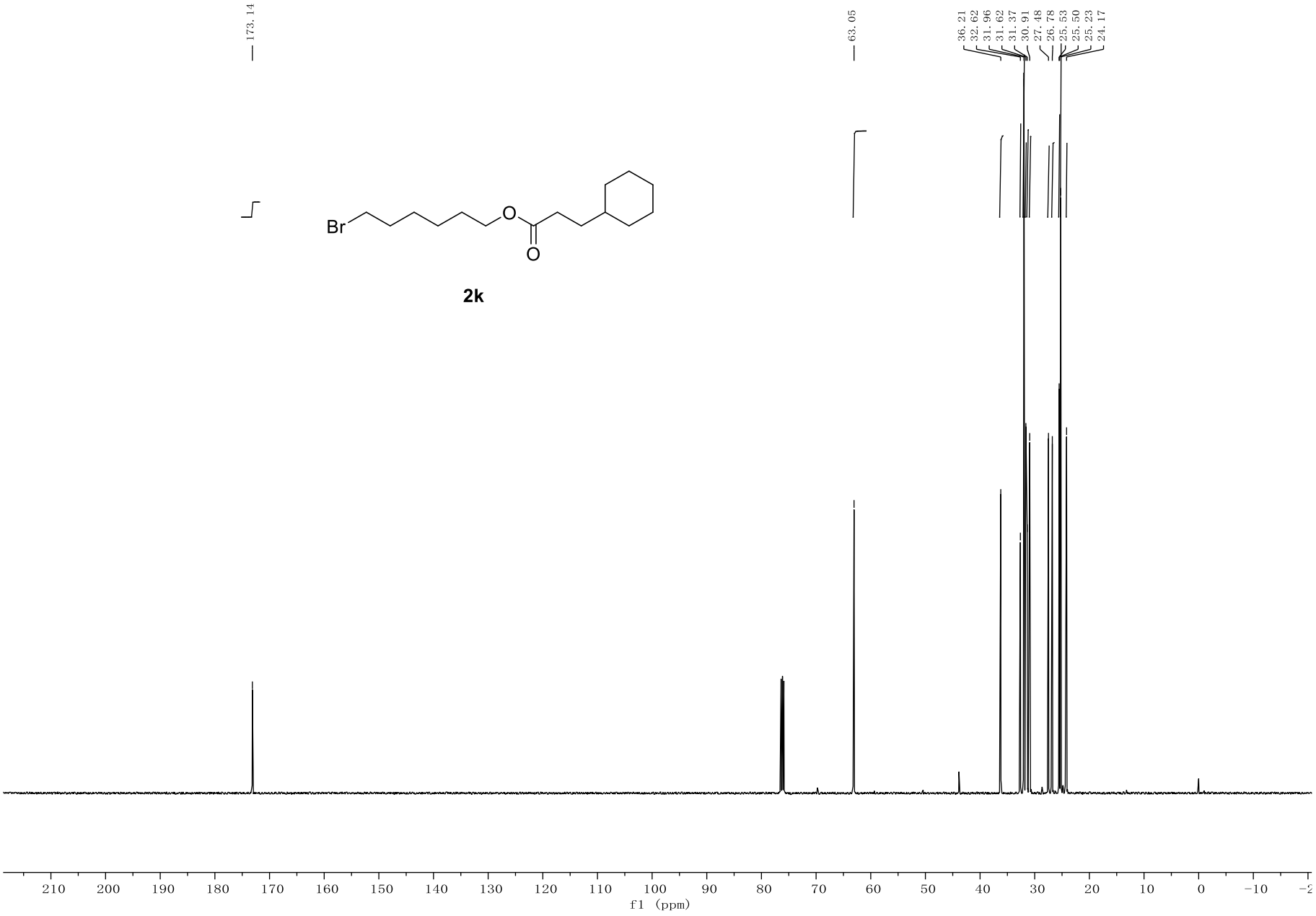

Figure S5 ^{1}H NMR Spectrum of 2l, related to Scheme 2

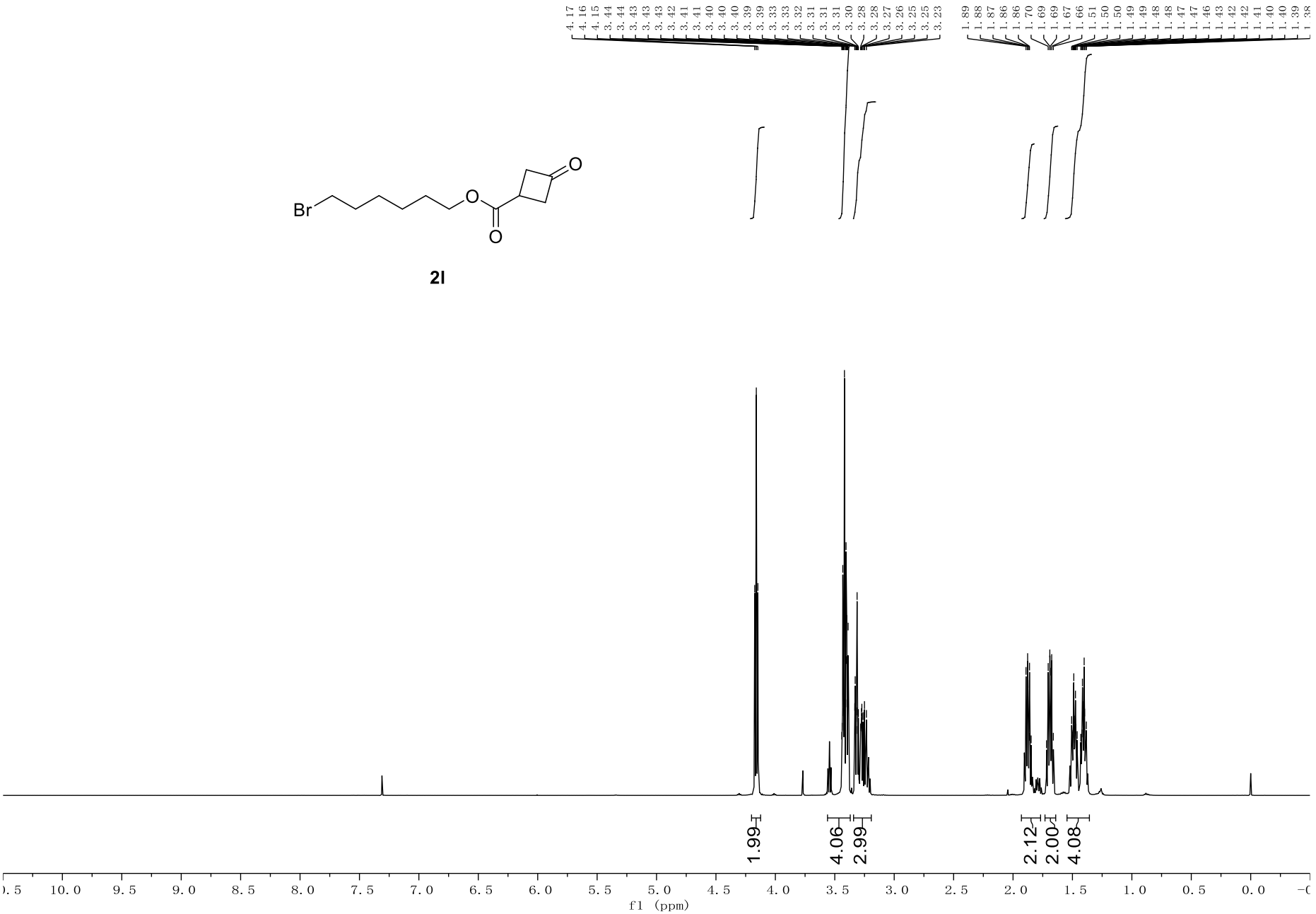

Figure S6 ^{13}C NMR Spectrum of 2l, related to Scheme 2

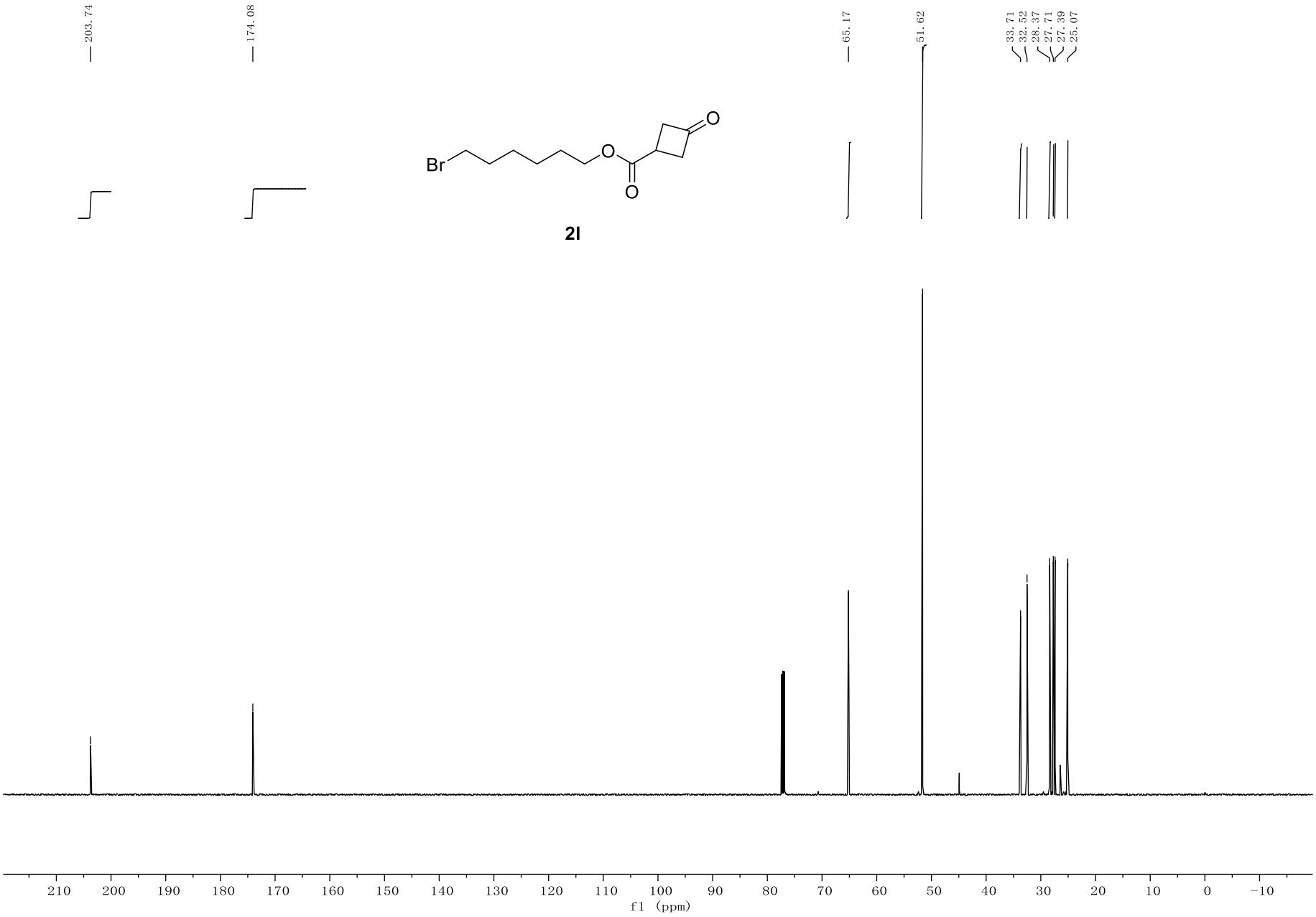

Figure S7 ^{1}H NMR Spectrum of 2o, related to Scheme 2

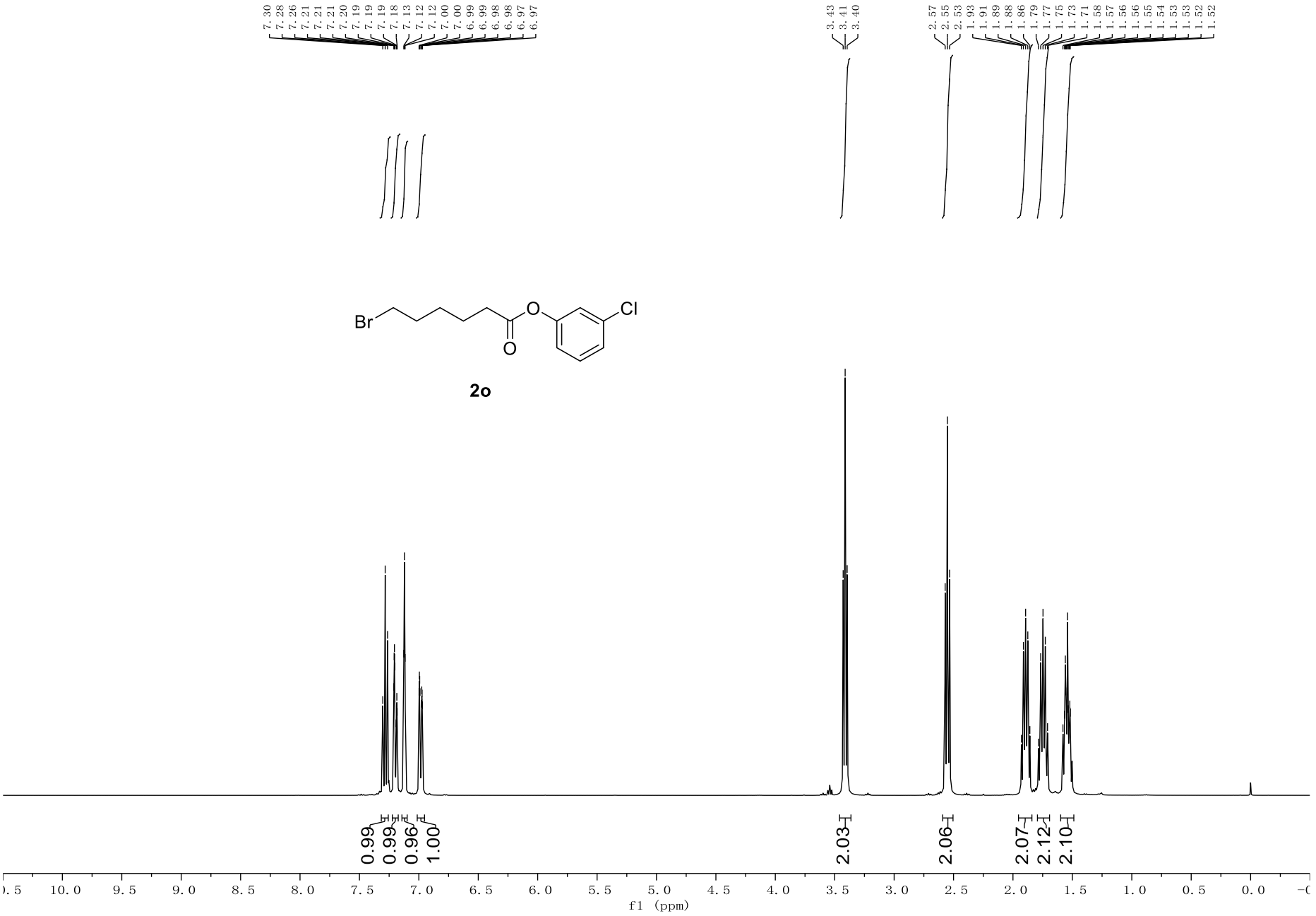

Figure S8 ^{13}C NMR Spectrum of 2o, related to Scheme 2

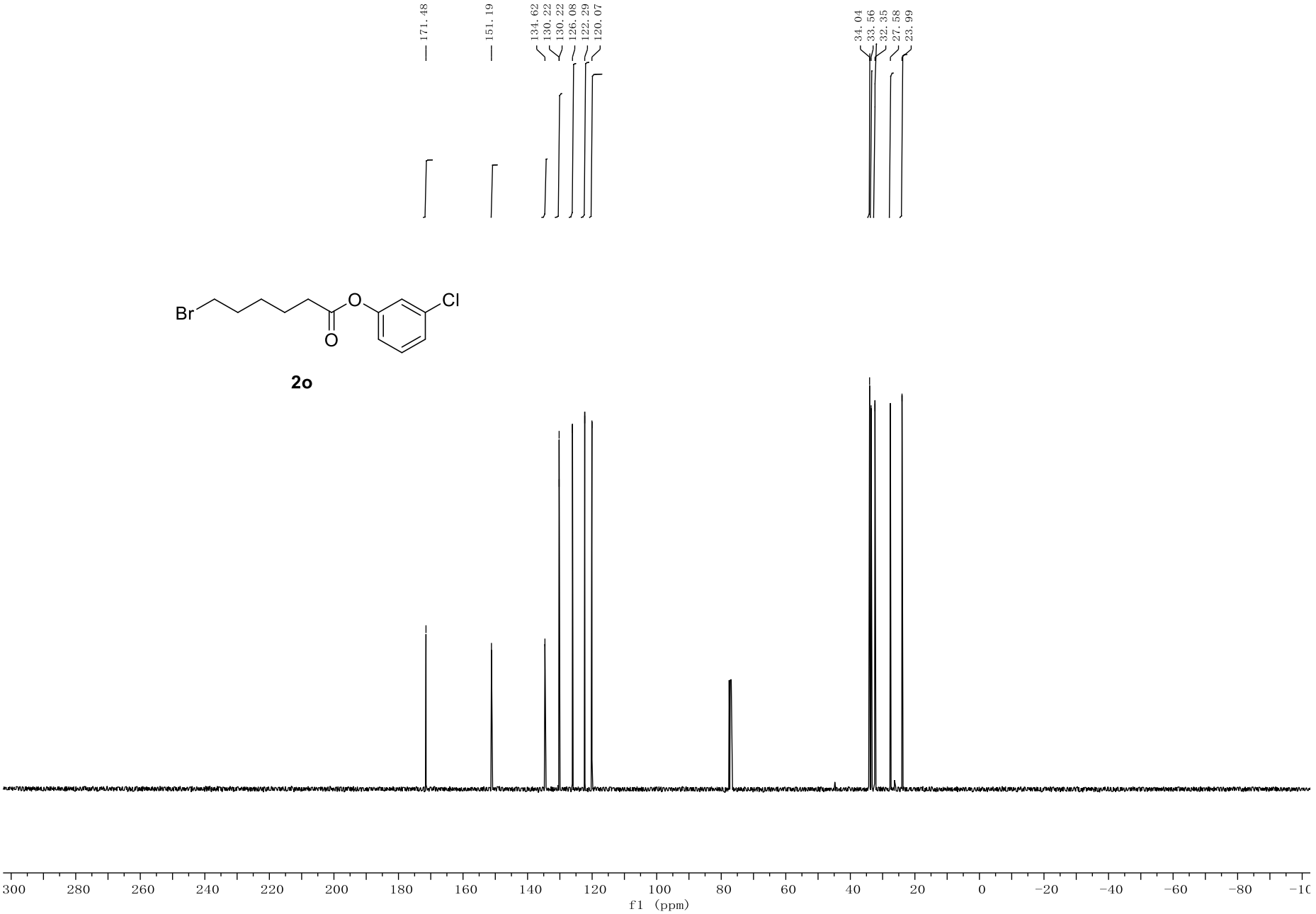

Figure S9 ^{1}H NMR Spectrum of 2q, related to Scheme 2

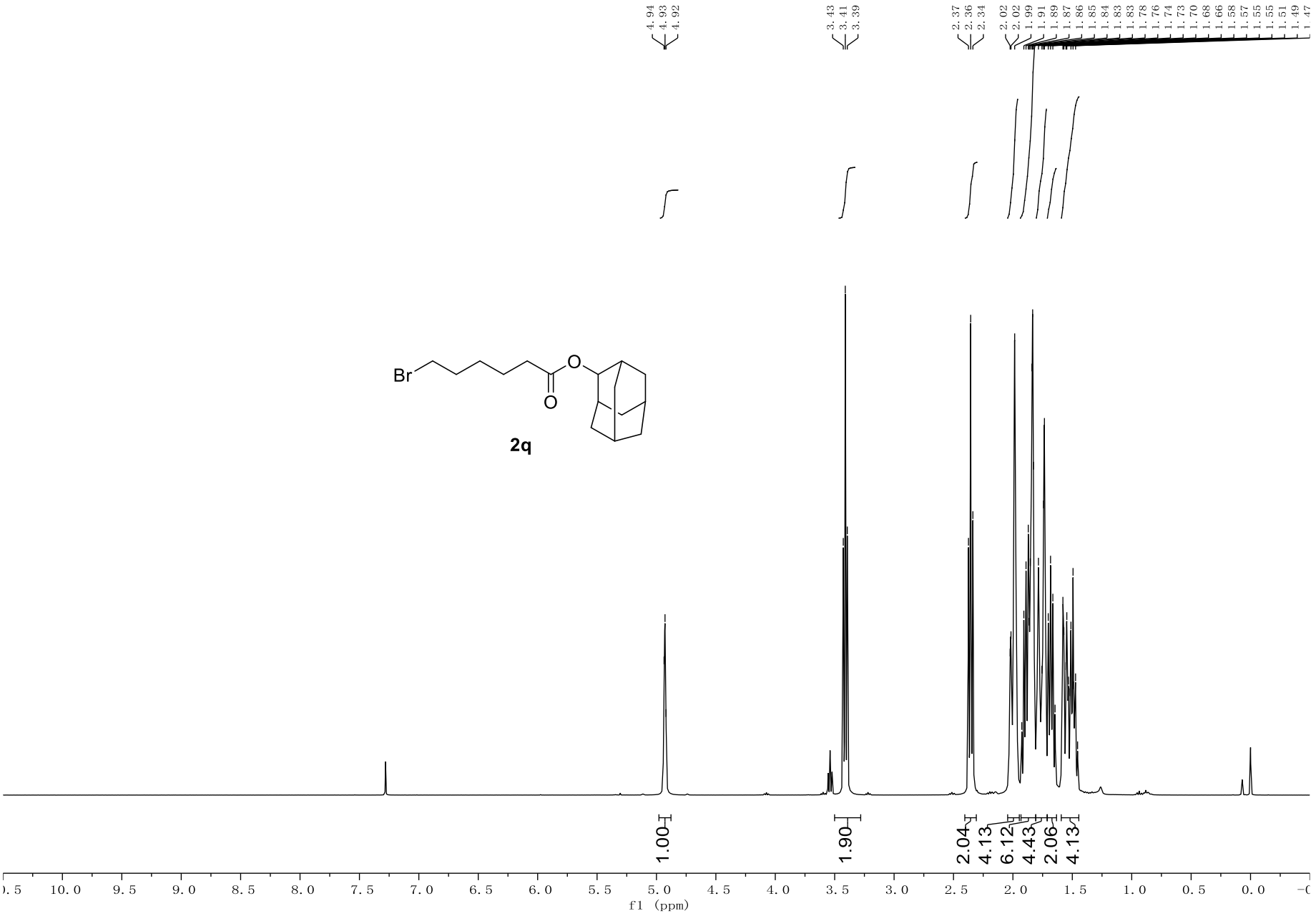

Figure S10 ^{13}C NMR Spectrum of 2q, related to Scheme 2

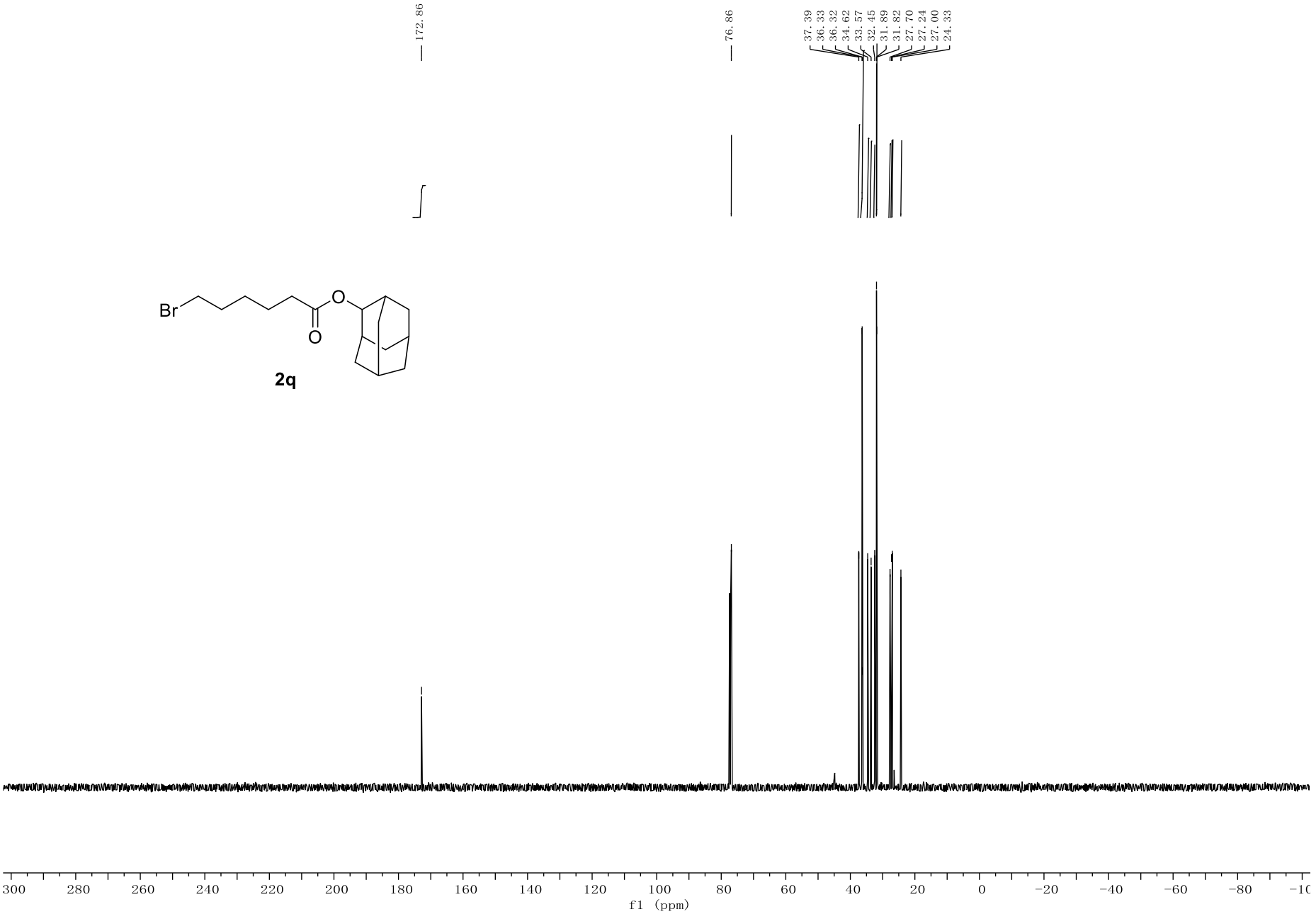

Figure S11 ^{1}H NMR Spectrum of 2r, related to Scheme 2

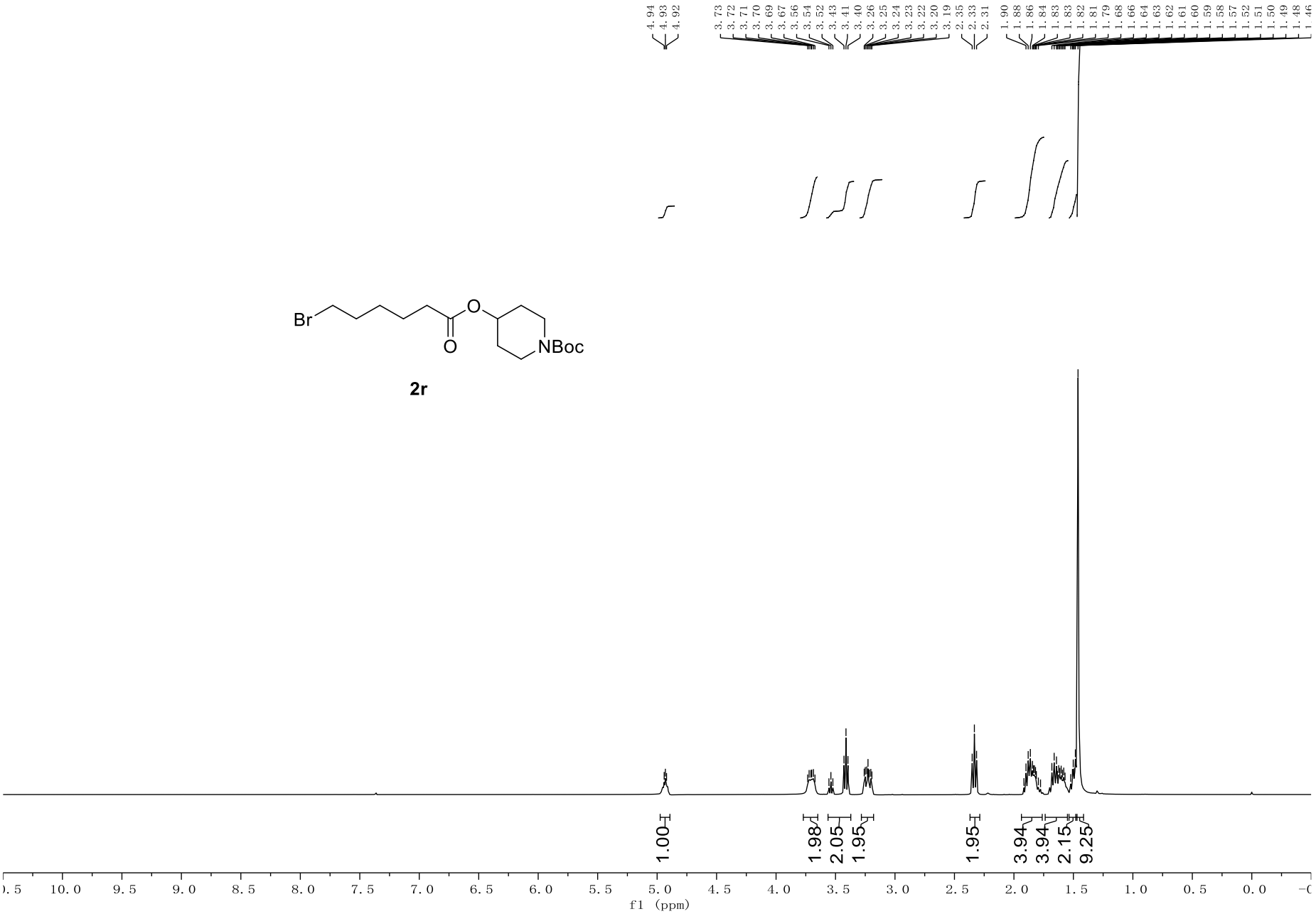

Figure S12 ^{13}C NMR Spectrum of 2r, related to Scheme 2

Figure S13 ^{1}H NMR Spectrum of 2t, related to Scheme 2

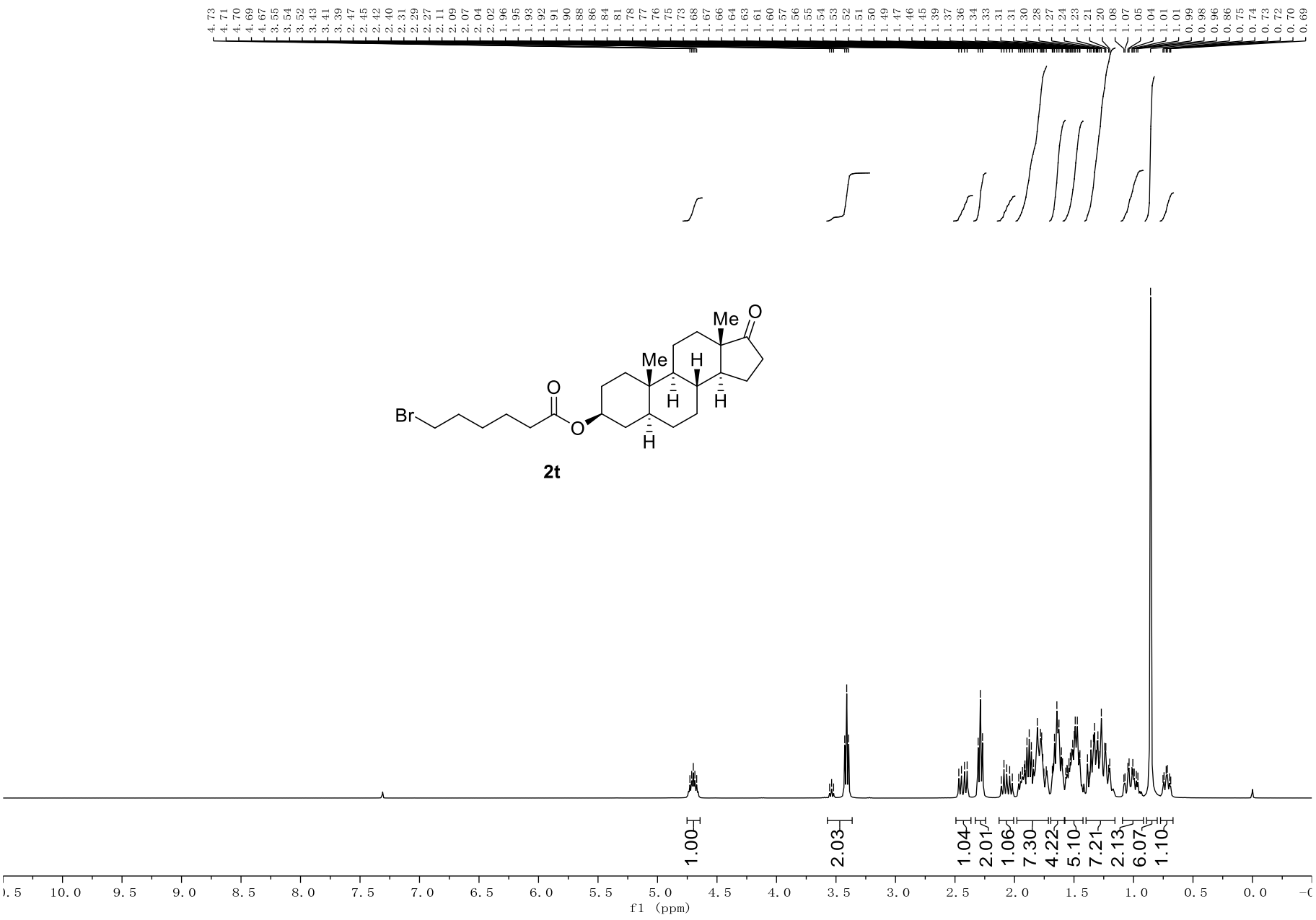

Figure S14 ^{13}C NMR Spectrum of 12t, related to Scheme 2

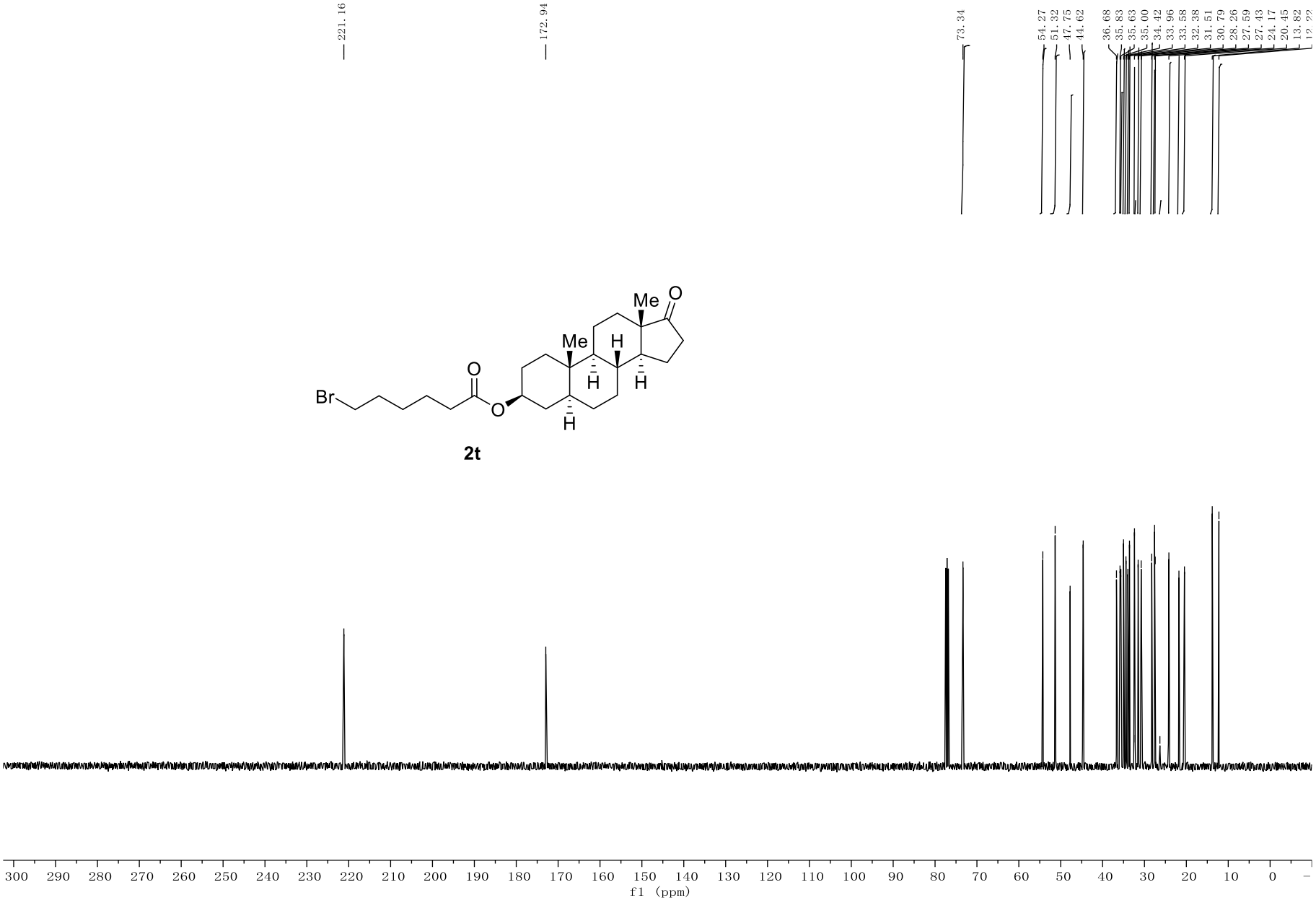

Figure S15 ^{1}H NMR Spectrum of 3a, related to Scheme 2

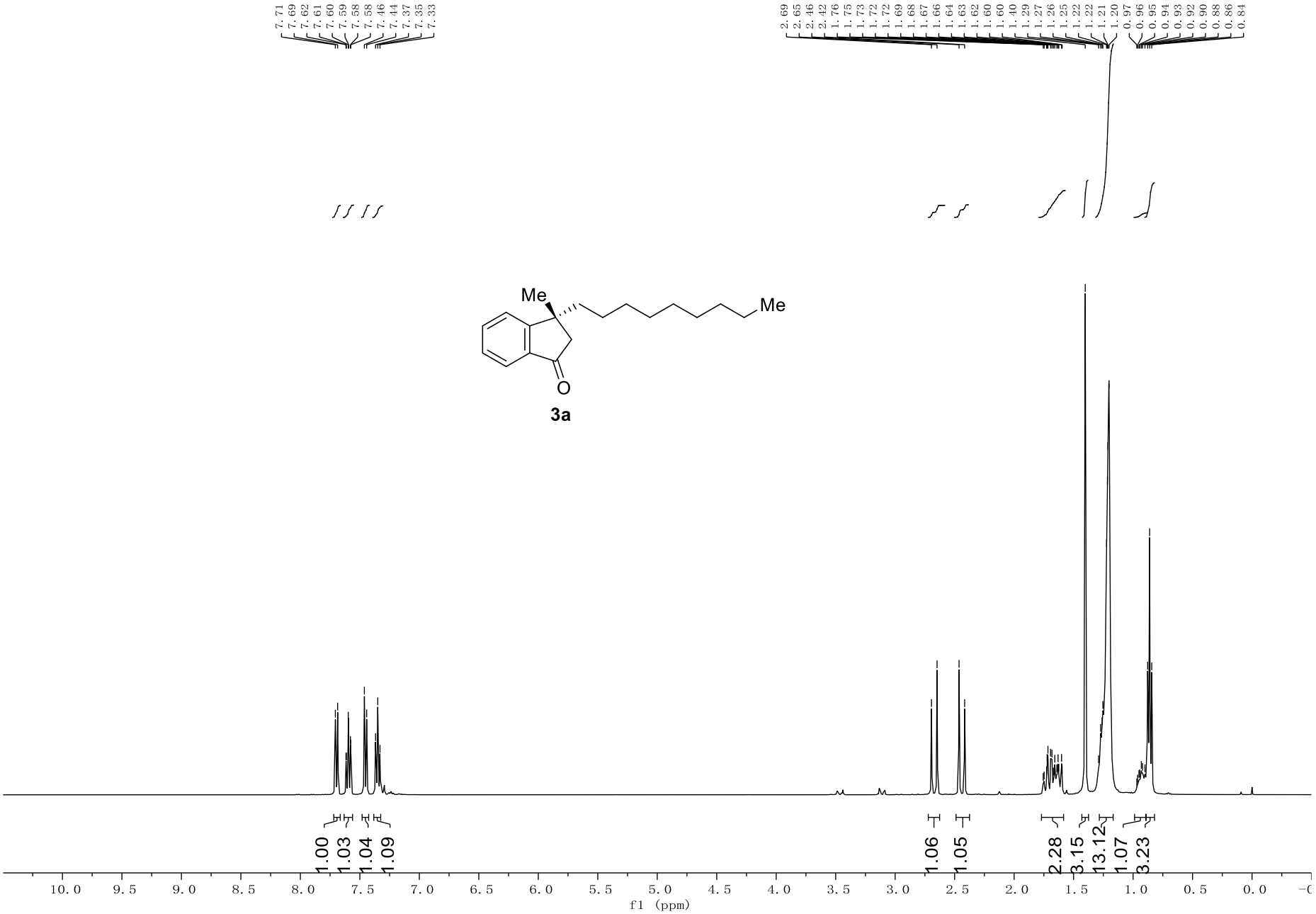

Figure S16 ^{13}C NMR Spectrum of 3a, related to Scheme 2

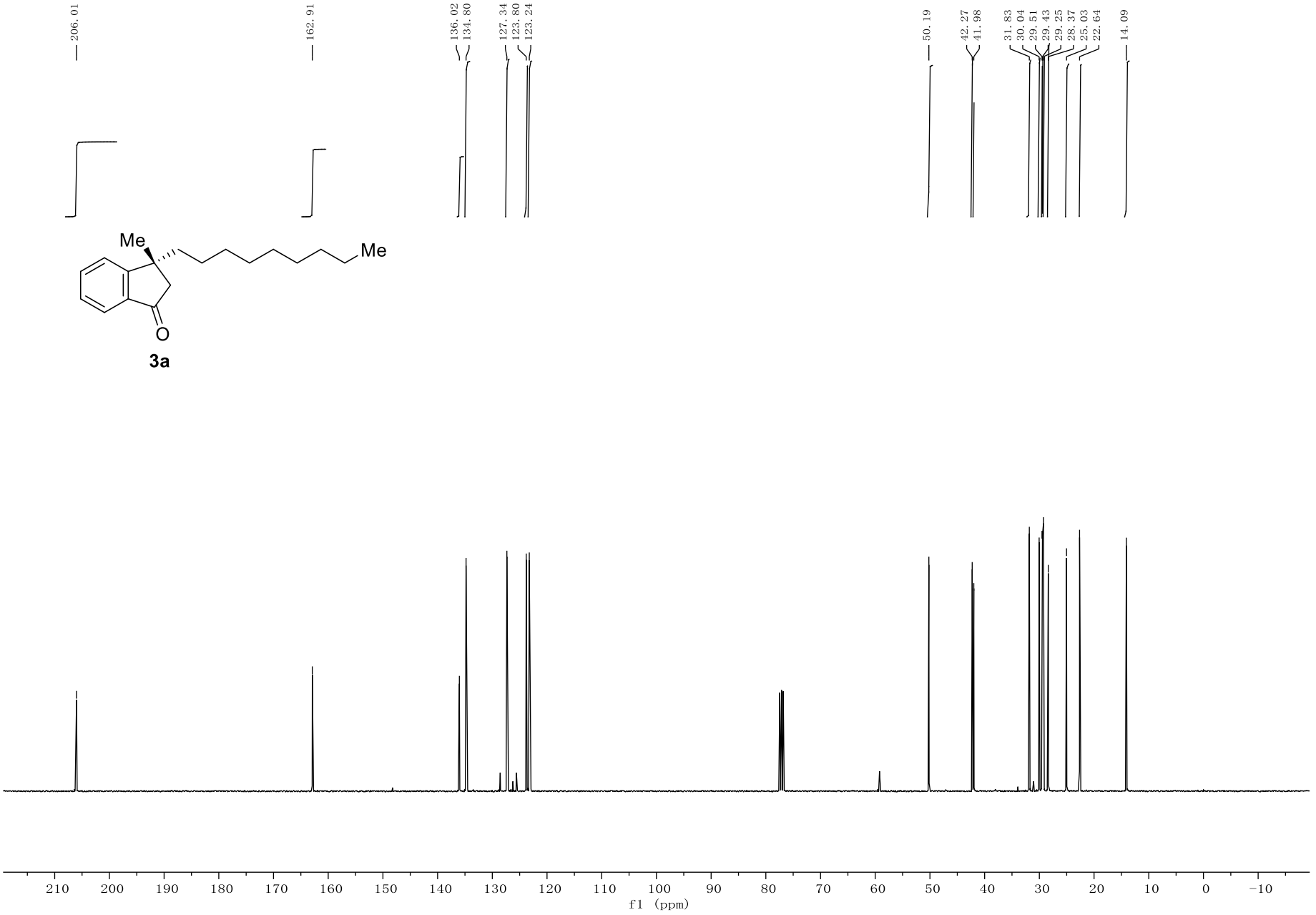

Figure S17 ^{1}H NMR Spectrum of 3b, related to Scheme 2

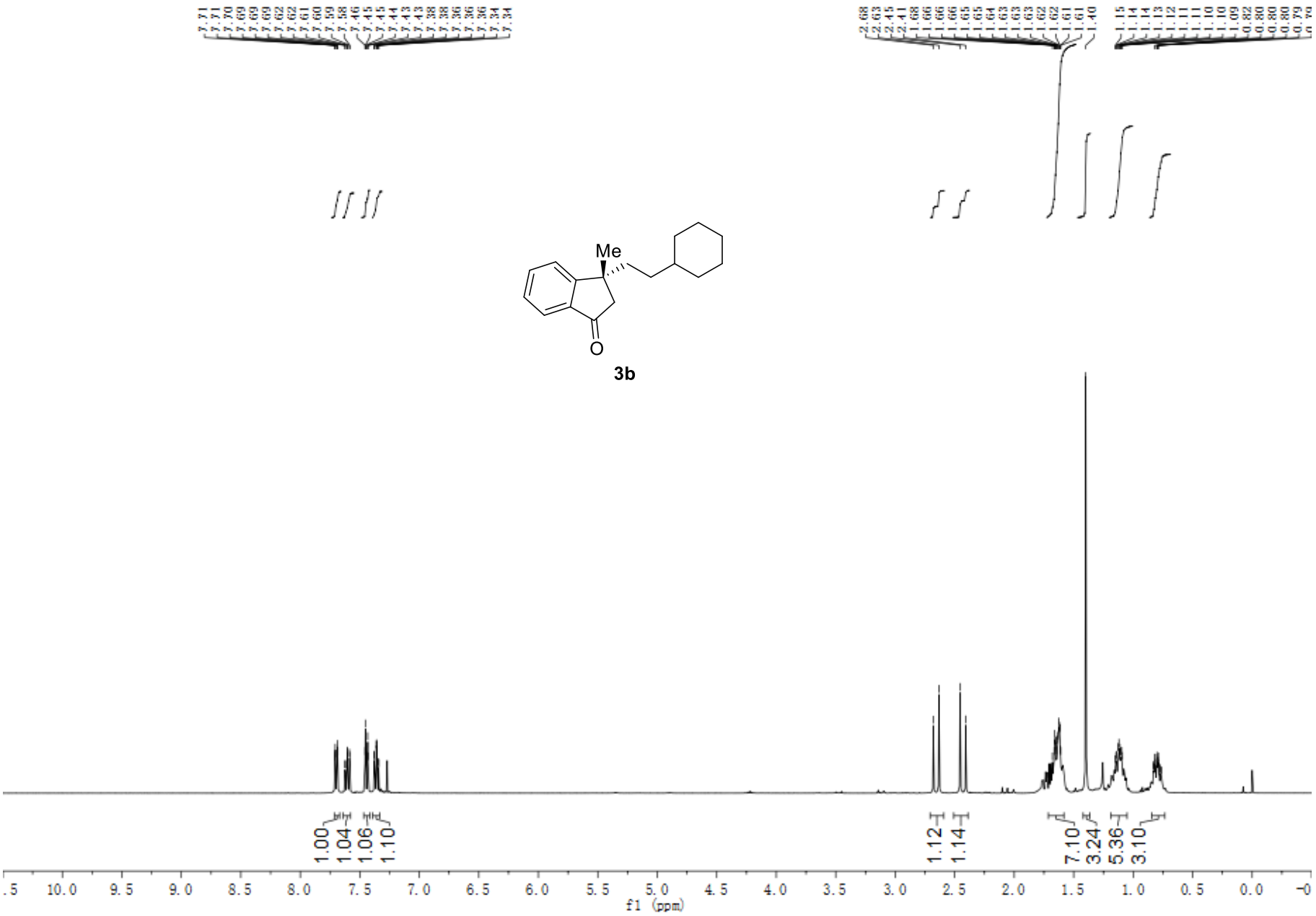

Figure S18 ^{13}C NMR Spectrum of 3b, related to Scheme 2

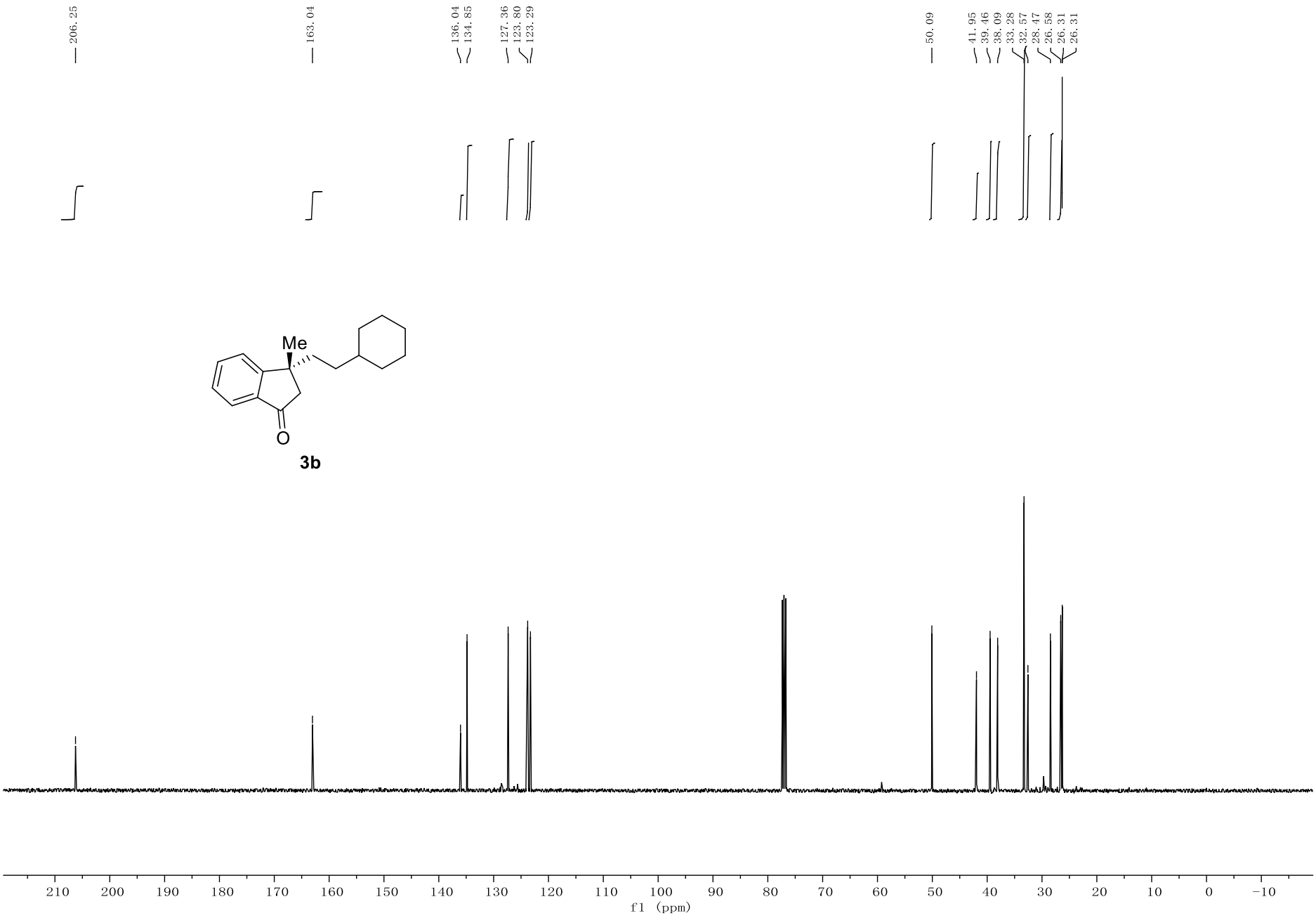

Figure S19 ^{1}H NMR Spectrum of 3c, related to Scheme 2

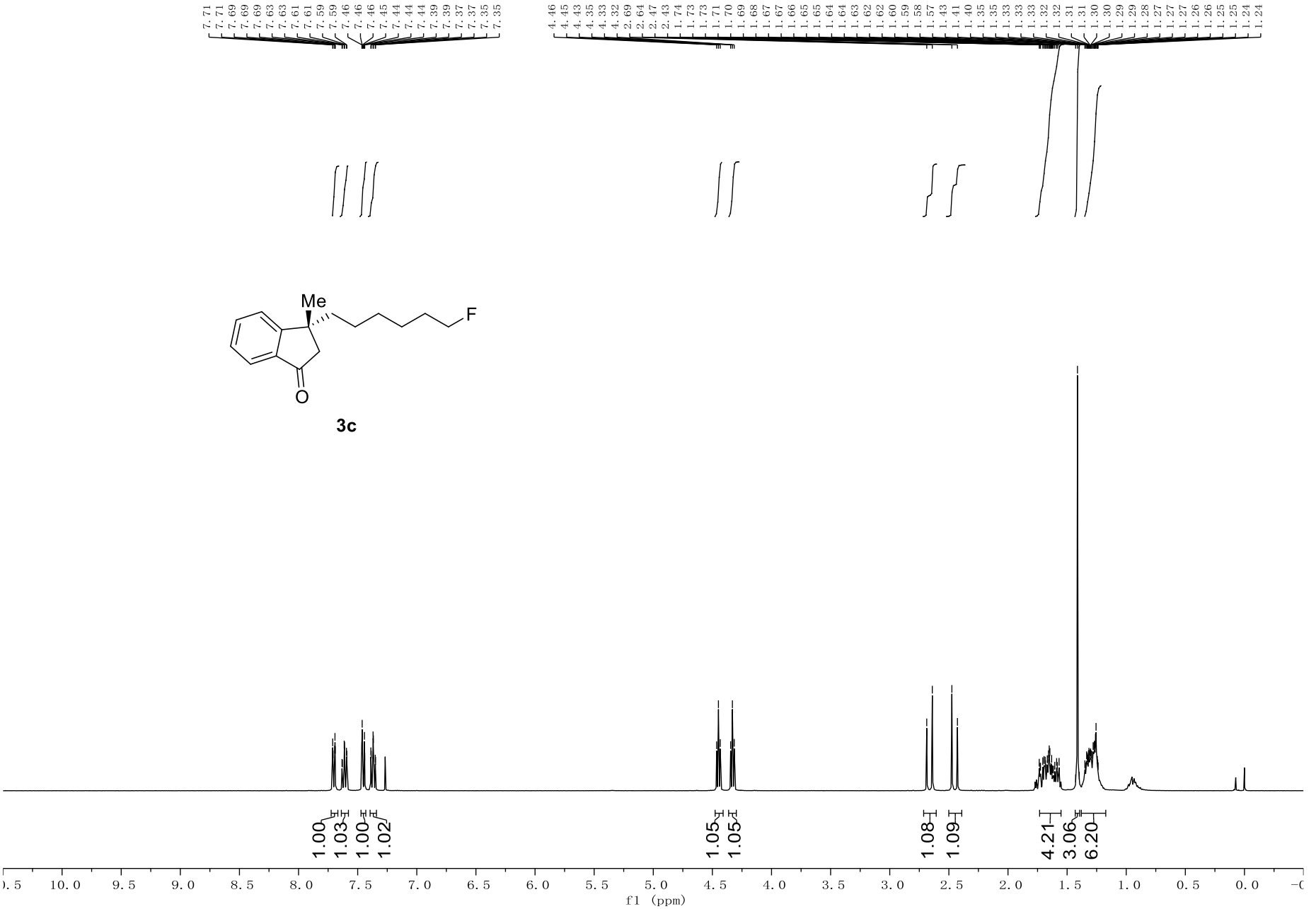

Figure S20 ^{13}C NMR Spectrum of 3c, related to Scheme 2

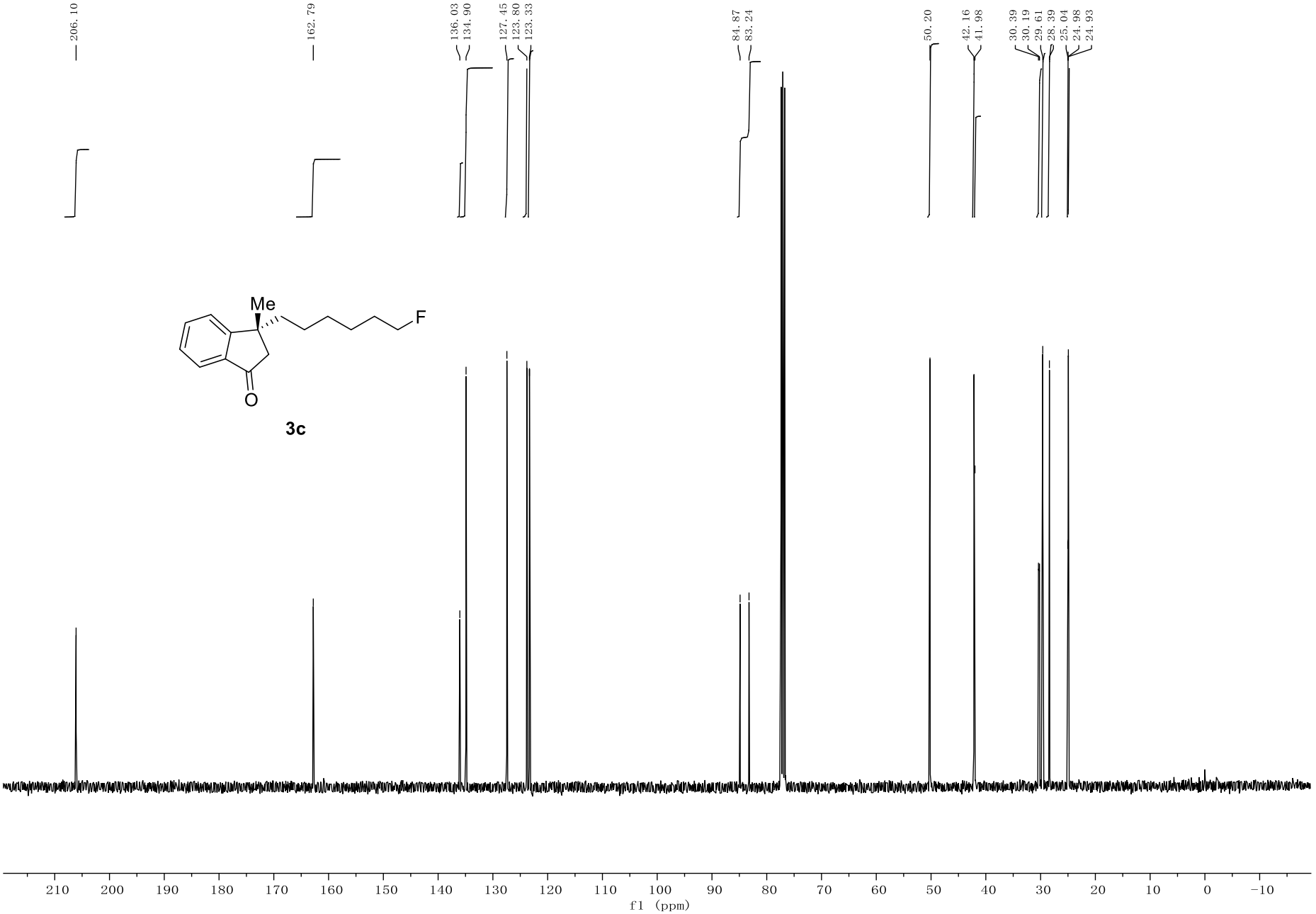

Figure S21 ^{19}F NMR Spectrum of 3c, related to Scheme 2

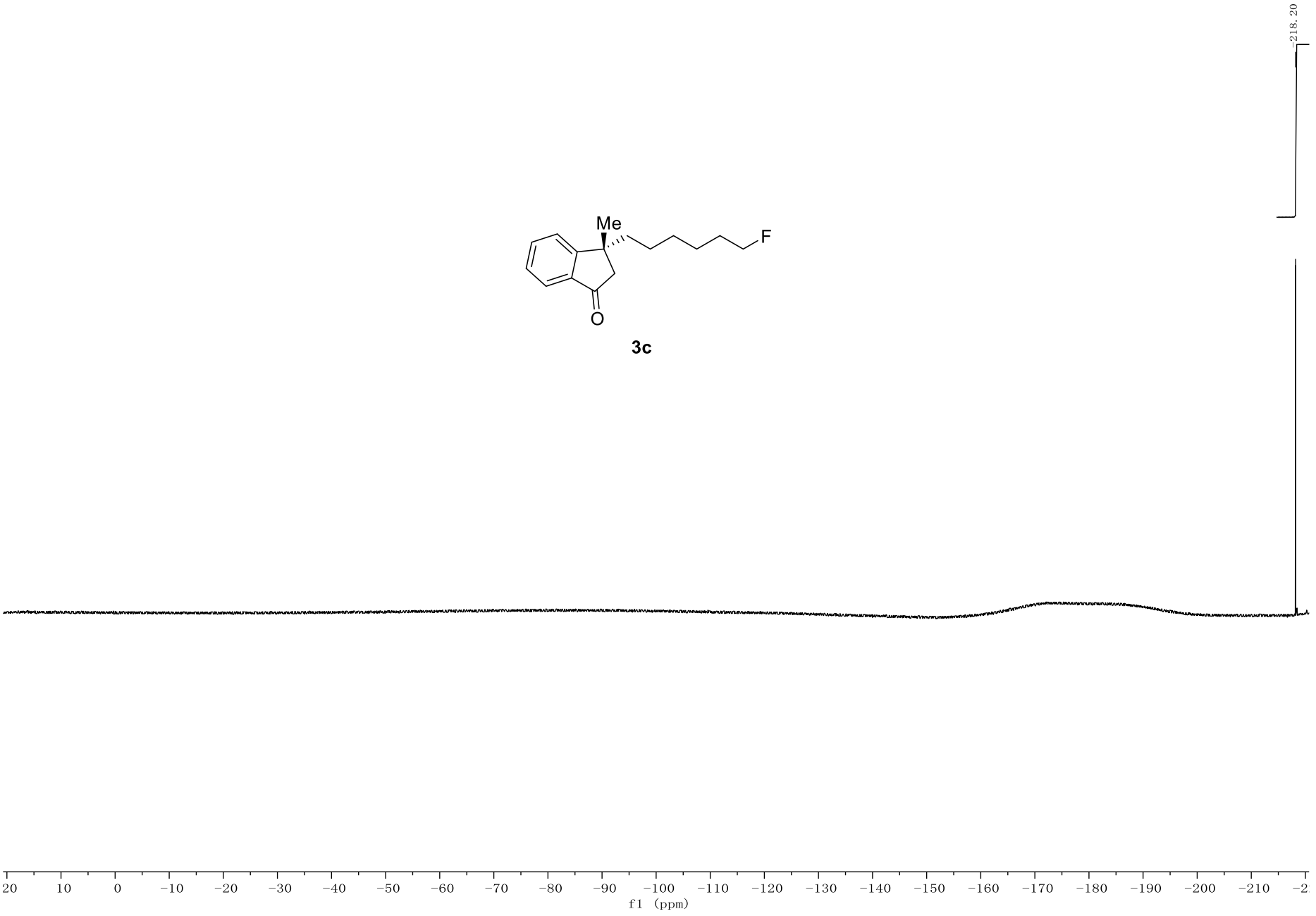

Figure S22 ^{1}H NMR Spectrum of 3d, related to Scheme 2

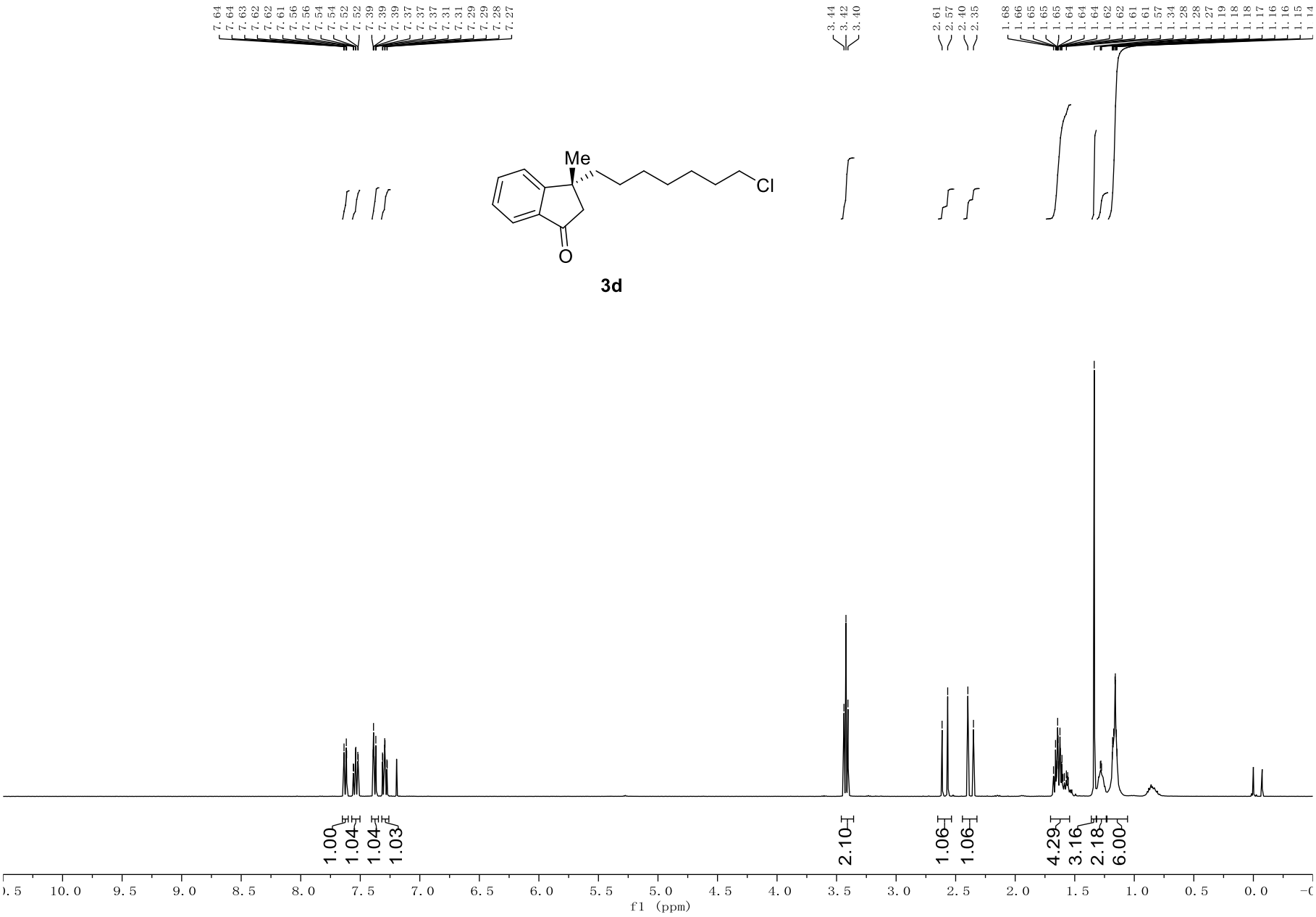

Figure S23 ^{13}C NMR Spectrum of 3d, related to Scheme 2

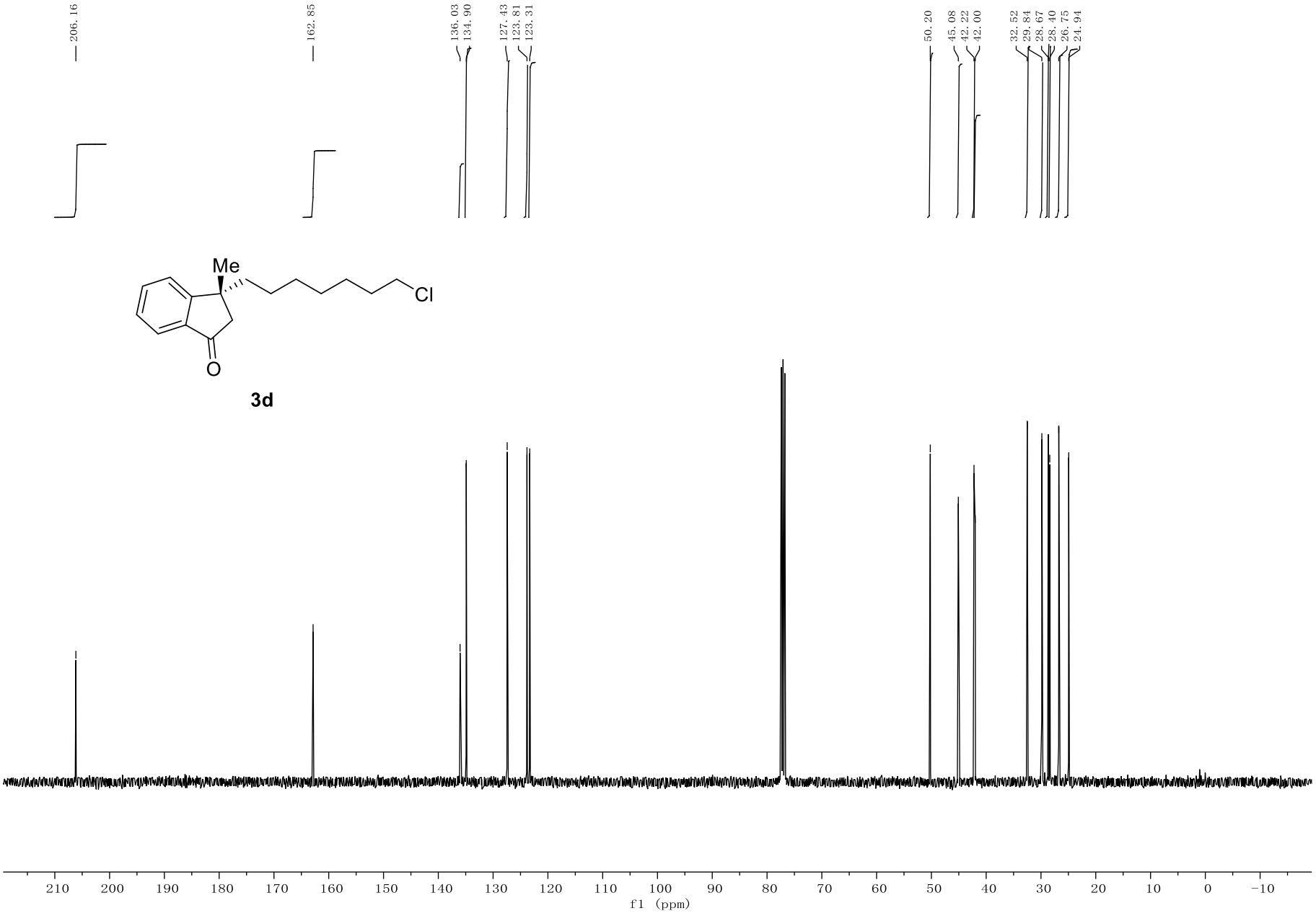

Figure S24 ^{1}H NMR Spectrum of 3e, related to Scheme 2

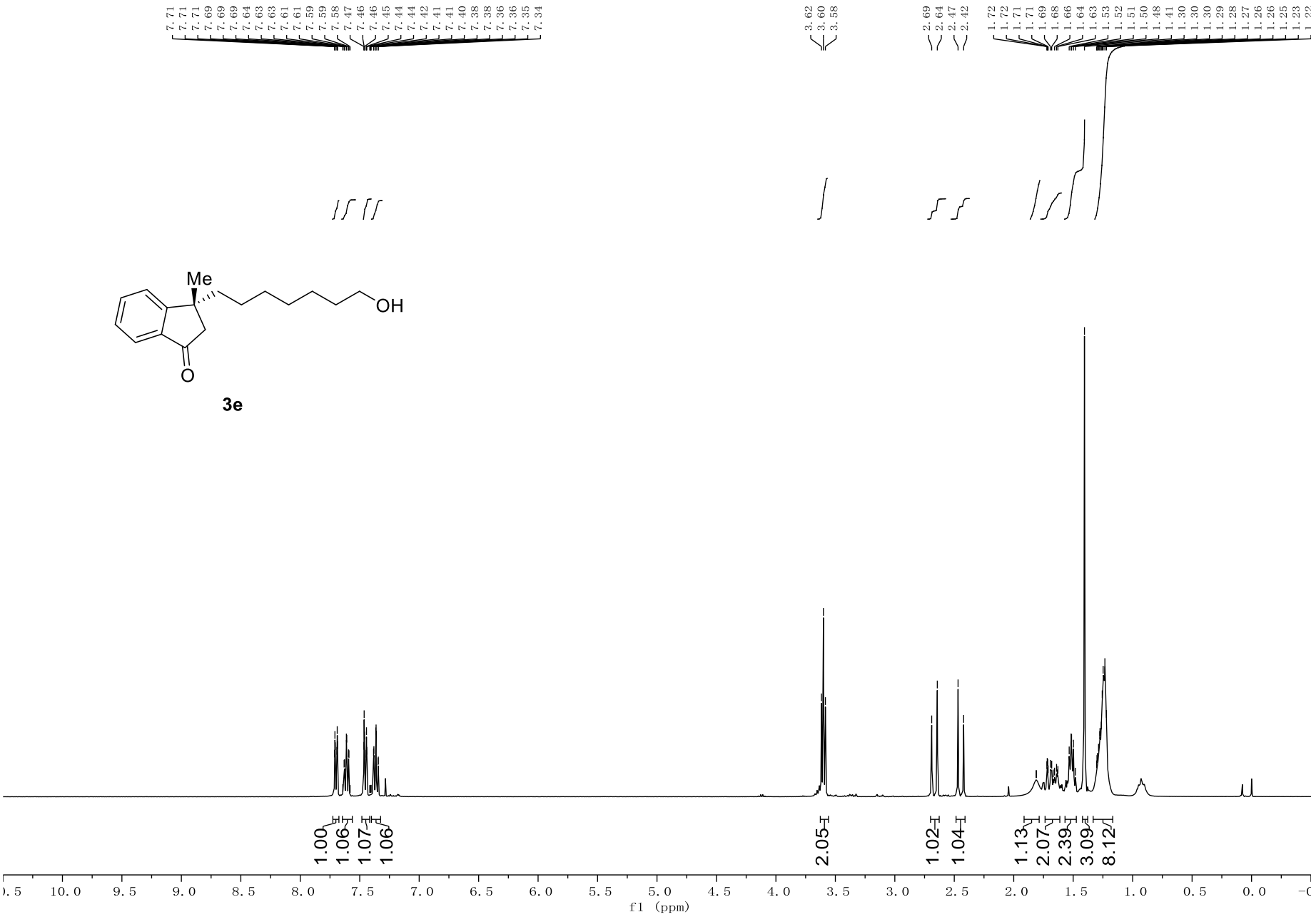

Figure S25 ^{13}C NMR Spectrum of 3e, related to Scheme 2

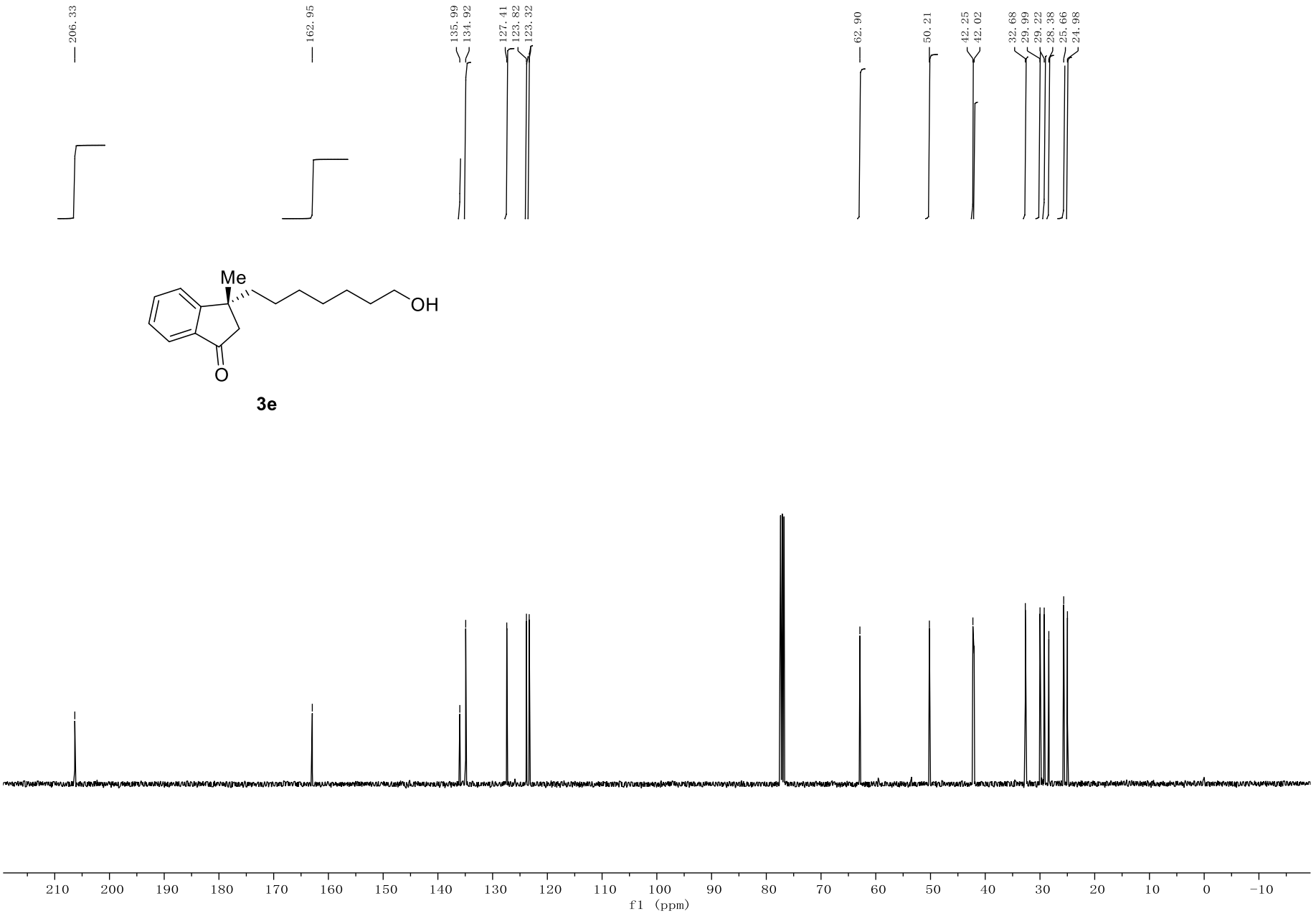

Figure S26 ^{1}H NMR Spectrum of 3f, related to Scheme 2

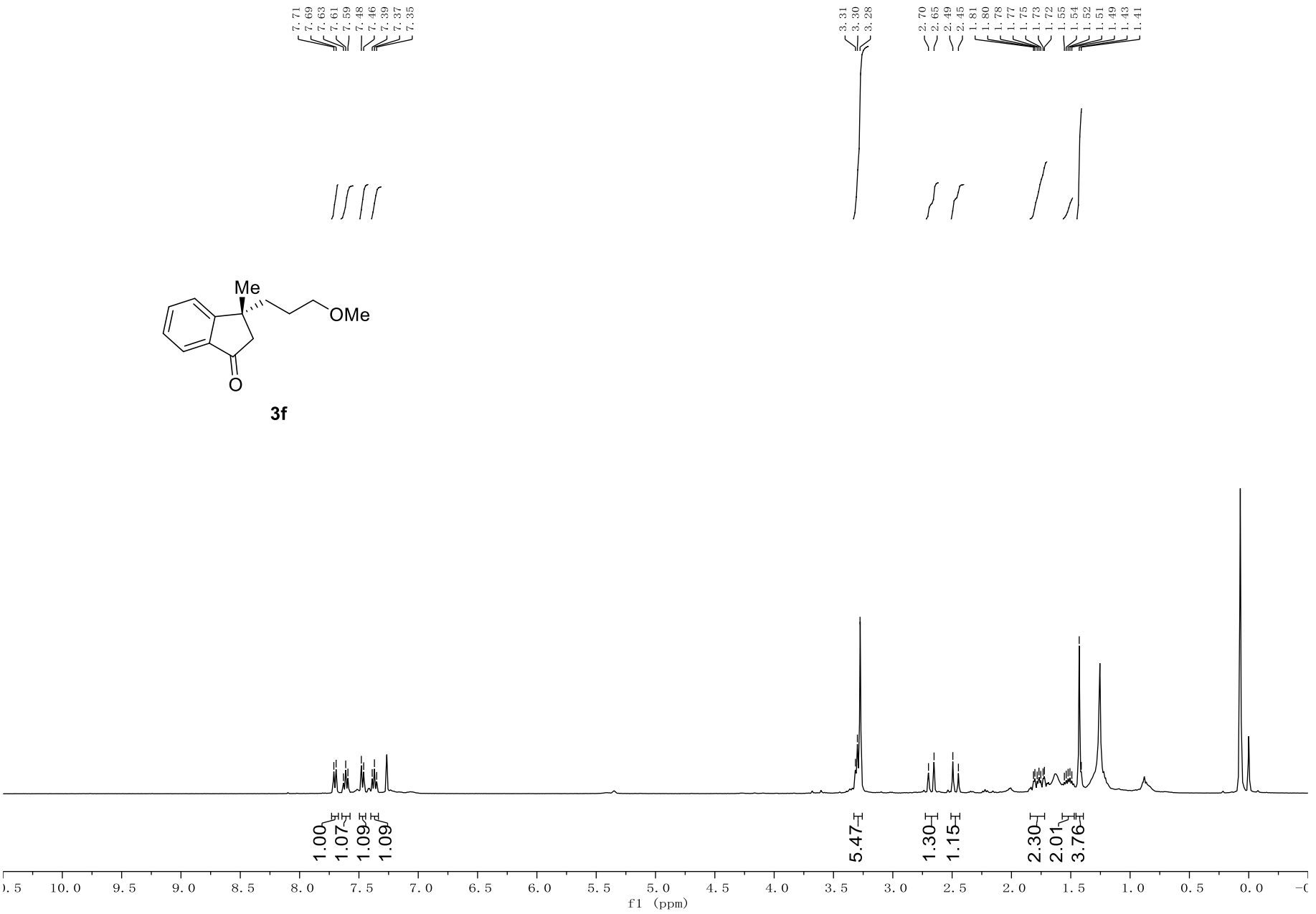

Figure S27 ^{13}C NMR Spectrum of 3f, related to Scheme 2

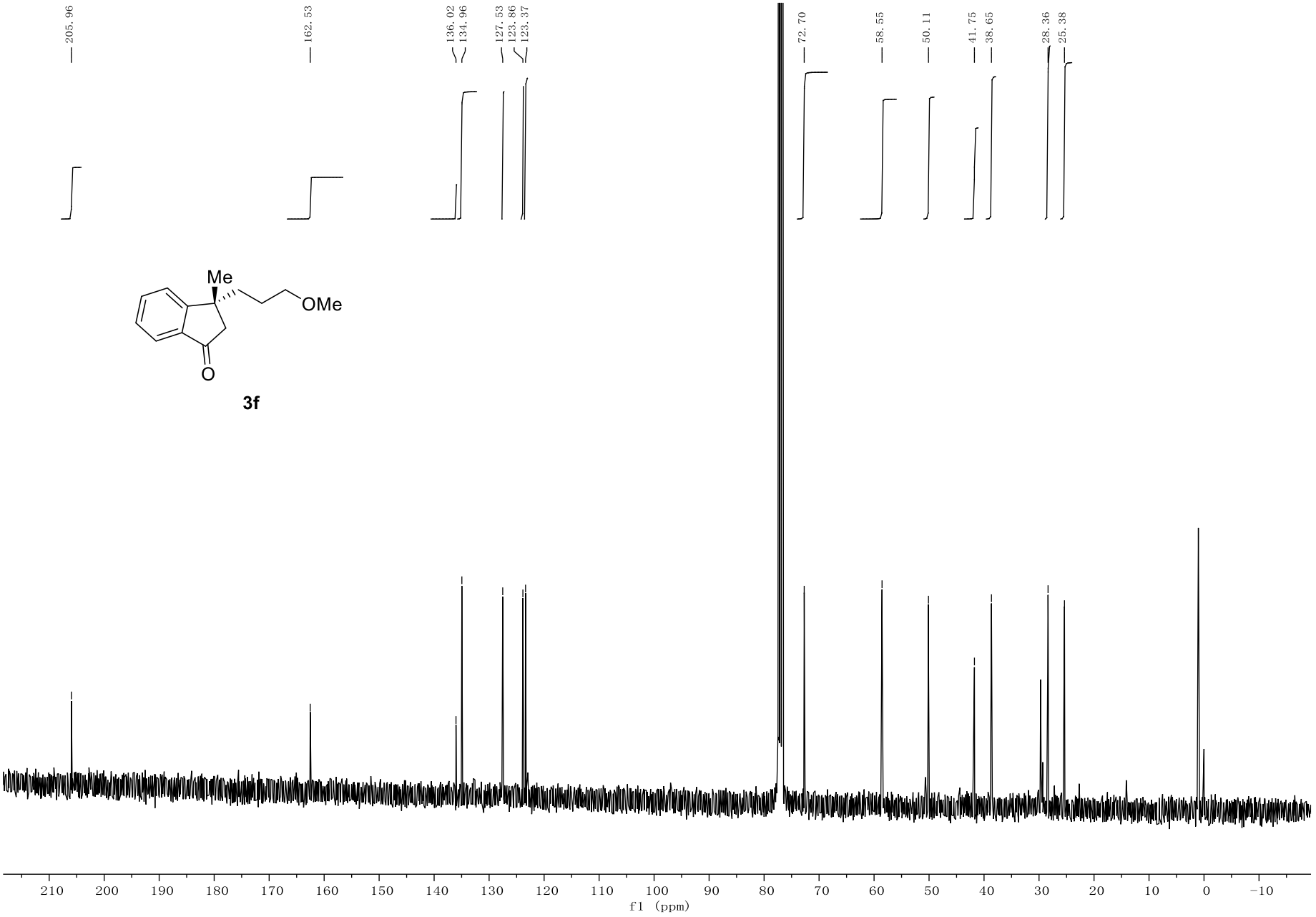

Figure S28 ^{1}H NMR Spectrum of 3g, related to Scheme 2

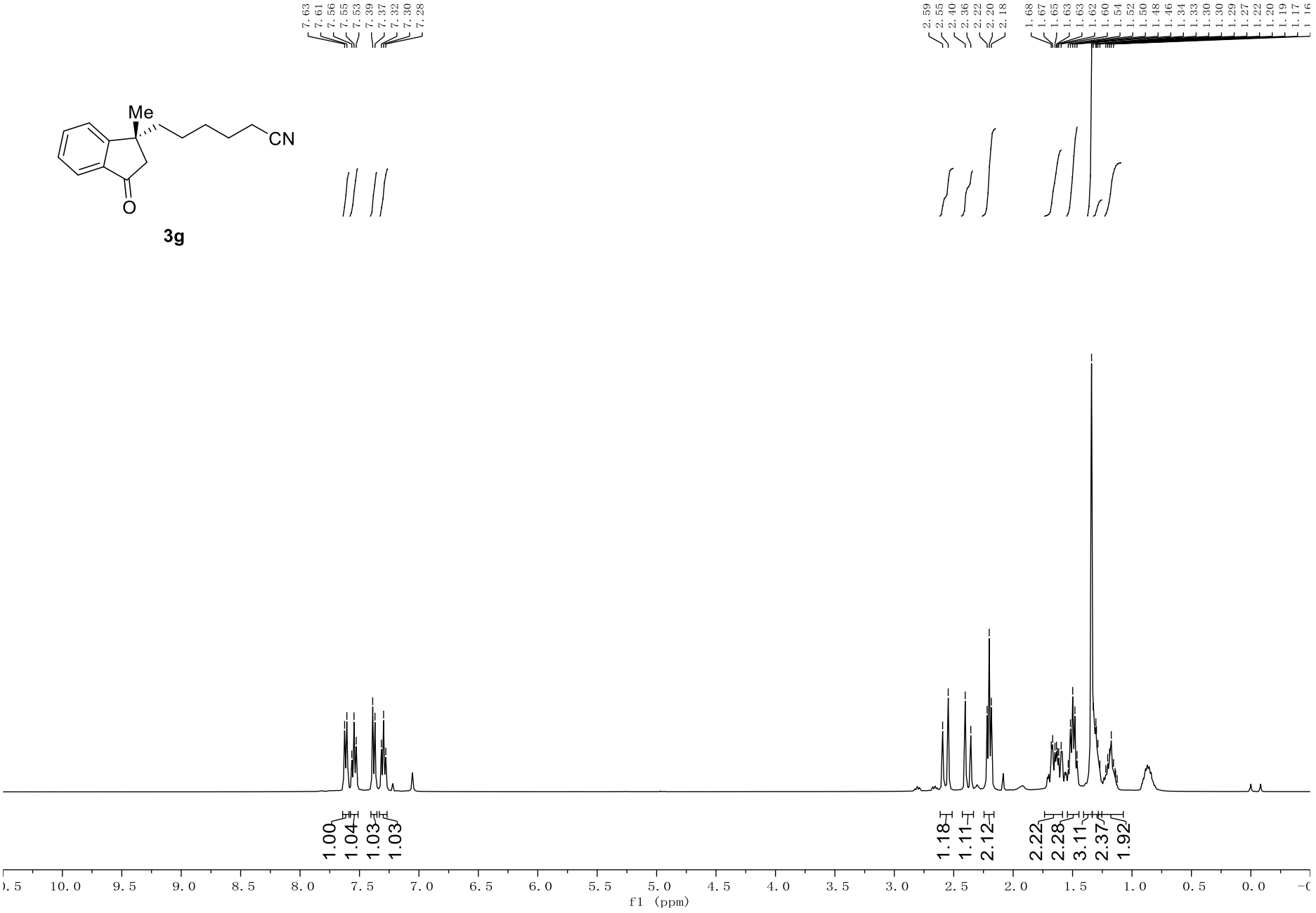

Figure S29 ^{13}C NMR Spectrum of 3g, related to Scheme 2

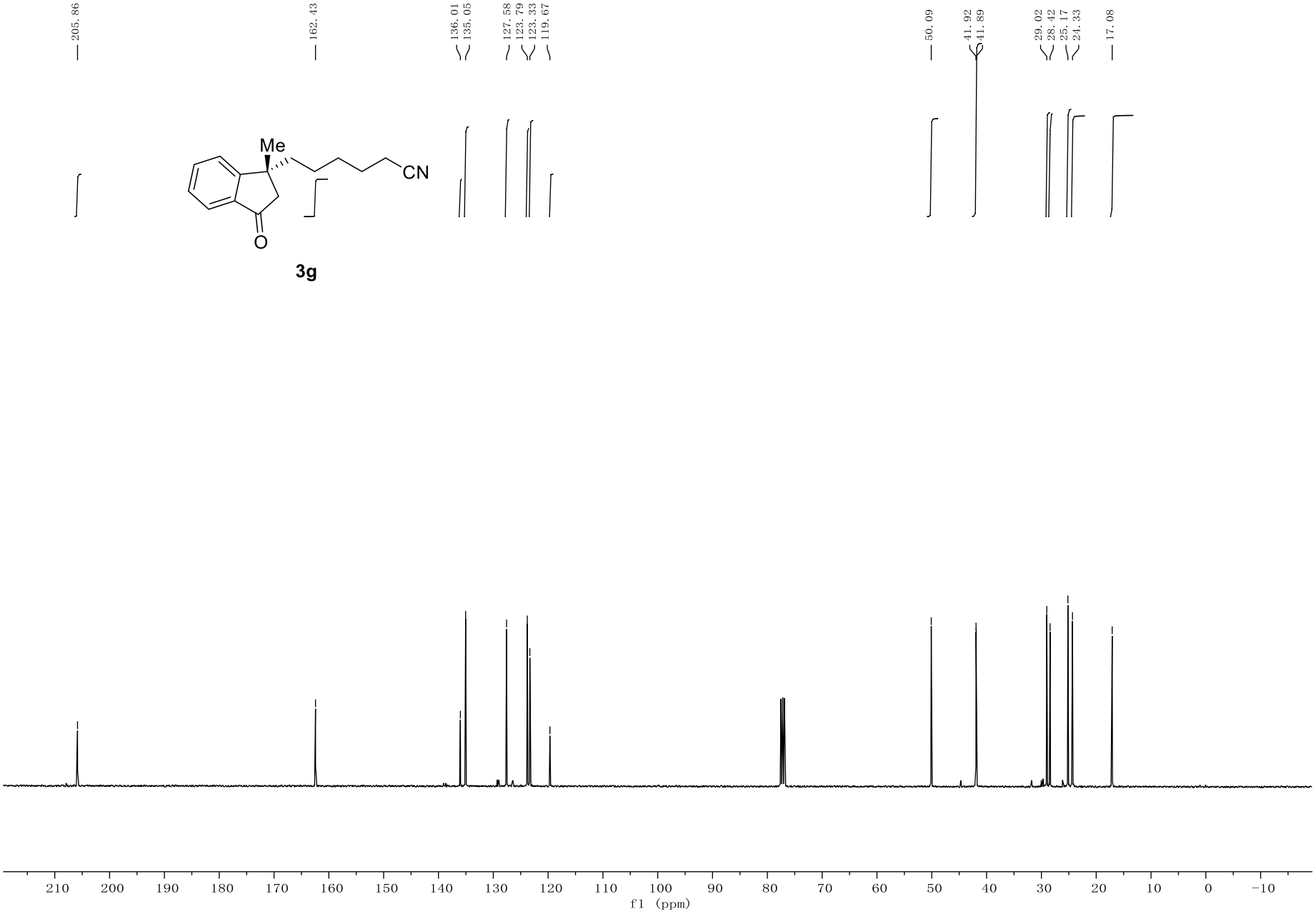

Figure S30 ^{1}H NMR Spectrum of 3h, related to Scheme 2

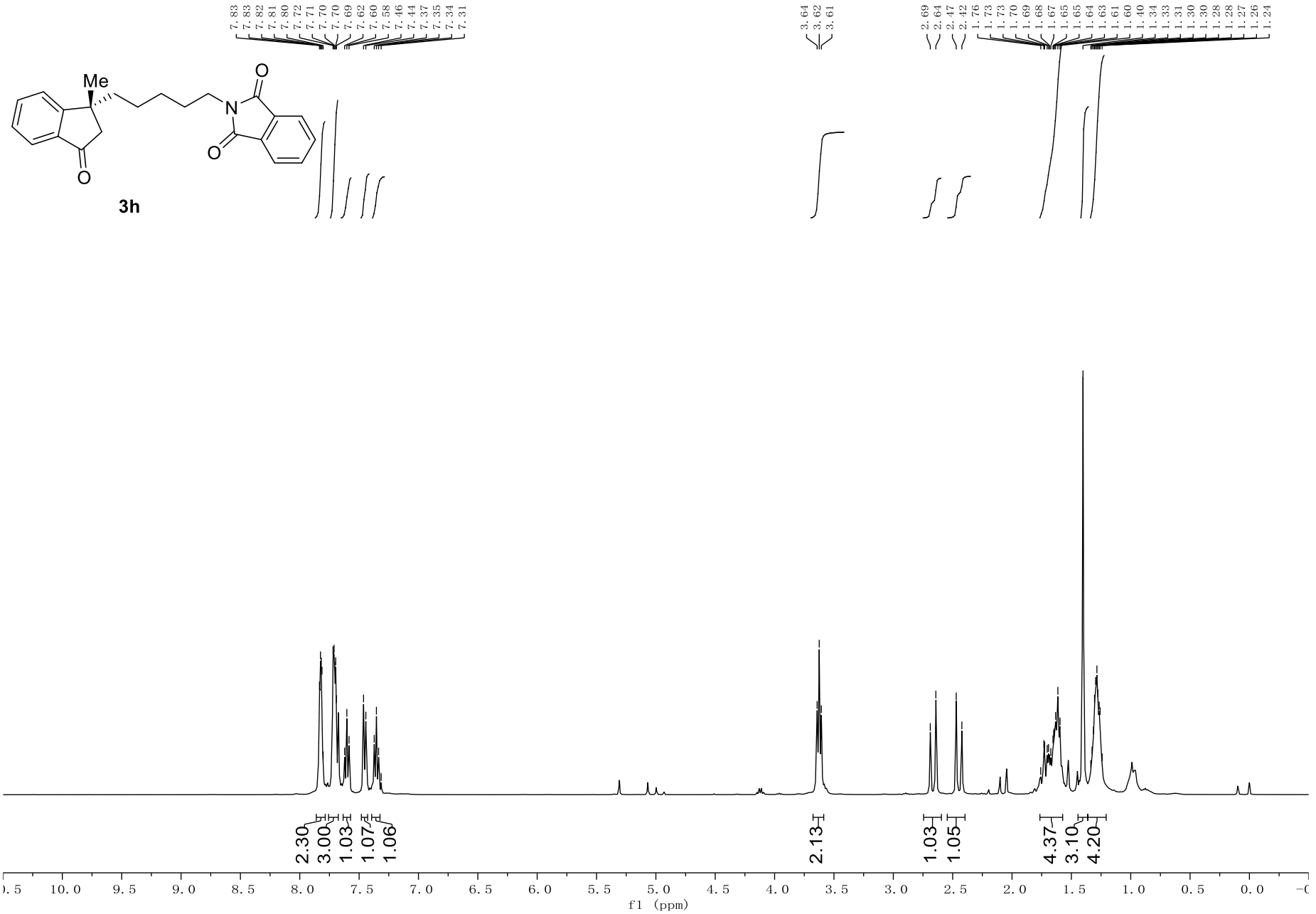

Figure S31 ^{13}C NMR Spectrum of 3h, related to Scheme 2

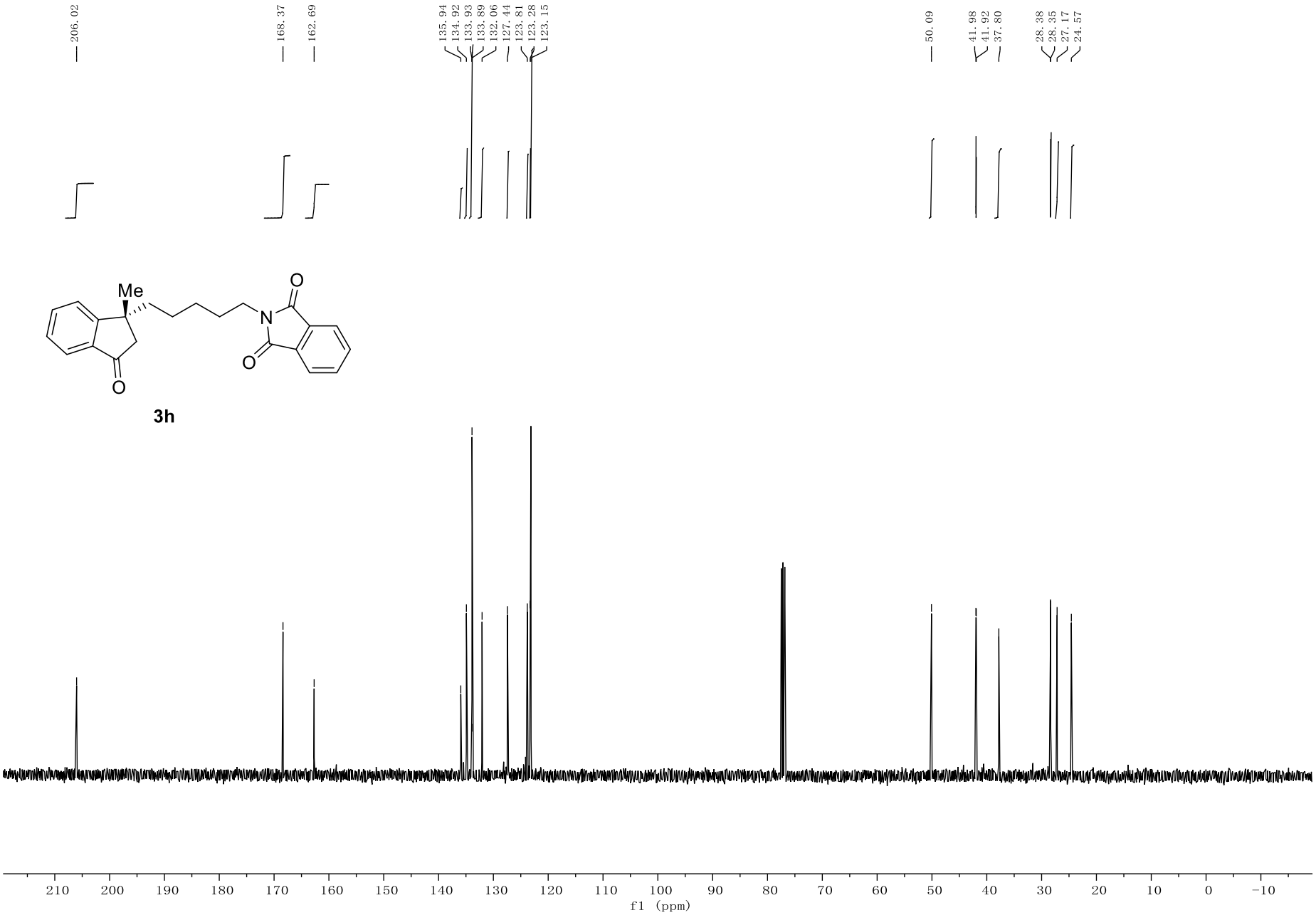

Figure S32 ^{1}H NMR Spectrum of 3i, related to Scheme 2

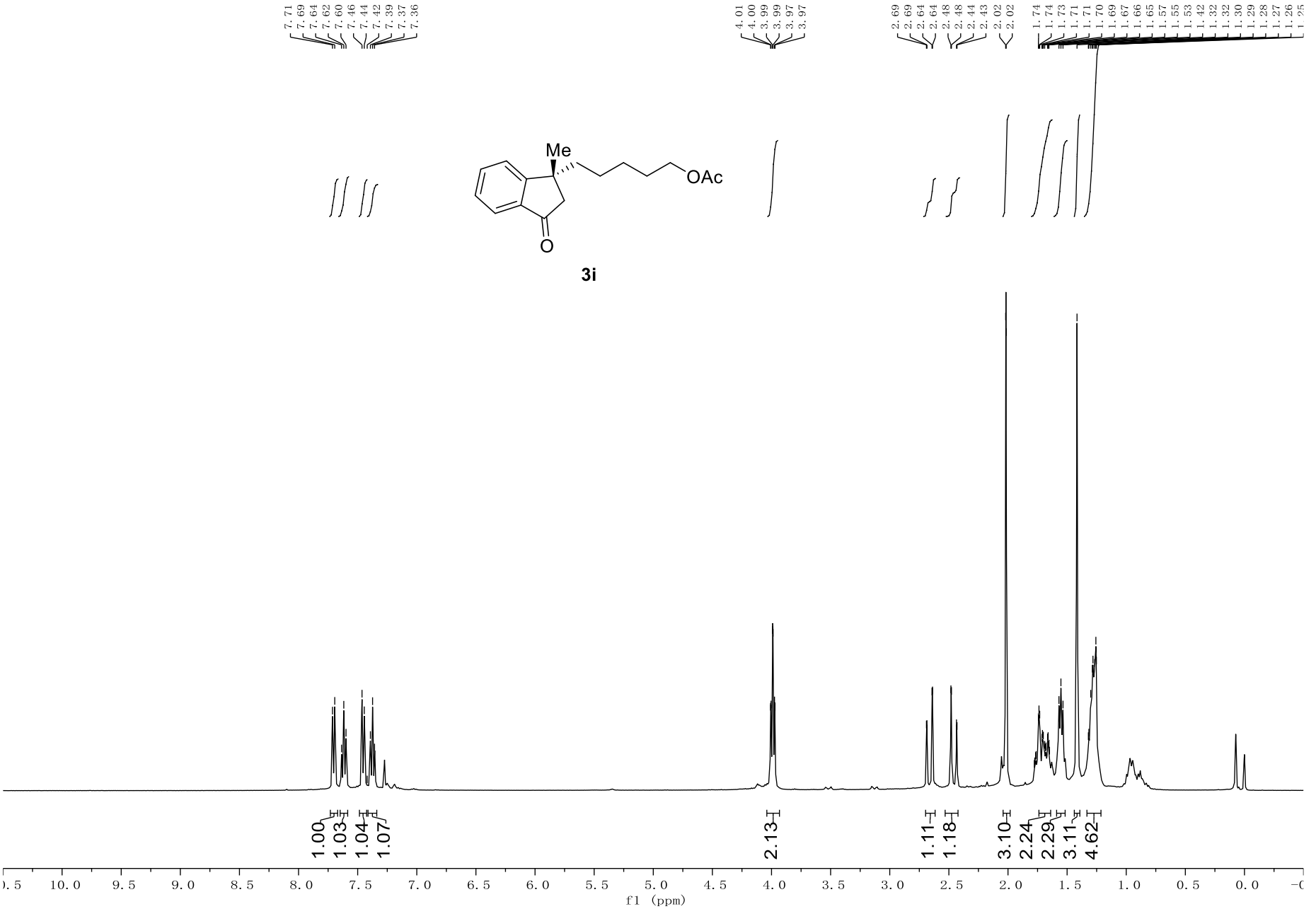

Figure S33 ^{13}C NMR Spectrum of 3i, related to Scheme 2

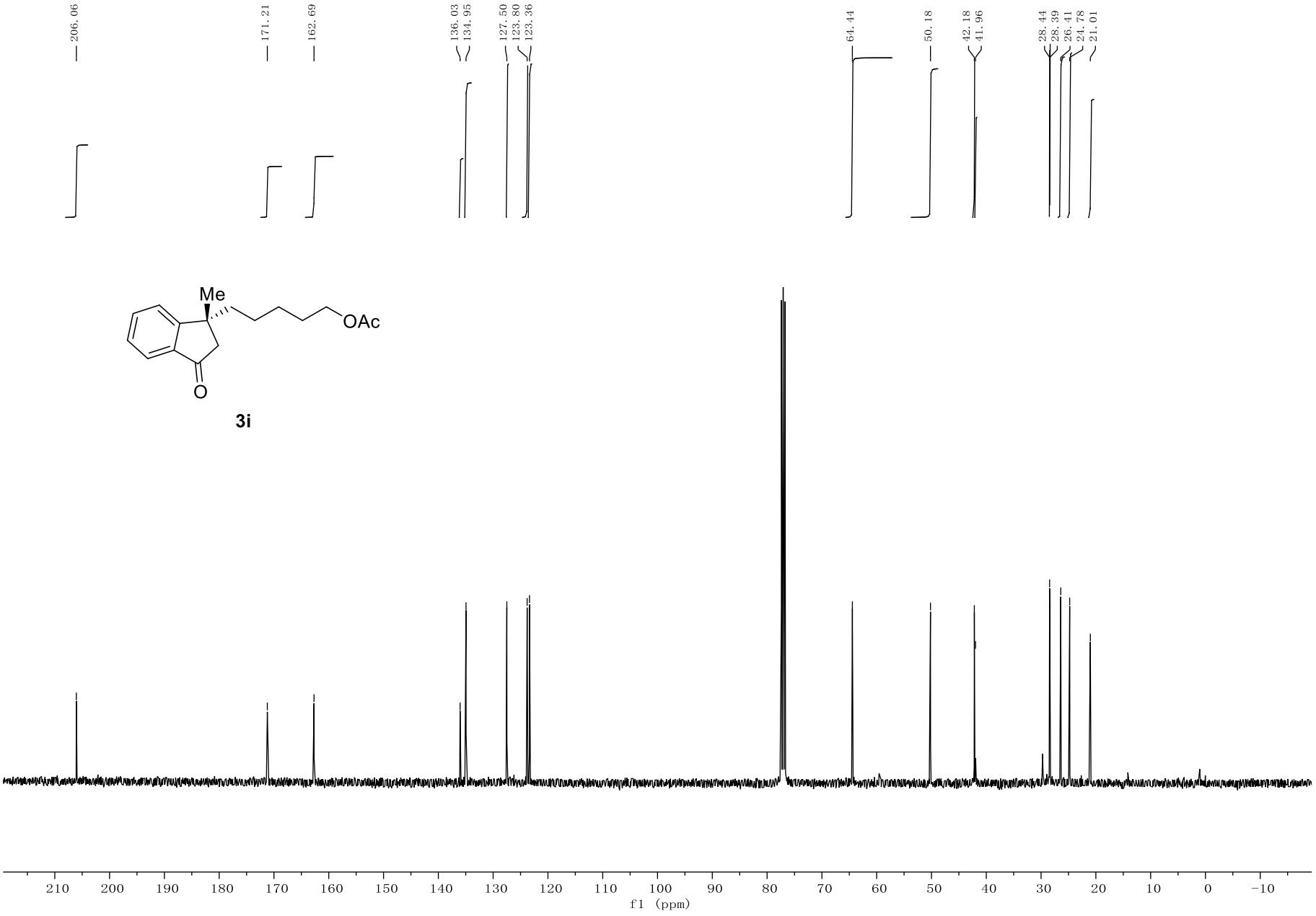

Figure S34 ^{1}H NMR Spectrum of 3j, related to Scheme 2

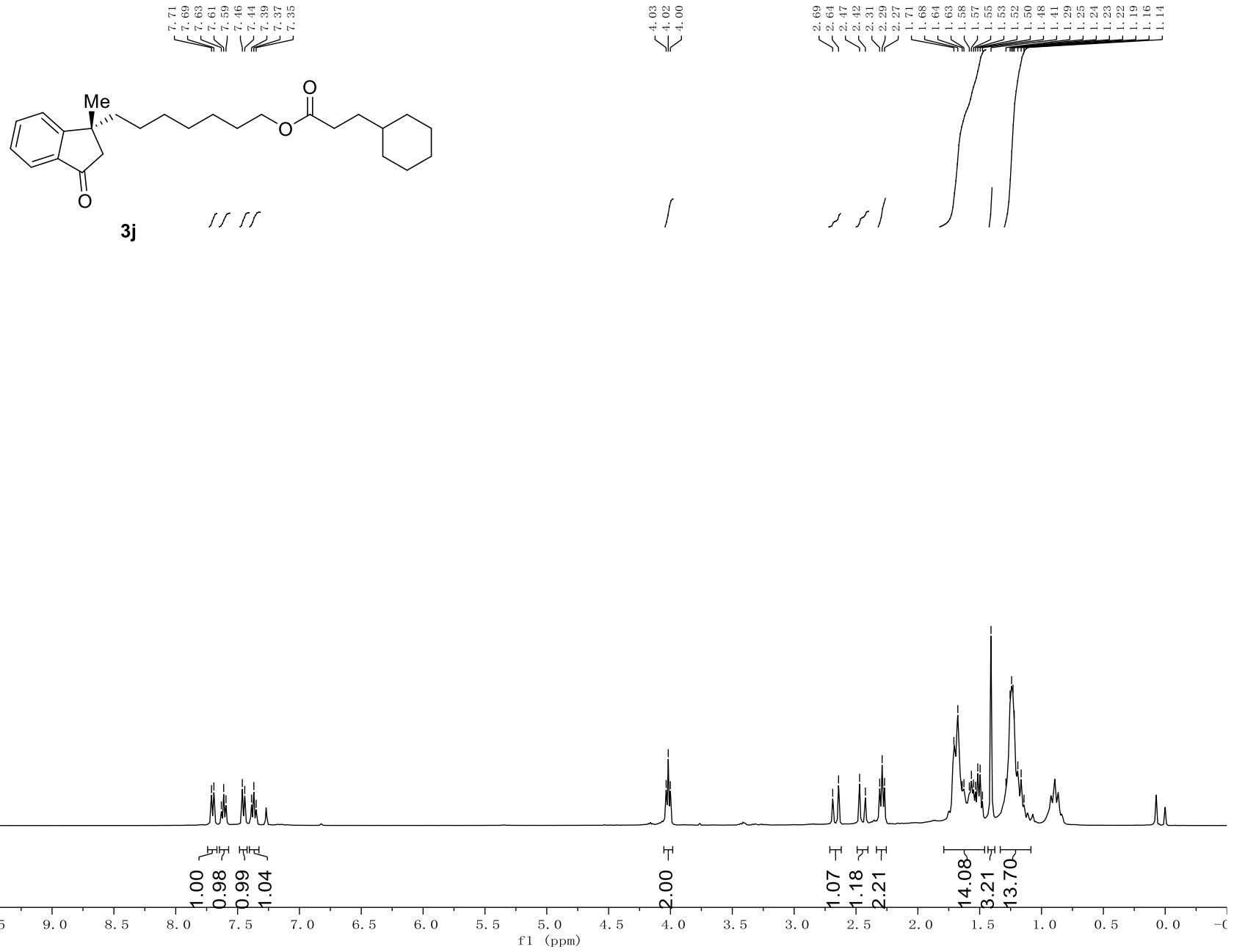

Figure S35 ^{13}C NMR Spectrum of 3j, related to Scheme 2

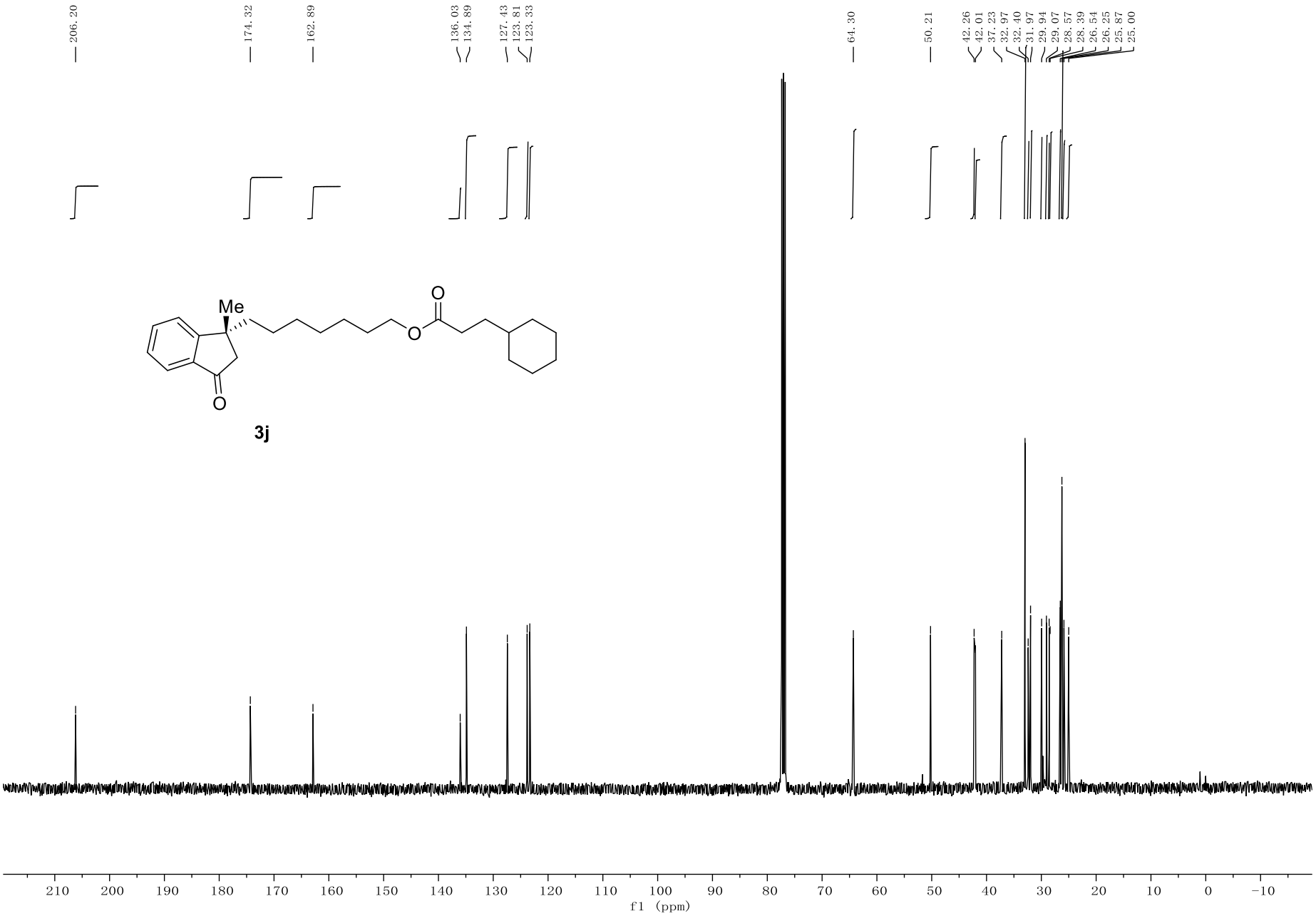

Figure S36 ^{1}H NMR Spectrum of 3k, related to Scheme 2

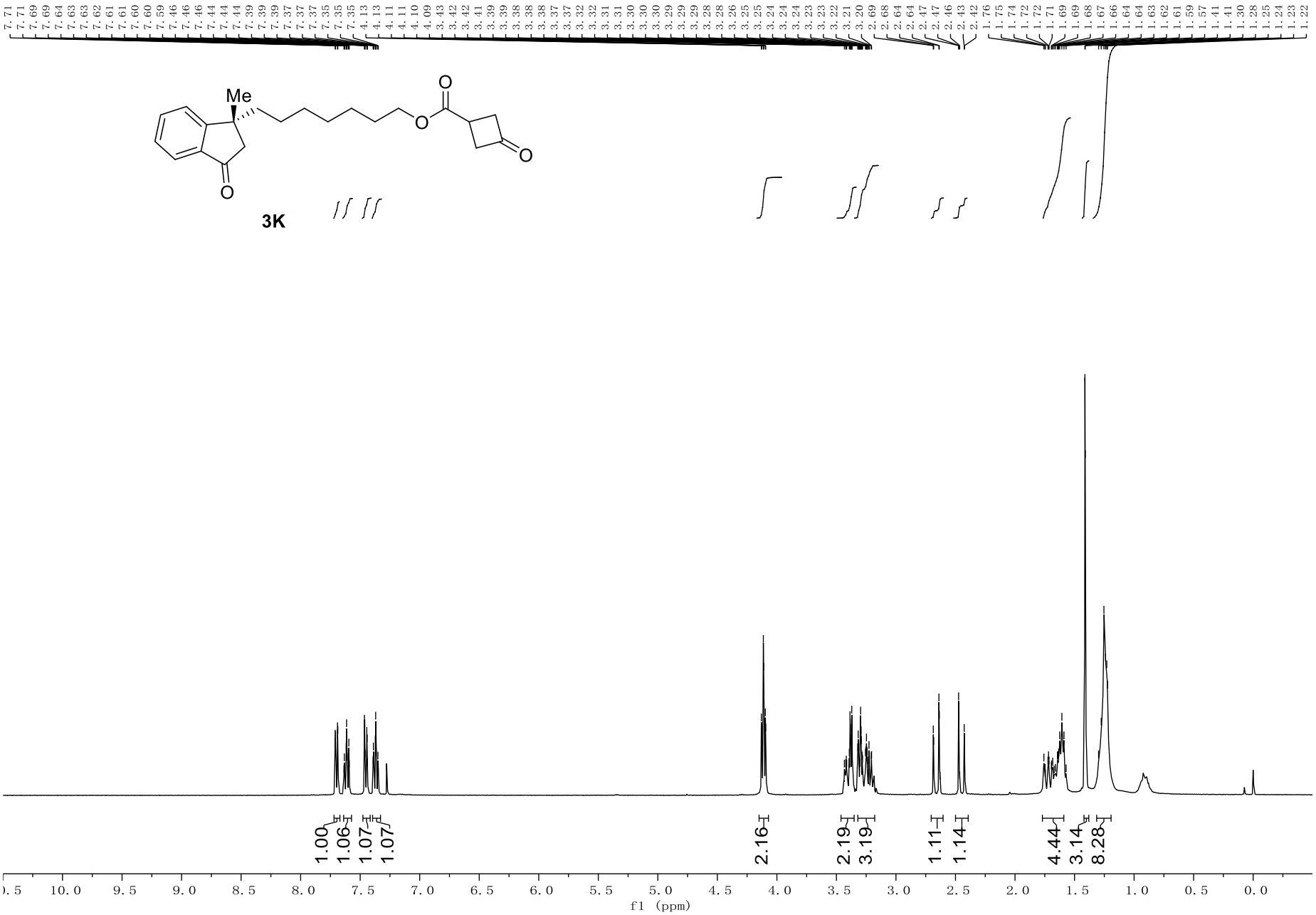

Figure S37 ^{13}C NMR Spectrum of 3k, related to Scheme 2

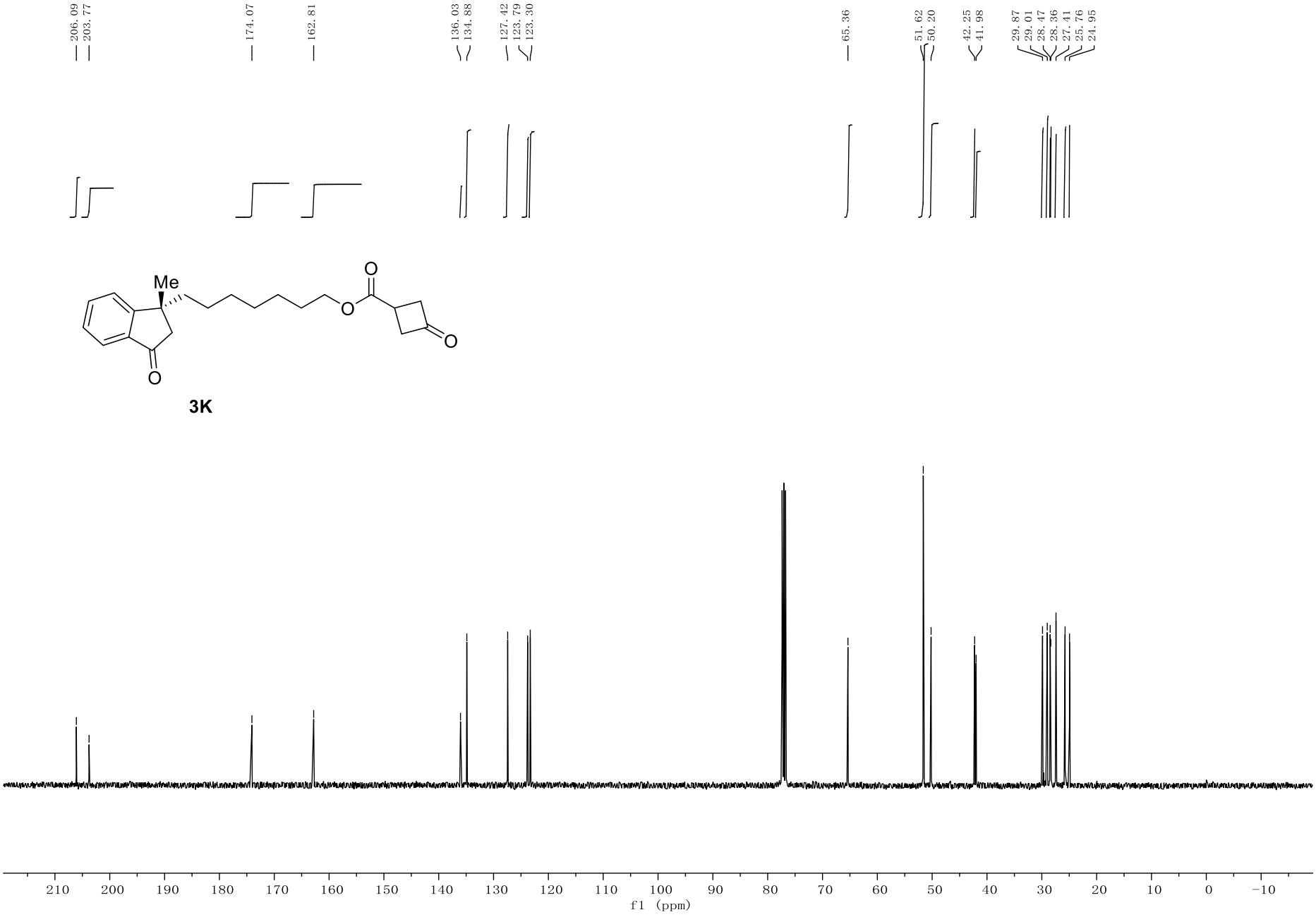

Figure S38 ^{1}H NMR Spectrum of 3l, related to Scheme 2

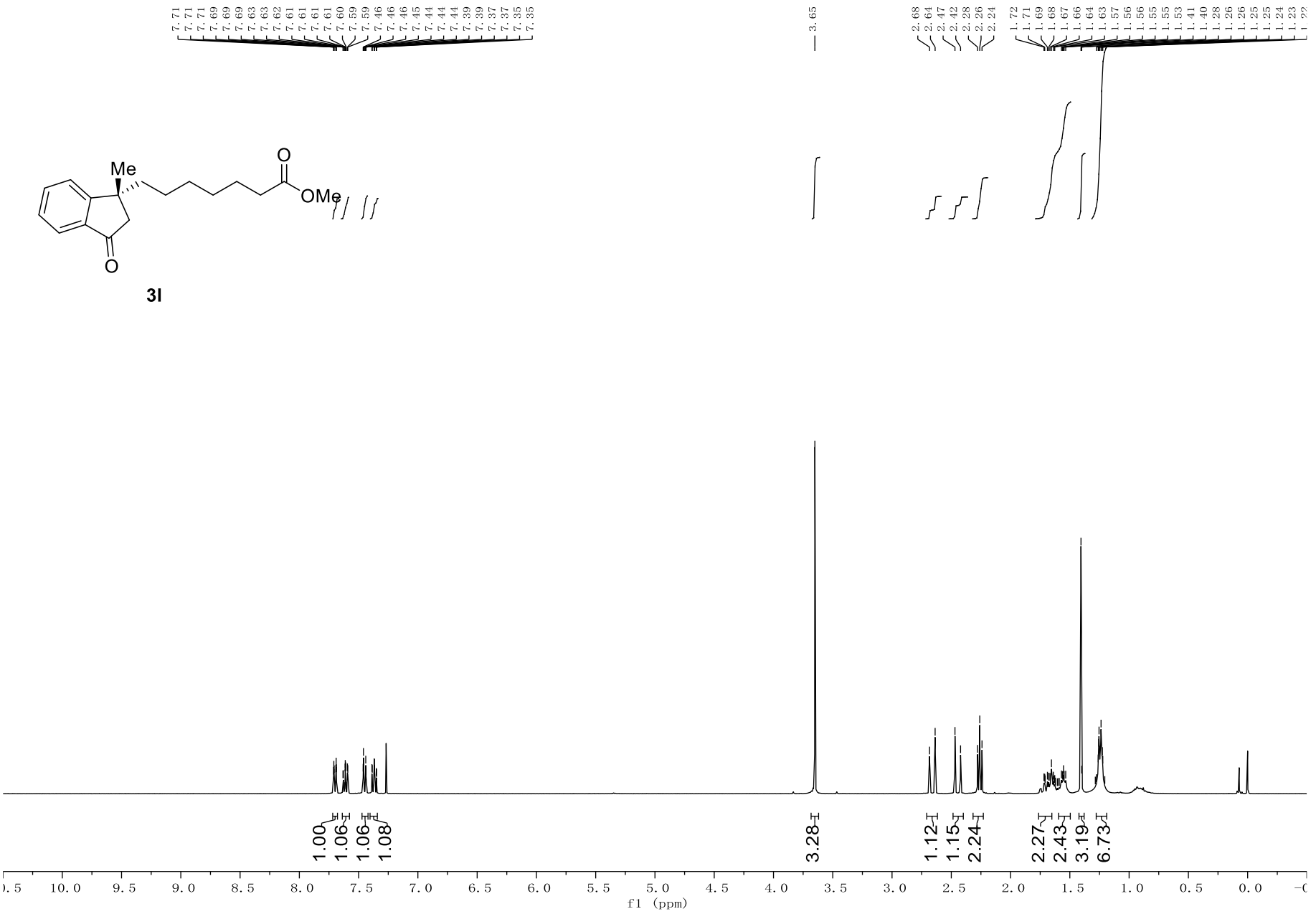

Figure S39 ^{13}C NMR Spectrum of 3l, related to Scheme 2

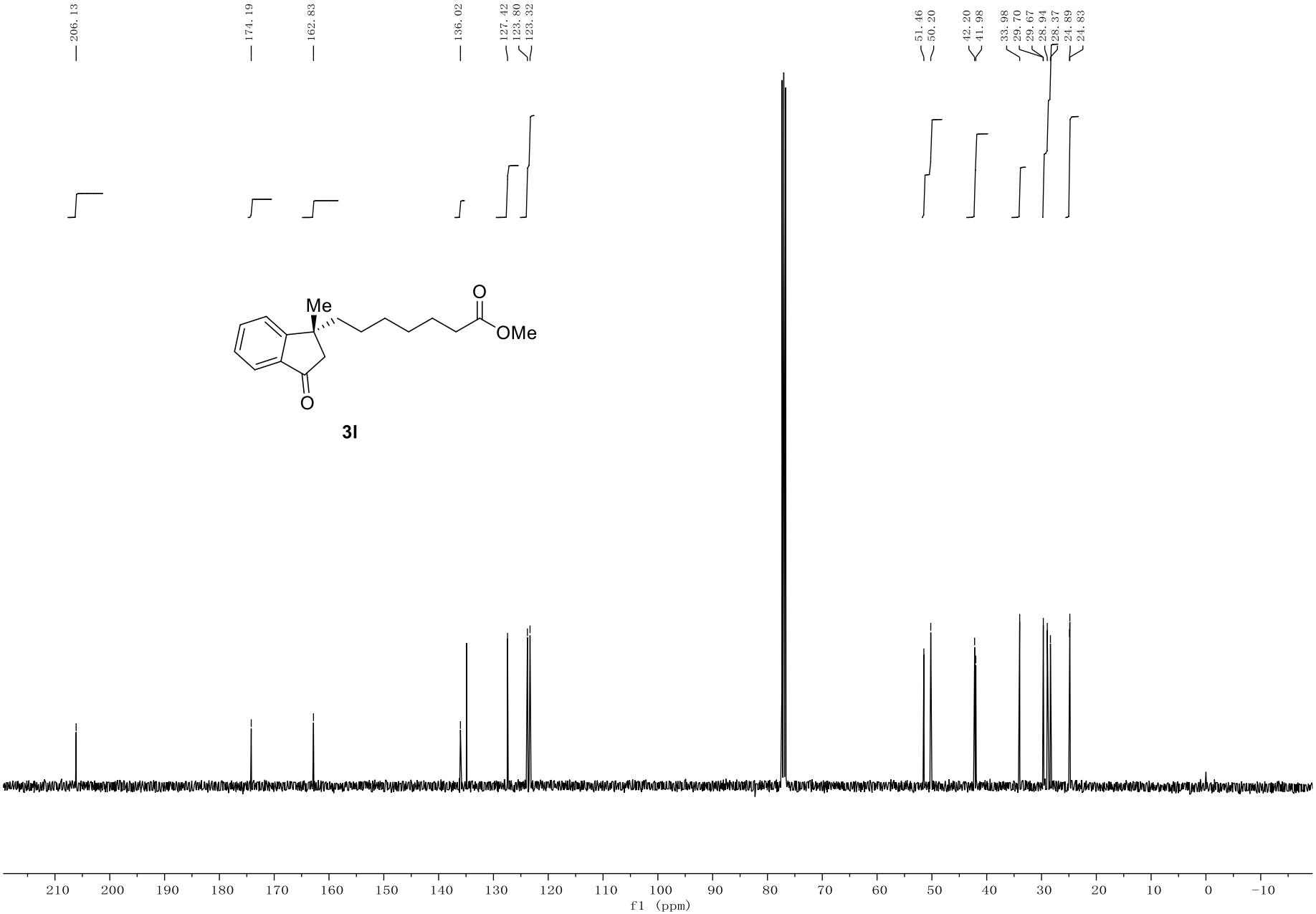

Figure S40 ^{1}H NMR Spectrum of 3m, related to Scheme 2

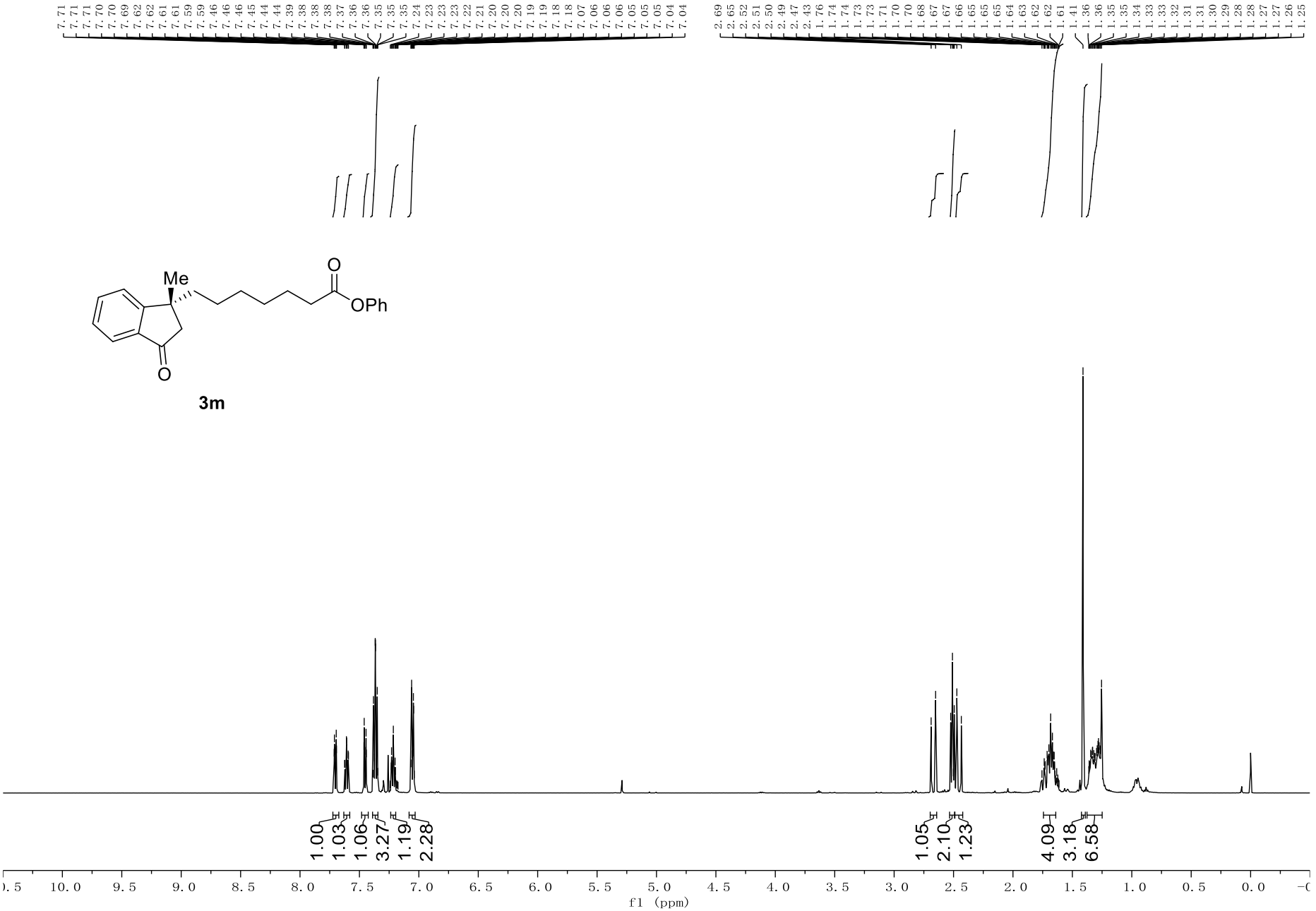

Figure S41 ^{13}C NMR Spectrum of 3m, related to Scheme 2

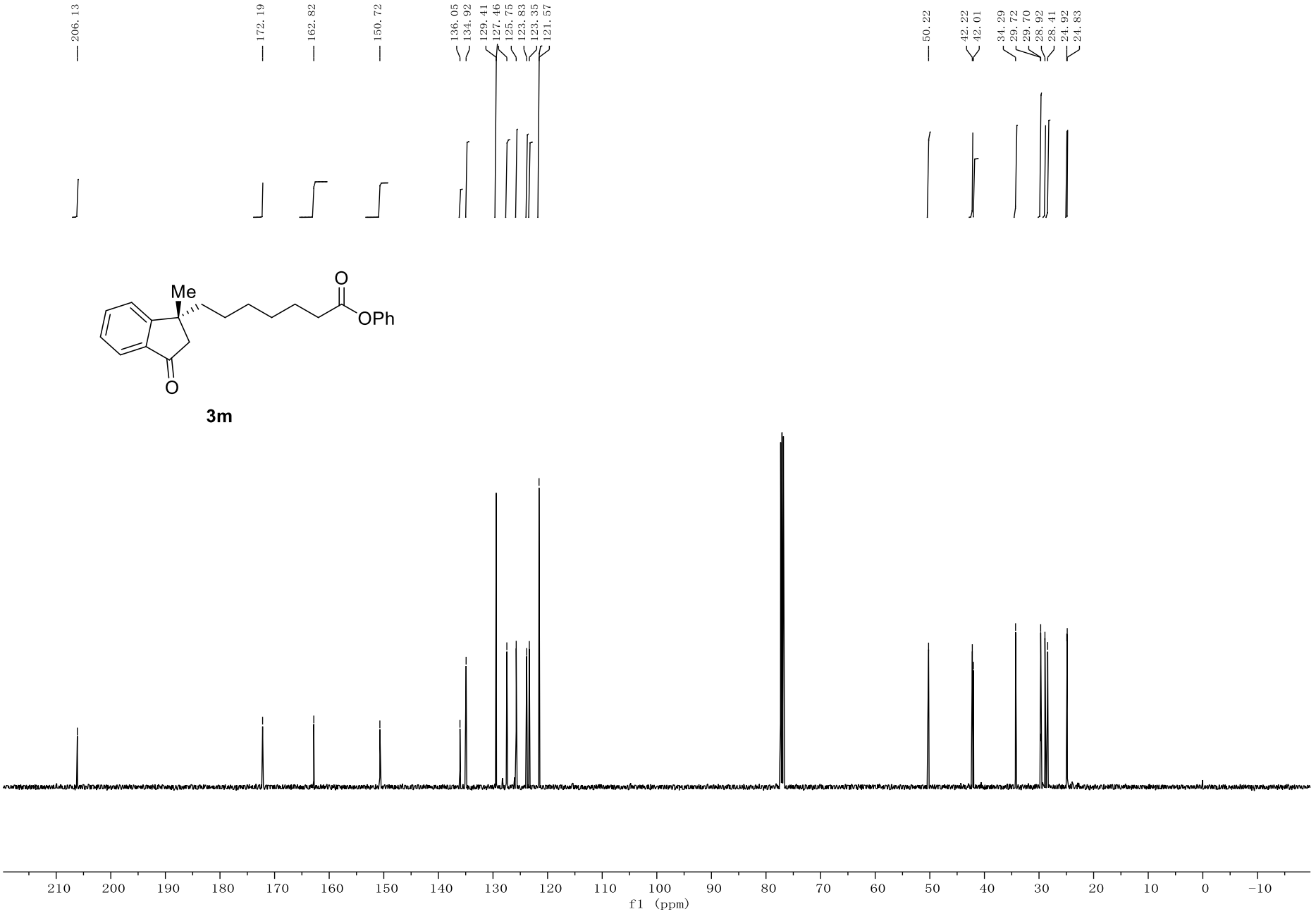

Figure S42 ^{1}H NMR Spectrum of 3n, related to Scheme 2

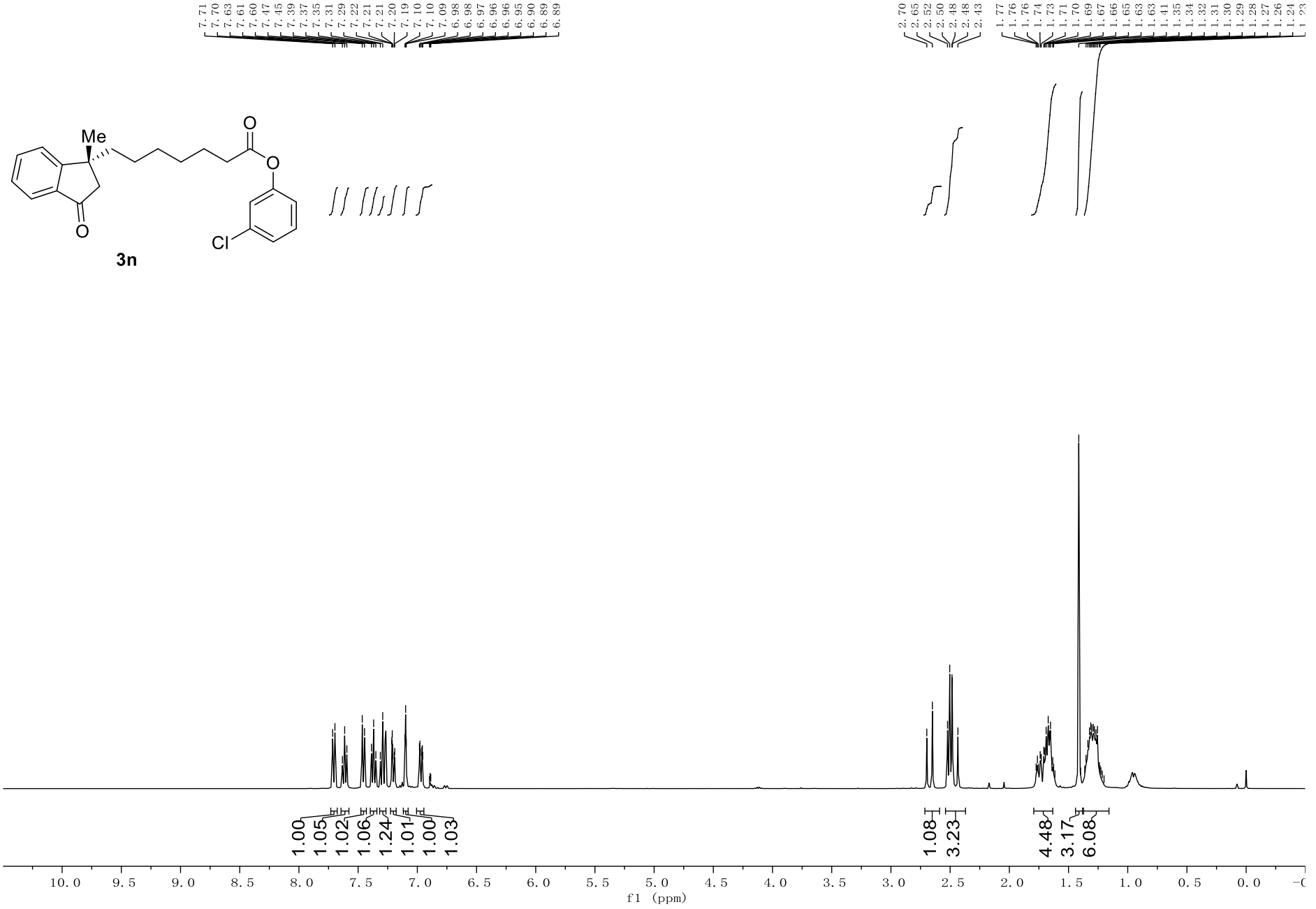

Figure S43 ^{13}C NMR Spectrum of 3n, related to Scheme 2

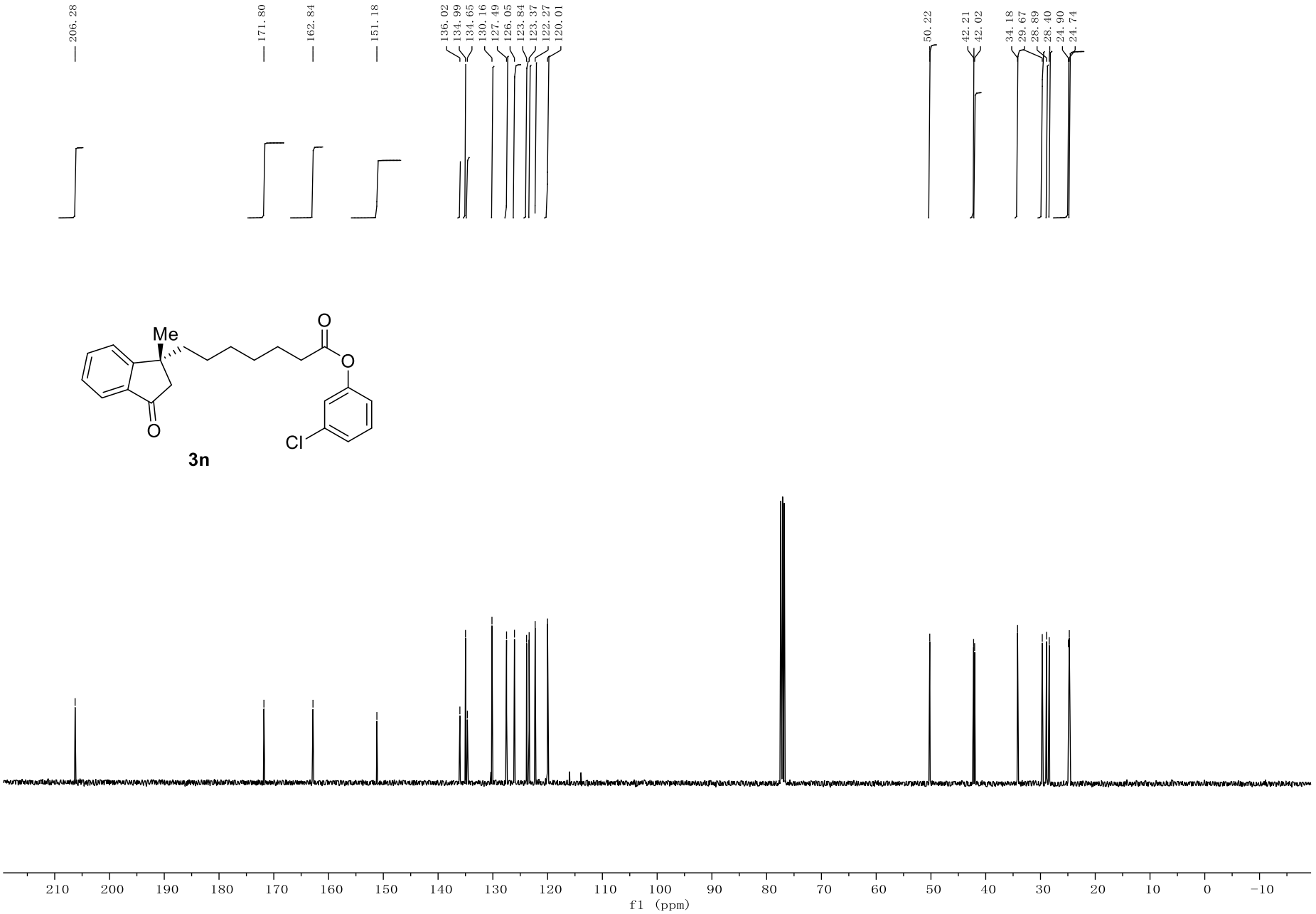

Figure S44 ^{1}H NMR Spectrum of 3o, related to Scheme 2

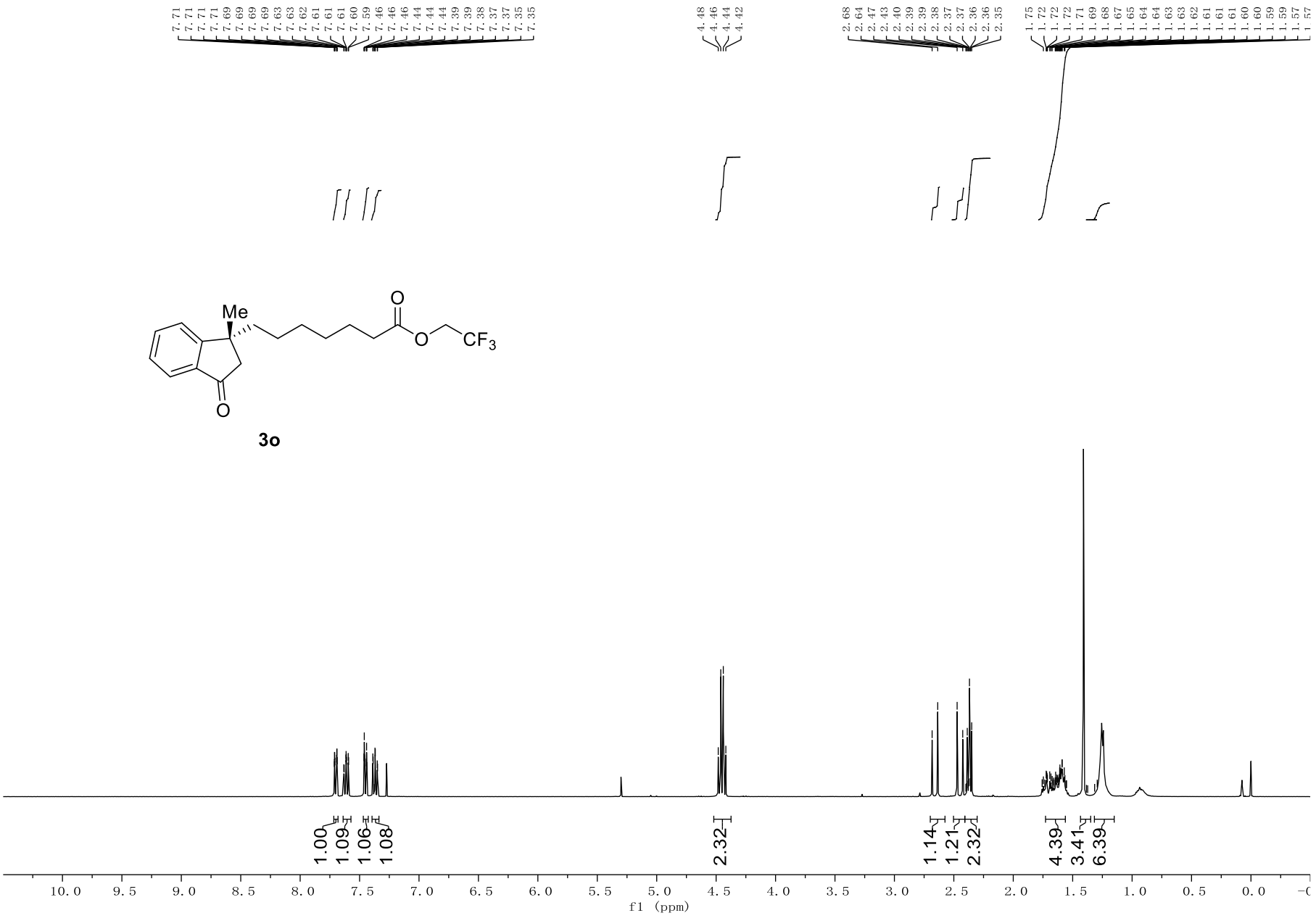

Figure S45 ^{13}C NMR Spectrum of 3o, related to Scheme 2

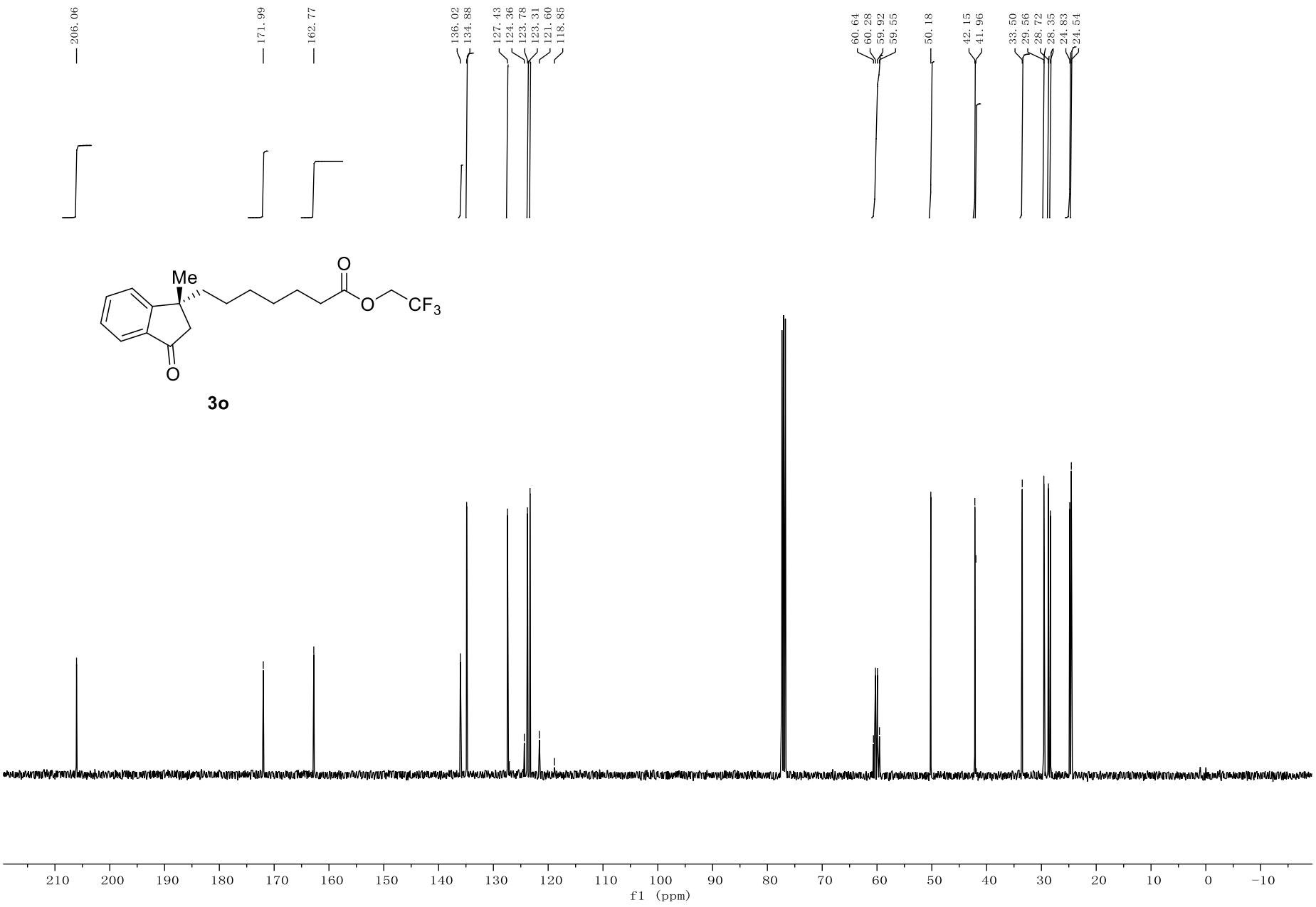

Figure S46 ^{19}F NMR Spectrum of 3o, related to Scheme 2

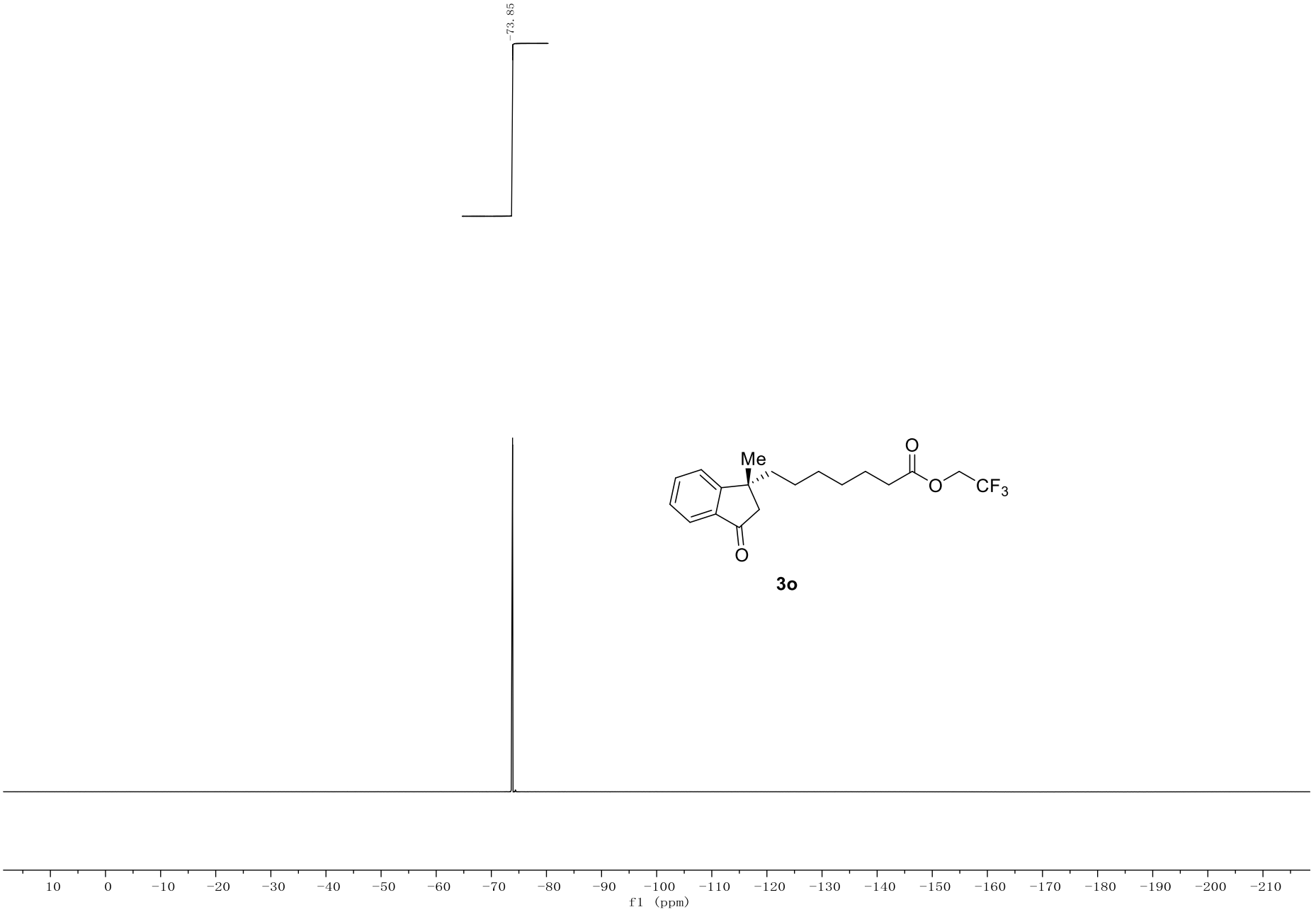

Figure S47 ^{1}H NMR Spectrum of 3p, related to Scheme 2

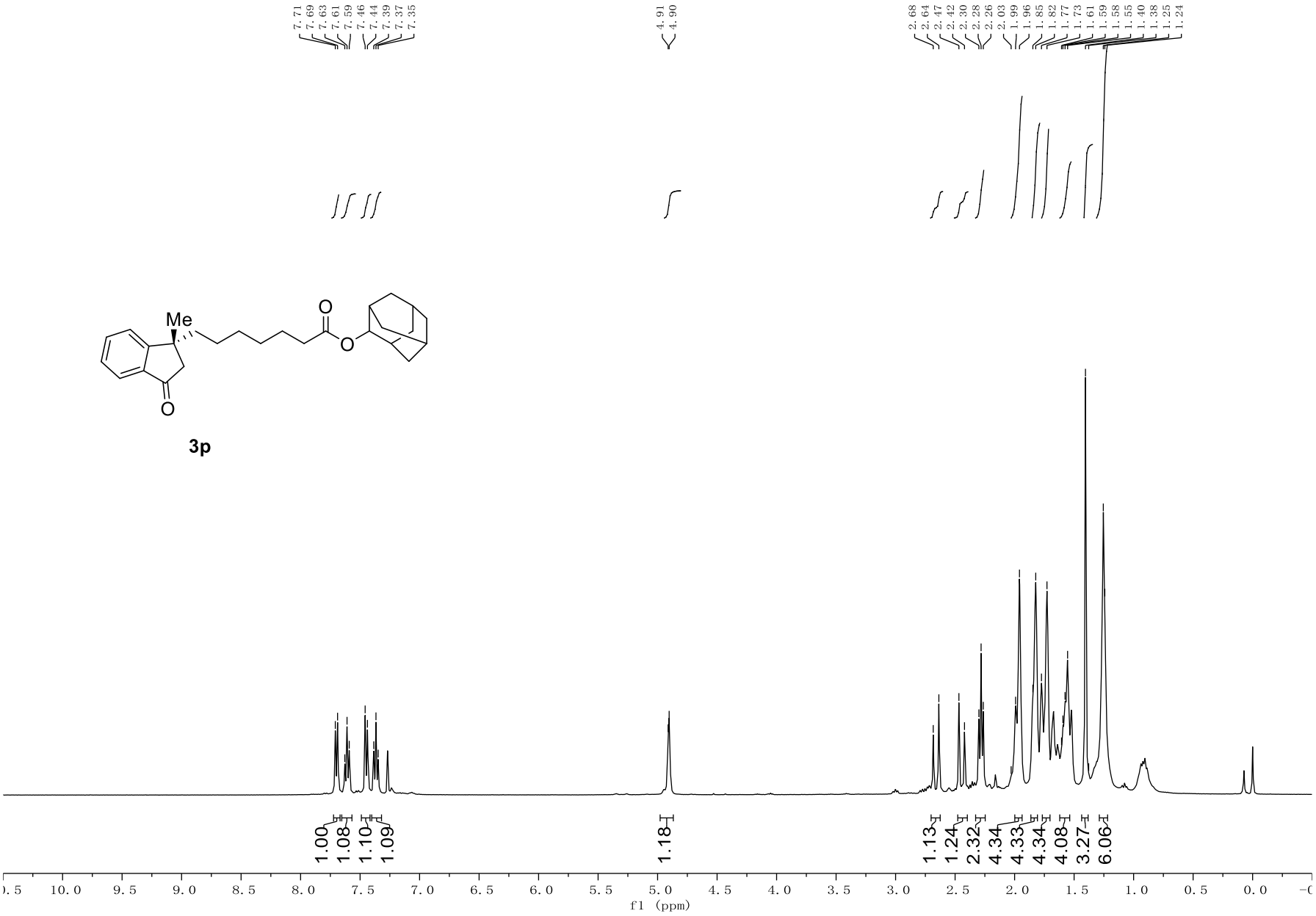

Figure S48 ^{13}C NMR Spectrum of 3p, related to Scheme 2

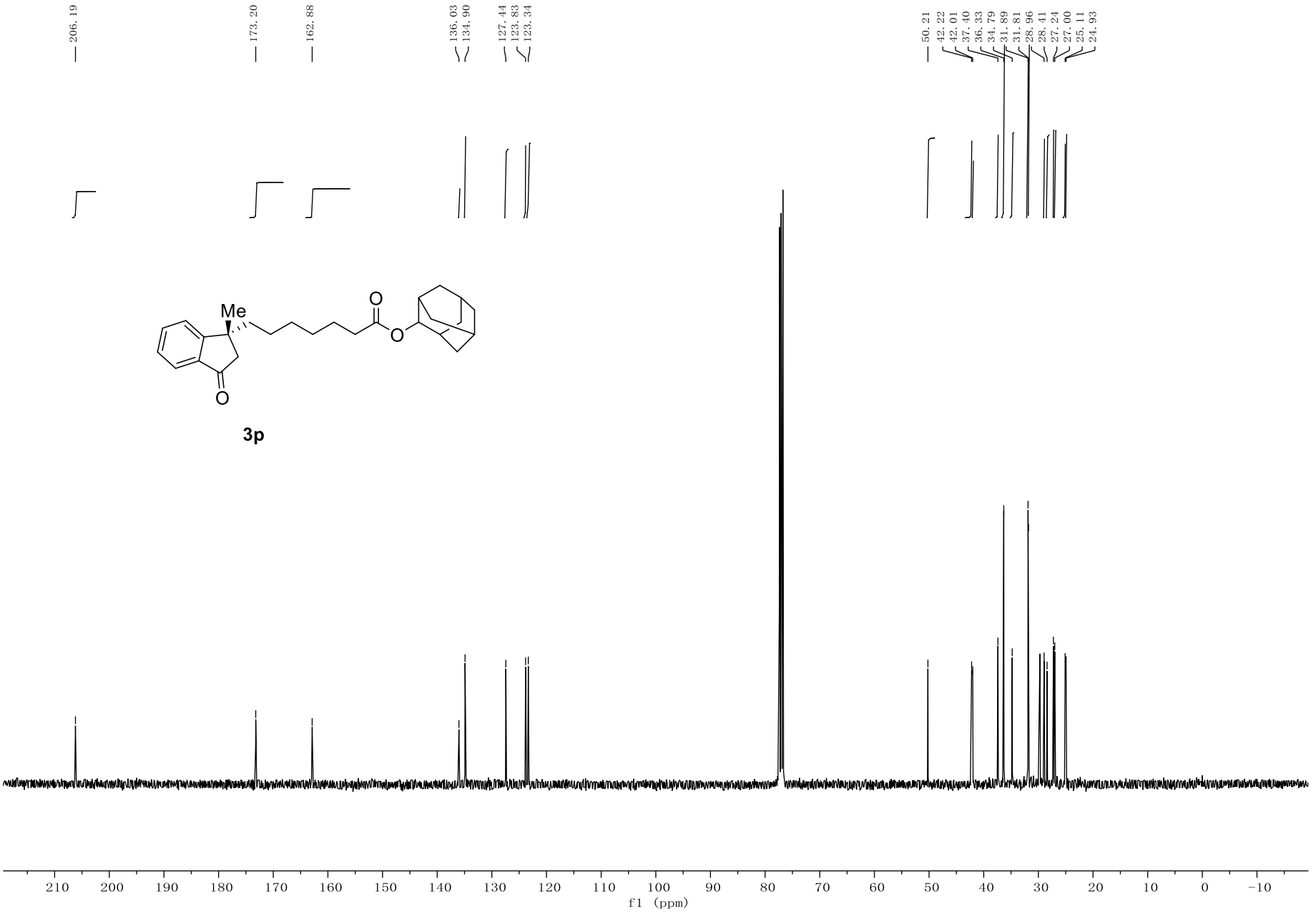

Figure S49 ^{1}H NMR Spectrum of 3q, related to Scheme 2

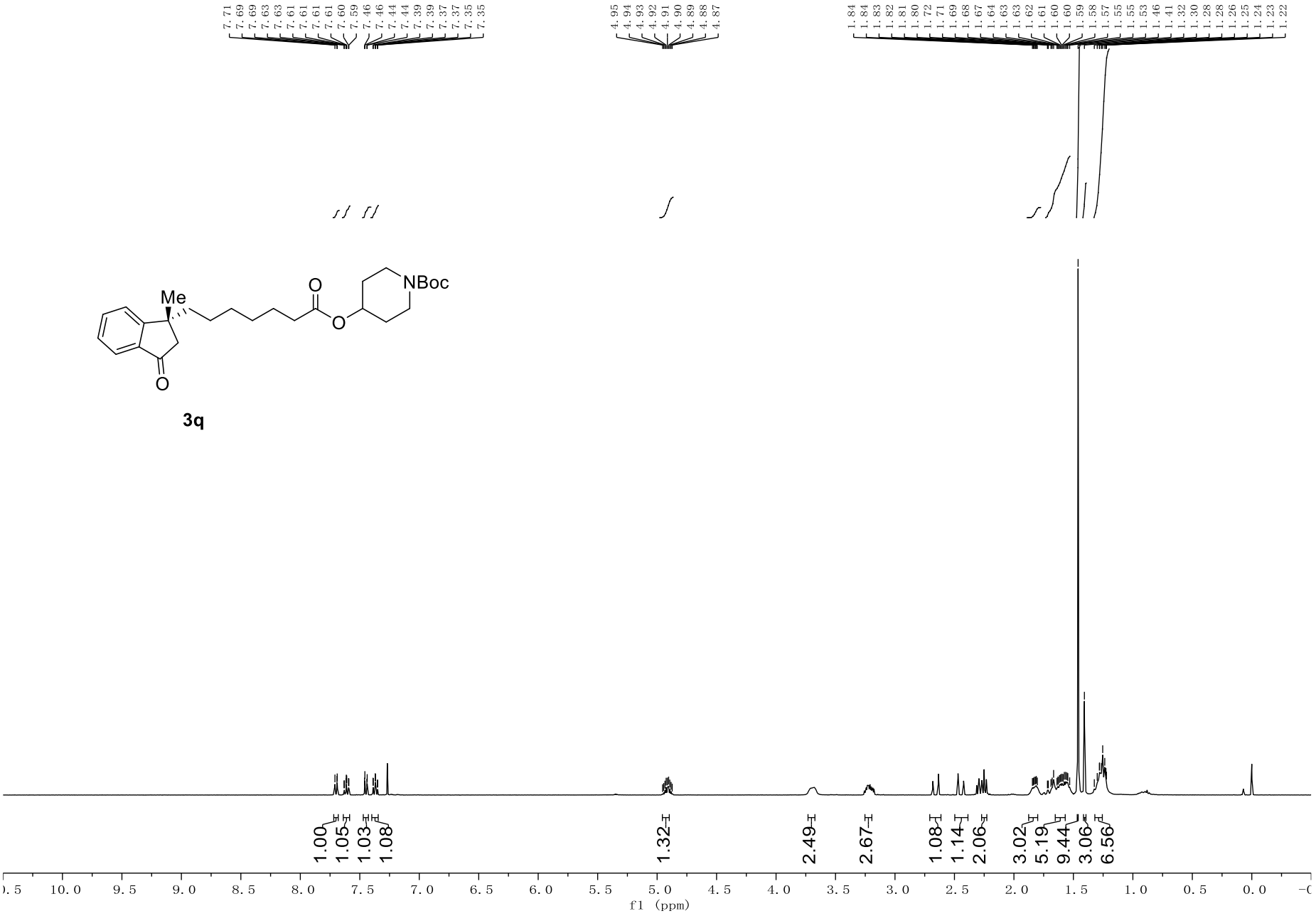

3q

Figure S50 ^{13}C NMR Spectrum of 3q, related to Scheme 2

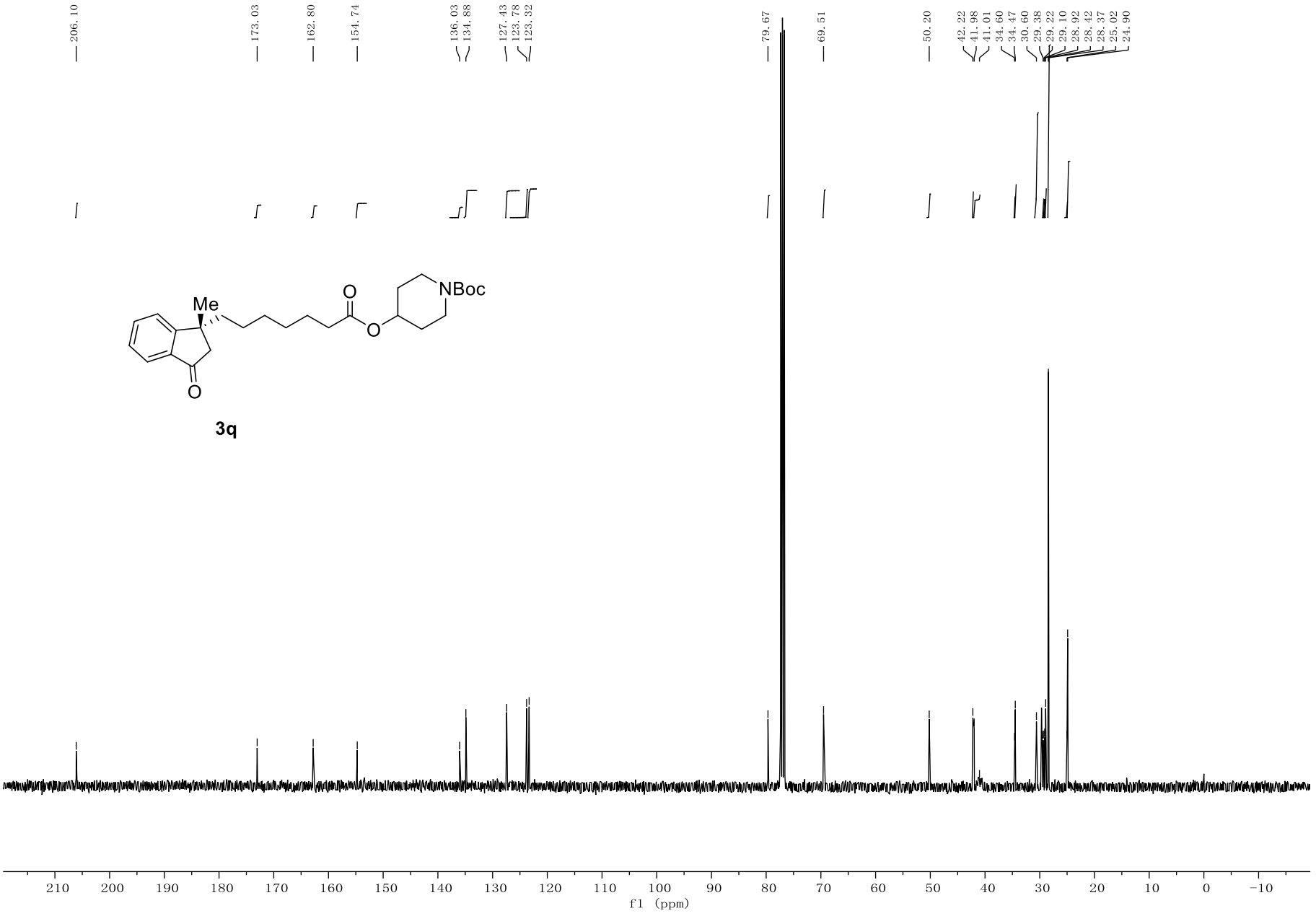

Figure S51 ^{1}H NMR Spectrum of 3r, related to Scheme 2

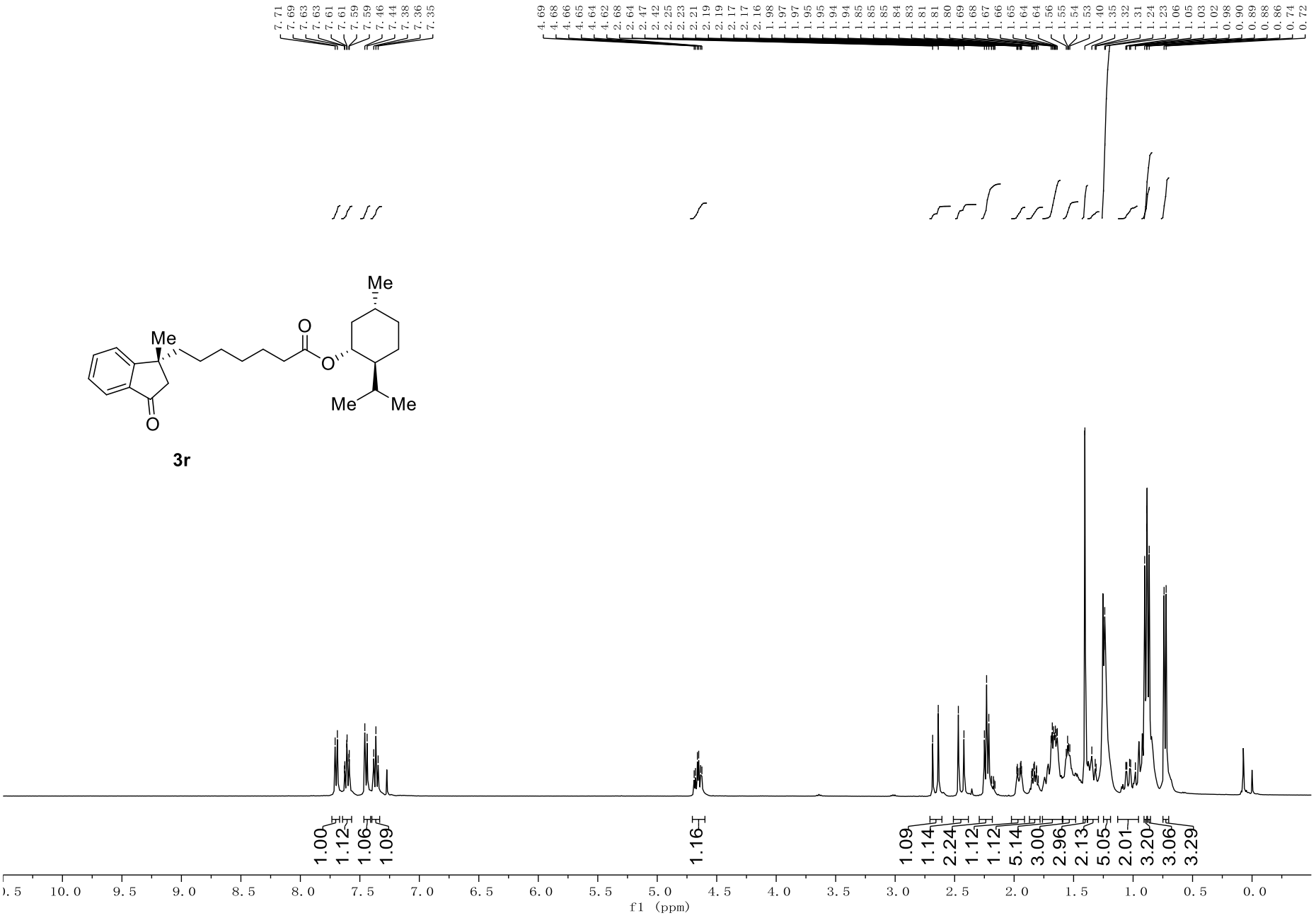

Figure S52 ^{13}C NMR Spectrum of 3r, related to Scheme 2

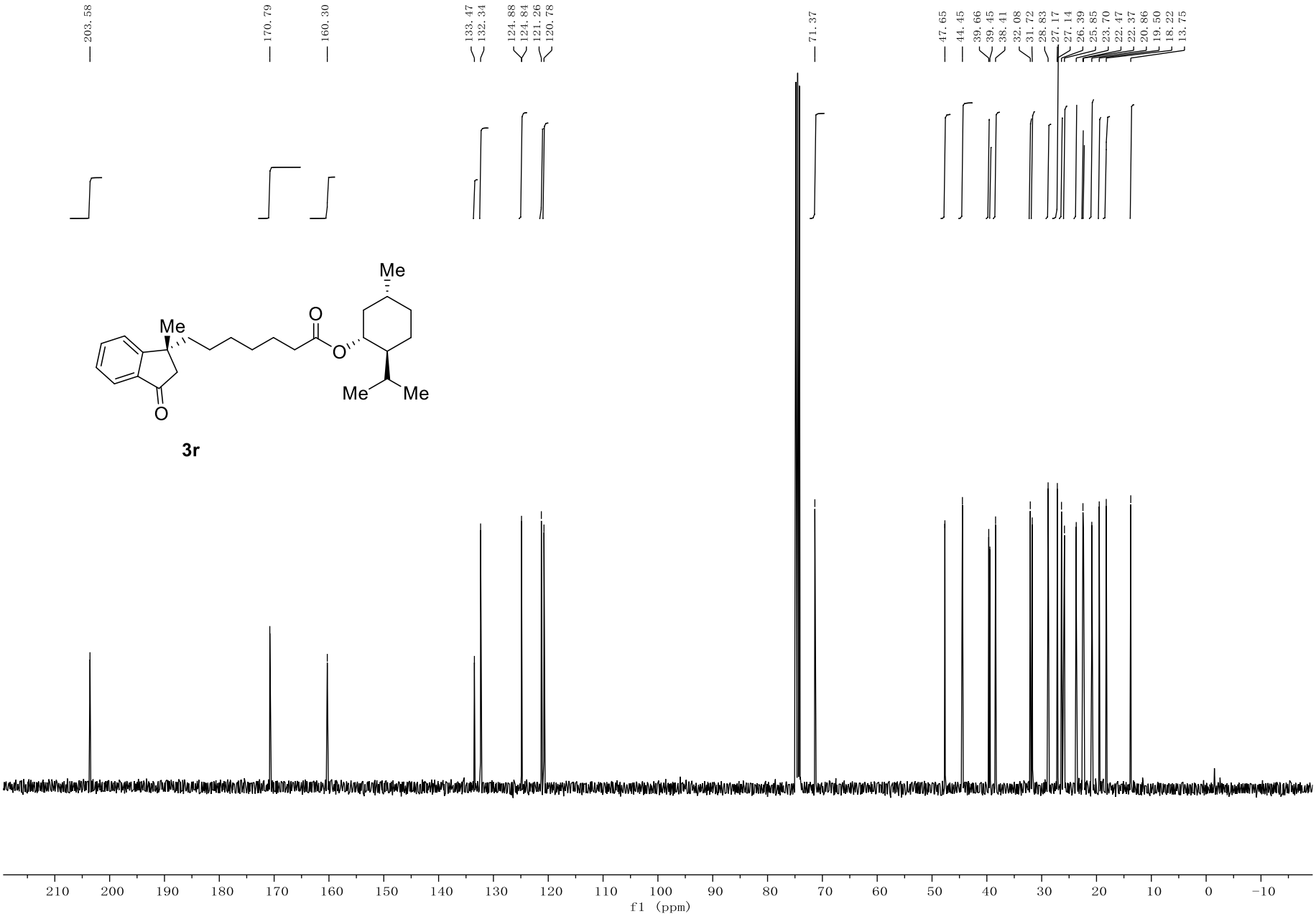

Figure S53 ^{1}H NMR Spectrum of 3s, related to Scheme 2

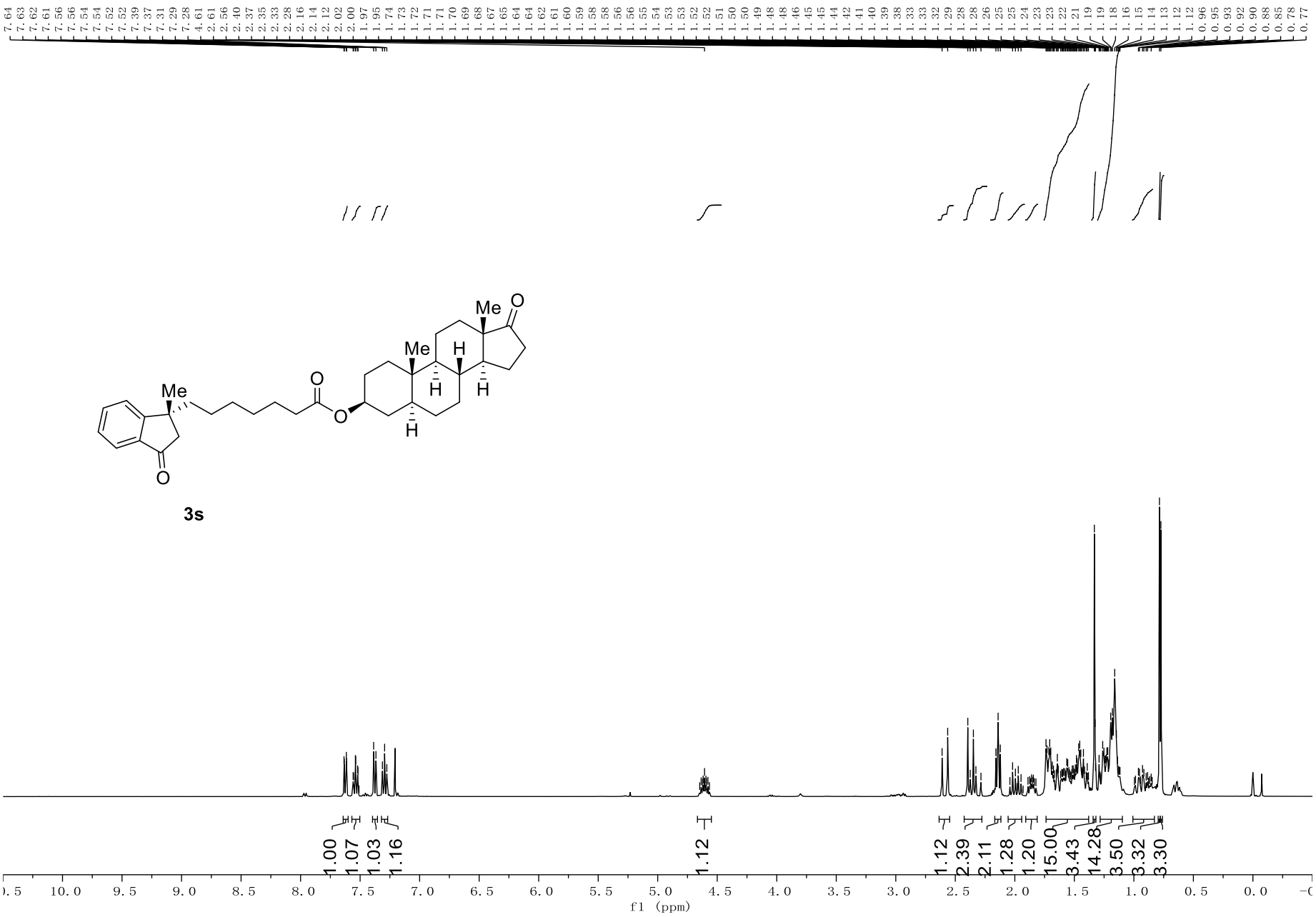

Figure S54 ^{13}C NMR Spectrum of 3a, related to Scheme 2

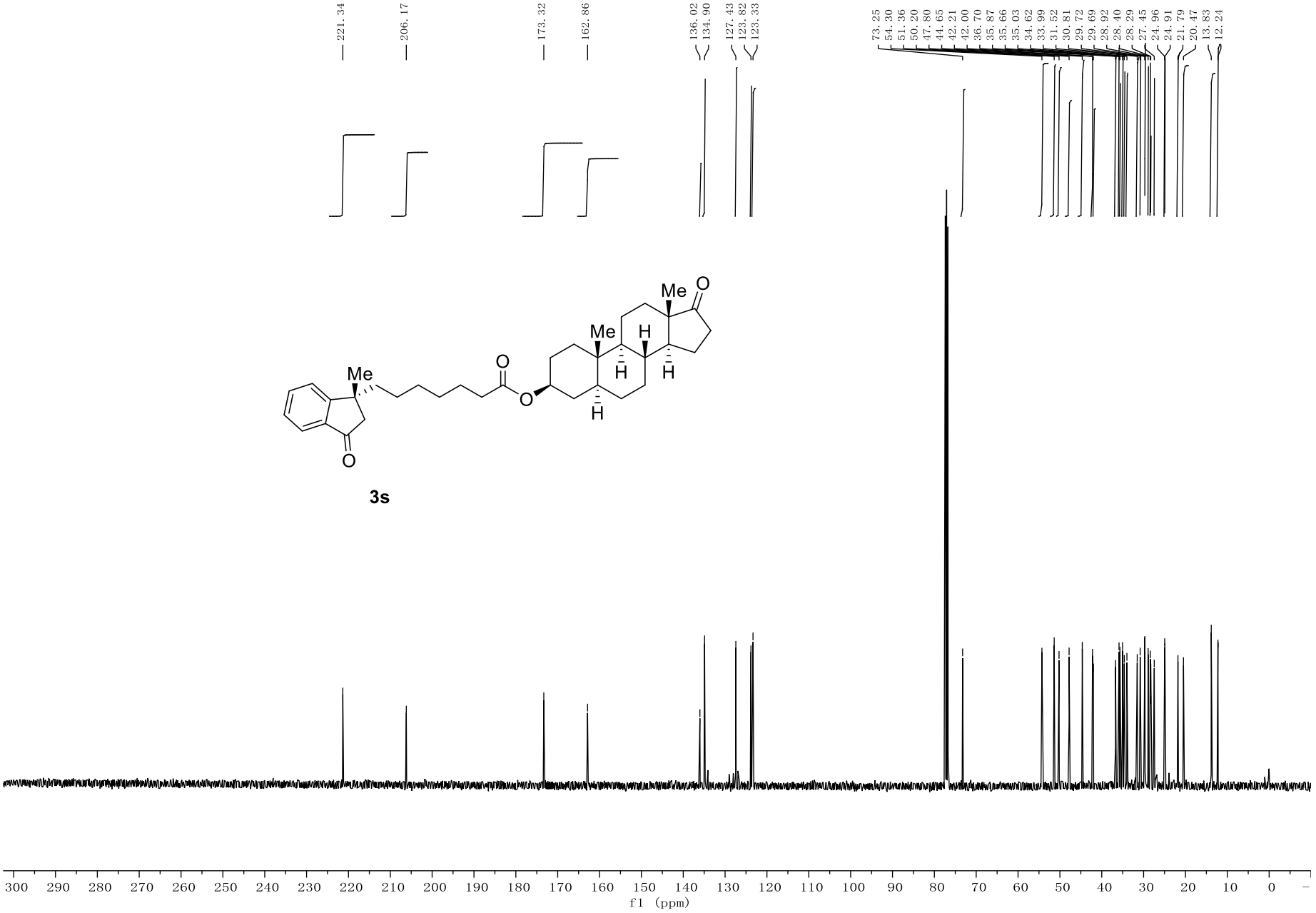

Figure S55 ^{1}H NMR Spectrum of 3t, related to Scheme 2

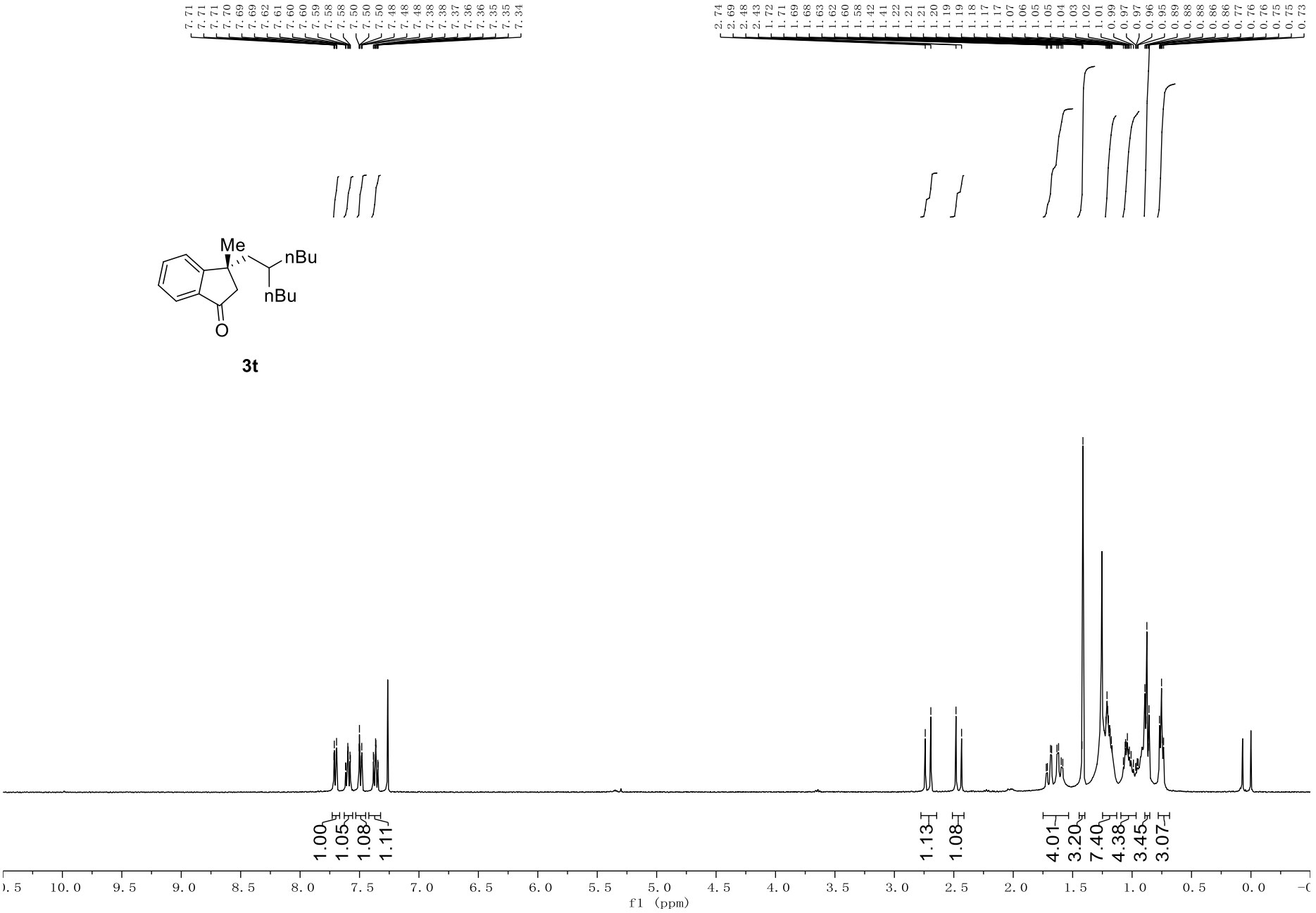

Figure S56 ^{13}C NMR Spectrum of 3t, related to Scheme 2

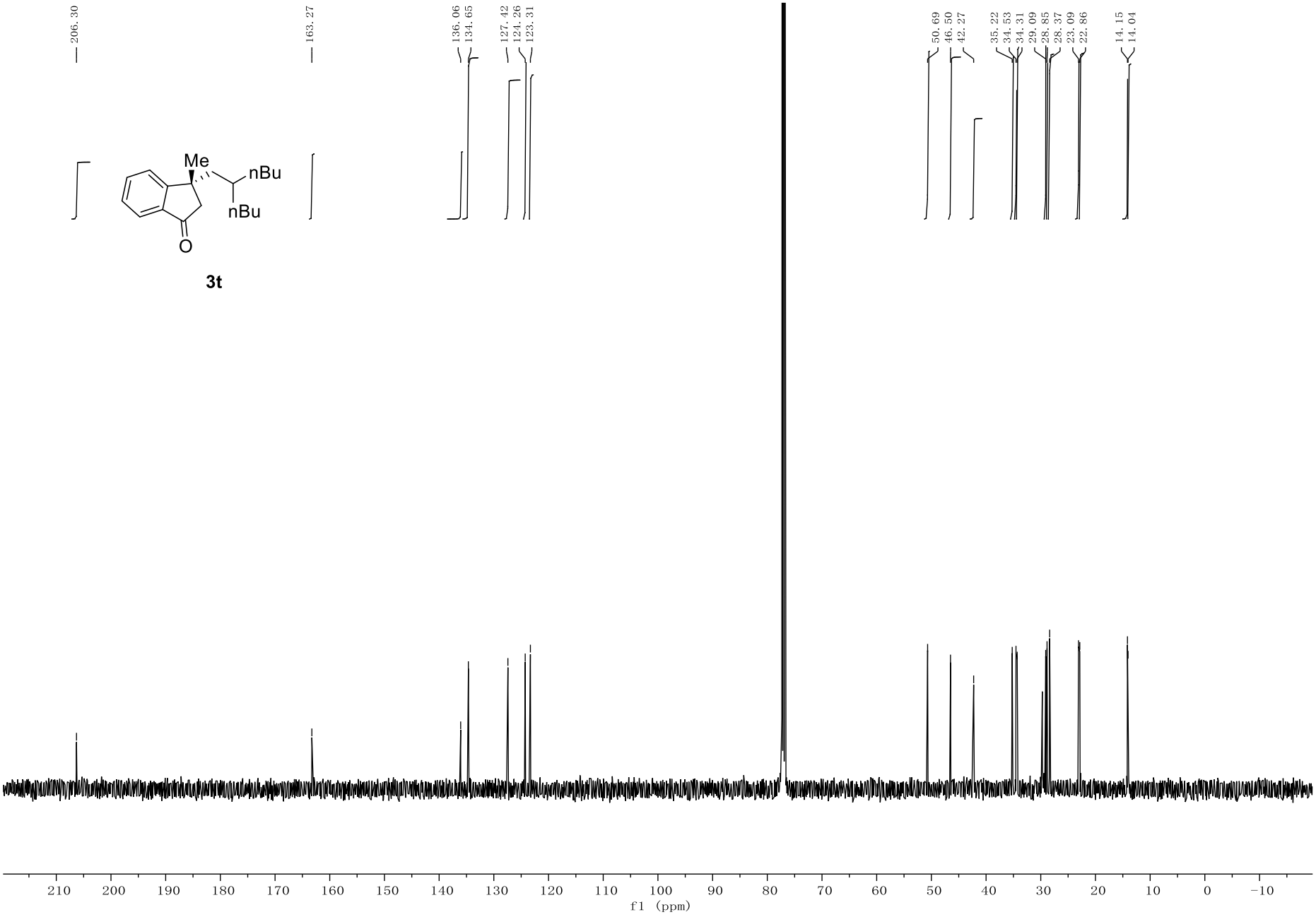

Figure S57 ^{1}H NMR Spectrum of 3u, related to Scheme 2

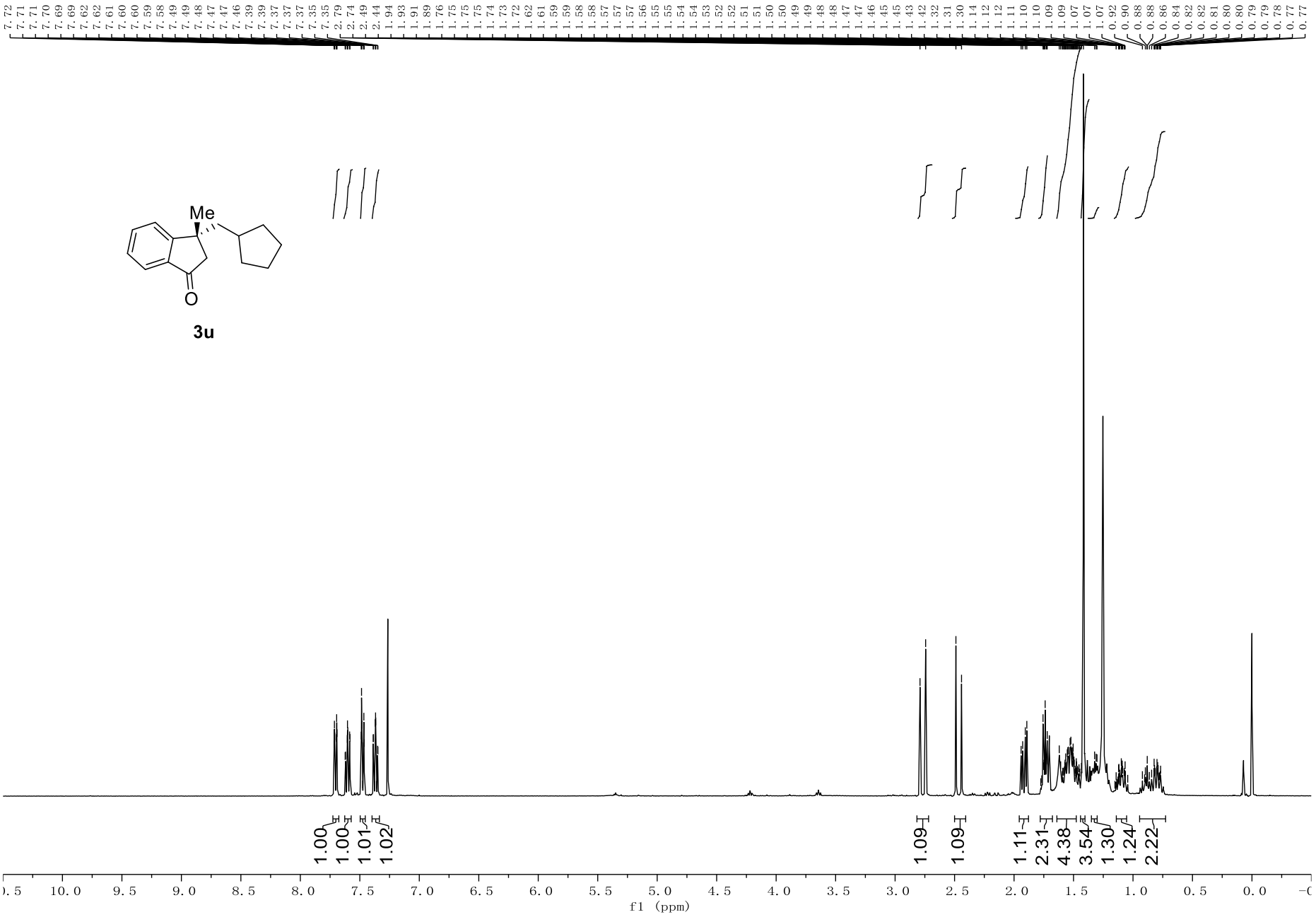

Figure S58 ^{13}C NMR Spectrum of 3u, related to Scheme 2

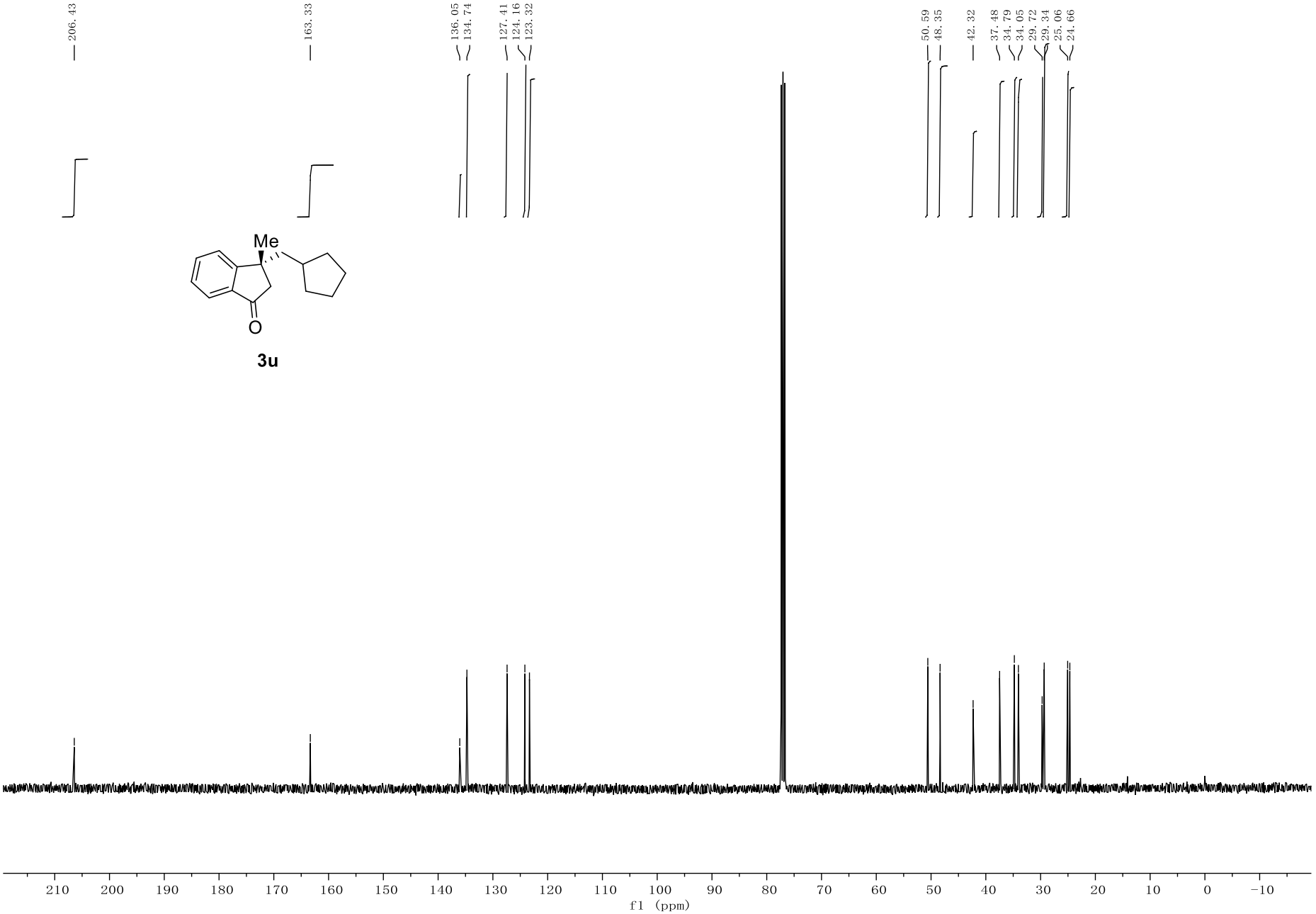

Figure S59 ^{1}H NMR Spectrum of 3v, related to Scheme 2

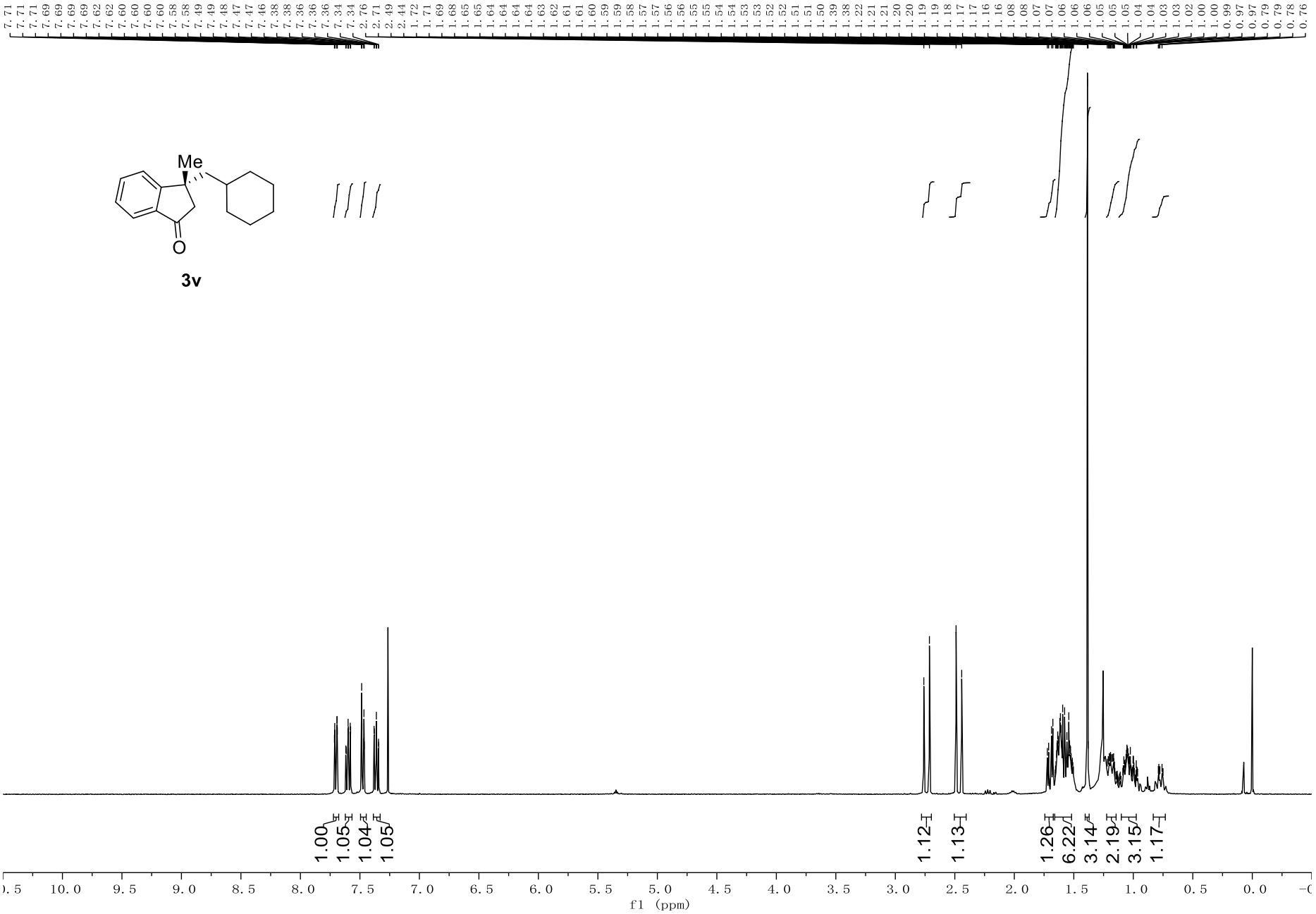

Figure S60 ^{13}C NMR Spectrum of 3v, related to Scheme 2

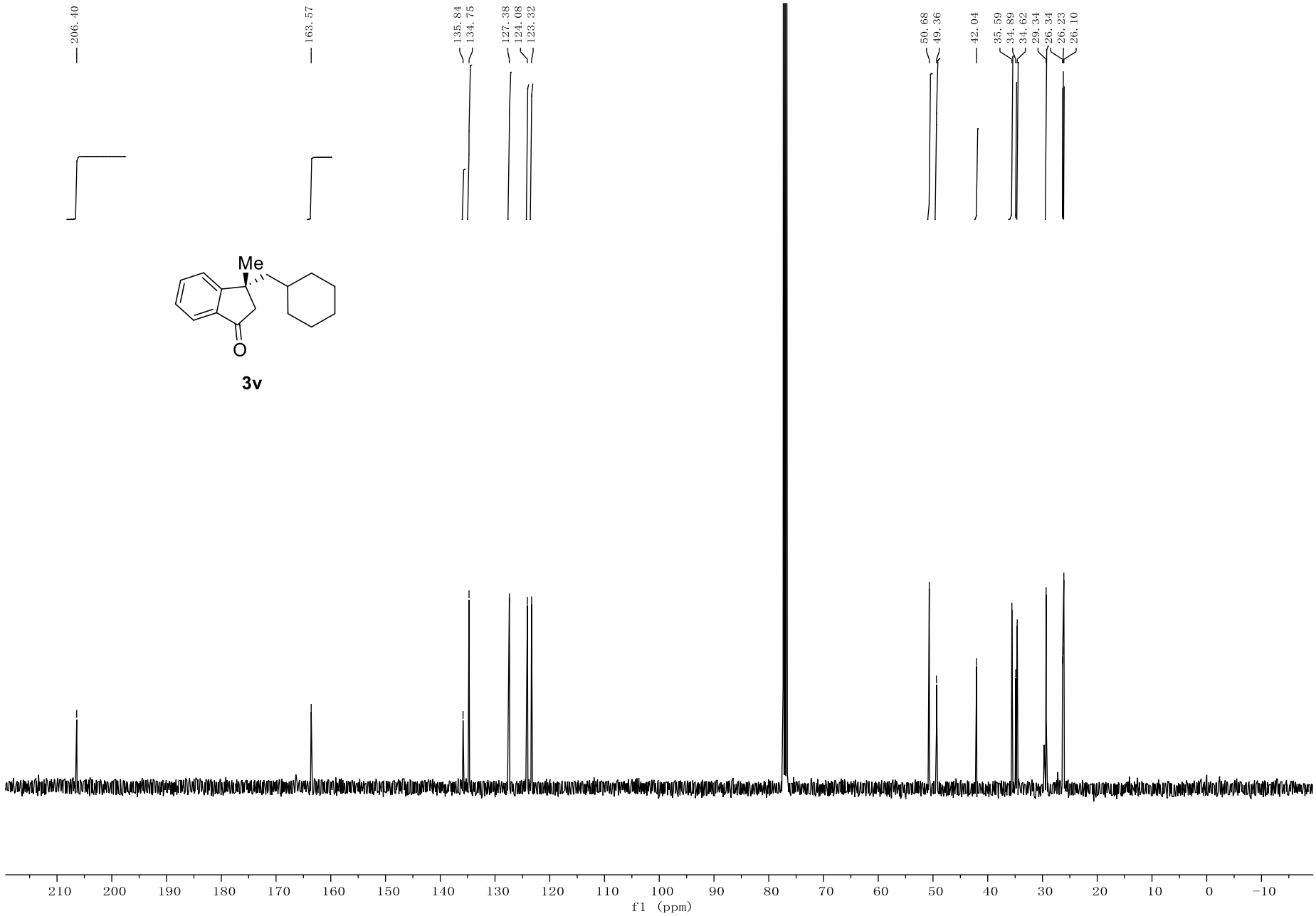

Figure S61 ^{1}H NMR Spectrum of 3w, related to Scheme 2

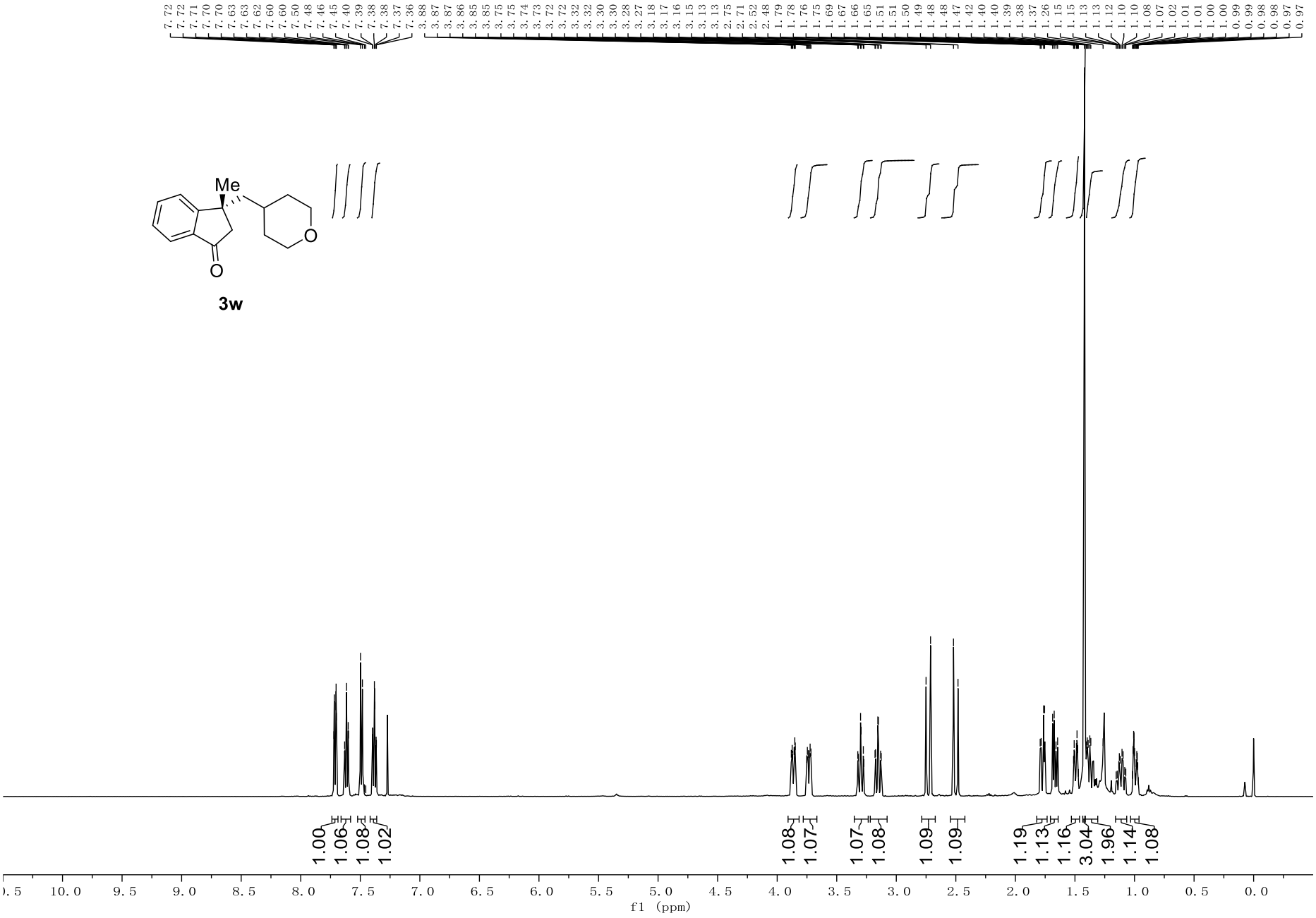

Figure S62 ^{13}C NMR Spectrum of 3w, related to Scheme 2

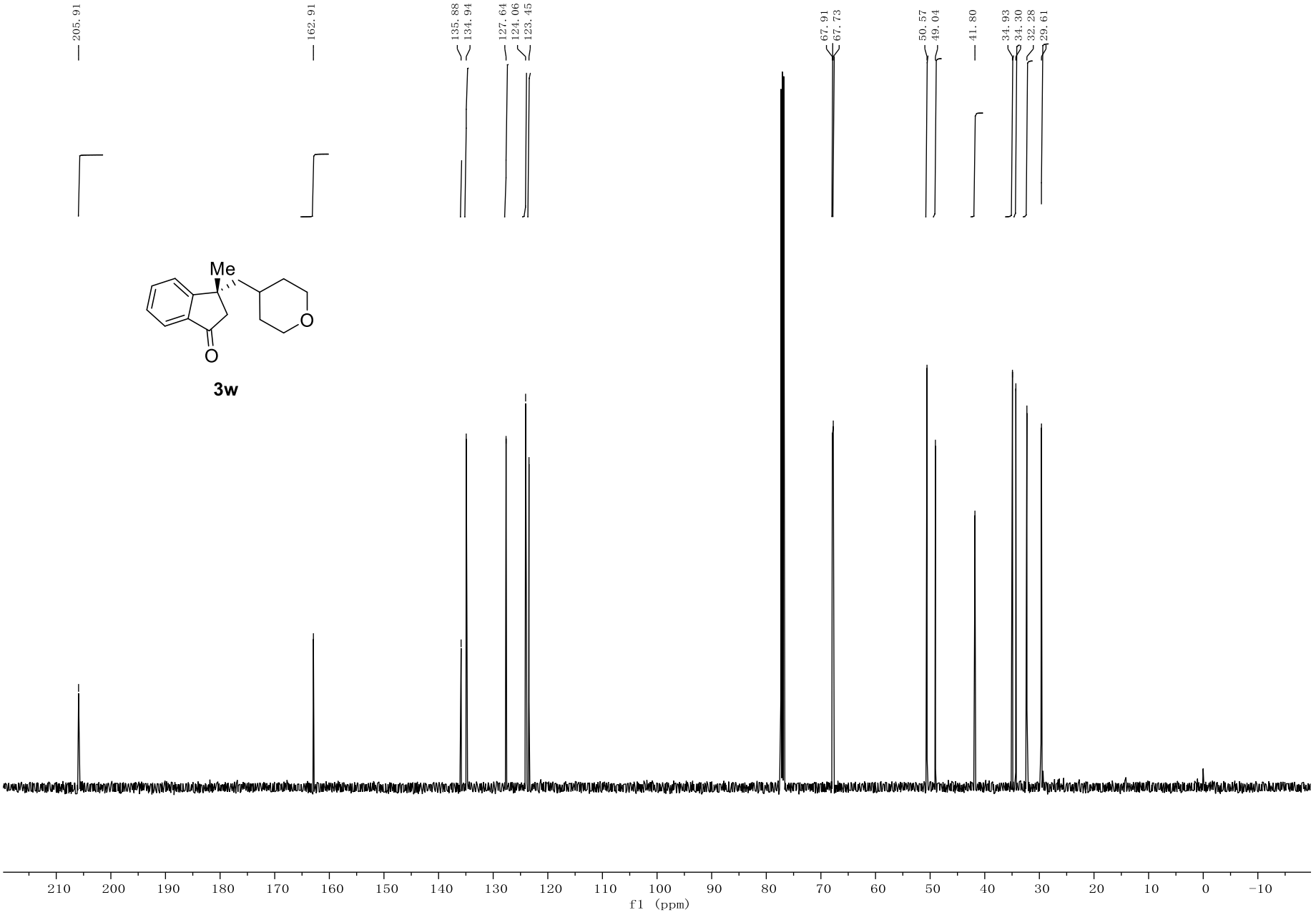

Figure S63 ^{1}H NMR Spectrum of 3w, related to Scheme 2

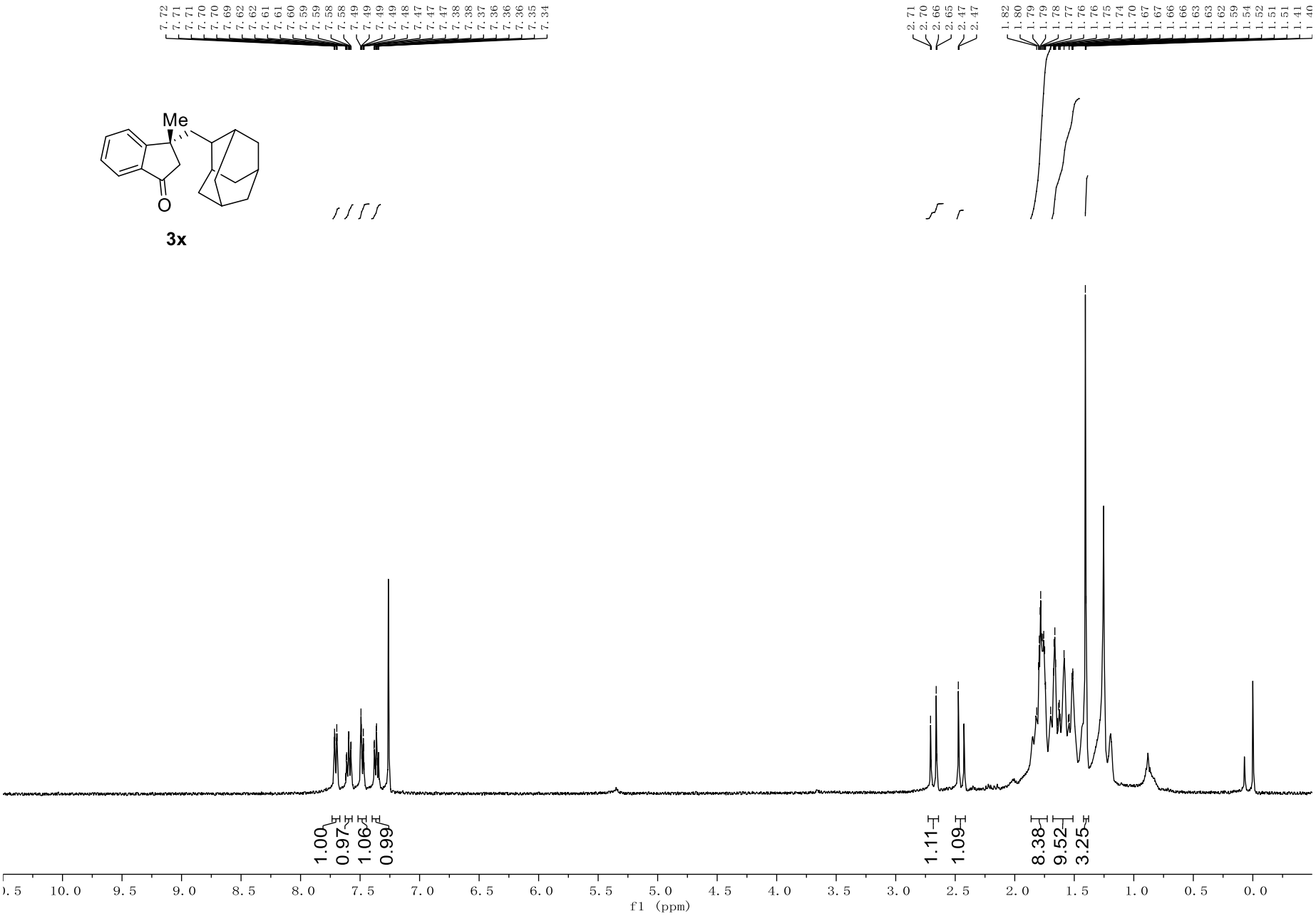

Figure S64 ^{13}C NMR Spectrum of 3w, related to Scheme 2

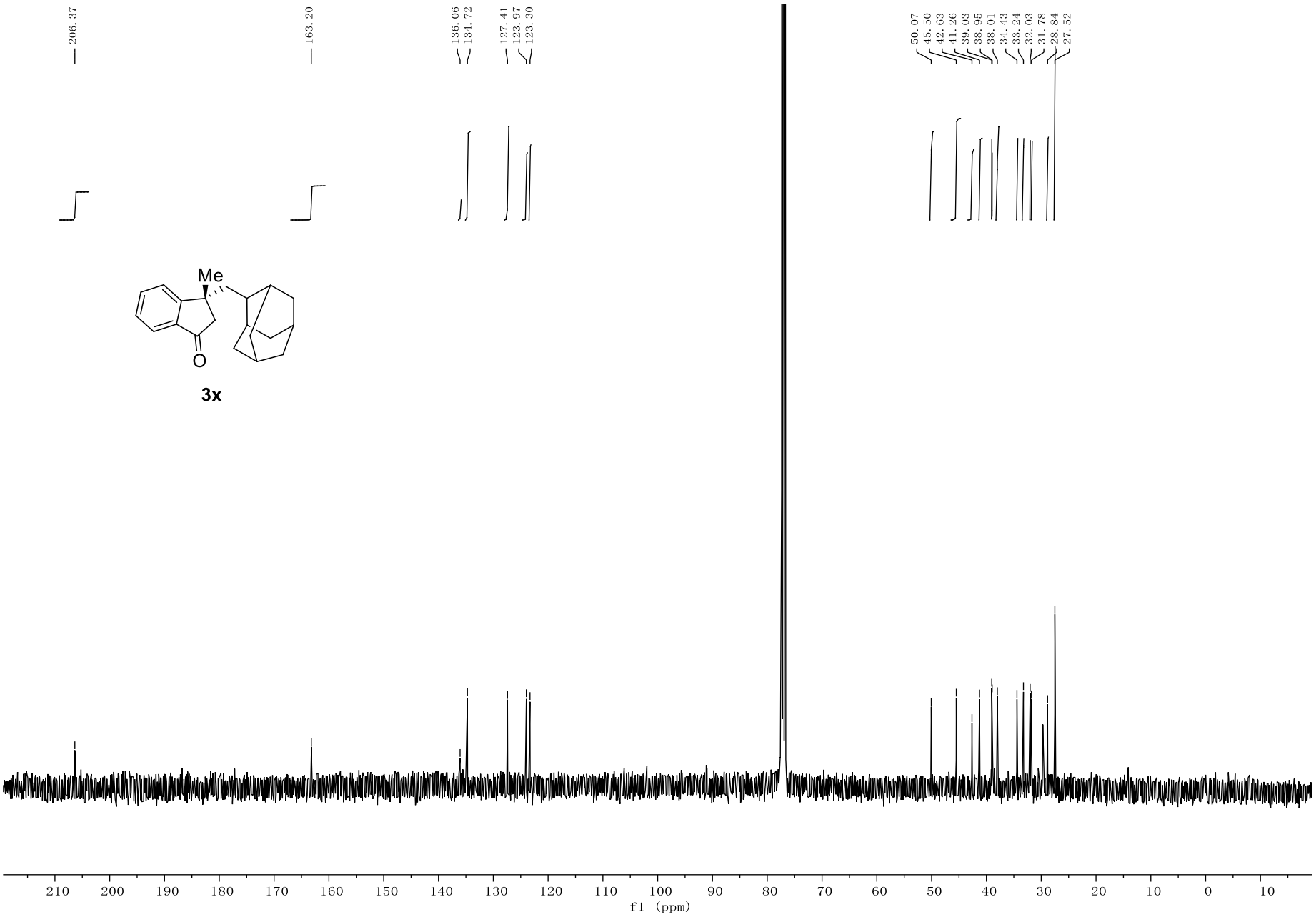

Figure S65 ^{1}H NMR Spectrum of 3y, related to Scheme 2

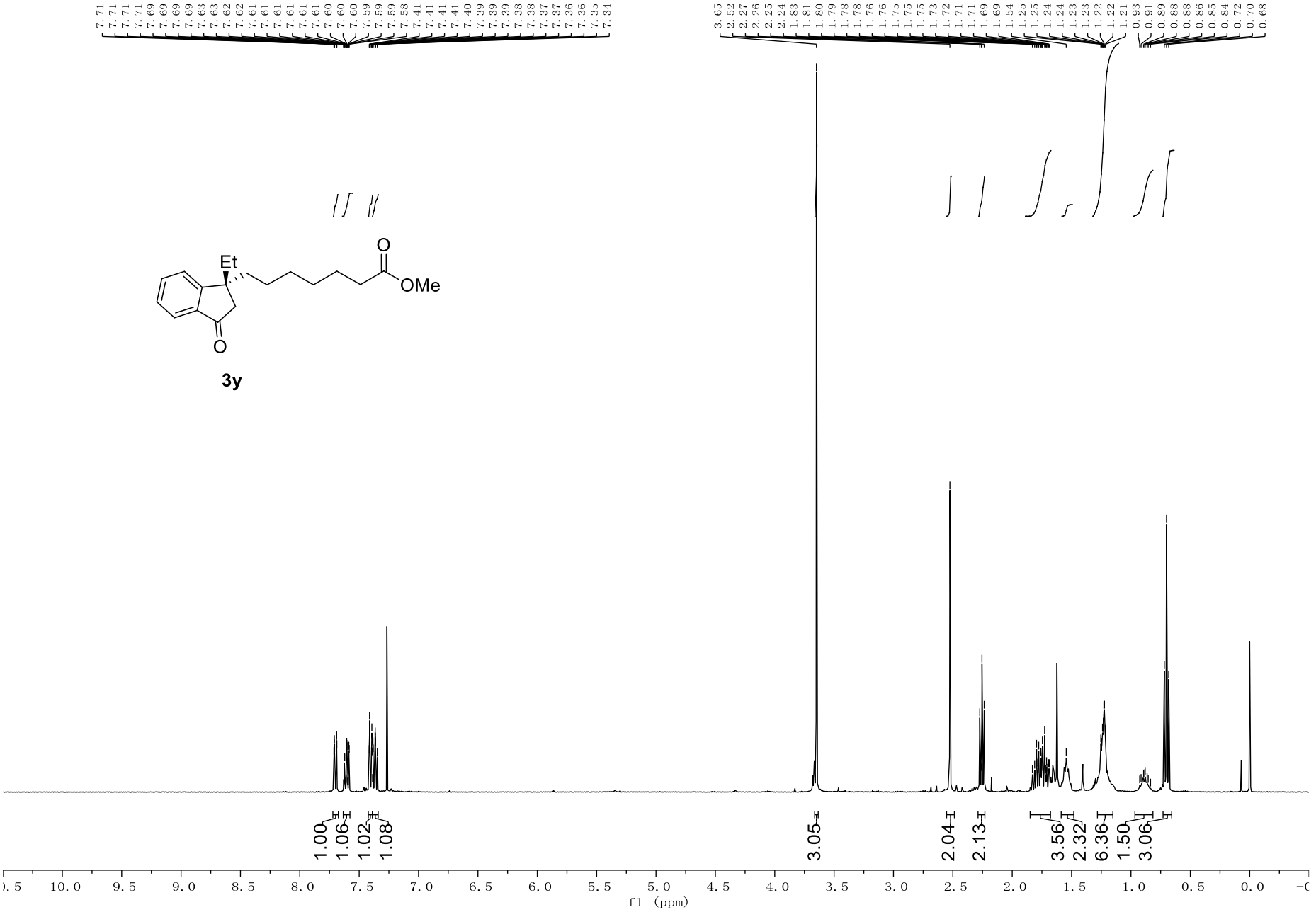

Figure S66 ^{13}C NMR Spectrum of 3y, related to Scheme 2

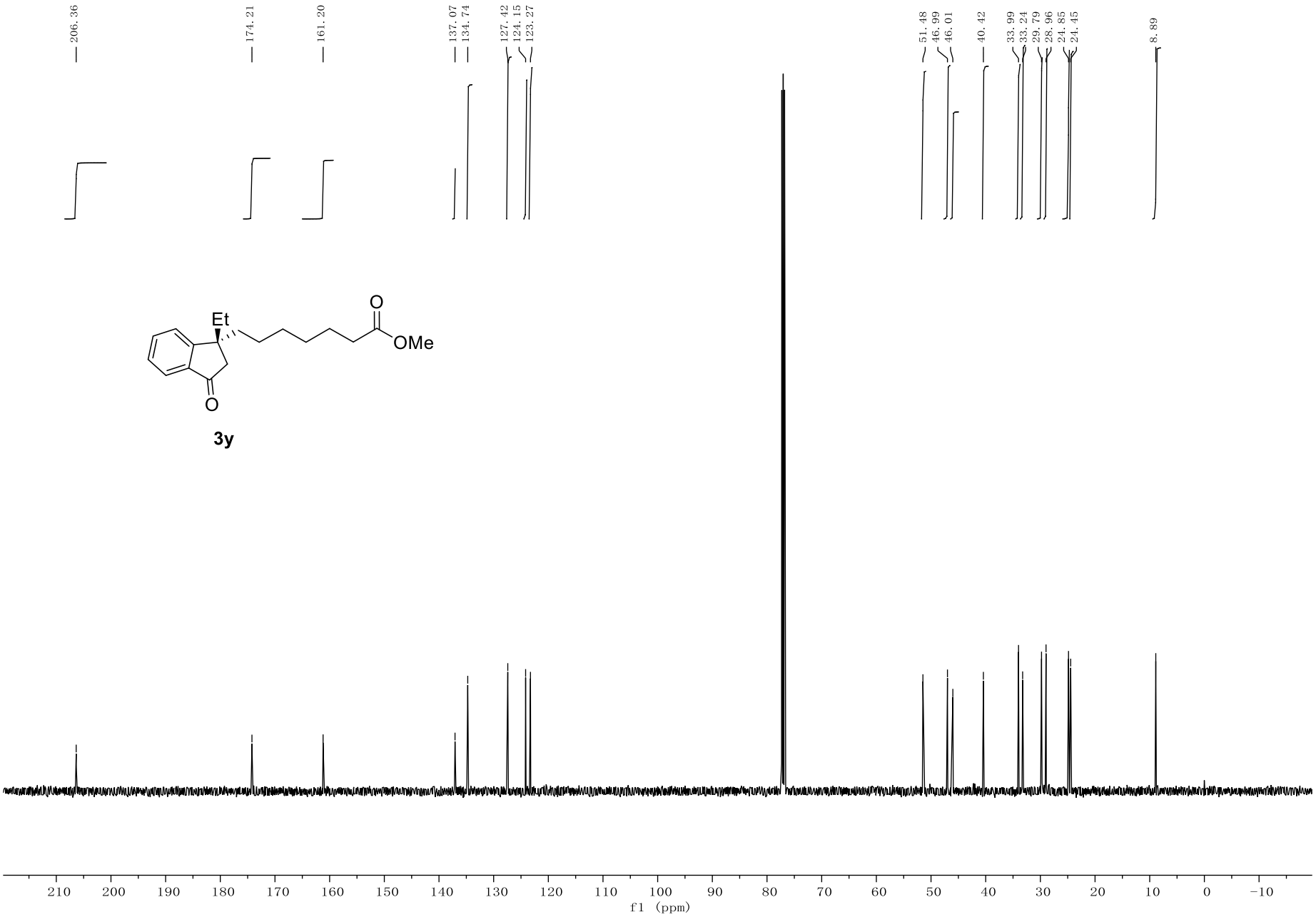

Figure S67 ^{1}H NMR Spectrum of 3z, related to Scheme 2

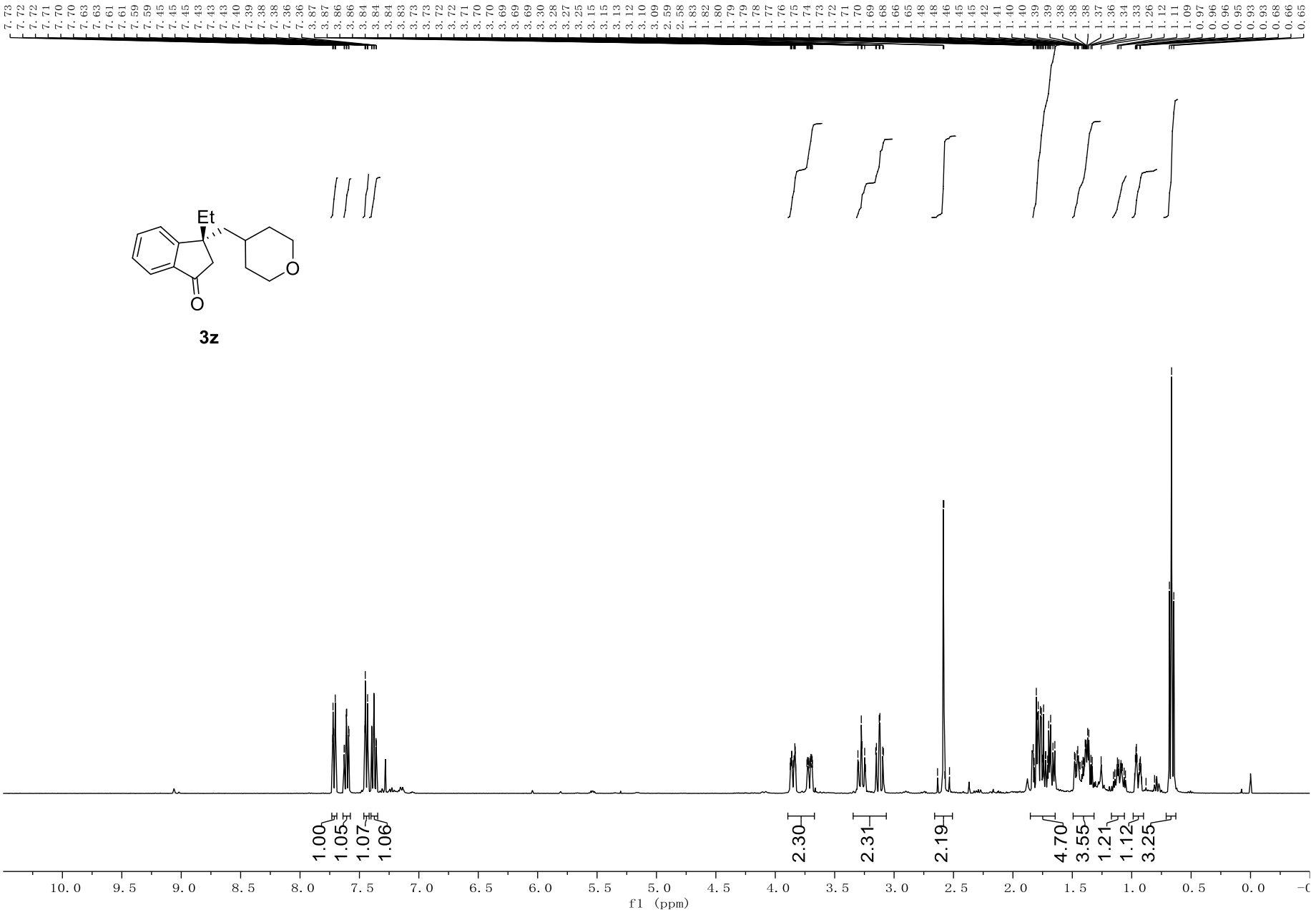

Figure S68 ^{13}C NMR Spectrum of 3z, related to Scheme 2

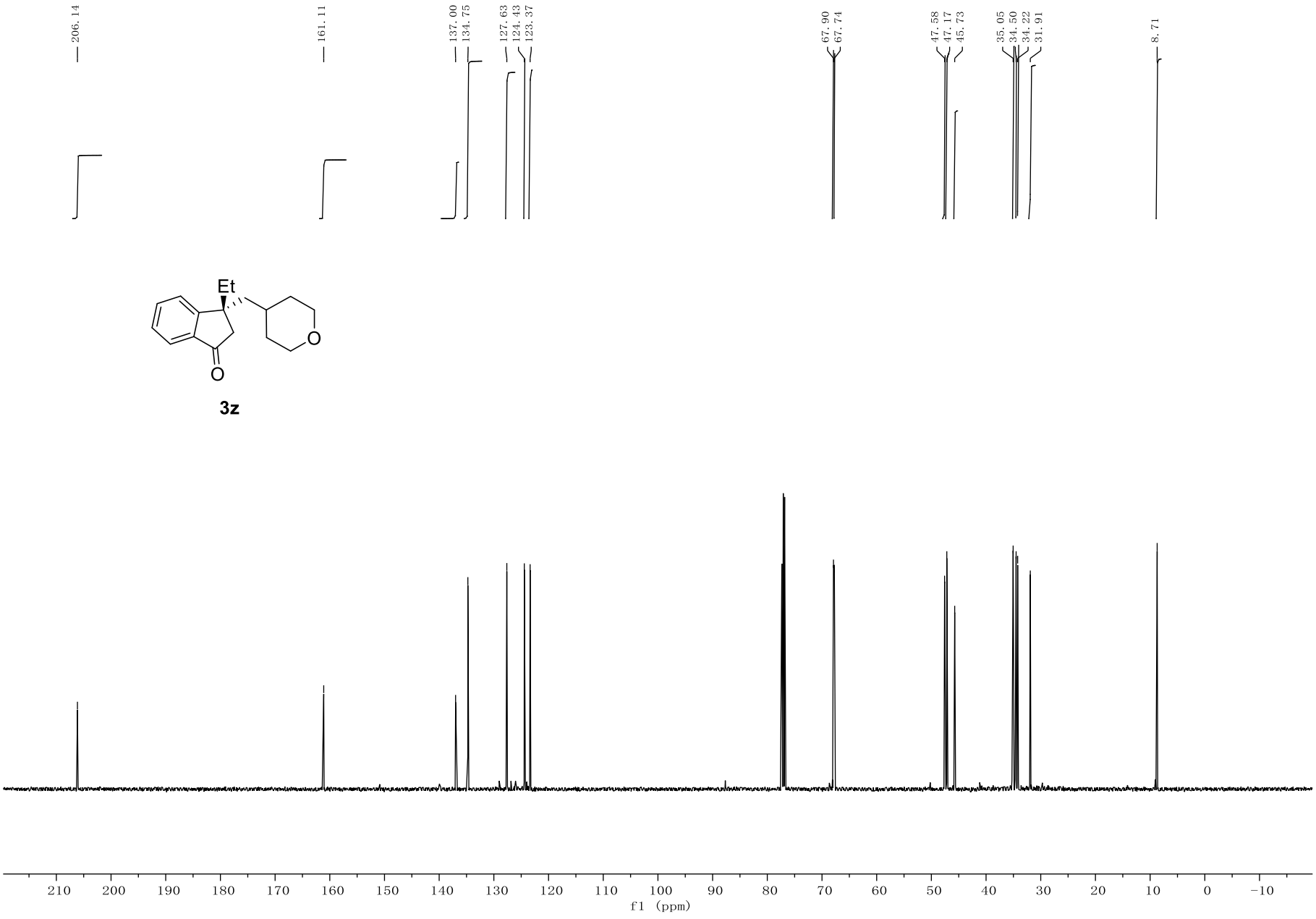

Figure S69 ^{1}H NMR Spectrum of 3aa, related to Scheme 2

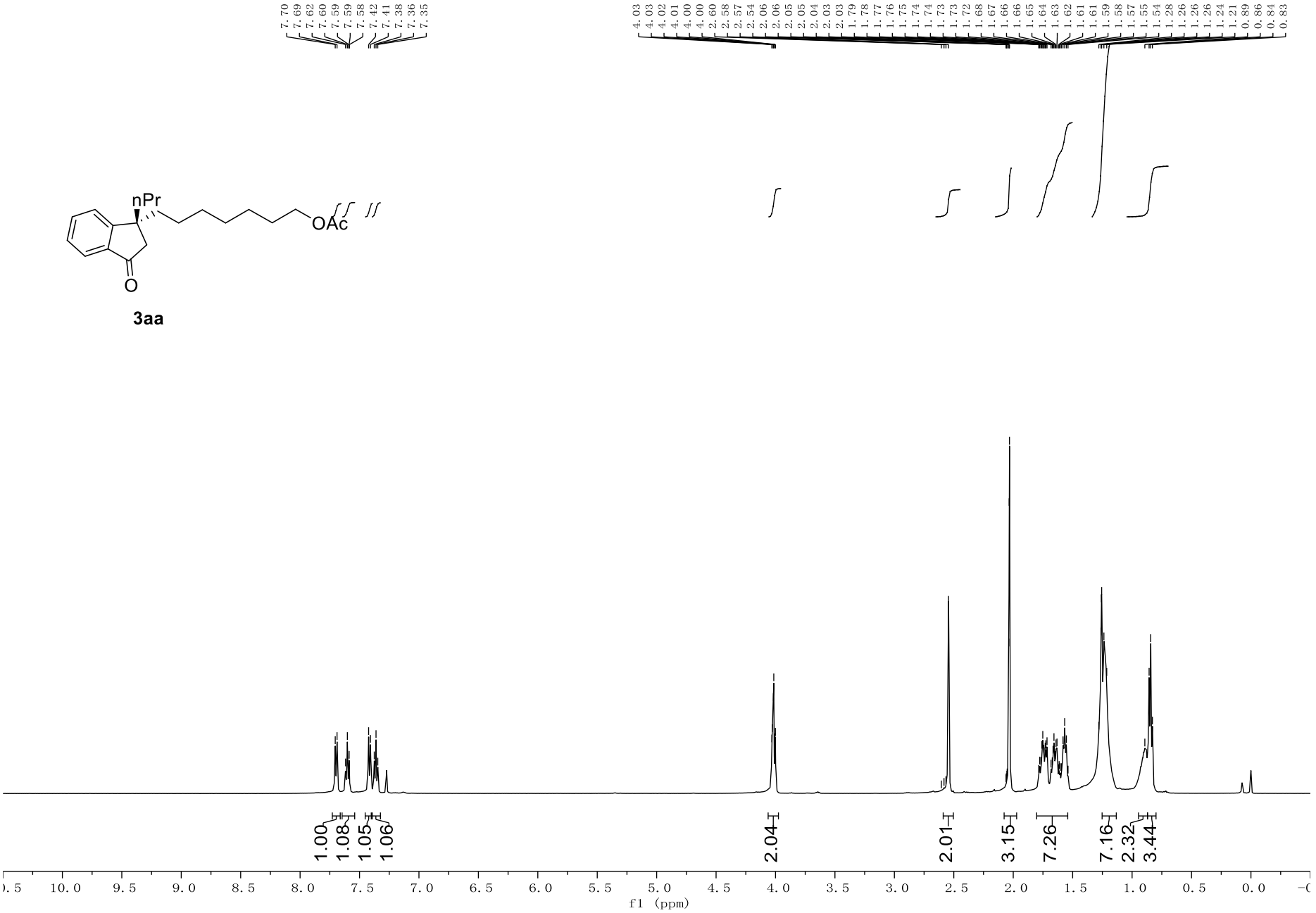

Figure S70 ^{13}C NMR Spectrum of 3aa, related to Scheme 2

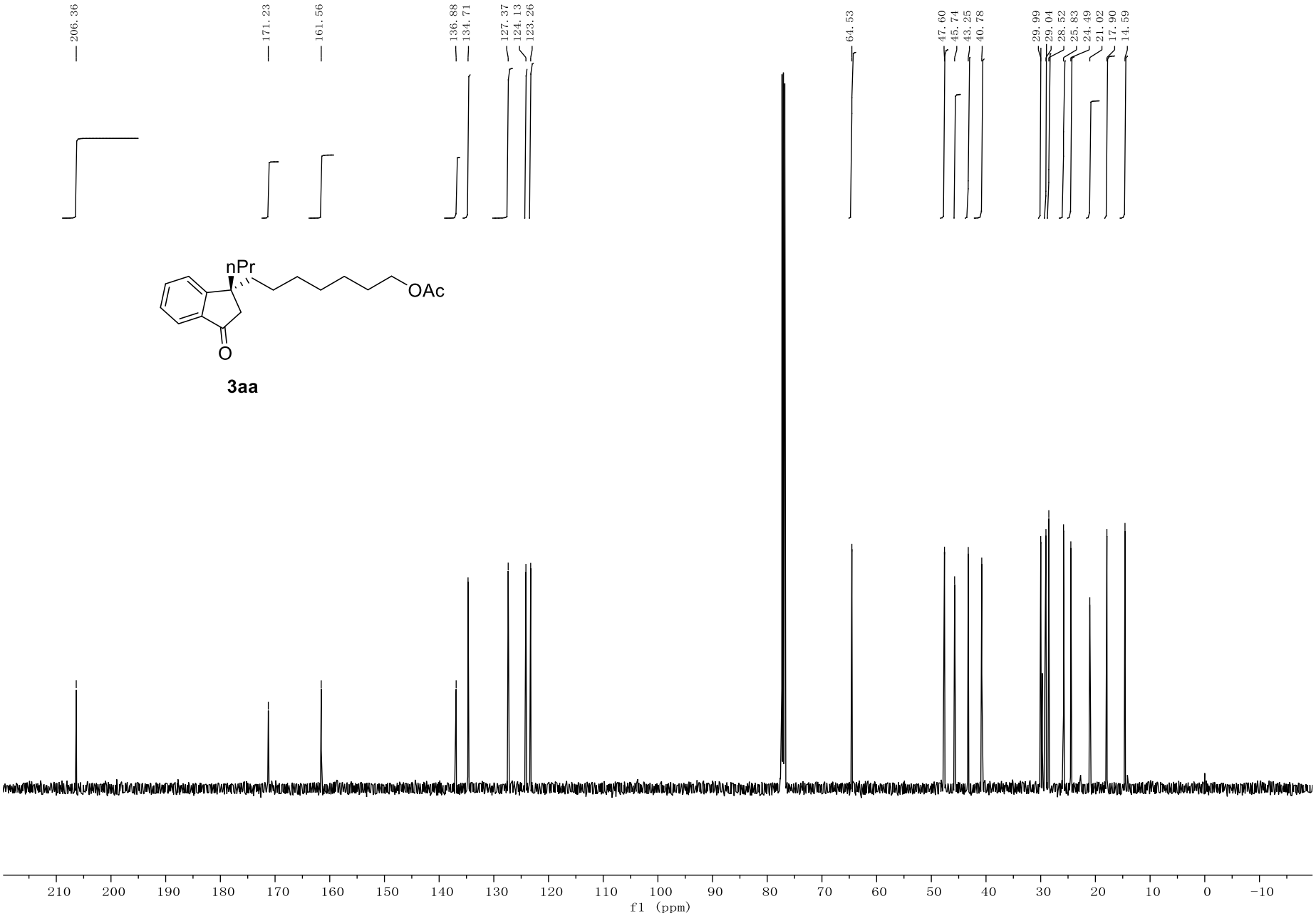

Figure S71 ^{1}H NMR Spectrum of 3ab, related to Scheme 2

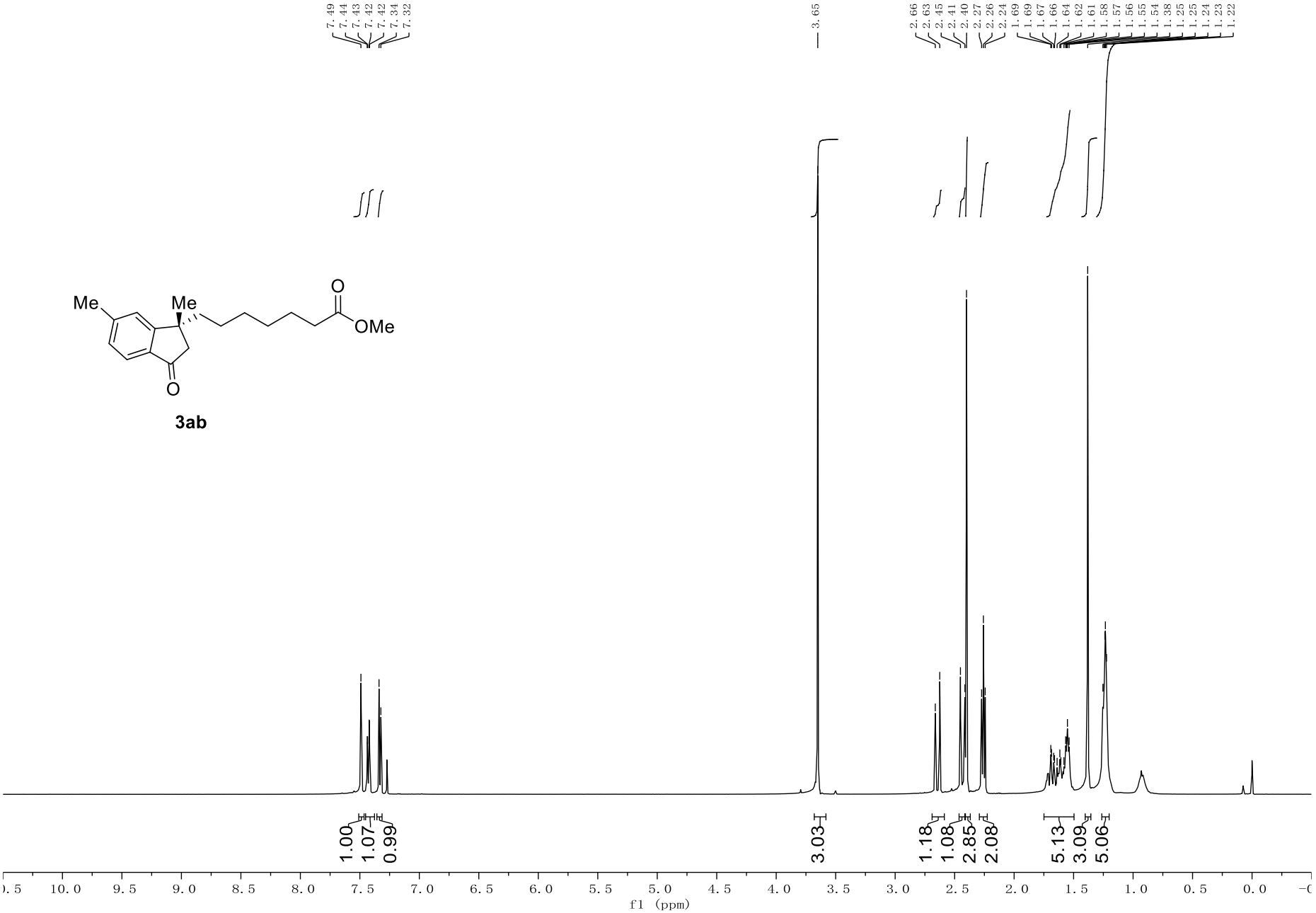

Figure S72 ^{1}H NMR Spectrum of 3ab, related to Scheme 2

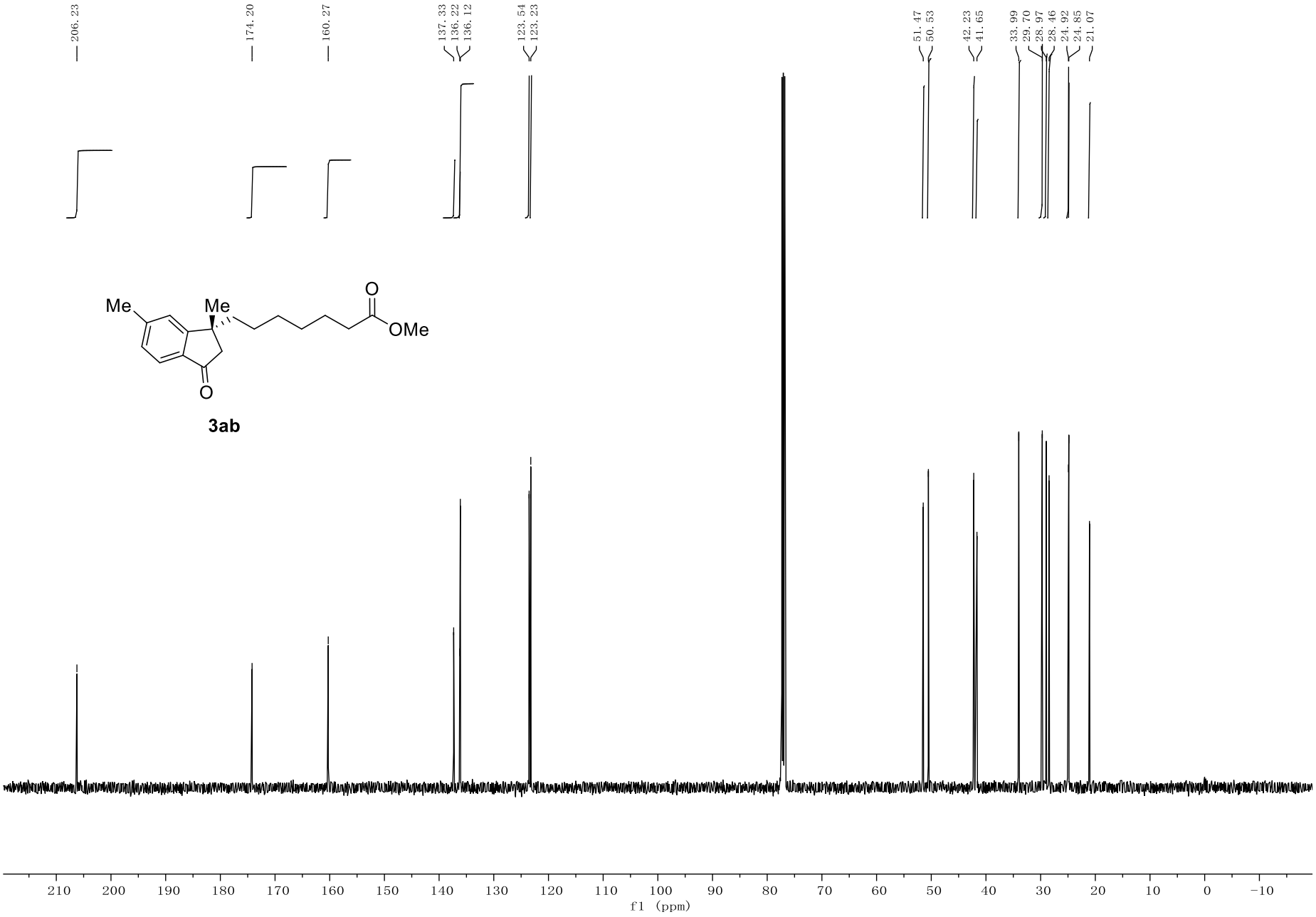

Figure S73 ^{1}H NMR Spectrum of 3ac, related to Scheme 2

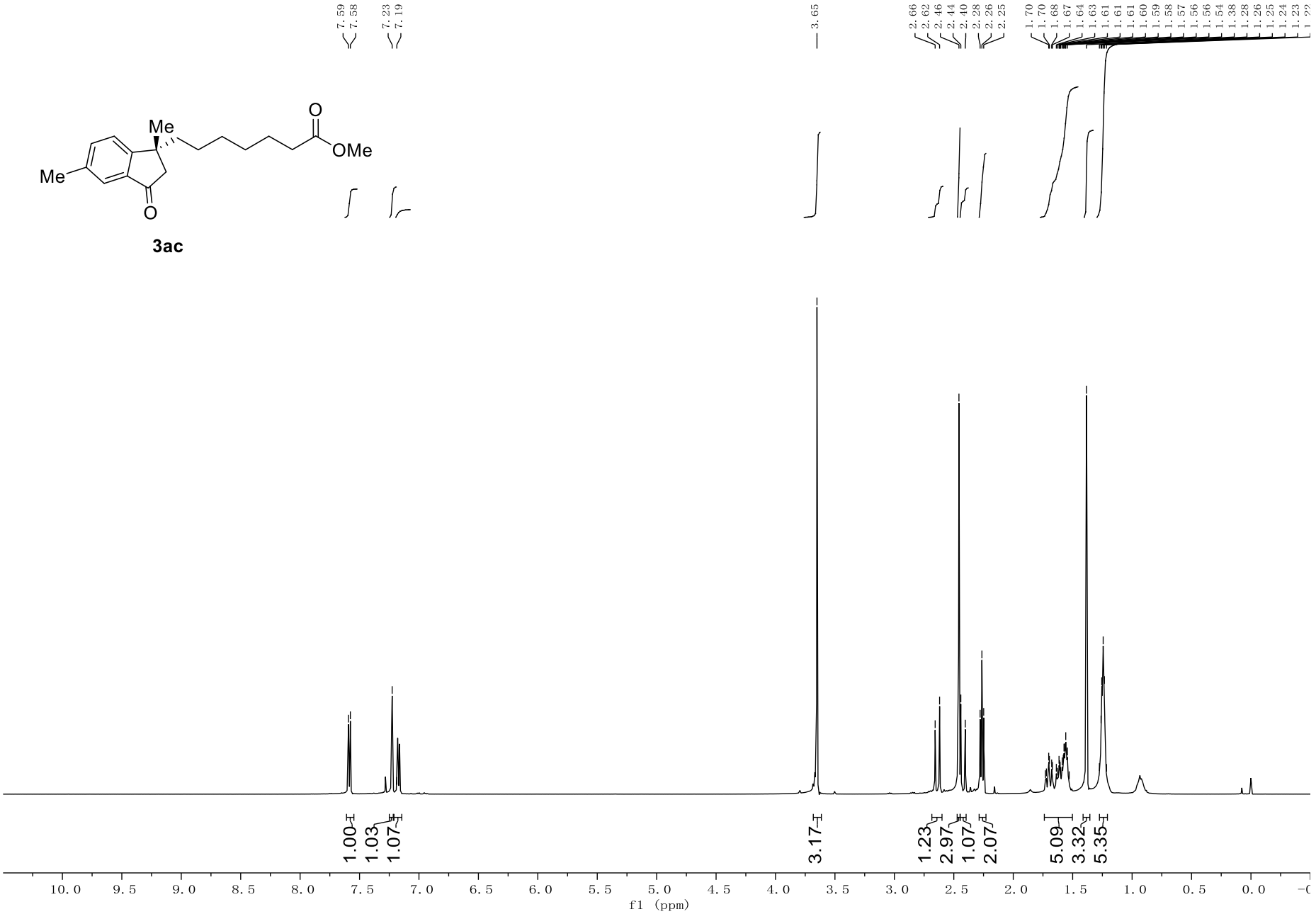

Figure S74 ^{13}C NMR Spectrum of 3ac, related to Scheme 2

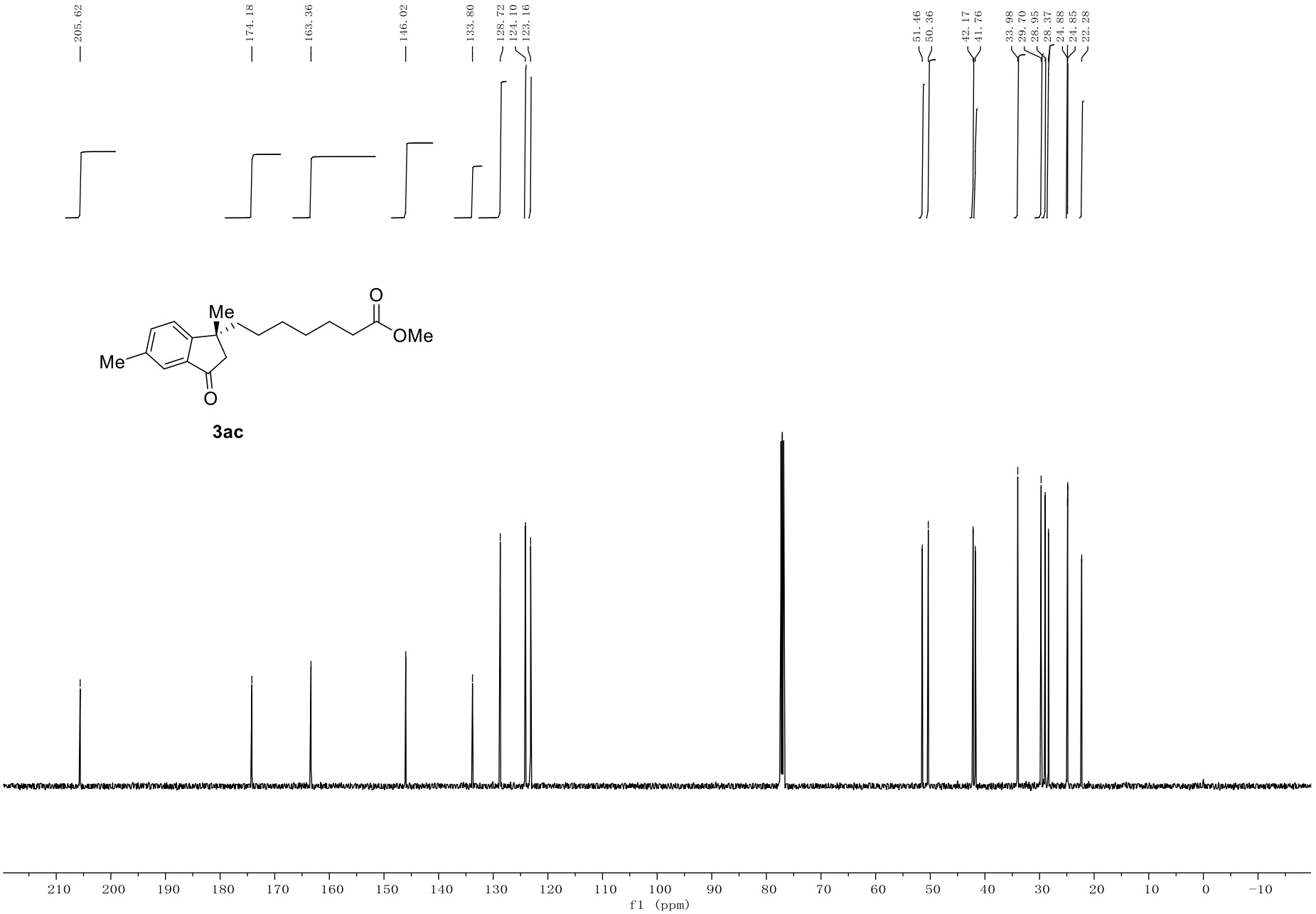

Figure S75 ^{1}H NMR Spectrum of 3ad, related to Scheme 2

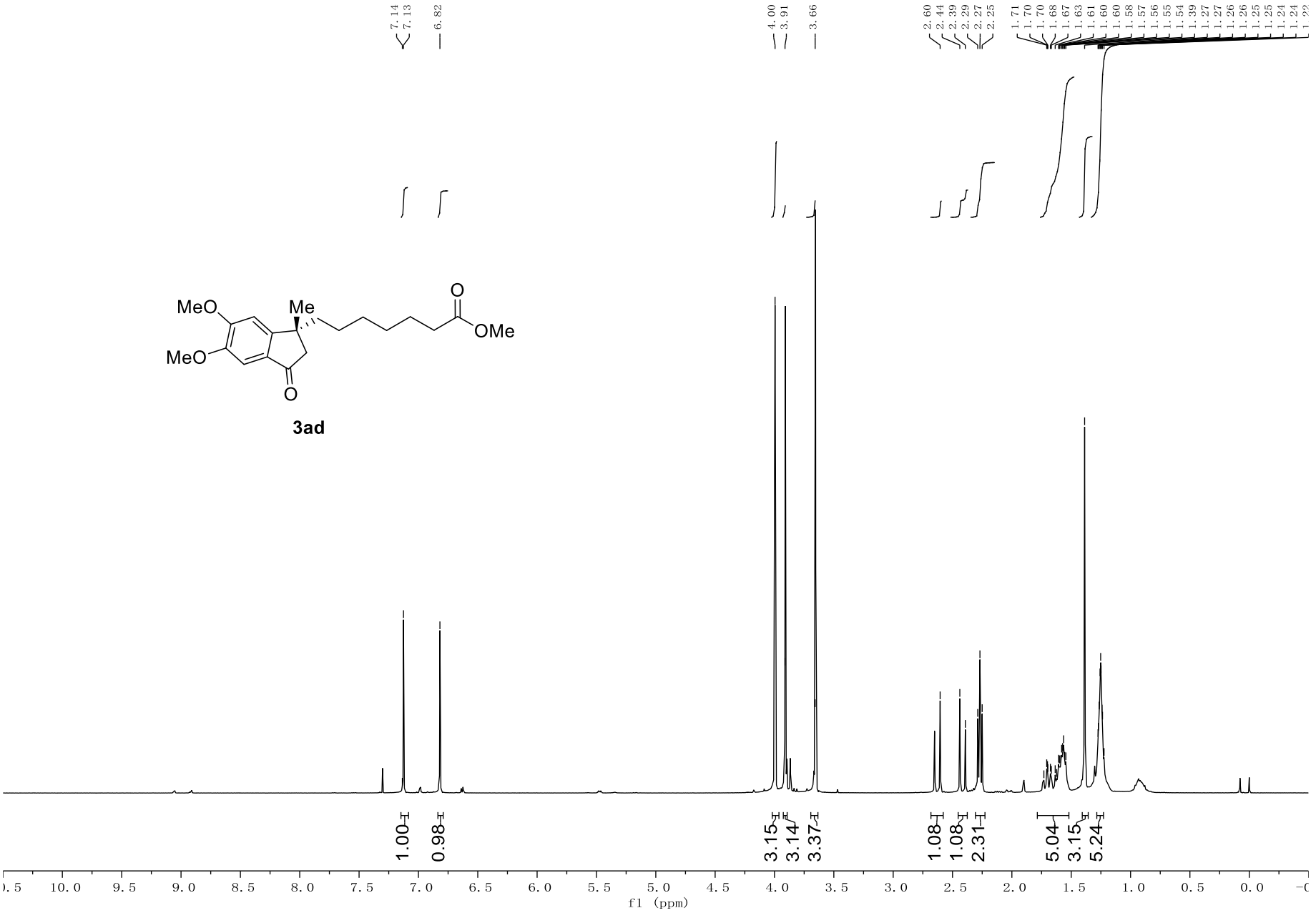

Figure S76 ^{13}C NMR Spectrum of 3ad, related to Scheme 2

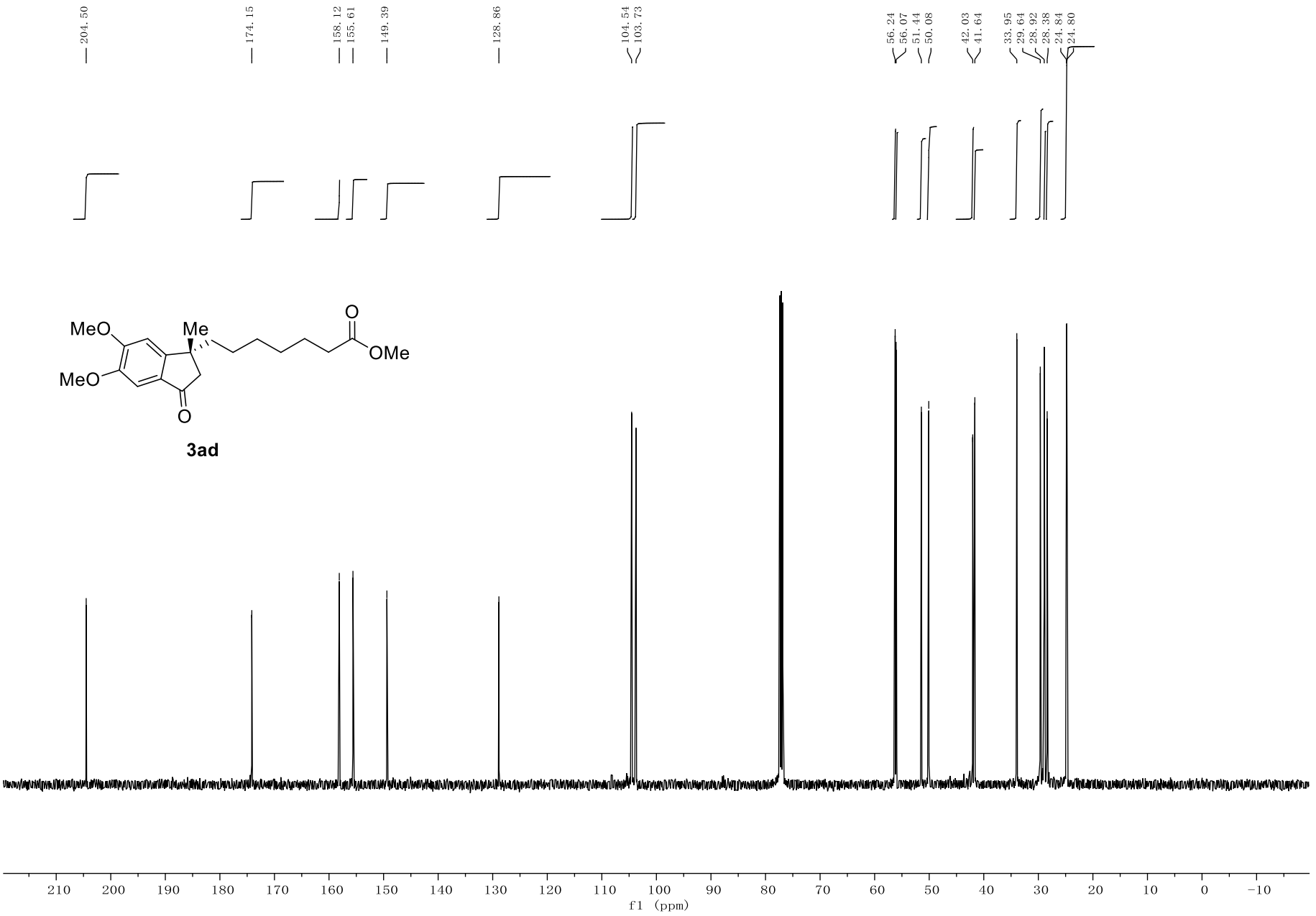

Figure S77 ^{1}H NMR Spectrum of 3ae, related to Scheme 2

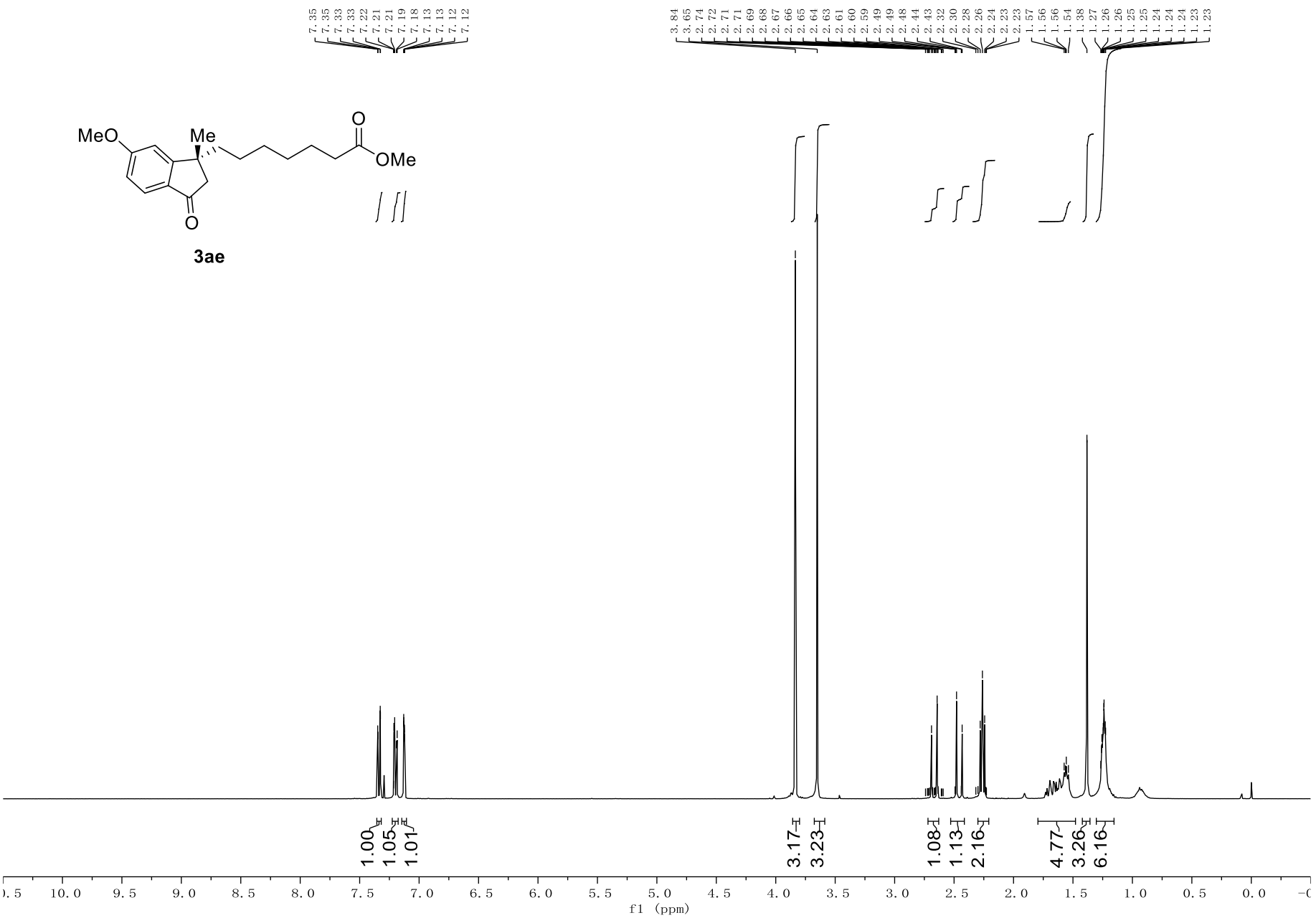

Figure S78 ^{13}C NMR Spectrum of 3ae, related to Scheme 2

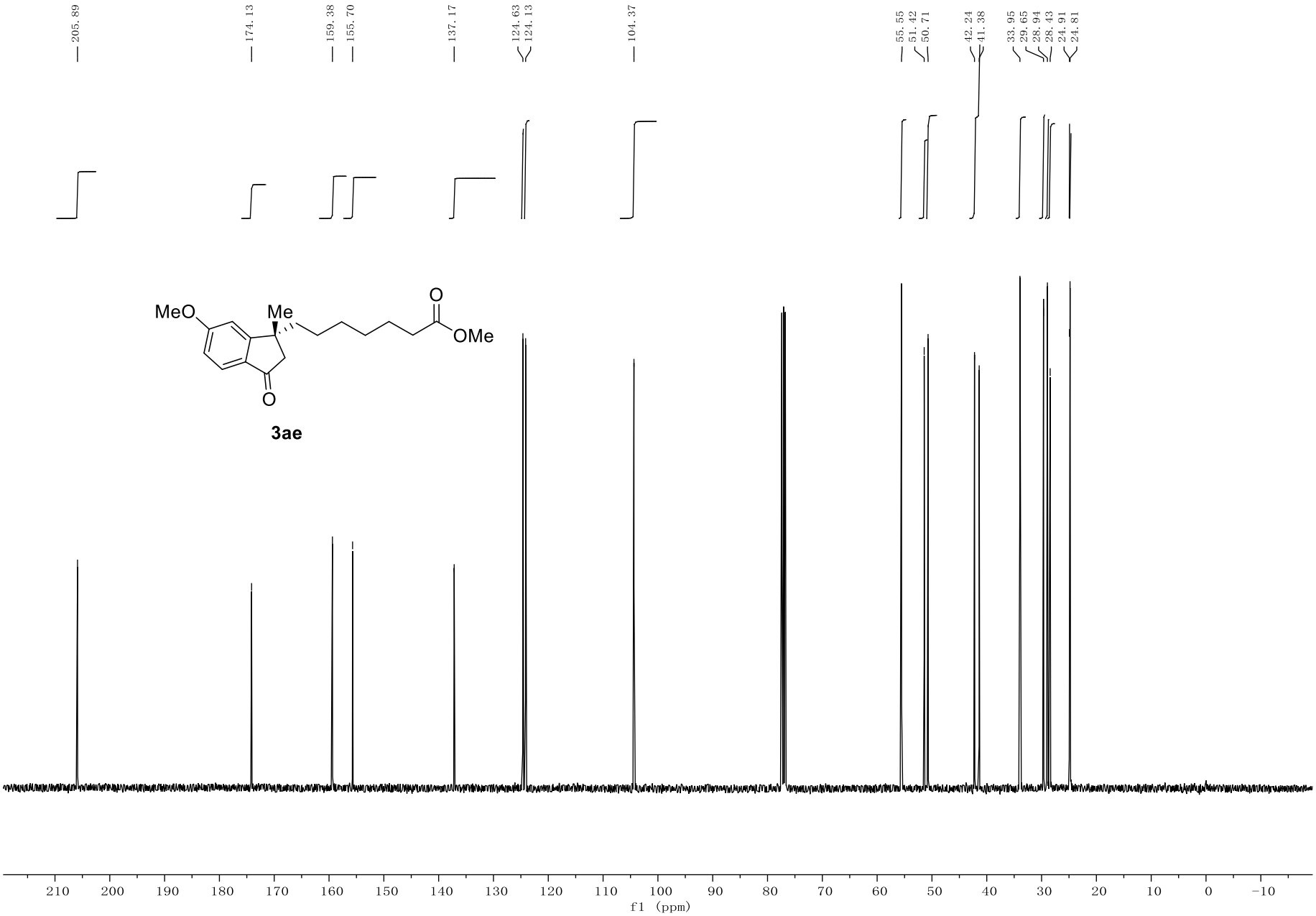

Figure S79 ^{1}H NMR Spectrum of 3af, related to Scheme 2

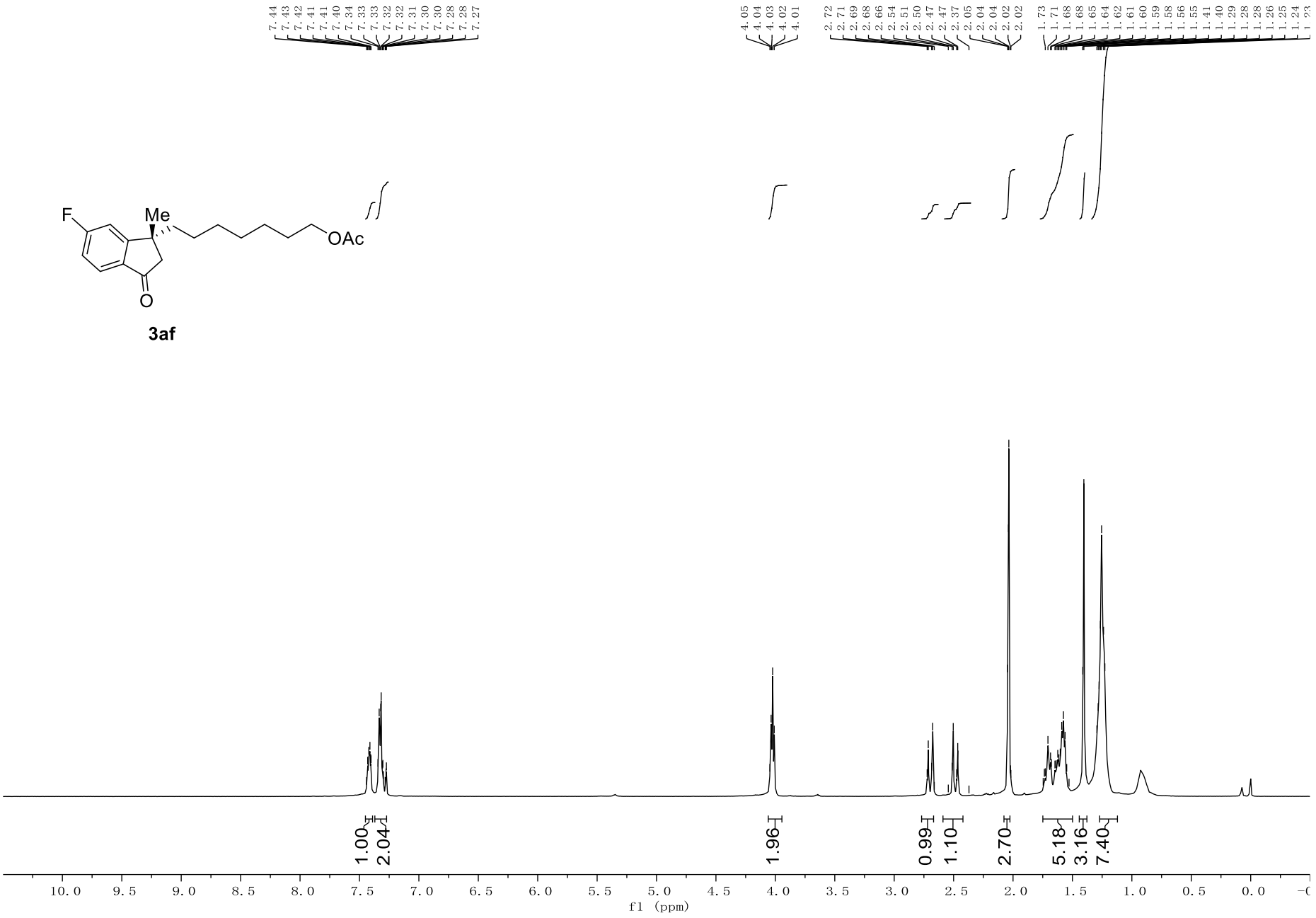

Figure S80 ^{13}C NMR Spectrum of 3af, related to Scheme 2

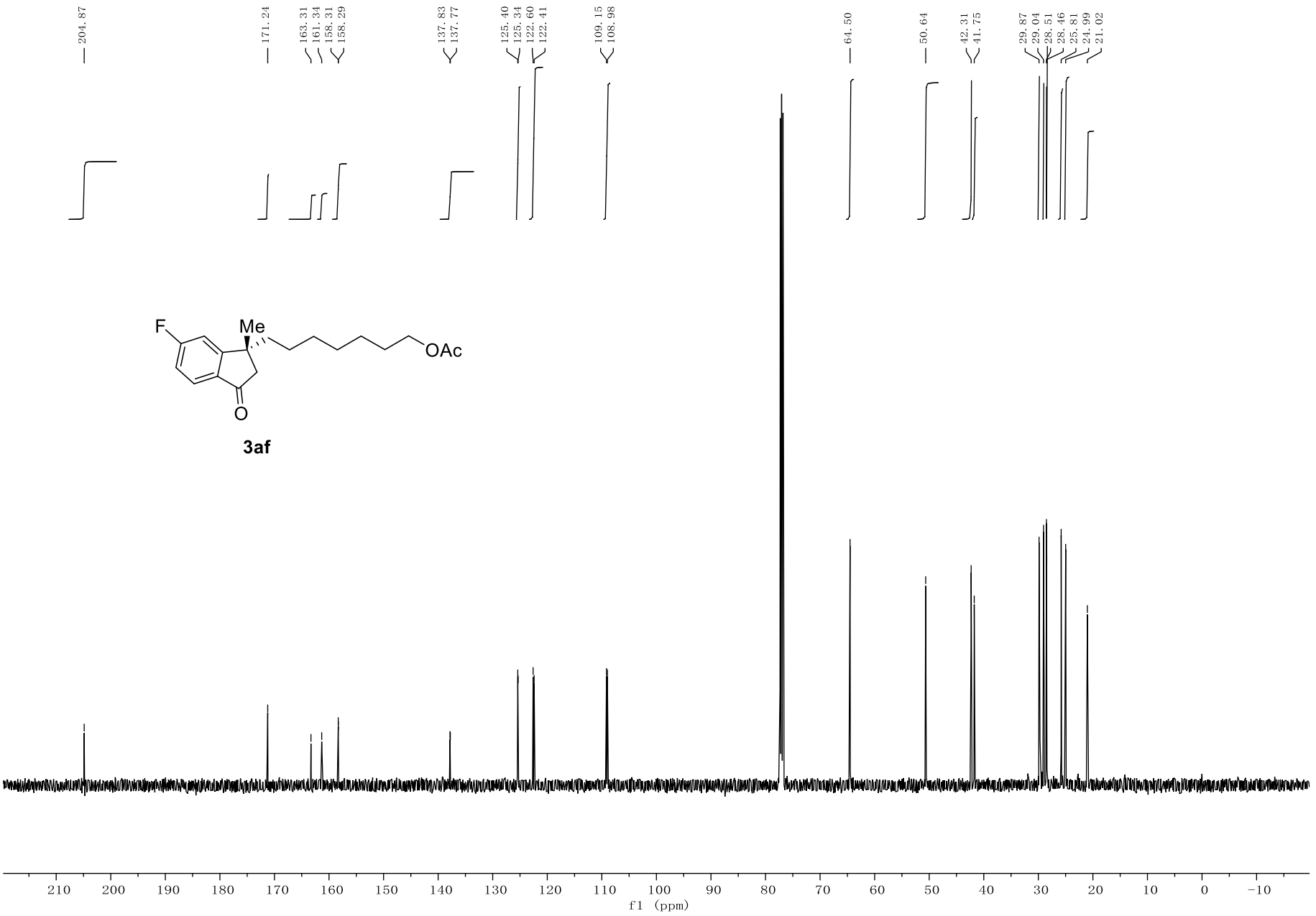

Figure S81 ^{19}F NMR Spectrum of 3af, related to Scheme 2

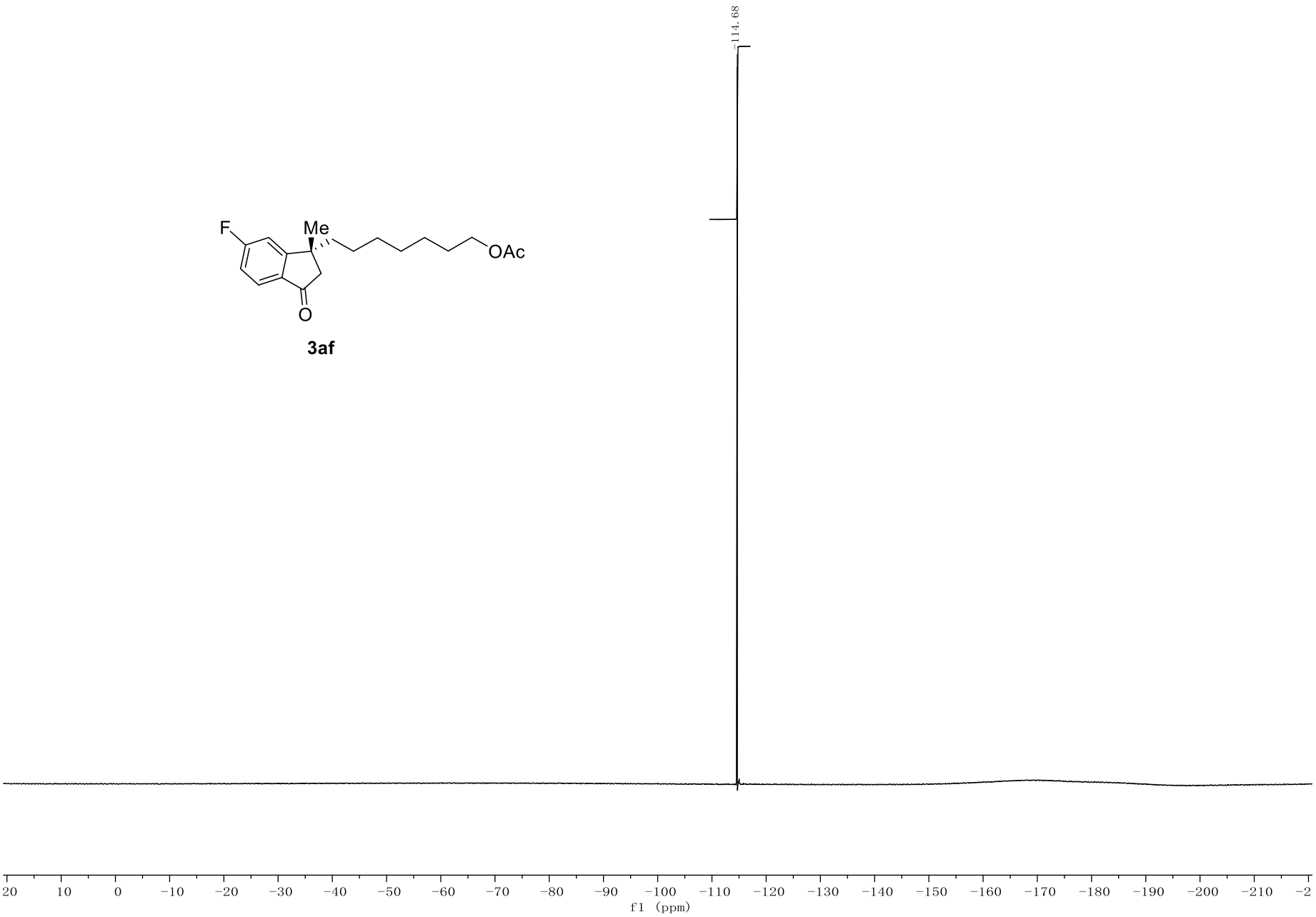

Figure S82 ^{1}H NMR Spectrum of 3ag, related to Scheme 2

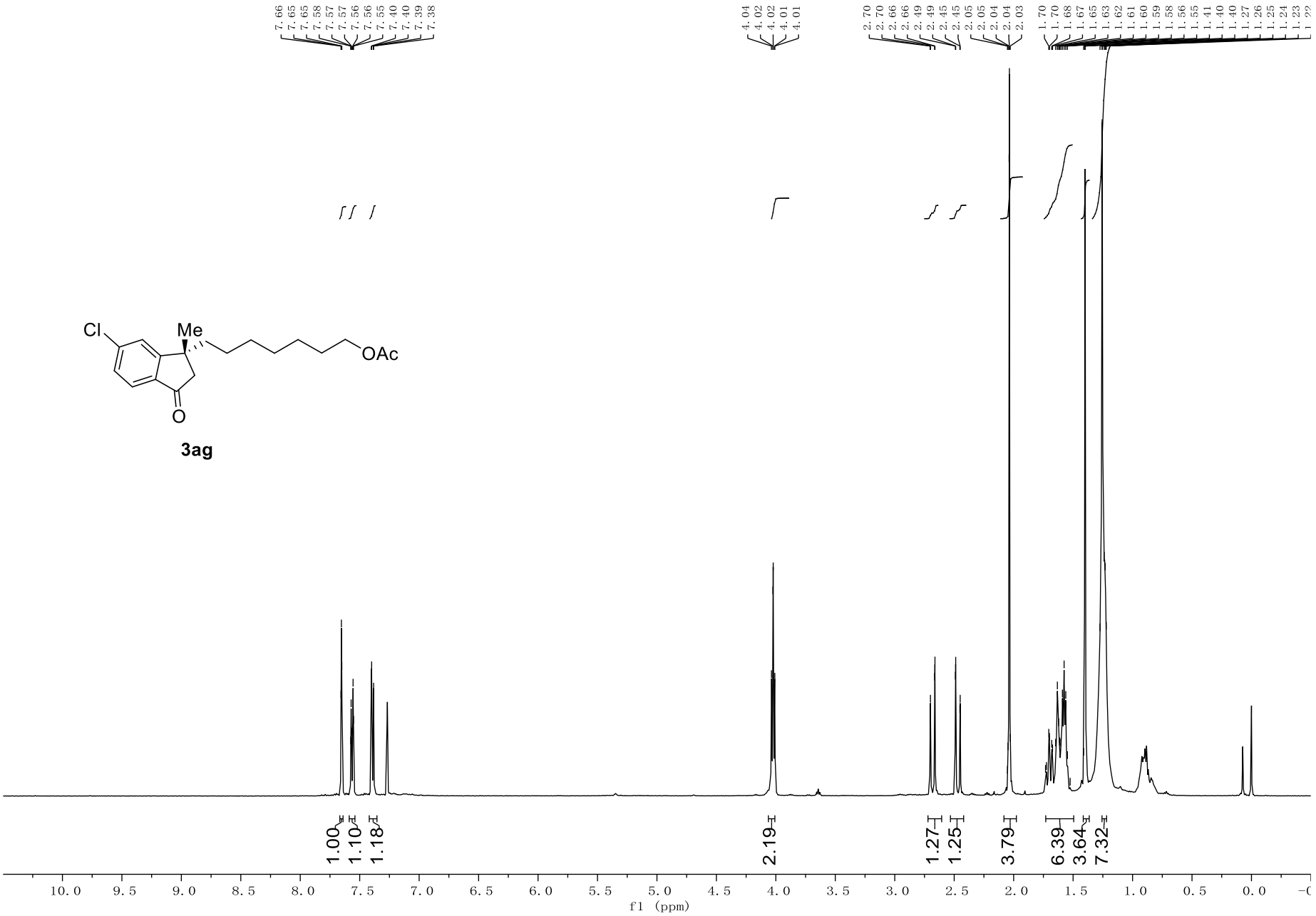

Figure S83 ^{13}C NMR Spectrum of 3ag, related to Scheme 2

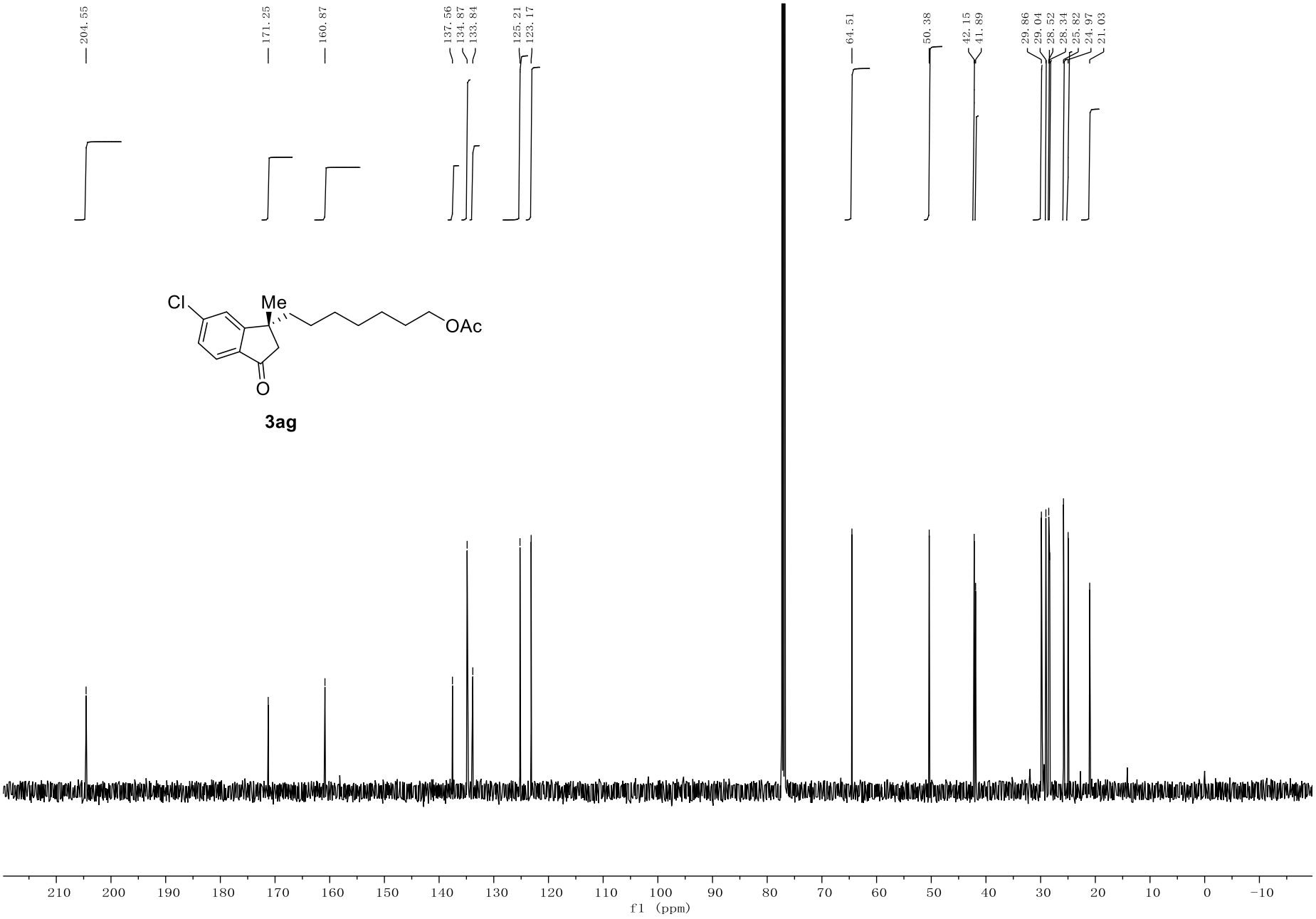

Figure S84 ^{1}H NMR Spectrum of 9, related to Scheme 4

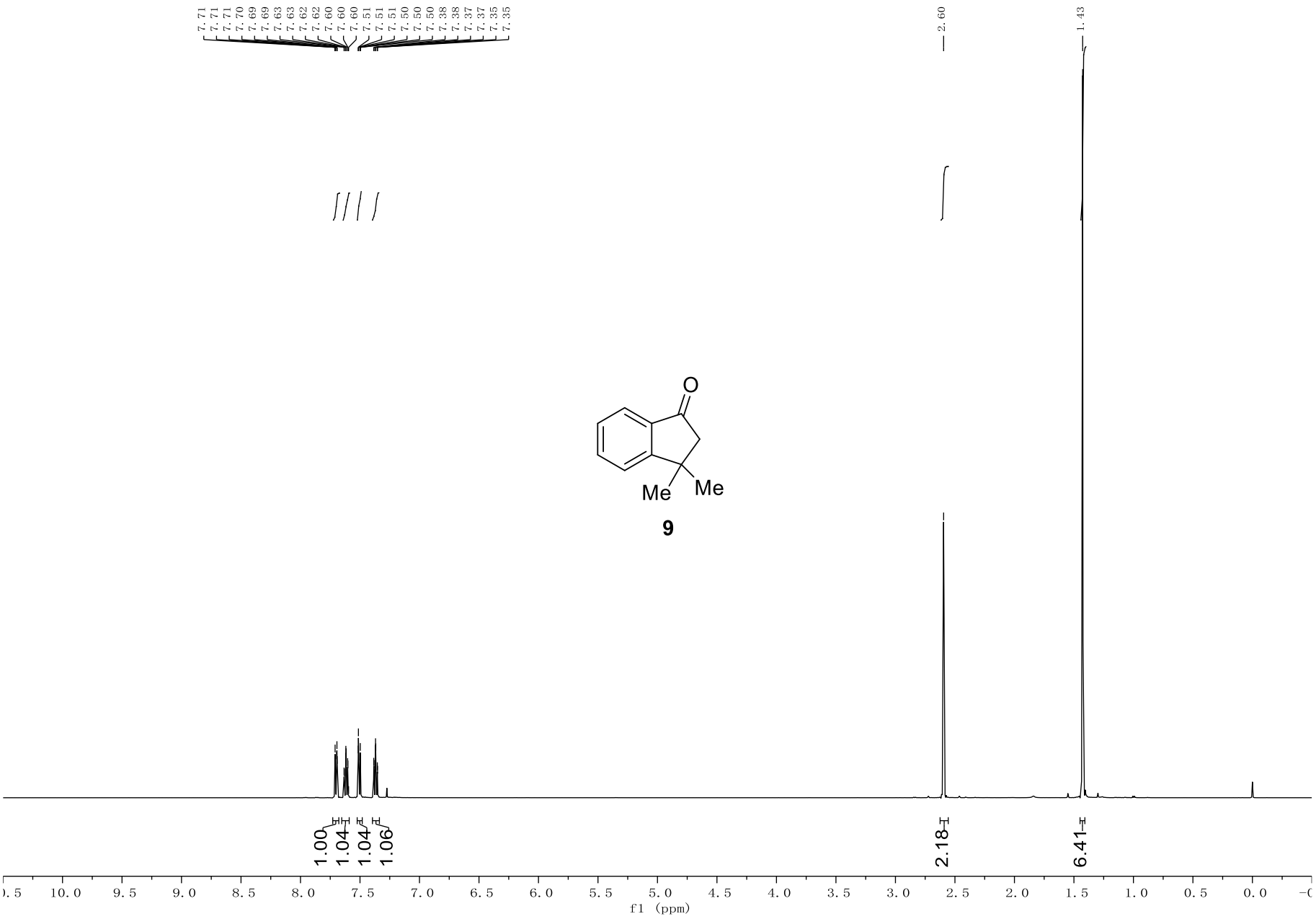

Figure S85 ^{13}C NMR Spectrum of 9, related to Scheme 4

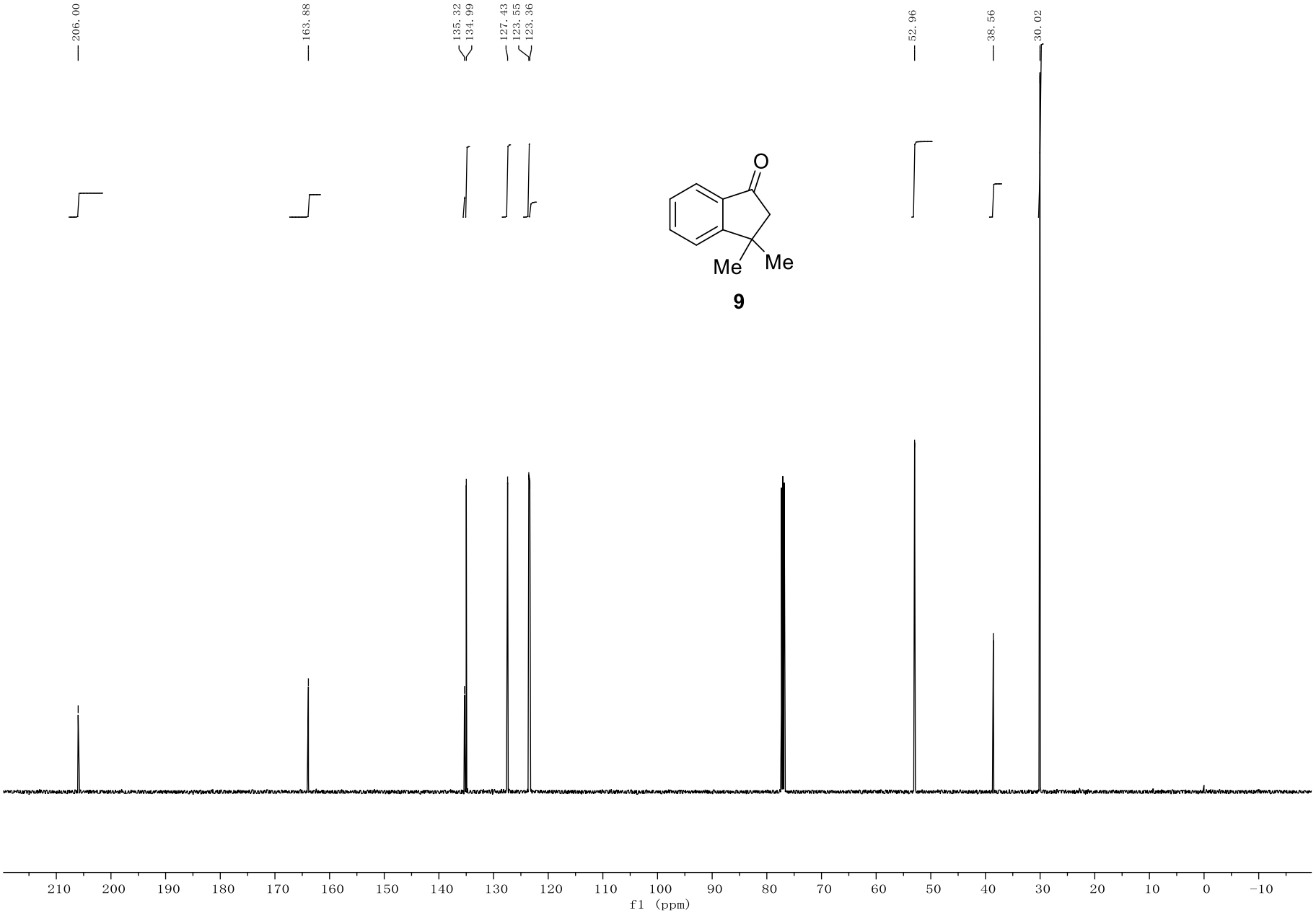

Figure S86 ^{1}H NMR Spectrum of 10, related to Scheme 4

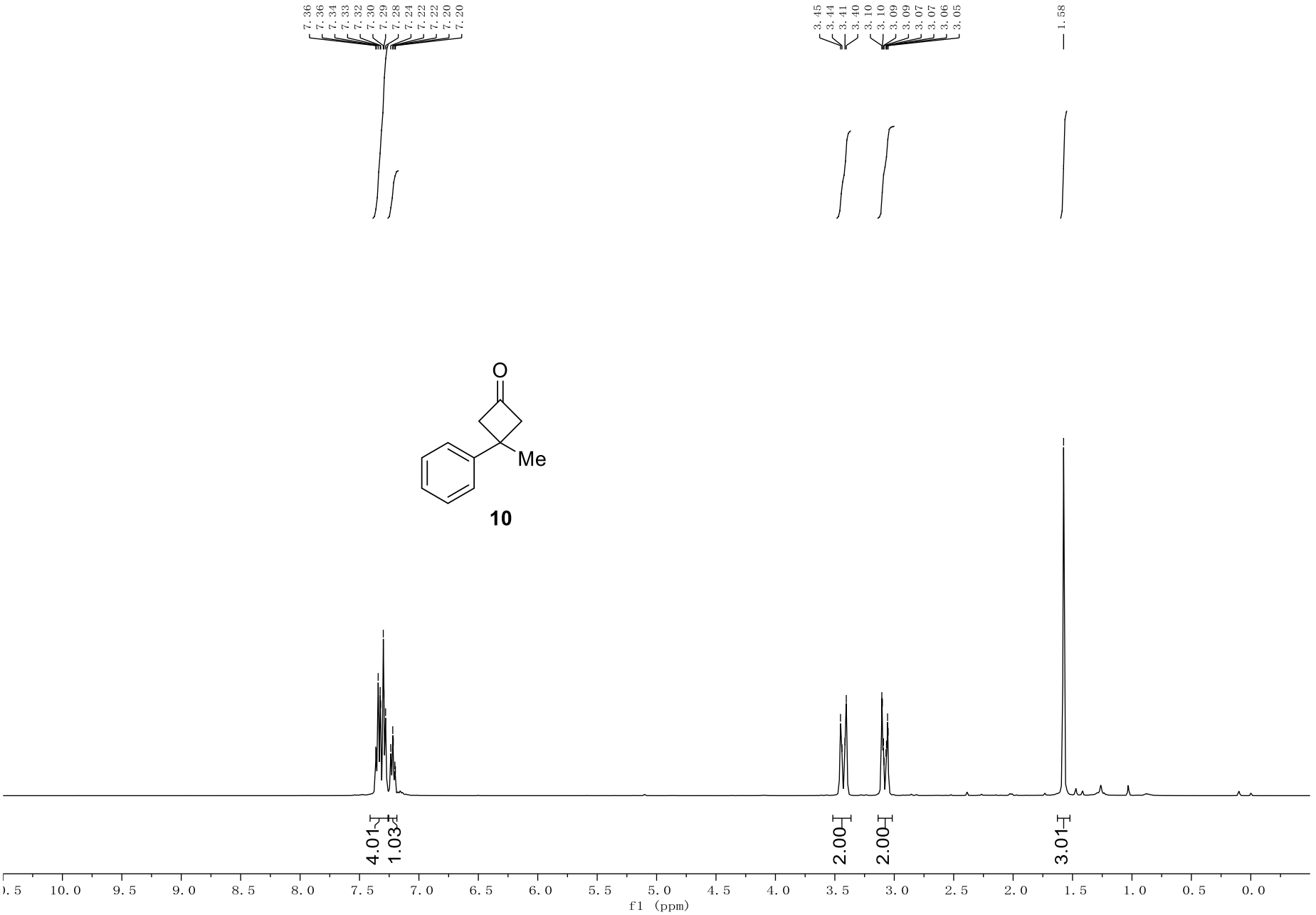

Figure S87 ^{13}C NMR Spectrum of 10, related to Scheme 4

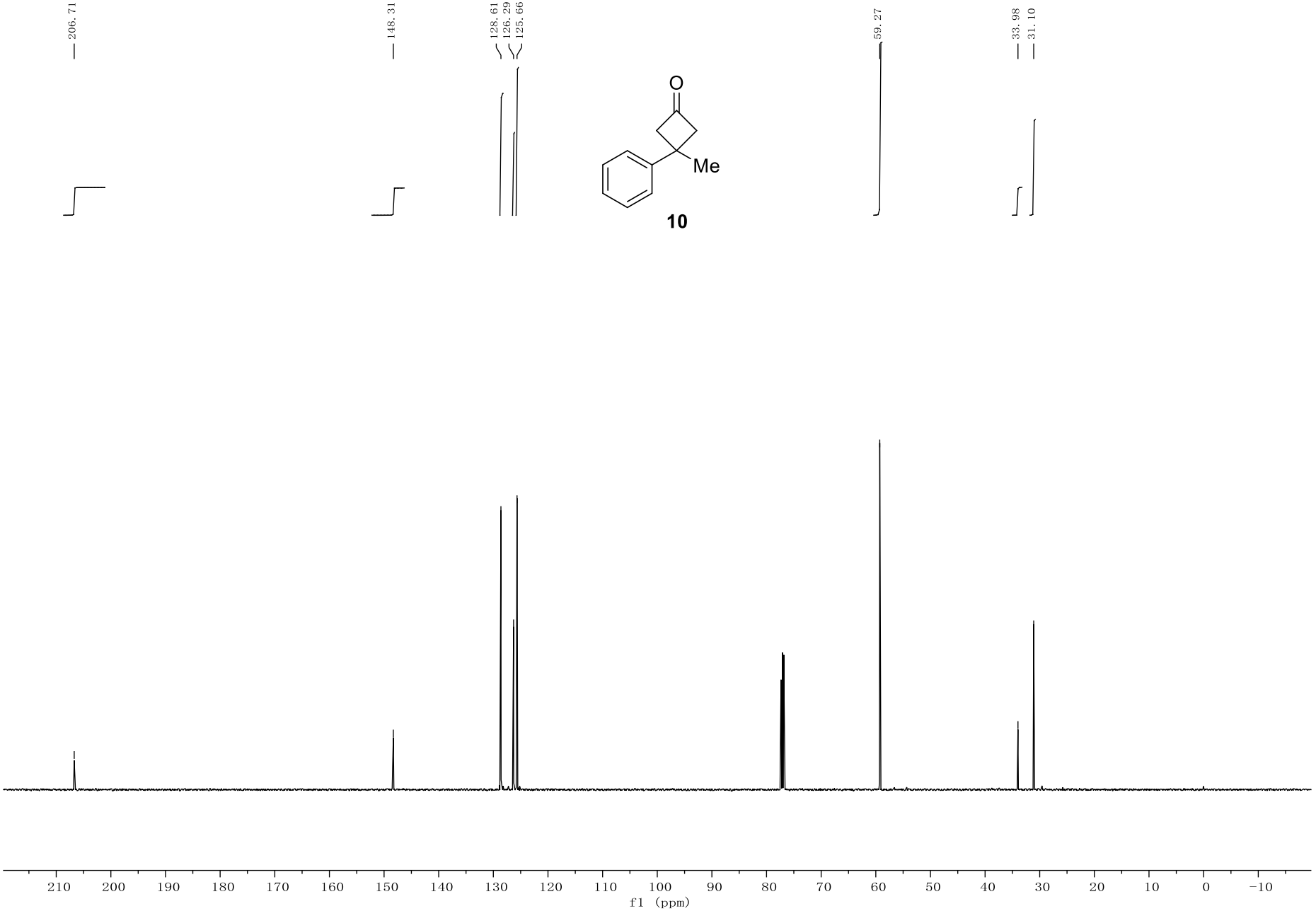

Figure S88 ^{1}H NMR Spectrum of 18, related to Scheme 4

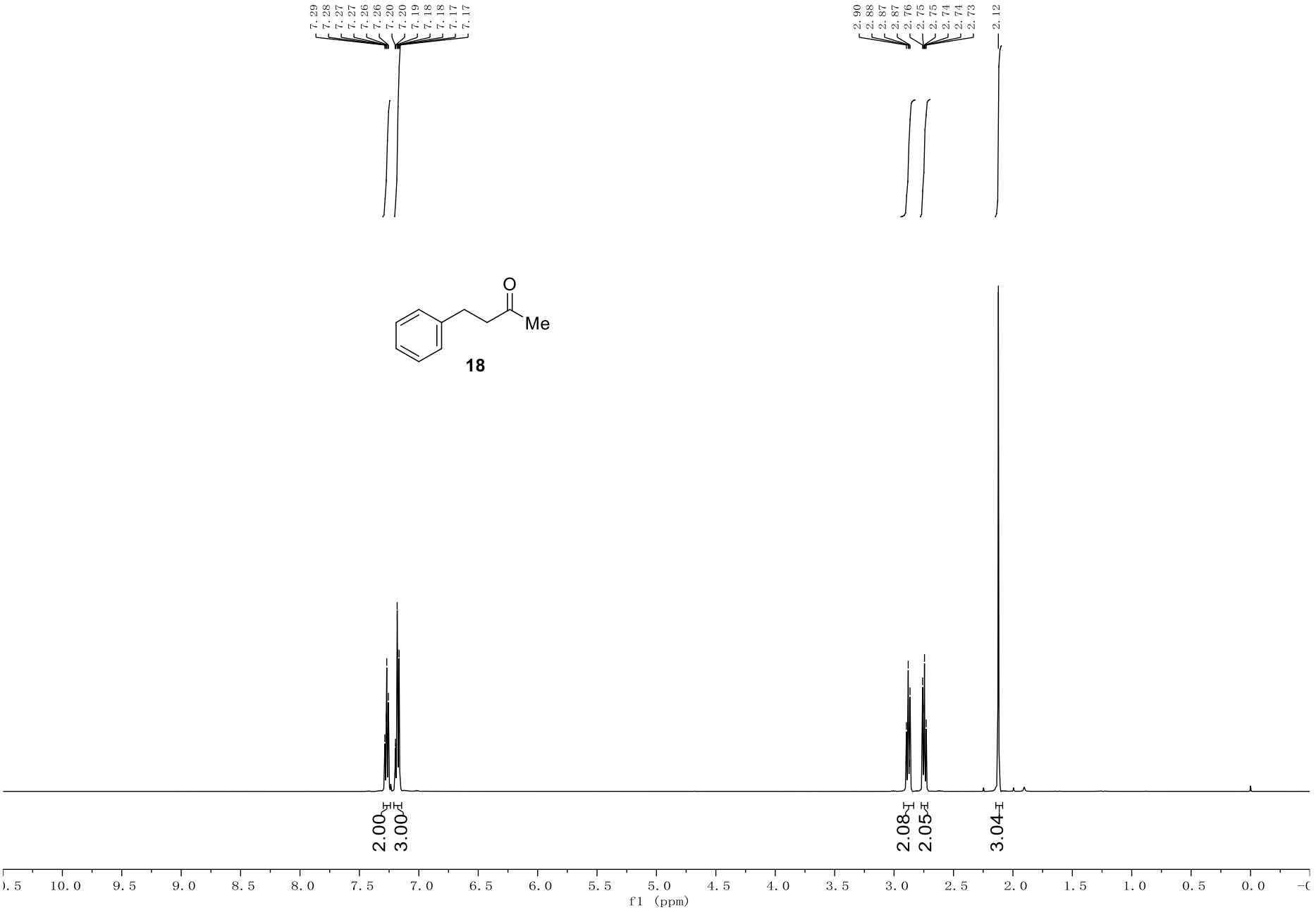

Figure S89 ^{13}C NMR Spectrum of 18, related to Scheme 4

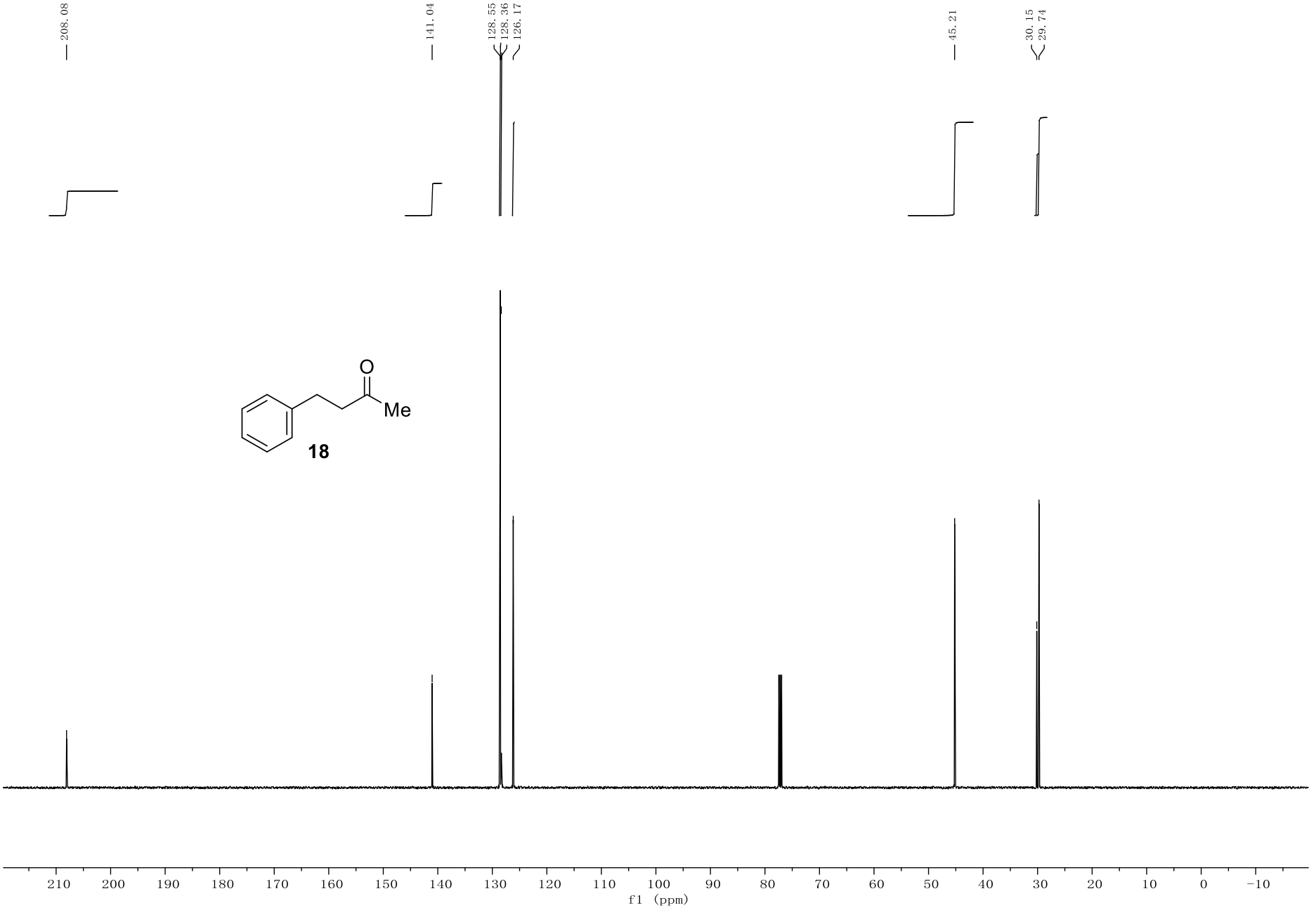

Figure S90 ^{1}H NMR Spectrum of 3ah, related to Scheme 4

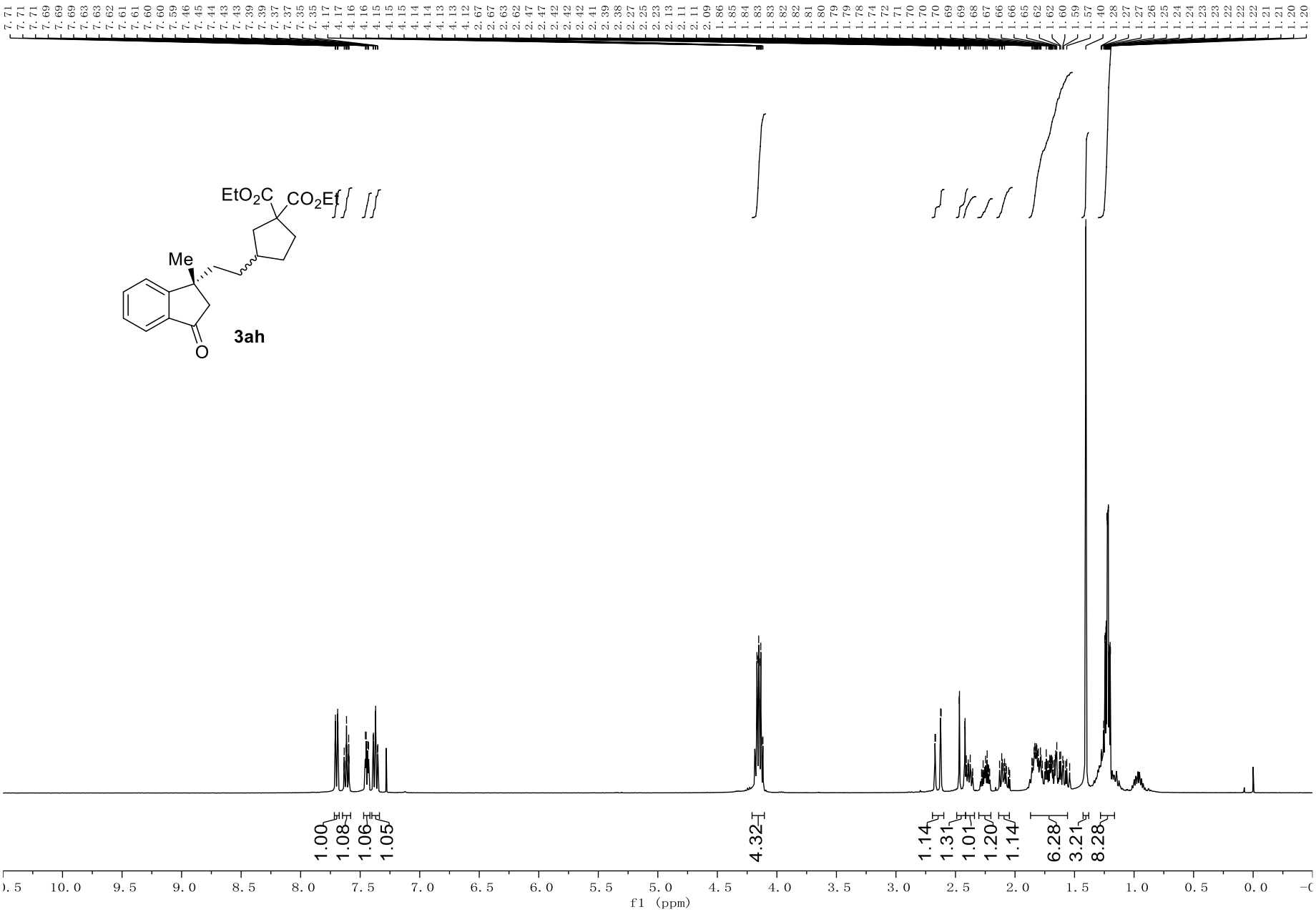

Figure S91 ^{13}C NMR Spectrum of 3ah, related to Scheme 4

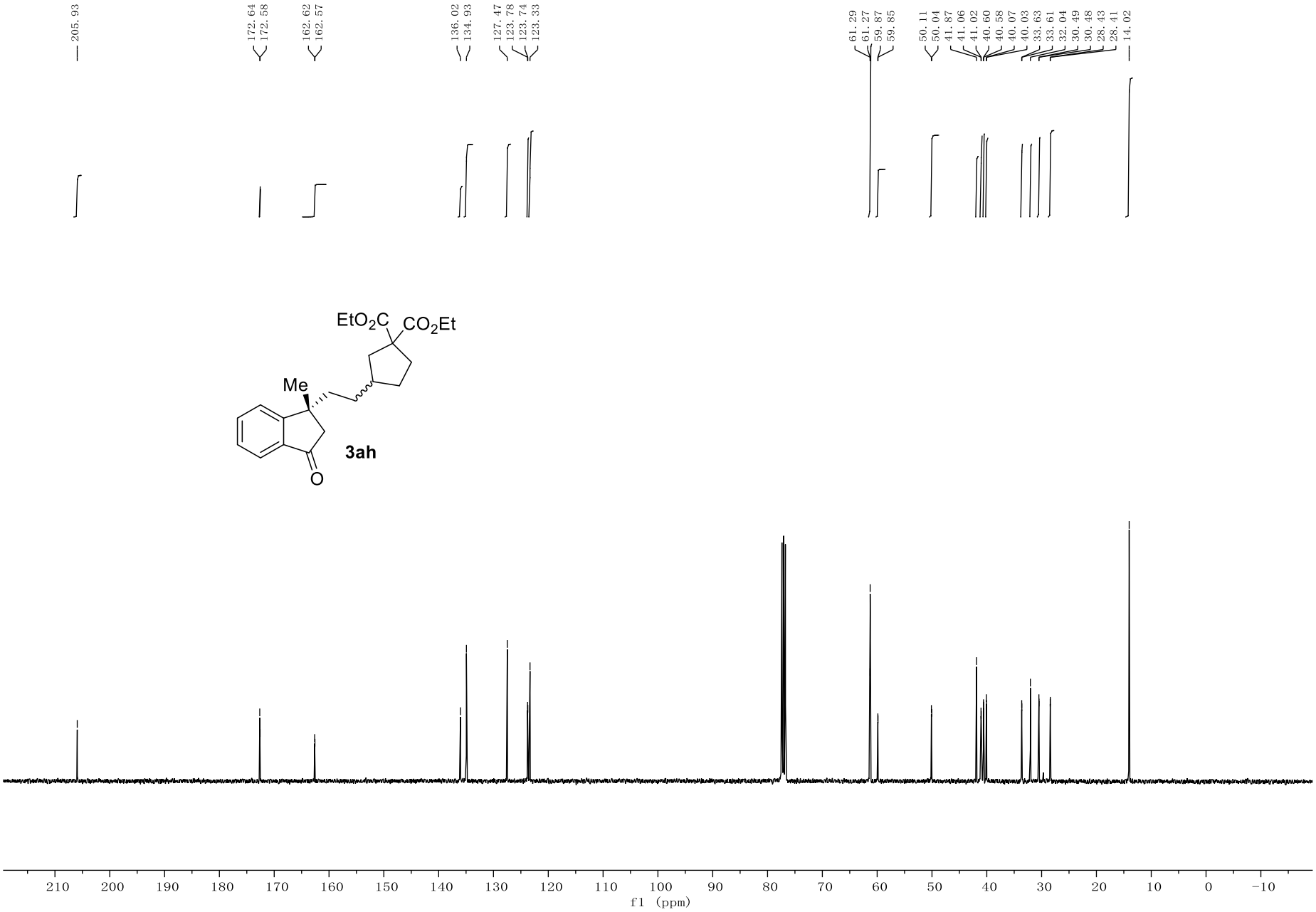

Figure S92 ^{1}H NMR Spectrum of 4, related to Scheme 3

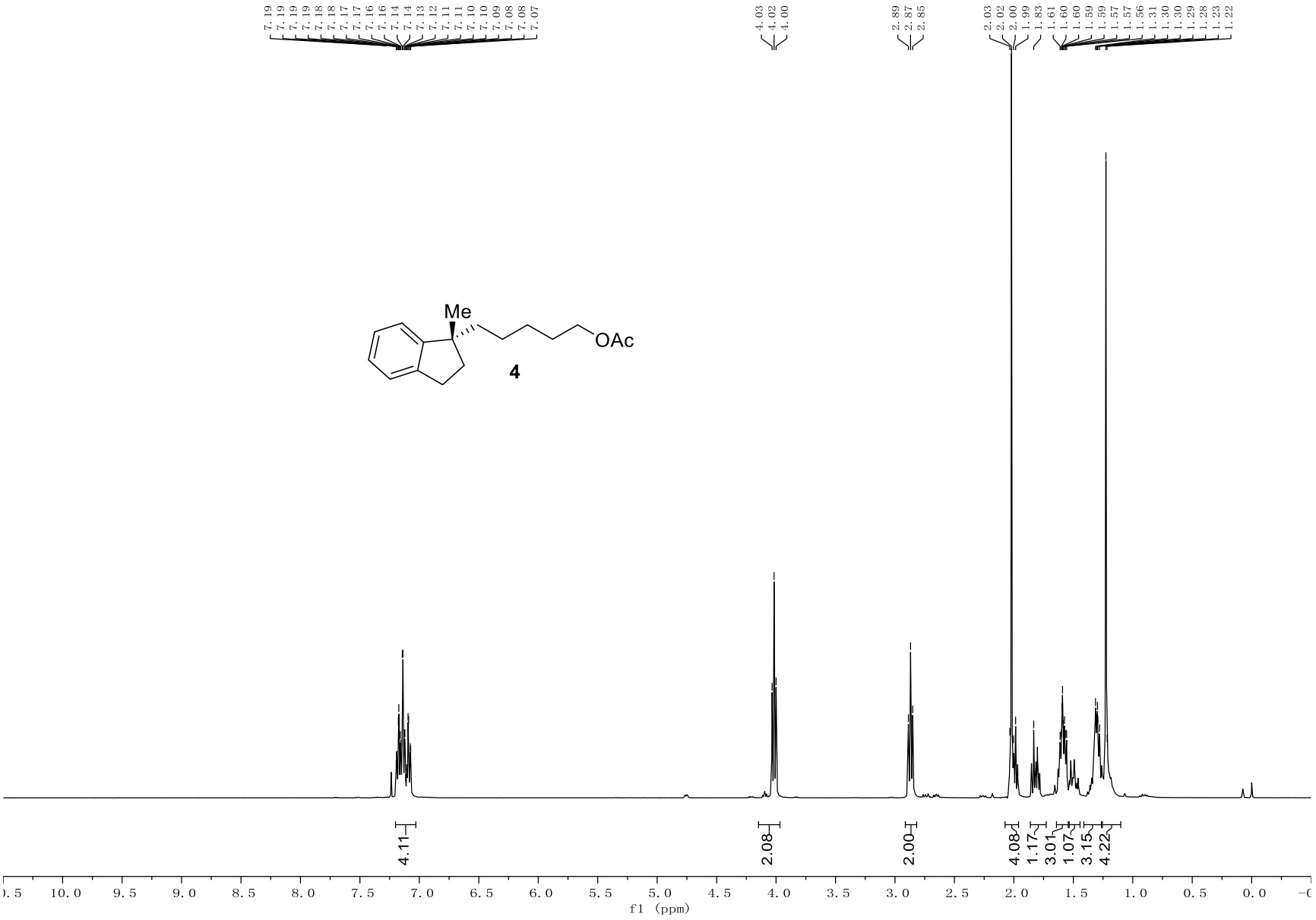

Figure S93 ^{13}C NMR Spectrum of 4, related to Scheme 3

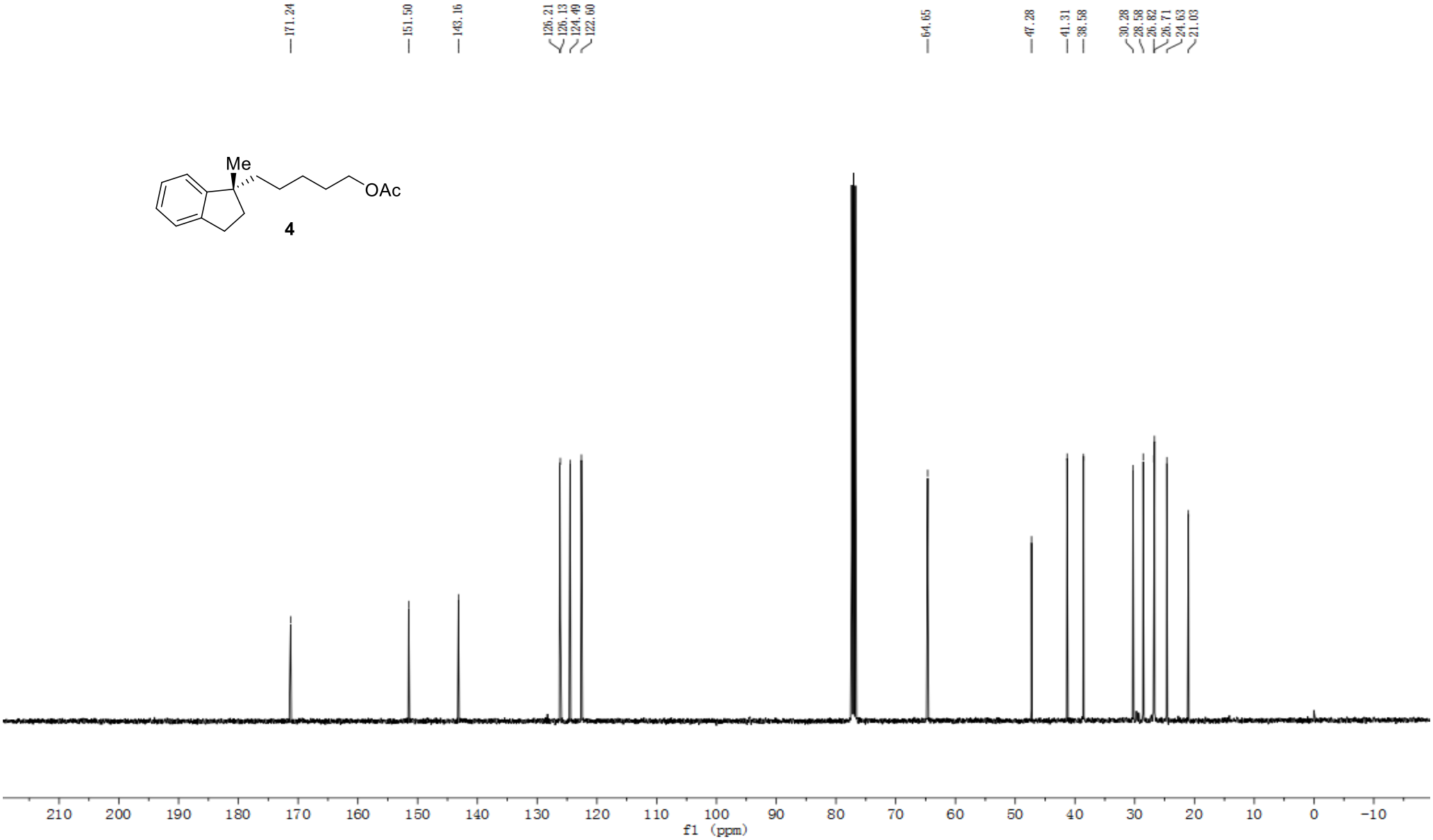

Figure S94 ^{1}H NMR Spectrum of 5, related to Scheme 3

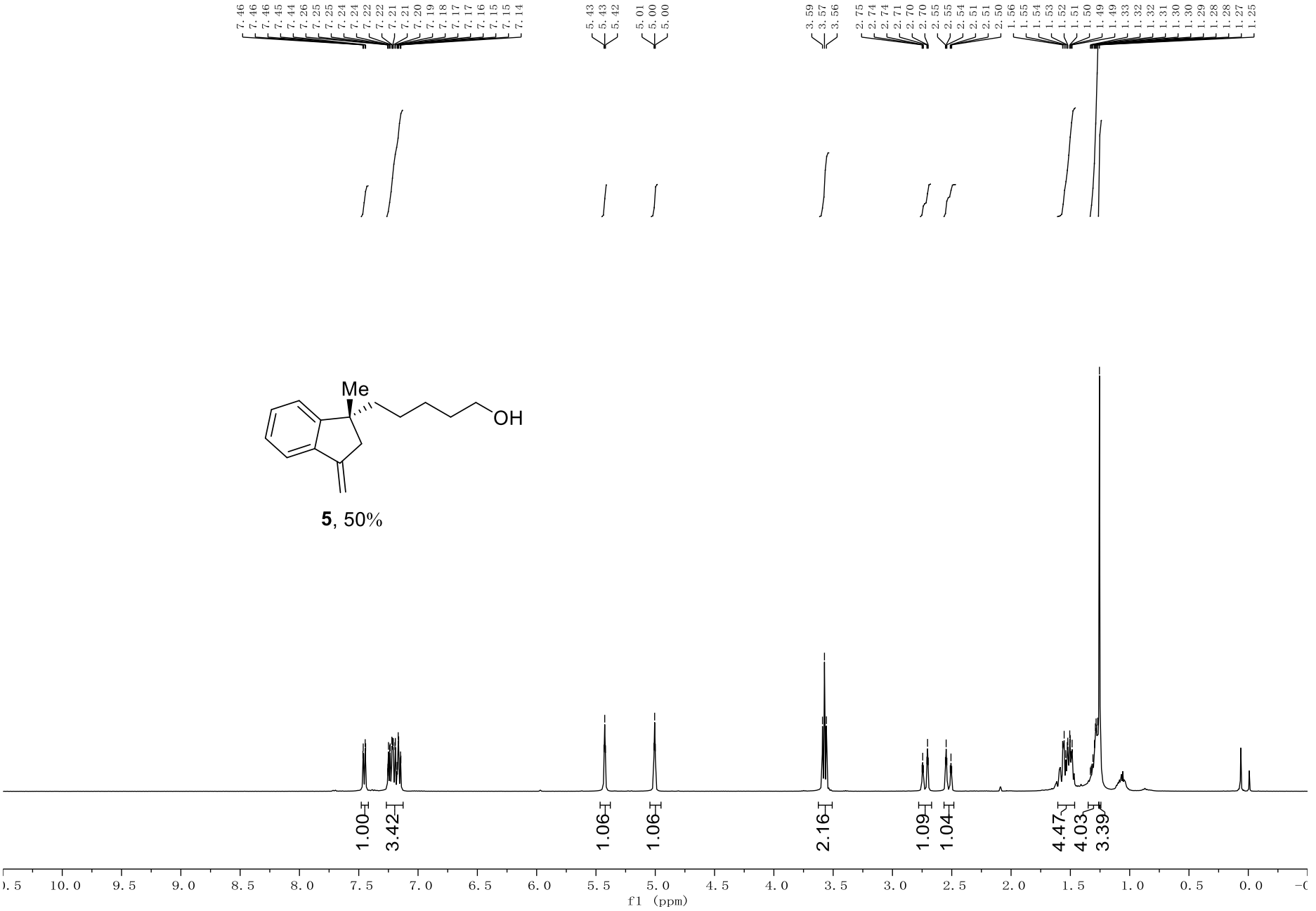

Figure S95 ^{13}C NMR Spectrum of 5, related to Scheme 3

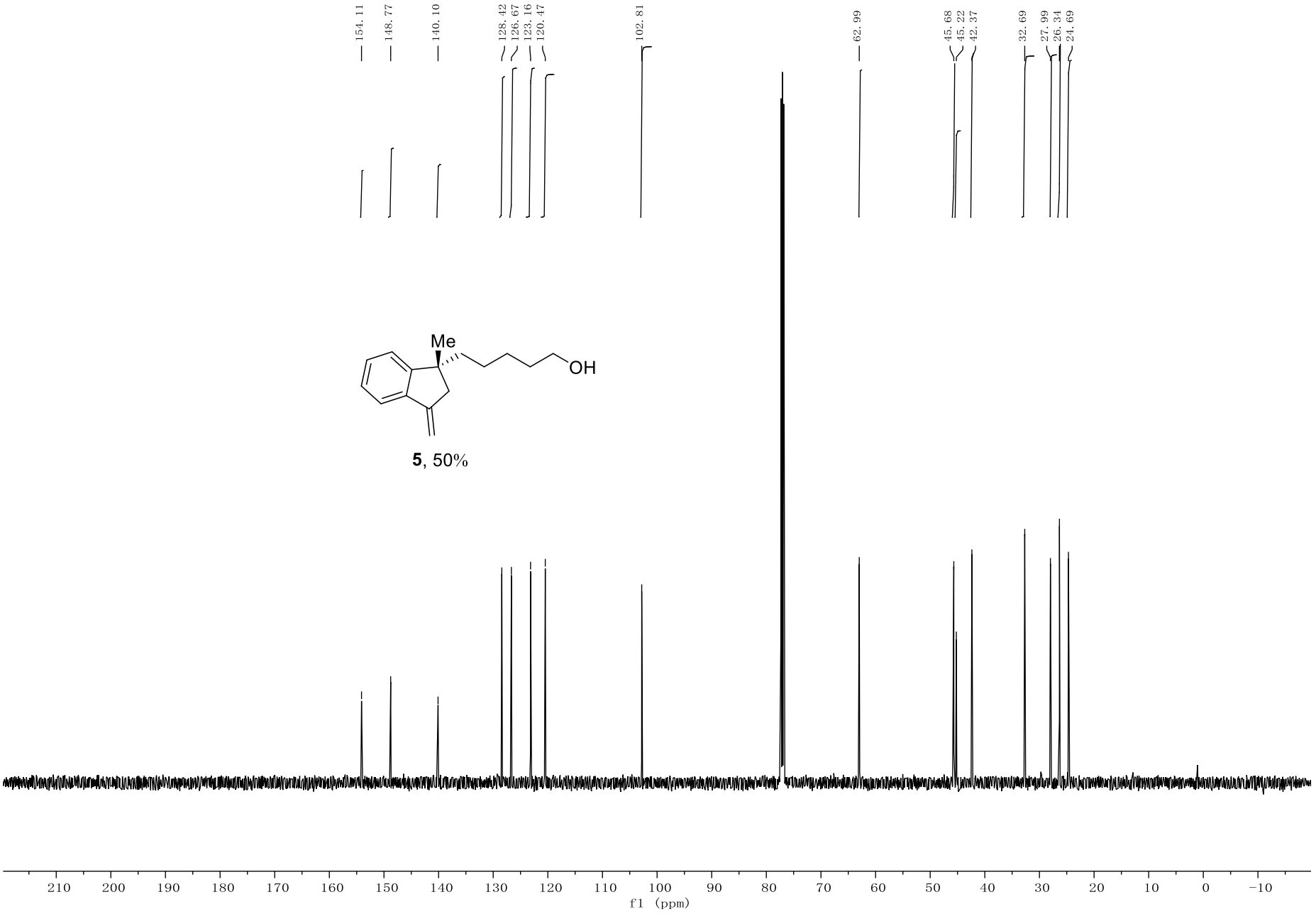

Figure S96 ^{1}H NMR Spectrum of 6, related to Scheme 3

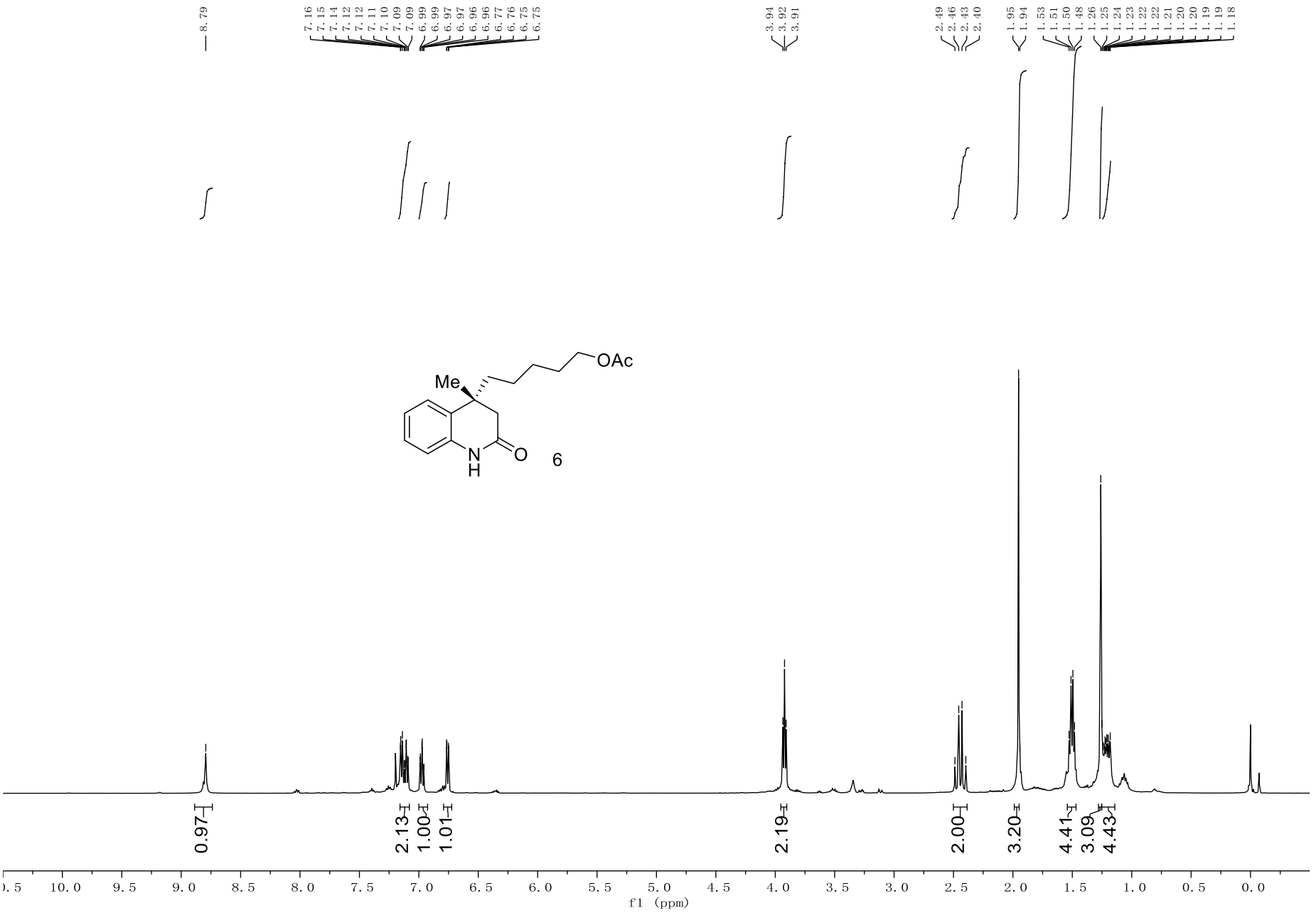

Figure S97 ^{13}C NMR Spectrum of 6, related to Scheme 3

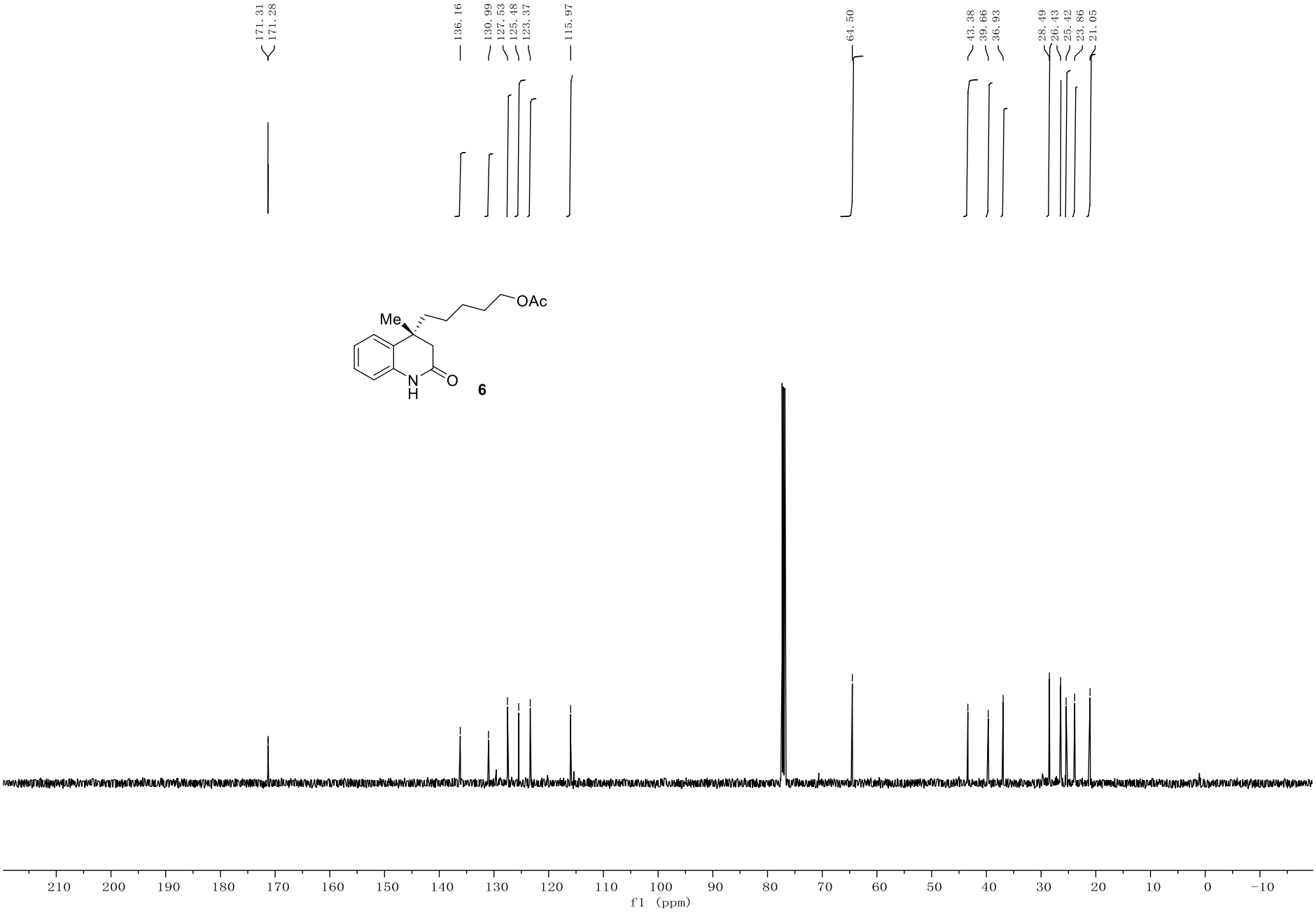

Figure S98 HPLC Data and Chromatograms of 3a, related to Scheme 2

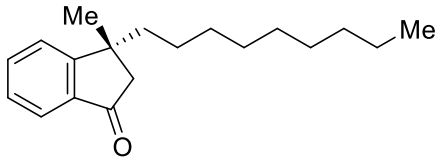

3a

HPLC (Chiralpak IC): t_R= 13.7 (minor), 15.3 (major)
Condition: 95:5 n-Hexane: *i*-PrOH, flow rate 0.5 mL/min, 25℃. 254nm.

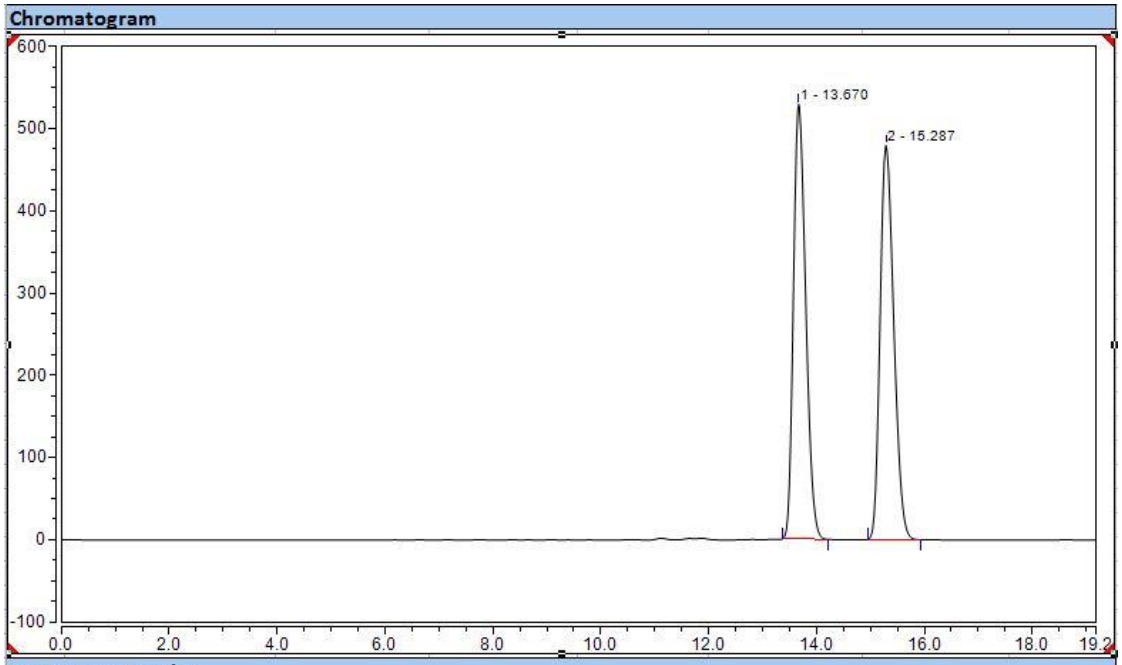

Integration Results

No.	Peak Name	Retention Time min	Area mAU*min	Height mAU	Relative Area %	Relative Height %	Amount n.a.
1		13.670	139.055	528.405	49.73	52.45	n.a.
2		15.287	140.550	479.038	50.27	47.55	n.a.
Total:			**279.606**	**1007.442**	**100.00**	**100.00**	

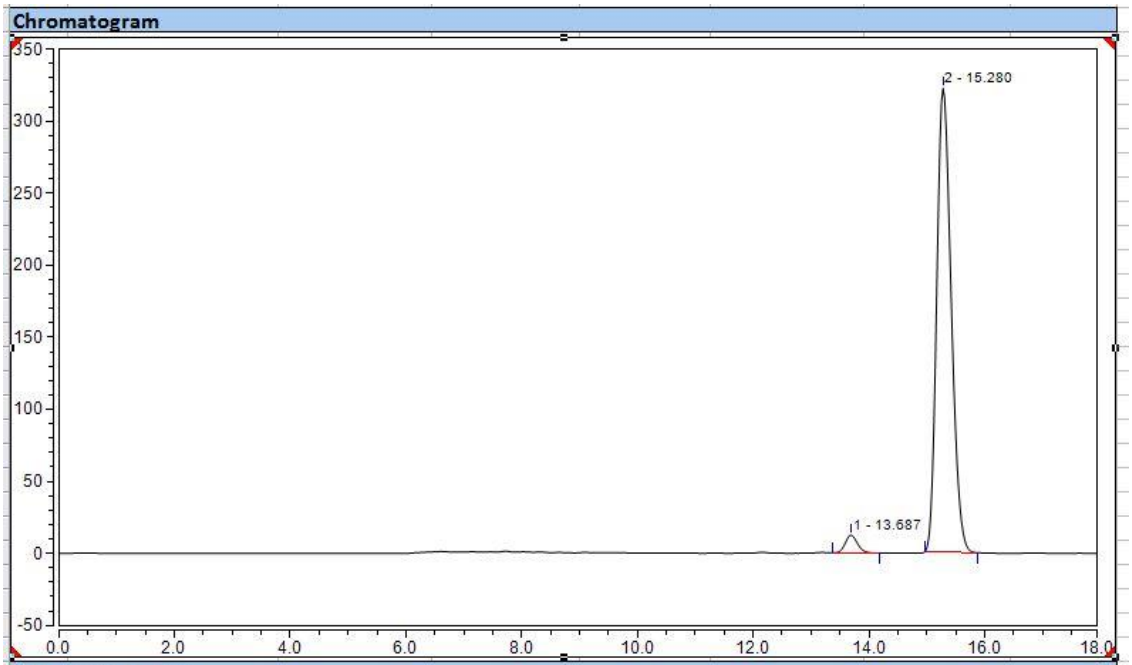

Integration Results

No.	Peak Name	Retention Time min	Area mAU*min	Height mAU	Relative Area %	Relative Height %	Amount n.a.
1		13.687	3.064	12.449	3.19	3.72	n.a.
2		15.280	93.007	322.305	96.81	96.28	n.a.
Total:			**96.071**	**334.754**	**100.00**	**100.00**	

Figure S99 HPLC Data and Chromatograms of 3b, related to Scheme 2

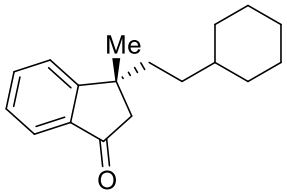

3b

HPLC (Chiralpak IC): t_R= 15.9 (minor), 18.4 (major)
Condition: 95:5 n-Hexane: i-PrOH, flow rate 0.5 mL/min, 25℃.
254nm

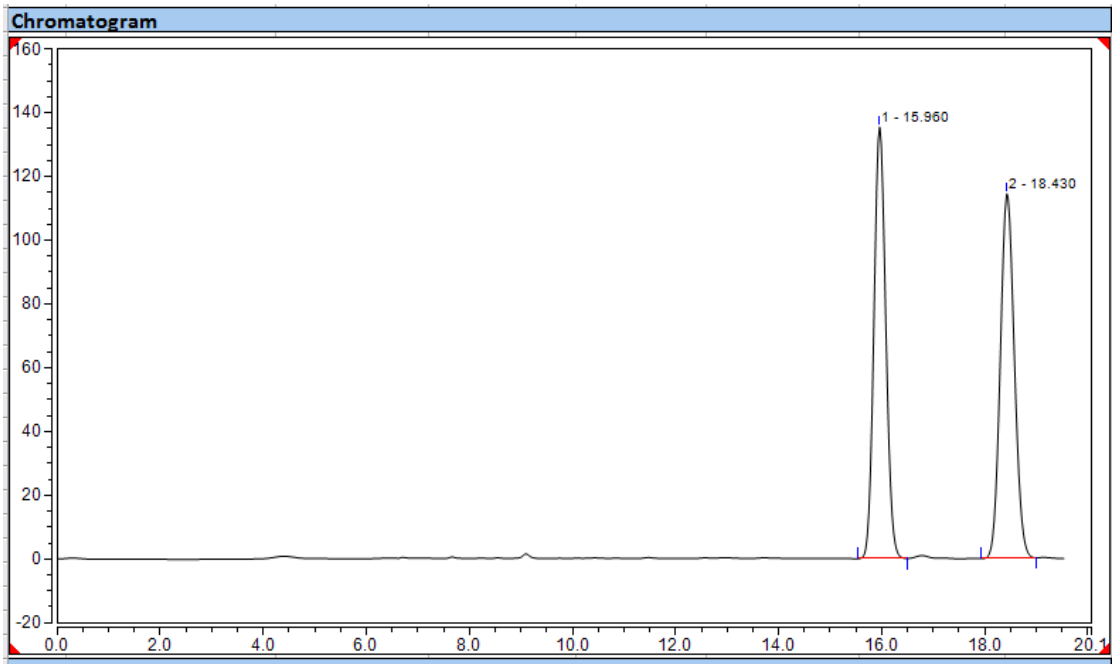

Integration Results

No.	Peak Name	Retention Time min	Area mAU*min	Height mAU	Relative Area %	Relative Height %	Amount n.a.
1		15.960	35.894	135.396	49.86	54.21	n.a.
2		18.430	36.100	114.371	50.14	45.79	n.a.
Total:			**71.993**	**249.767**	**100.00**	**100.00**	

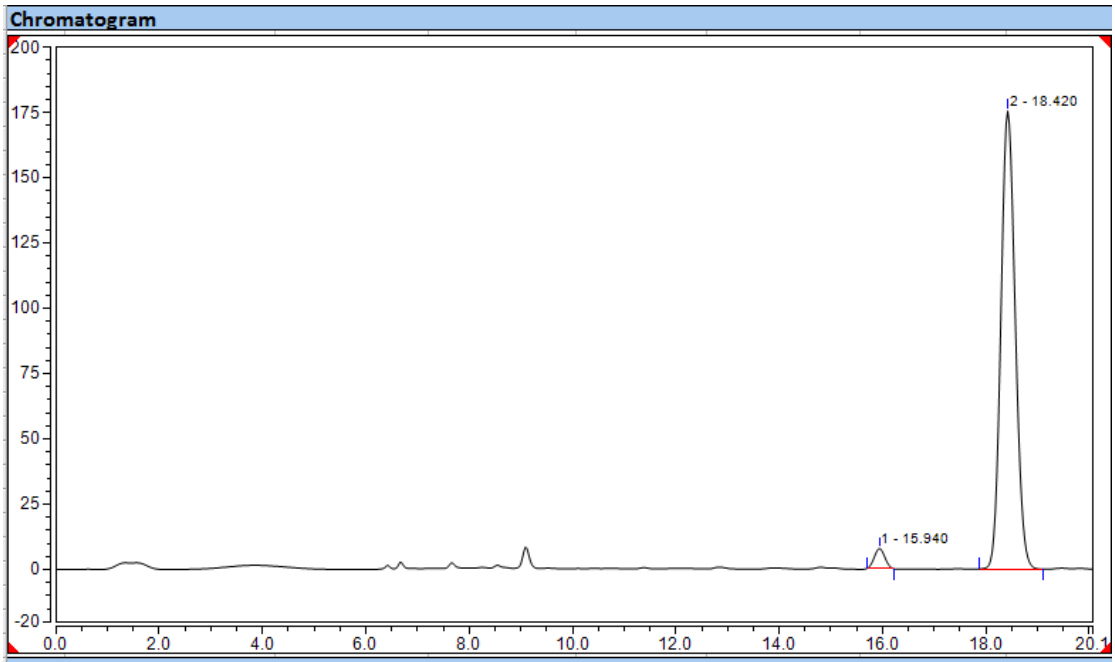

Integration Results

No.	Peak Name	Retention Time min	Area mAU*min	Height mAU	Relative Area %	Relative Height %	Amount n.a.
1		15.940	1.777	7.650	3.06	4.18	n.a.
2		18.420	56.347	175.441	96.94	95.82	n.a.
Total:			**58.125**	**183.091**	**100.00**	**100.00**	

Figure S100 HPLC Data and Chromatograms of 3c, related to Scheme 2

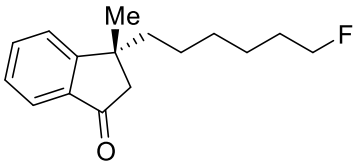

HPLC (Chiralpak IC): t_R= 32.0 (minor), 32.6 (major)
Condition: 95:5 n-Hexane: *i*-PrOH, flow rate 0.5 mL/min, 25℃.
254nm

3c

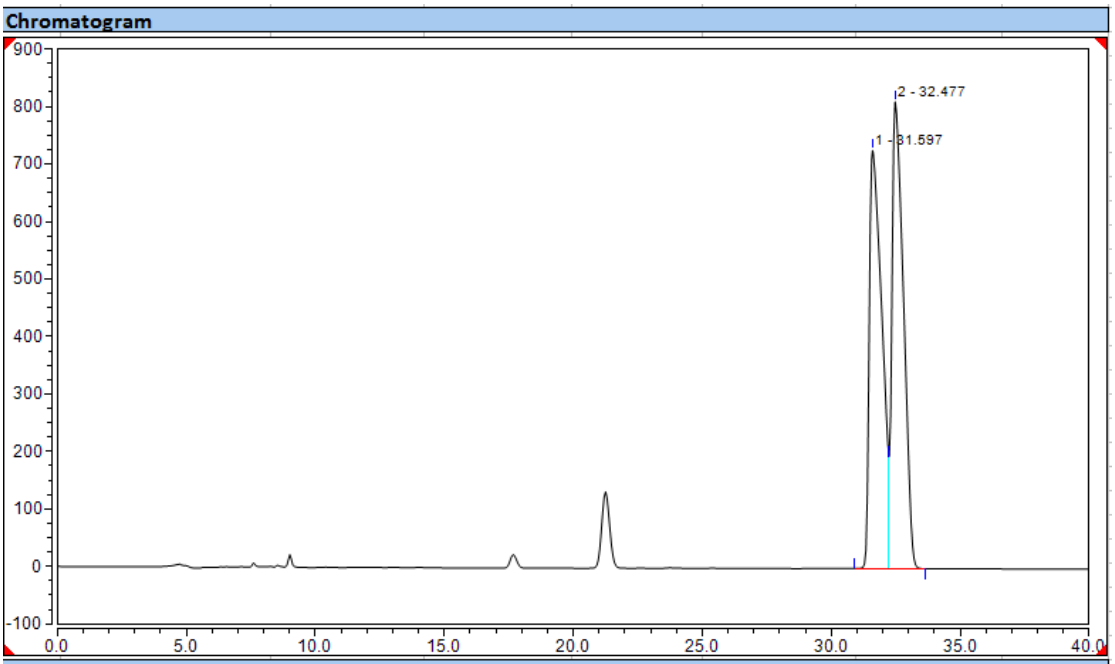

Integration Results

No.	Peak Name	Retention Time min	Area mAU*min	Height mAU	Relative Area %	Relative Height %	Amount n.a.
1		31.597	411.303	727.597	49.45	47.25	n.a.
2		32.477	420.501	812.442	50.55	52.75	n.a.
Total:			**831.805**	**1540.038**	**100.00**	**100.00**	

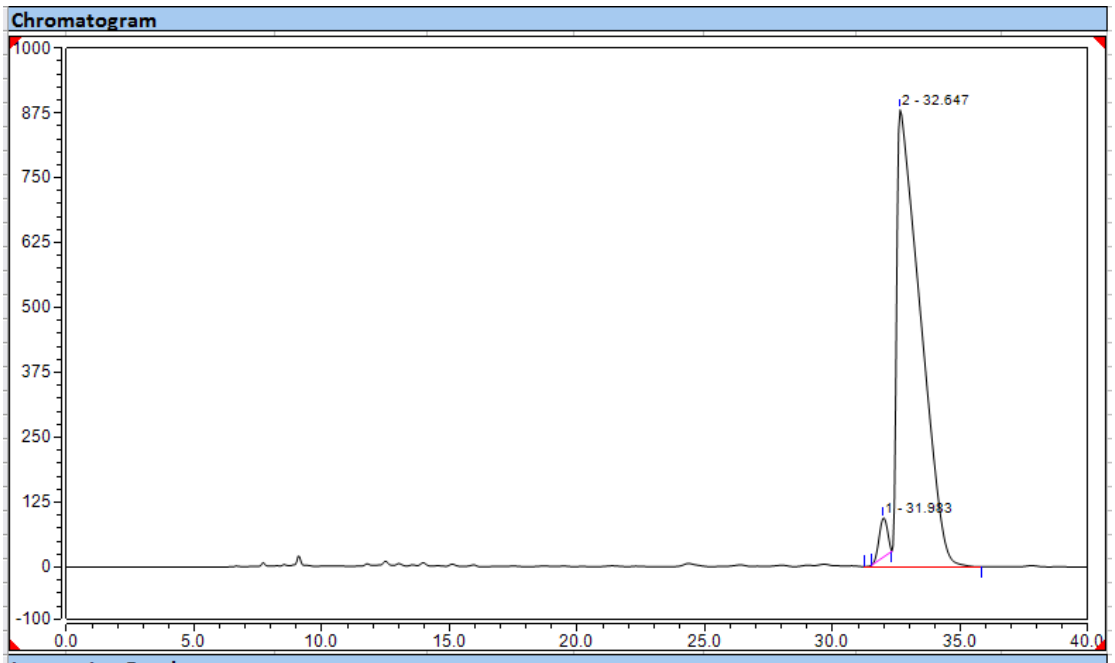

Integration Results

No.	Peak Name	Retention Time min	Area mAU*min	Height mAU	Relative Area %	Relative Height %	Amount n.a.
1		31.983	28.389	75.615	2.89	7.91	n.a.
2		32.647	952.461	880.495	97.11	92.09	n.a.
Total:			**980.850**	**956.110**	**100.00**	**100.00**	

Figure S101 HPLC Data and Chromatograms of 3d, related to Scheme 2

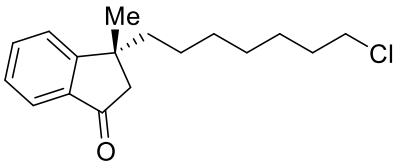

HPLC (Chiralpak IC): t_R= 29.0 (minor), 30.2 (major)
Condition: 95:5 n-Hexane: i-PrOH, flow rate 0.5 mL/min, 25℃.
254nm

3d

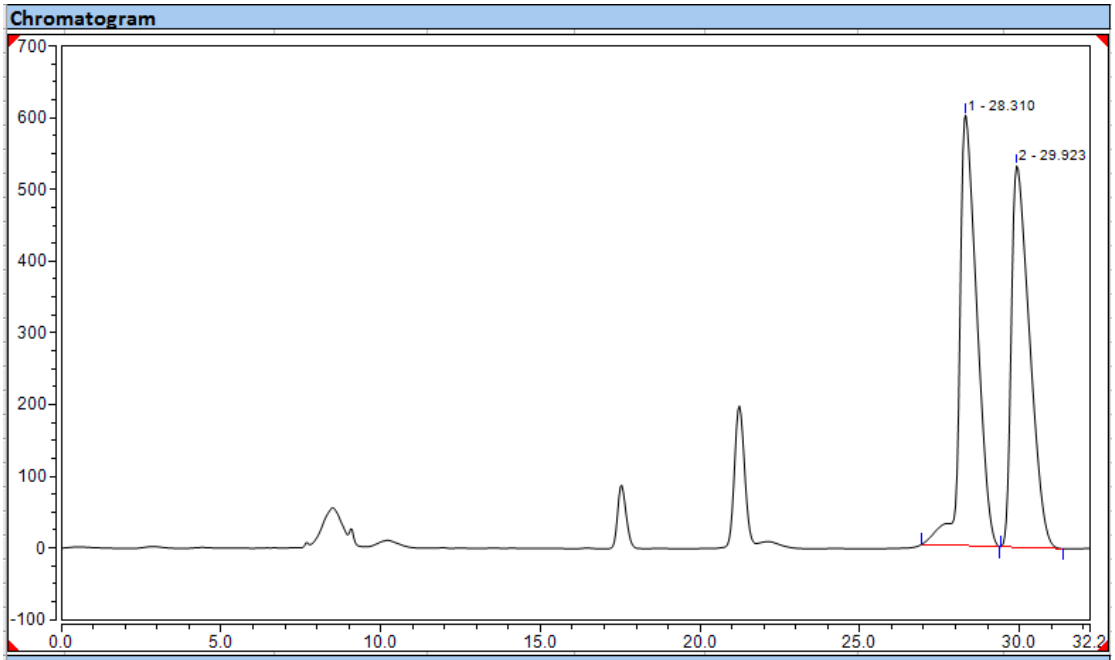

Integration Results

No.	Peak Name	Retention Time min	Area mAU*min	Height mAU	Relative Area %	Relative Height %	Amount n.a.
1		28.310	376.171	600.416	51.64	52.99	n.a.
2		29.923	352.336	532.680	48.36	47.01	n.a.
Total:			**728.507**	**1133.096**	**100.00**	**100.00**	

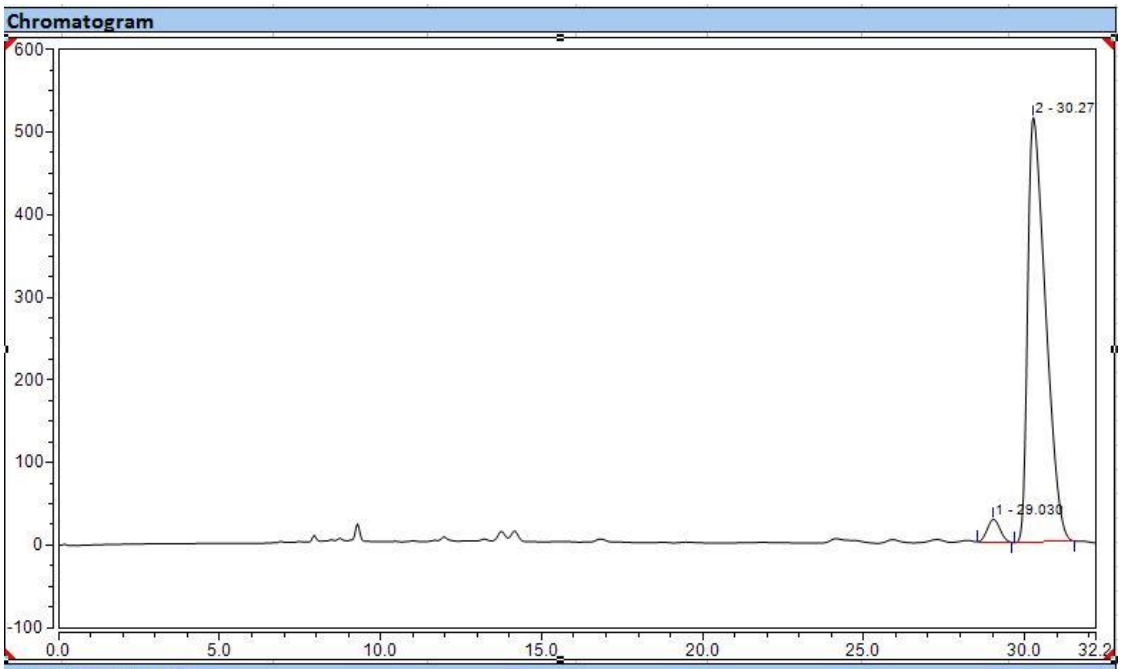

Integration Results

No.	Peak Name	Retention Time min	Area mAU*min	Height mAU	Relative Area %	Relative Height %	Amount n.a.
1		29.030	12.586	27.488	3.67	5.08	n.a.
2		30.270	330.820	513.855	96.33	94.92	n.a.
Total:			**343.406**	**541.344**	**100.00**	**100.00**	

Figure S102 HPLC Data and Chromatograms of 3e, related to Scheme 2

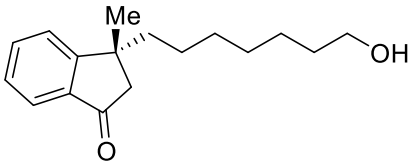

HPLC (Chiralpak ADH): t_R= 12.6 (minor), 11.7 (major)
Condition: 80:20 n-Hexane: i-PrOH, flow rate 0.5 mL/min, 25°C.
254nm

3e

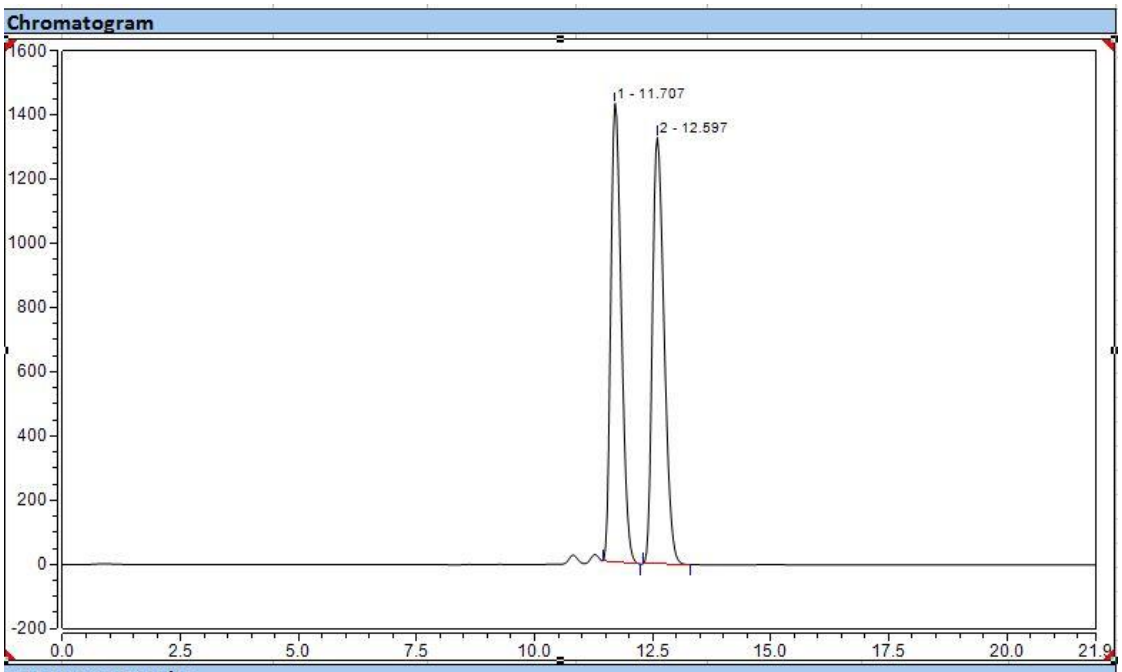

Integration Results

No.	Peak Name	Retention Time min	Area mAU*min	Height mAU	Relative Area %	Relative Height %	Amount n.a.
1		11.707	369.963	1428.718	49.24	51.82	n.a.
2		12.597	381.390	1328.358	50.76	48.18	n.a.
Total:			**751.353**	**2757.076**	**100.00**	**100.00**	

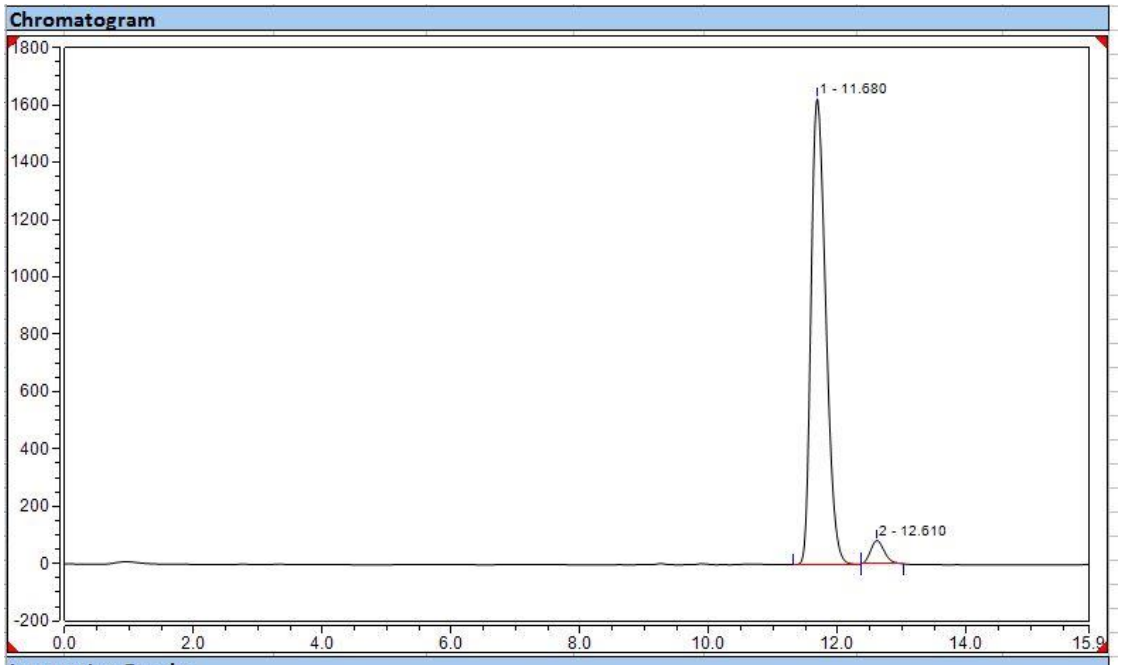

Integration Results

No.	Peak Name	Retention Time min	Area mAU*min	Height mAU	Relative Area %	Relative Height %	Amount n.a.
1		11.680	430.515	1624.430	95.48	95.19	n.a.
2		12.610	20.388	82.012	4.52	4.81	n.a.
Total:			**450.903**	**1706.442**	**100.00**	**100.00**	

Figure S103 HPLC Data and Chromatograms of 3f, related to Scheme 2

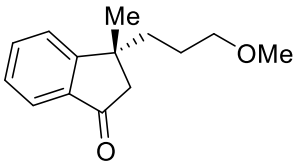

HPLC (Chiralcel OJH): t_R= 12.6 (minor), 12.0 (major)
Condition: 90:10 n-Hexane: i-PrOH, flow rate 0.5 mL/min, 25℃.
254nm

3f

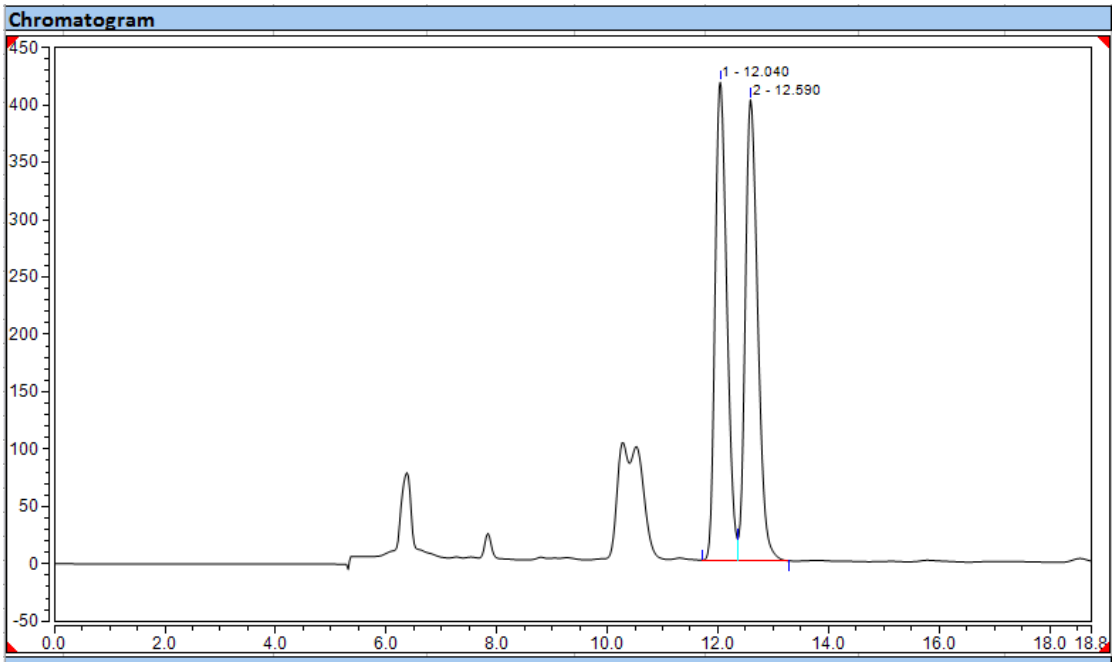

Integration Results

No.	Peak Name	Retention Time min	Area mAU*min	Height mAU	Relative Area %	Relative Height %	Amount n.a.
1		12.040	102.050	416.909	49.29	50.92	n.a.
2		12.590	104.978	401.775	50.71	49.08	n.a.
Total:			**207.028**	**818.684**	**100.00**	**100.00**	

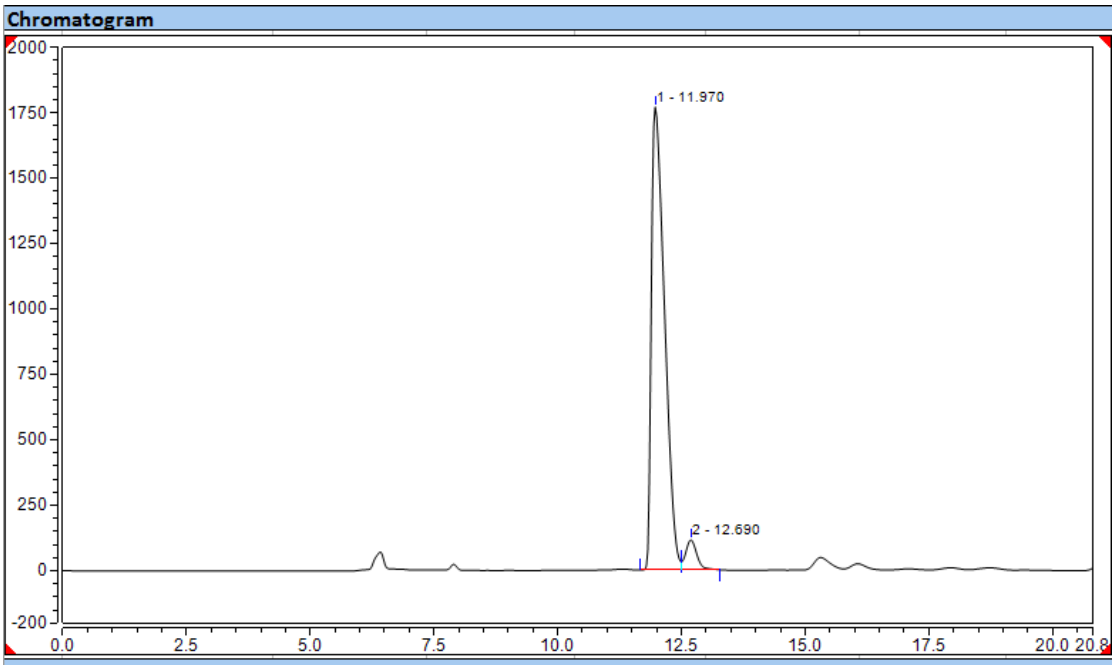

Integration Results

No.	Peak Name	Retention Time min	Area mAU*min	Height mAU	Relative Area %	Relative Height %	Amount n.a.
1		11.970	545.963	1769.385	94.79	93.90	n.a.
2		12.690	30.013	114.967	5.21	6.10	n.a.
Total:			**575.976**	**1884.352**	**100.00**	**100.00**	

Figure S104 HPLC Data and Chromatograms of 3g, related to Scheme 2

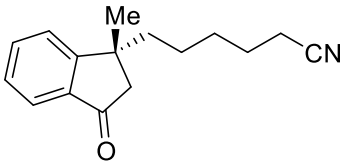

HPLC (Chiralcel ODH): t_R= 27.6 (minor), 25.4 (major)
Condition: 85:15 n-Hexane: i-PrOH, flow rate 0.5 mL/min, 25°C.
254nm

3g

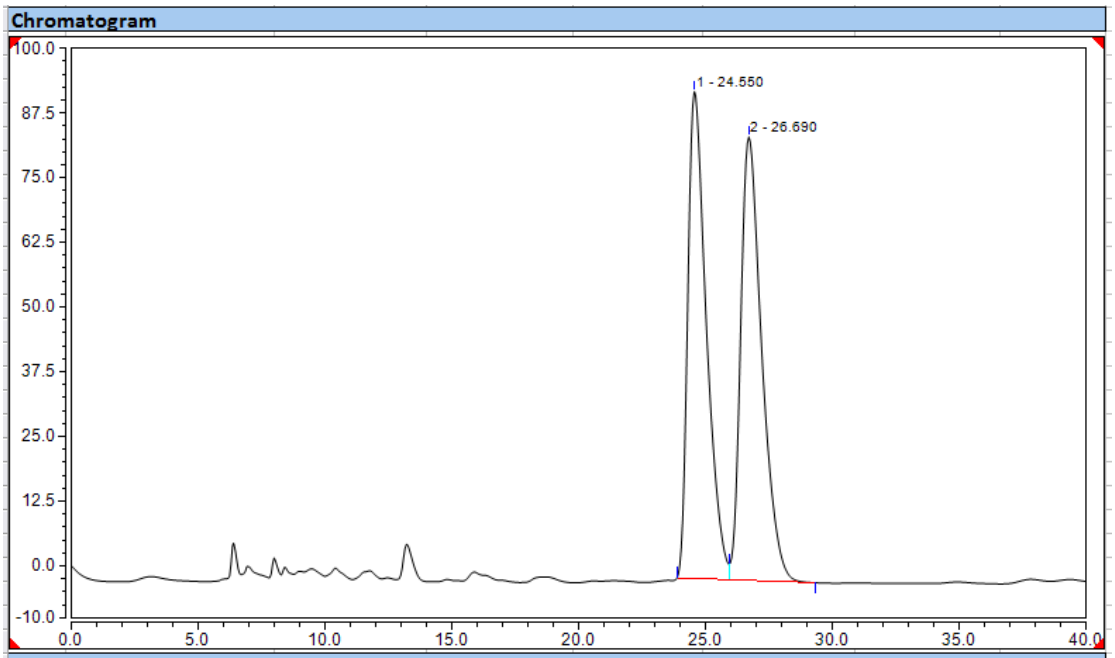

Integration Results

No.	Peak Name	Retention Time min	Area mAU*min	Height mAU	Relative Area %	Relative Height %	Amount n.a.
1		24.550	79.825	94.083	49.16	52.33	n.a.
2		26.690	82.557	85.710	50.84	47.67	n.a.
Total:			**162.382**	**179.793**	**100.00**	**100.00**	

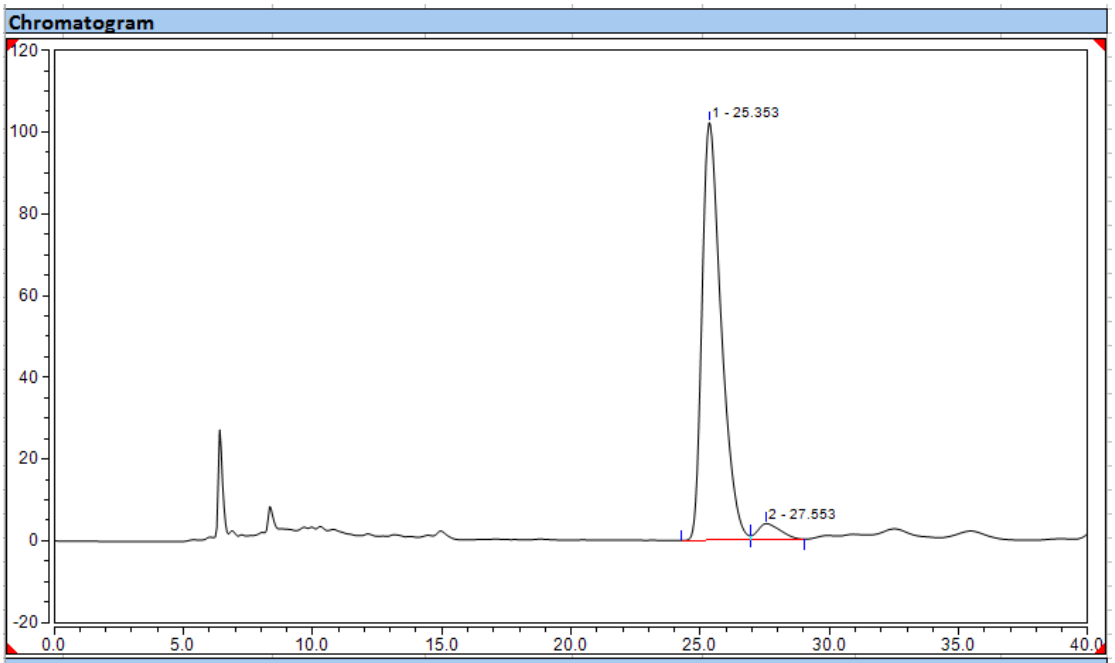

Integration Results

No.	Peak Name	Retention Time min	Area mAU*min	Height mAU	Relative Area %	Relative Height %	Amount n.a.
1		25.353	88.021	102.191	95.66	96.30	n.a.
2		27.553	3.998	3.930	4.34	3.70	n.a.
Total:			**92.019**	**106.121**	**100.00**	**100.00**	

Figure S105 HPLC Data and Chromatograms of 3h, related to Scheme 2

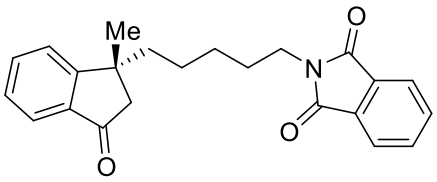

3h

HPLC (Chiralpak ADH): t_R= 30.2 (minor), 31.4 (major)
Condition: 85:15 n-Hexane: i-PrOH, flow rate 0.5 mL/min, 25℃. 254nm

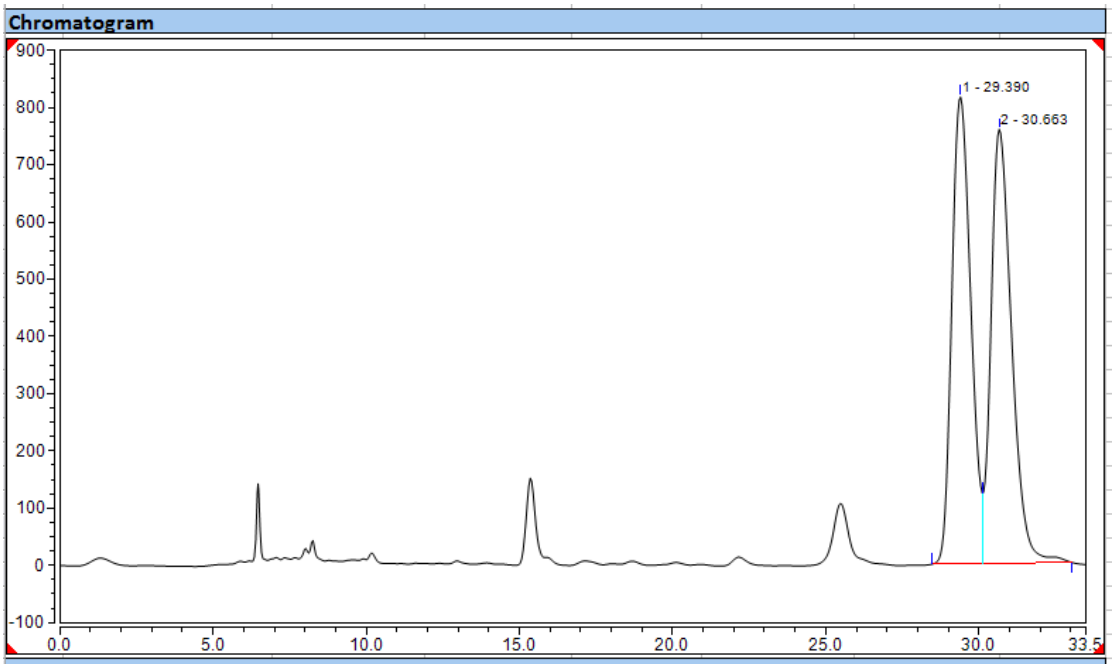

Integration Results

No.	Peak Name	Retention Time min	Area mAU*min	Height mAU	Relative Area %	Relative Height %	Amount n.a.
1		29.390	583.964	816.460	49.50	51.83	n.a.
2		30.663	595.781	758.805	50.50	48.17	n.a.
Total:			**1179.745**	**1575.265**	**100.00**	**100.00**	

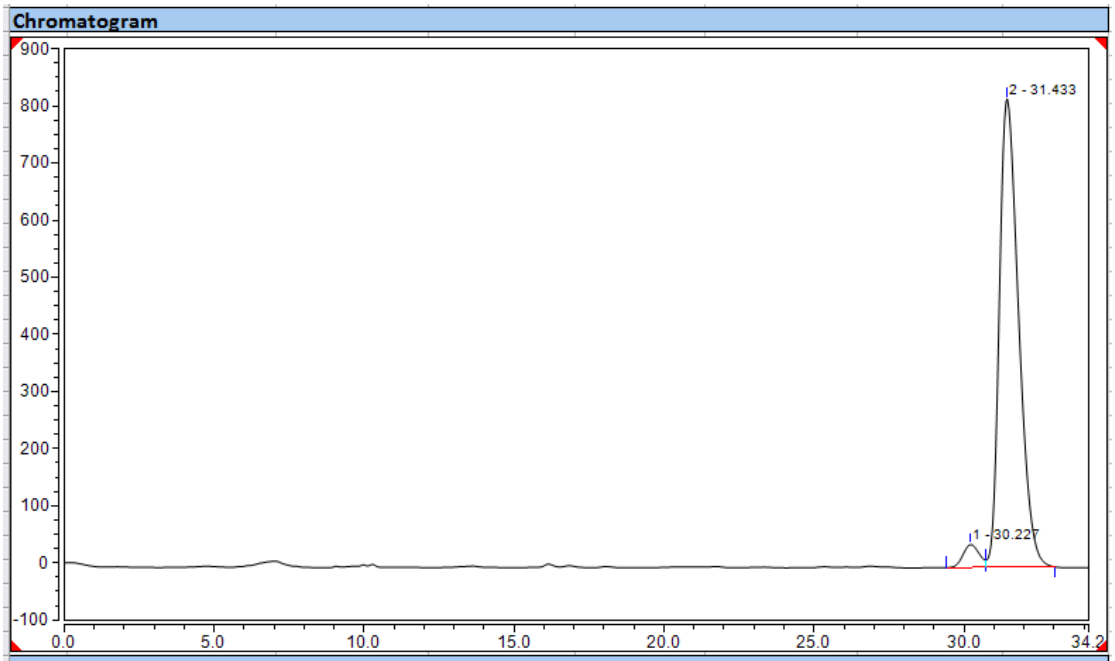

Integration Results

No.	Peak Name	Retention Time min	Area mAU*min	Height mAU	Relative Area %	Relative Height %	Amount n.a.
1		30.227	25.334	40.398	3.99	4.69	n.a.
2		31.433	610.039	820.129	96.01	95.31	n.a.
Total:			**635.373**	**860.527**	**100.00**	**100.00**	

Figure S106 HPLC Data and Chromatograms of 3i, related to Scheme 2

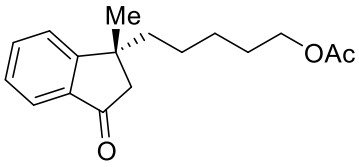

3i

HPLC (Chiralpak IB): t_R= 26.0 (minor), 22.4 (major)
Condition: 95:5 n-Hexane: i-PrOH, flow rate 0.4 mL/min, 25°C.
254nm

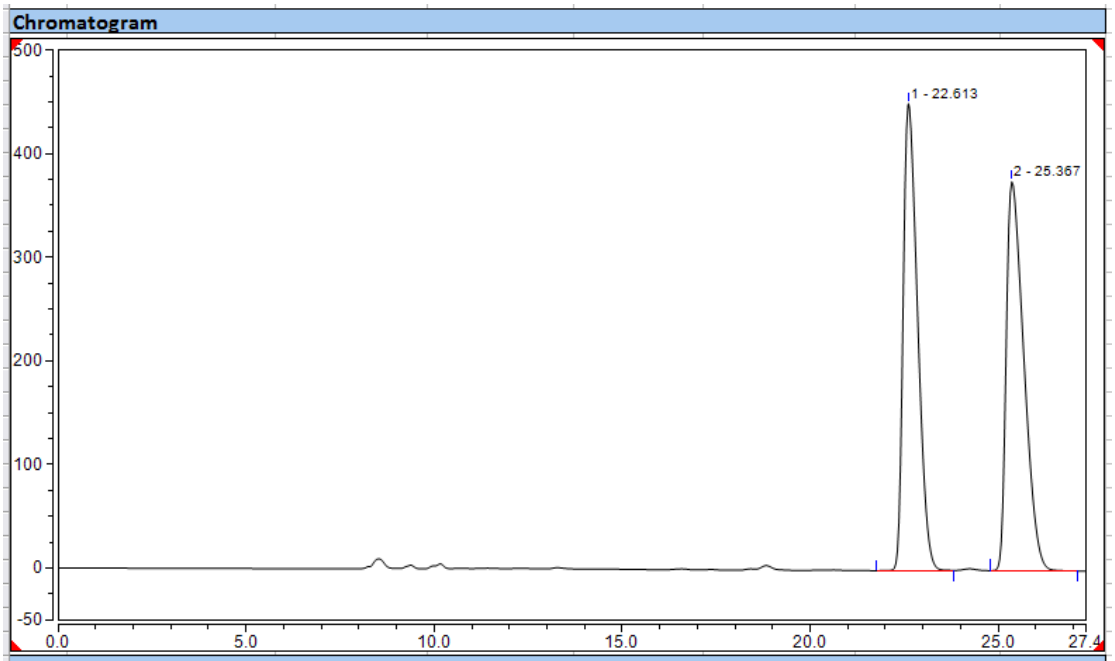

Integration Results

No.	Peak Name	Retention Time min	Area mAU*min	Height mAU	Relative Area %	Relative Height %	Amount n.a.
1		22.613	199.405	450.789	49.48	54.53	n.a.
2		25.367	203.572	375.871	50.52	45.47	n.a.
Total:			**402.977**	**826.660**	**100.00**	**100.00**	

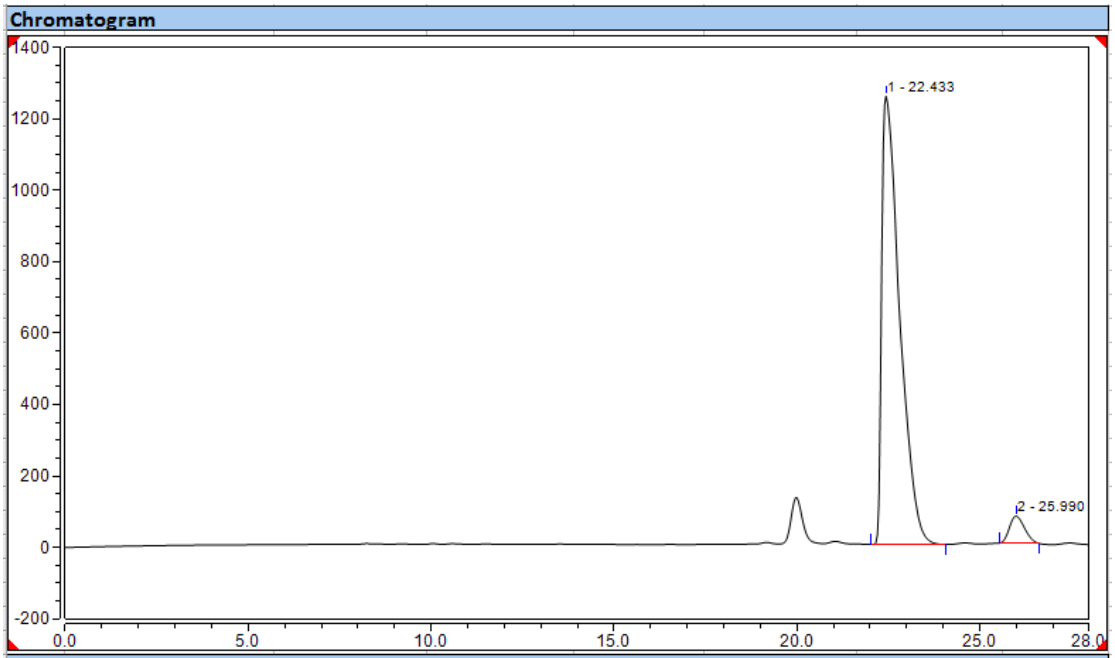

Integration Results

No.	Peak Name	Retention Time min	Area mAU*min	Height mAU	Relative Area %	Relative Height %	Amount n.a.
1		22.433	712.366	1254.962	95.17	94.29	n.a.
2		25.990	36.122	75.955	4.83	5.71	n.a.
Total:			**748.488**	**1330.917**	**100.00**	**100.00**	

Figure S107 HPLC Data and Chromatograms of 3j, related to Scheme 2

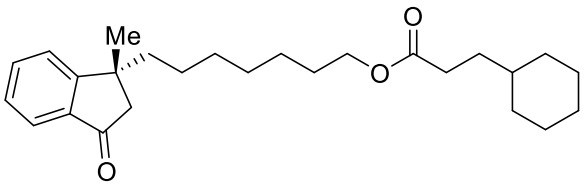

3j

HPLC (Chiralpak ADH): t_R= 19.8 (minor),18.4 (major)
Condition: 95:5 n-Hexane: i-PrOH, flow rate 0.5 mL/min, 25°C.
254nm

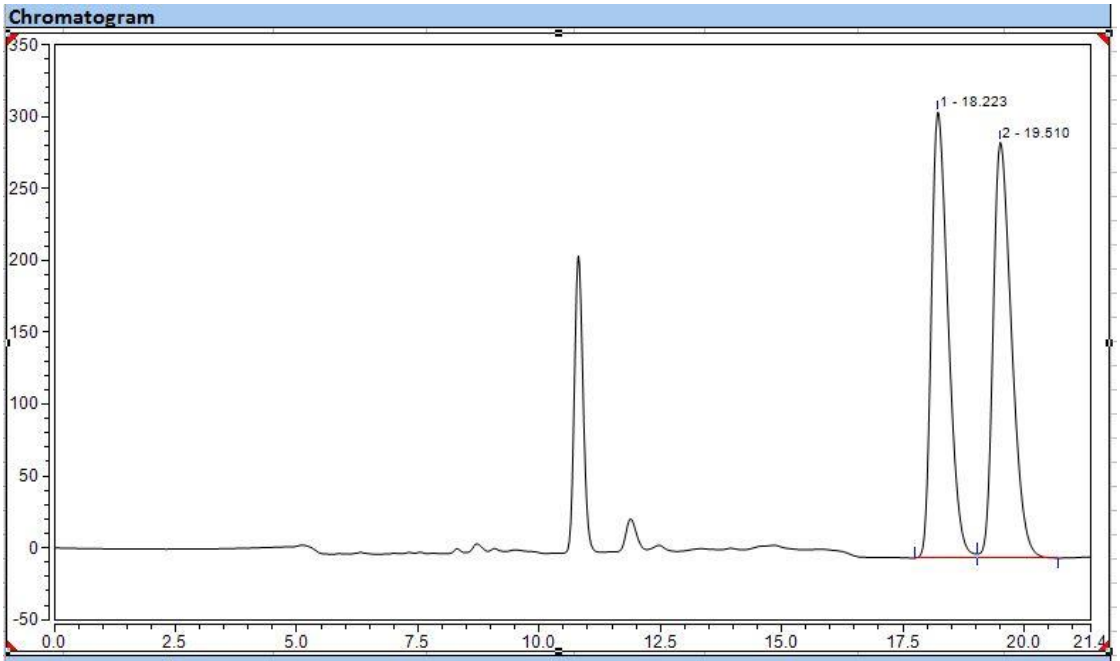

Integration Results

No.	Peak Name	Retention Time min	Area mAU*min	Height mAU	Relative Area %	Relative Height %	Amount n.a.
1		18.223	124.698	310.359	49.40	51.75	n.a.
2		19.510	127.737	289.322	50.60	48.25	n.a.
Total:			**252.436**	**599.681**	**100.00**	**100.00**	

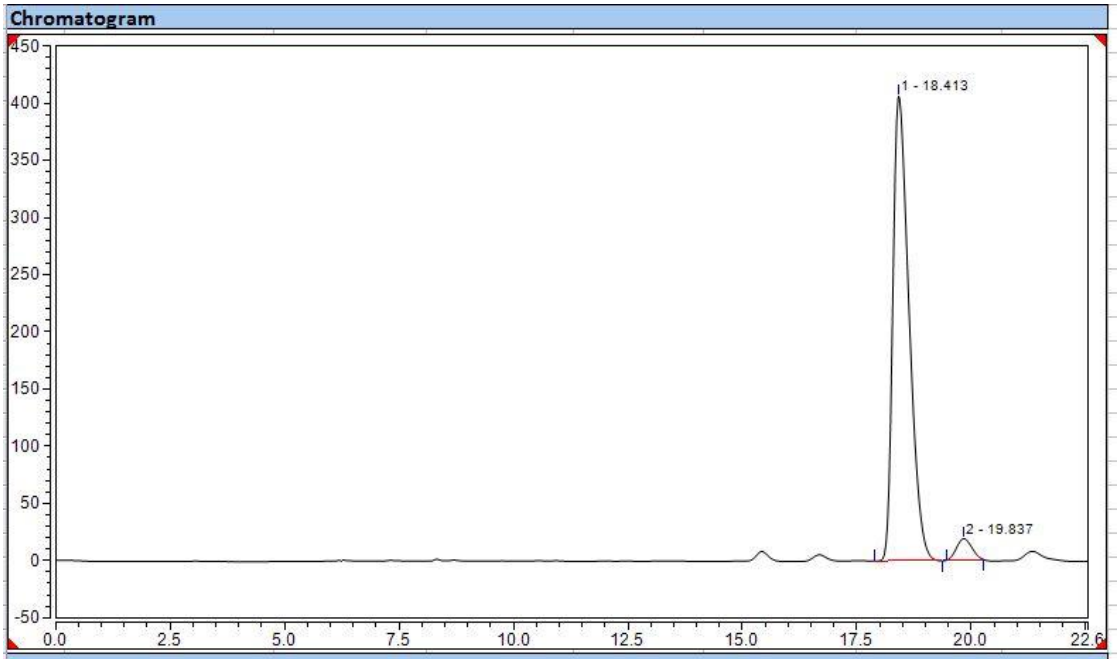

Integration Results

No.	Peak Name	Retention Time min	Area mAU*min	Height mAU	Relative Area %	Relative Height %	Amount n.a.
1		18.413	166.261	406.530	95.83	95.61	n.a.
2		19.837	7.229	18.677	4.17	4.39	n.a.
Total:			**173.491**	**425.207**	**100.00**	**100.00**	

Figure S108 HPLC Data and Chromatograms of 3k, related to Scheme 2

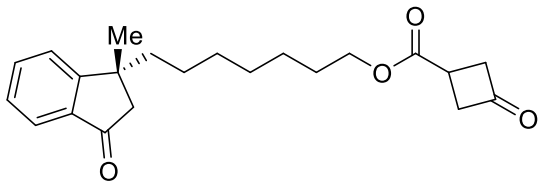

3K

HPLC (Chiralpak ADH): t_R= 31.7 (minor), 29.3 (major)
Condition: 90:10 n-Hexane: i-PrOH, flow rate 0.5 mL/min, 25°C.
254nm

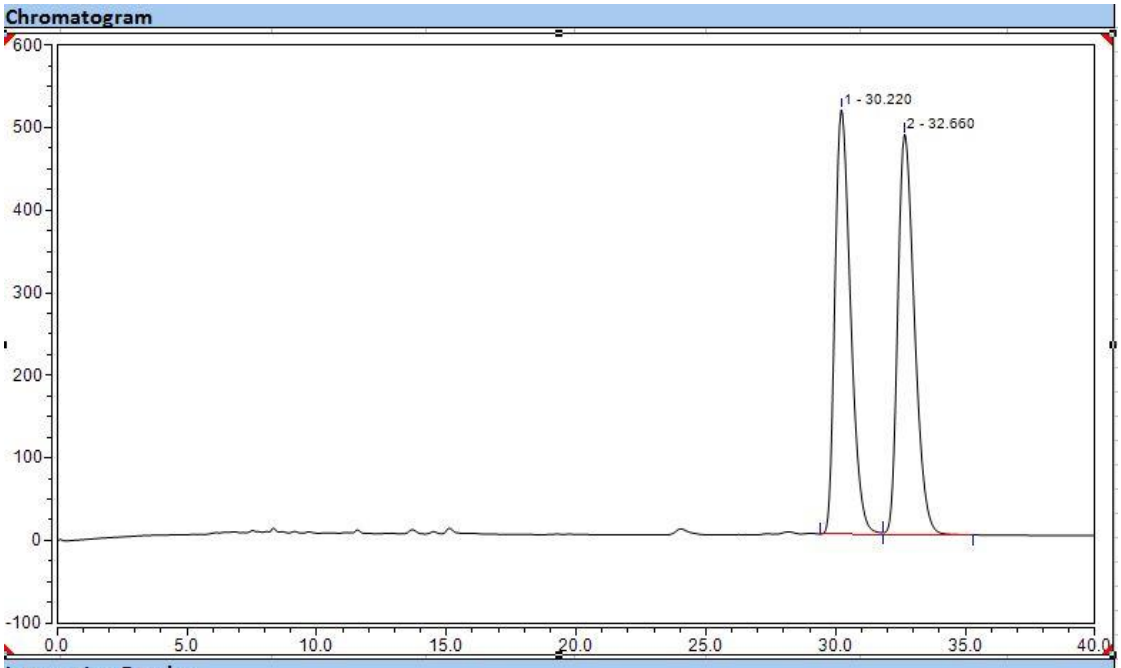

Integration Results

No.	Peak Name	Retention Time min	Area mAU*min	Height mAU	Relative Area %	Relative Height %	Amount n.a.
1		30.220	359.313	513.882	49.84	51.46	n.a.
2		32.660	361.672	484.711	50.16	48.54	n.a.
Total:			**720.985**	**998.593**	**100.00**	**100.00**	

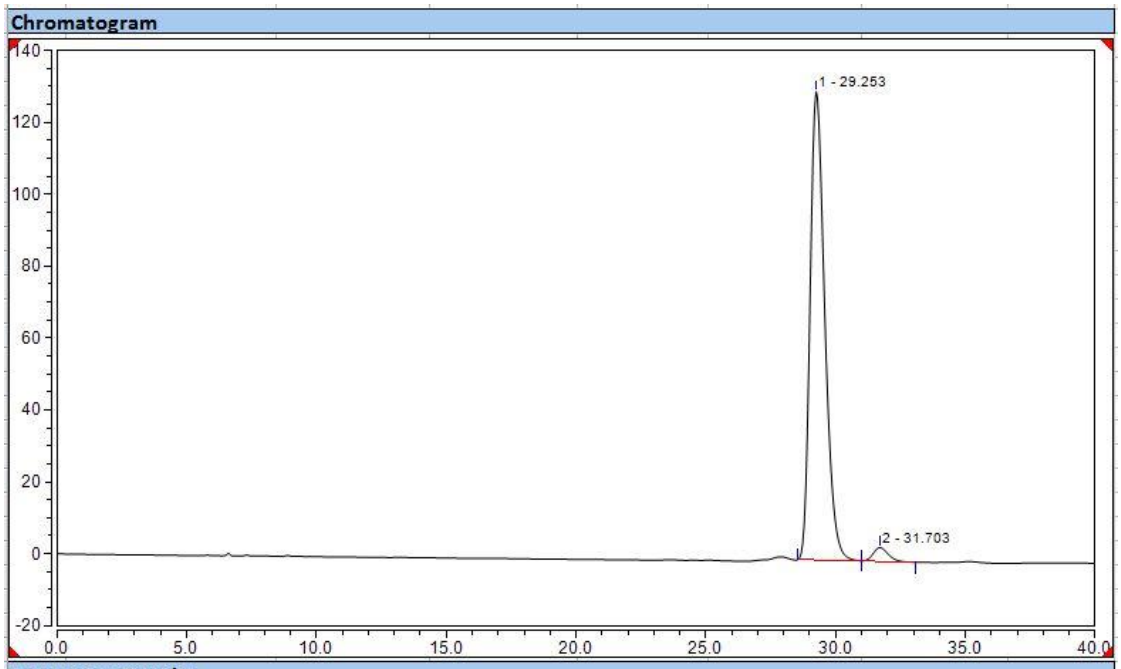

Integration Results

No.	Peak Name	Retention Time min	Area mAU*min	Height mAU	Relative Area %	Relative Height %	Amount n.a.
1		29.253	85.462	130.317	97.01	97.12	n.a.
2		31.703	2.633	3.861	2.99	2.88	n.a.
Total:			**88.095**	**134.179**	**100.00**	**100.00**	

Figure S109 HPLC Data and Chromatograms of 3l, related to Scheme 2

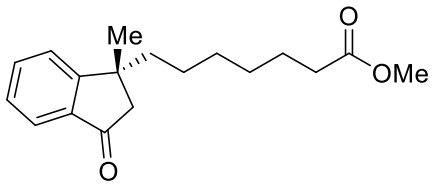

3l

HPLC (Chiralpak IB): t_R= 17.8 (minor), 15.1 (major)
Condition: 95:5 n-Hexane: i-PrOH, flow rate 0.5 mL/min, 25°C.
254nm

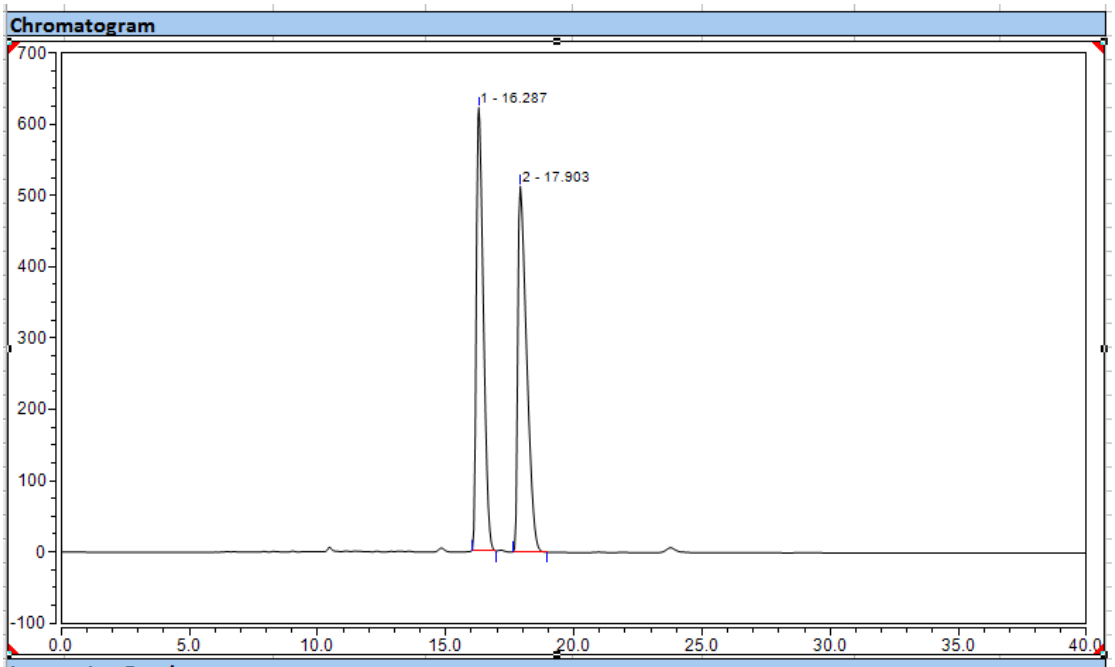

Integration Results

No.	Peak Name	Retention Time min	Area mAU*min	Height mAU	Relative Area %	Relative Height %	Amount n.a.
1		16.287	197.812	621.560	49.05	54.80	n.a.
2		17.903	205.490	512.688	50.95	45.20	n.a.
Total:			**403.302**	**1134.247**	**100.00**	**100.00**	

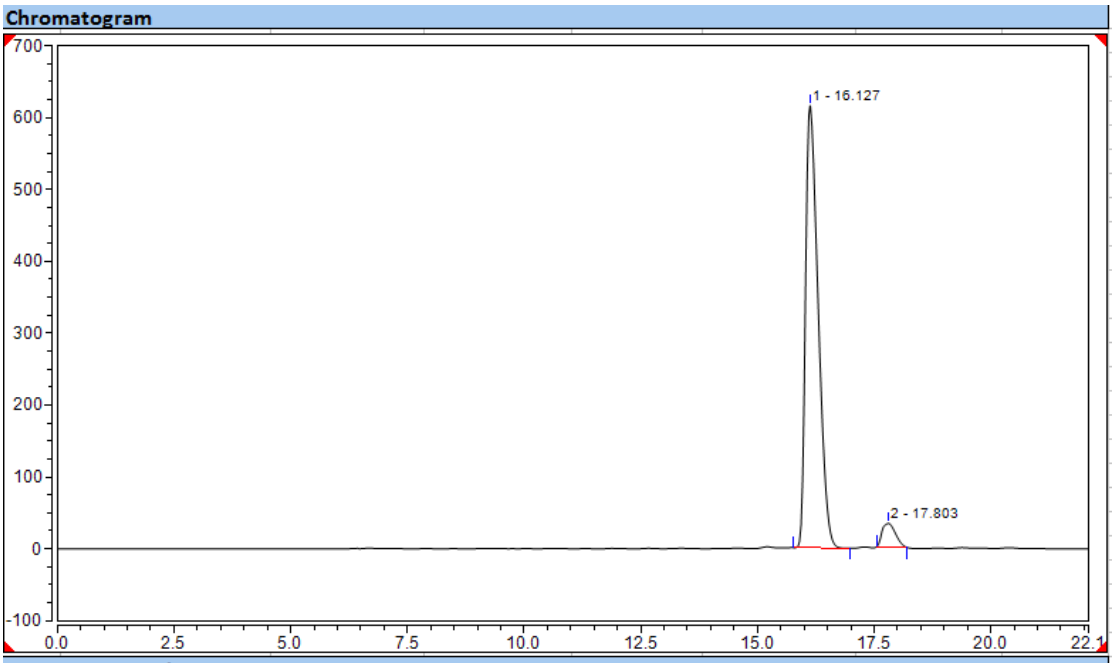

Integration Results

No.	Peak Name	Retention Time min	Area mAU*min	Height mAU	Relative Area %	Relative Height %	Amount n.a.
1		16.127	192.862	615.429	94.67	94.92	n.a.
2		17.803	10.861	32.934	5.33	5.08	n.a.
Total:			**203.722**	**648.363**	**100.00**	**100.00**	

Figure S110 HPLC Data and Chromatograms of 3m, related to Scheme 2

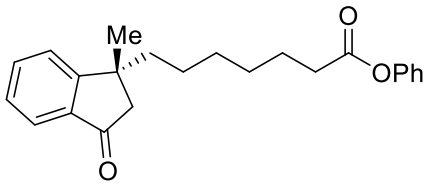

3m

HPLC (Chiralpak ADH): t_R= 24.4 (minor), 21.2 (major)
Condition: 90:10 n-Hexane: i-PrOH, flow rate 0.5 mL/min, 25°C.
254nm

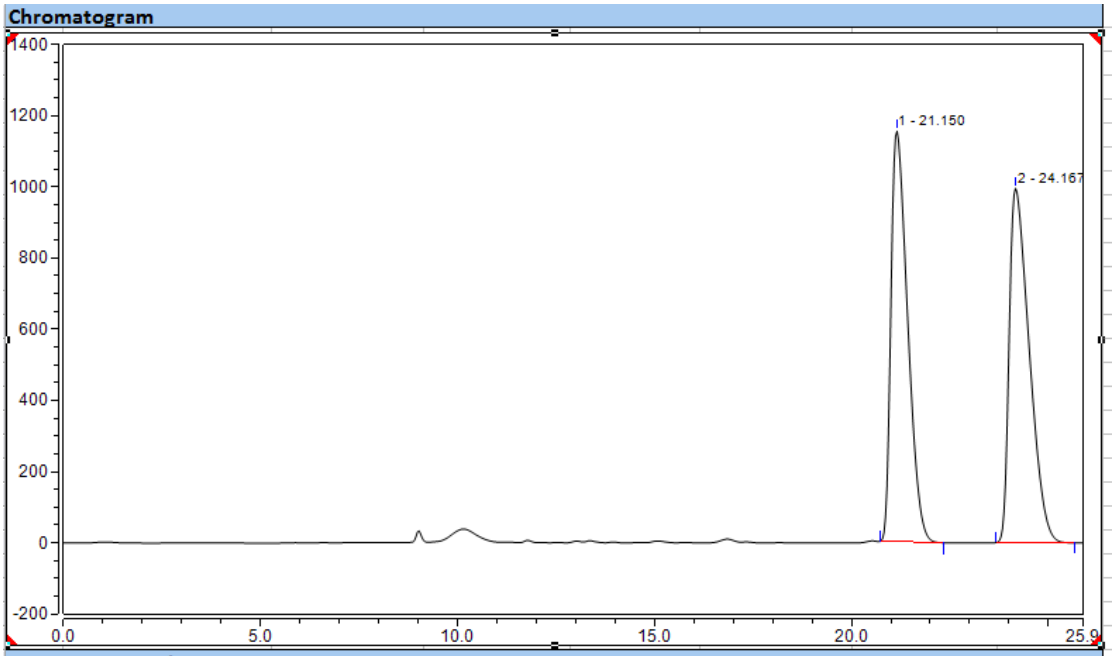

Integration Results

No.	Peak Name	Retention Time min	Area mAU*min	Height mAU	Relative Area %	Relative Height %	Amount n.a.
1		21.150	564.715	1153.981	49.08	53.69	n.a.
2		24.167	585.943	995.429	50.92	46.31	n.a.
Total:			**1150.658**	**2149.409**	**100.00**	**100.00**	

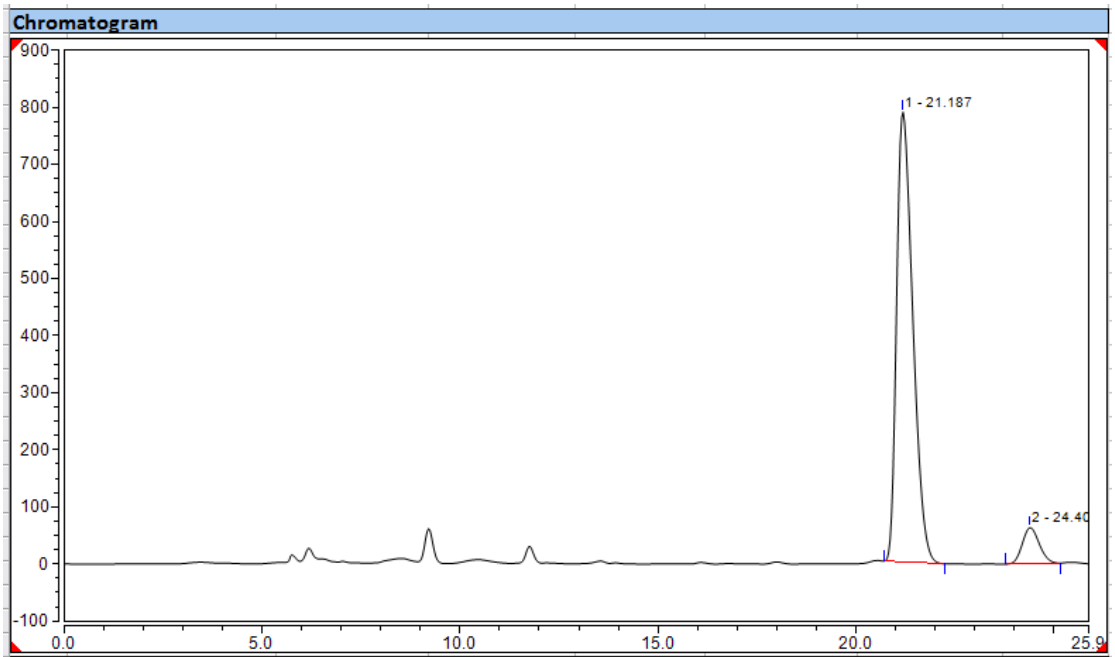

Integration Results

No.	Peak Name	Retention Time min	Area mAU*min	Height mAU	Relative Area %	Relative Height %	Amount n.a.
1		21.187	374.013	788.876	92.31	92.59	n.a.
2		24.403	31.172	63.179	7.69	7.41	n.a.
Total:			**405.185**	**852.055**	**100.00**	**100.00**	

Figure S111 HPLC Data and Chromatograms of 3n, related to Scheme 2

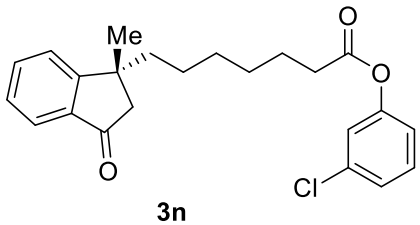

3n

HPLC (Chiralpak ADH): t_R= 23.0 (minor), 20.5 (major)
Condition: 90:10 n-Hexane: i-PrOH, flow rate 0.5 mL/min, 25°C.
254nm

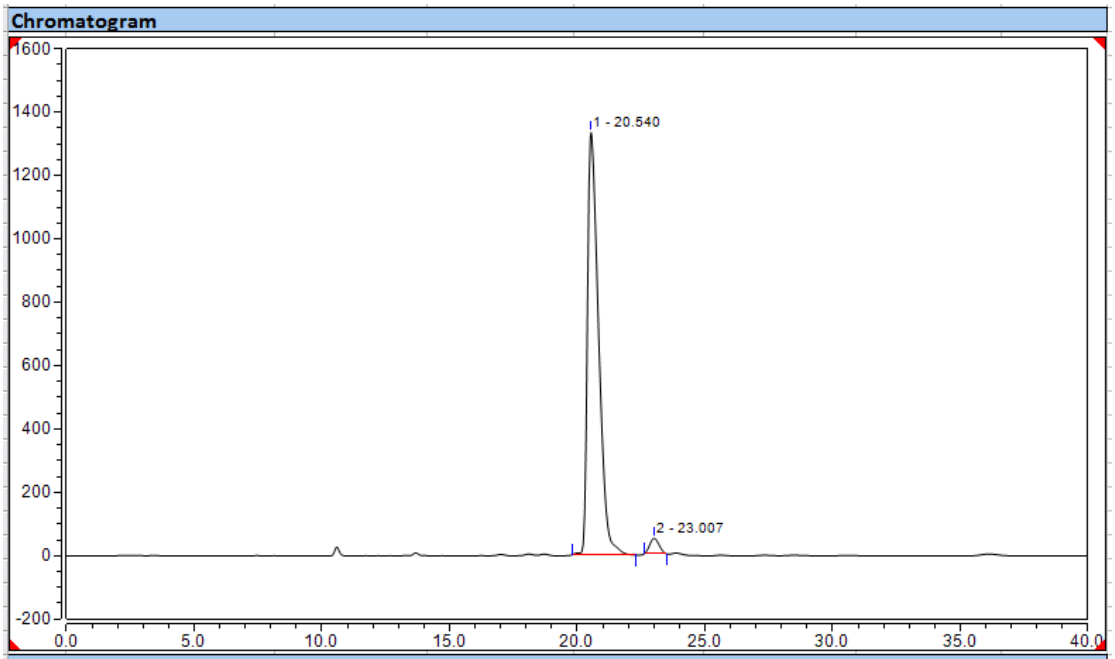

Integration Results

No.	Peak Name	Retention Time min	Area mAU*min	Height mAU	Relative Area %	Relative Height %	Amount n.a.
1		20.540	669.390	1333.106	96.98	96.43	n.a.
2		23.007	20.878	49.325	3.02	3.57	n.a.
Total:			**690.268**	**1382.431**	**100.00**	**100.00**	

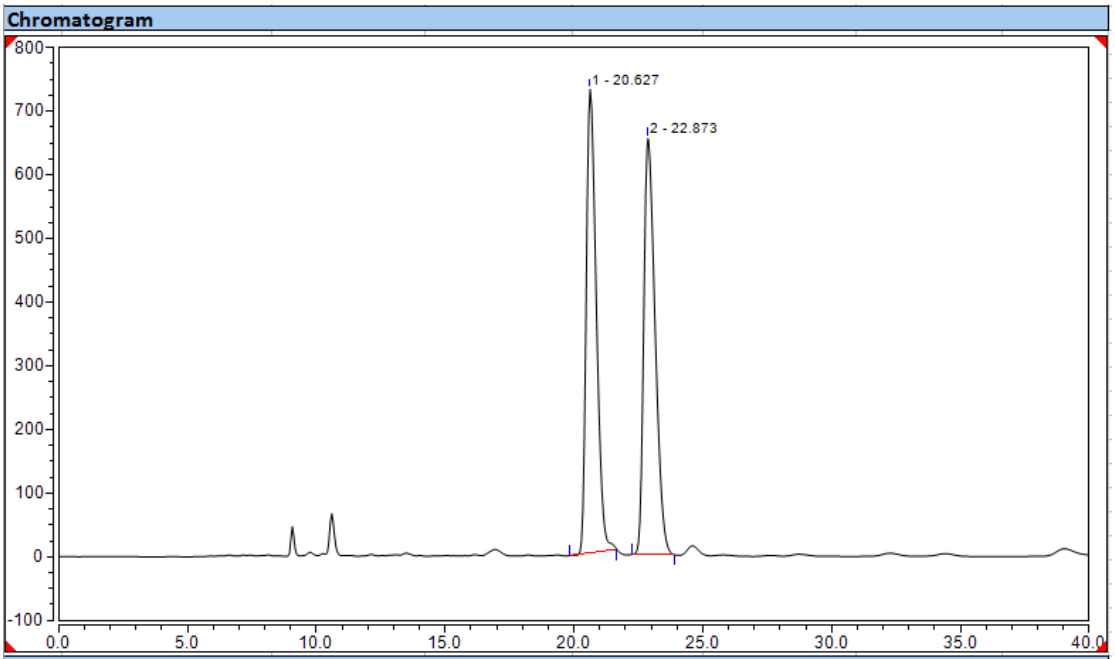

Integration Results

No.	Peak Name	Retention Time min	Area mAU*min	Height mAU	Relative Area %	Relative Height %	Amount n.a.
1		20.627	327.538	728.190	49.56	52.70	n.a.
2		22.873	333.318	653.451	50.44	47.30	n.a.
Total:			**660.856**	**1381.641**	**100.00**	**100.00**	

Figure S112 HPLC Data and Chromatograms of 3o, related to Scheme 2

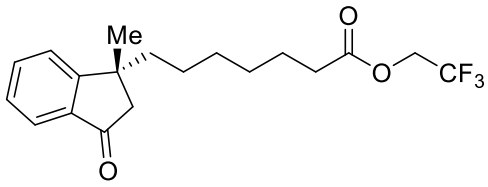

HPLC (Chiralpak IB): t_R= 16.1 (minor), 14.2 (major)
Condition: 95:5 n-Hexane: i-PrOH, flow rate 0.5 mL/min, 25°C.
254nm

3o

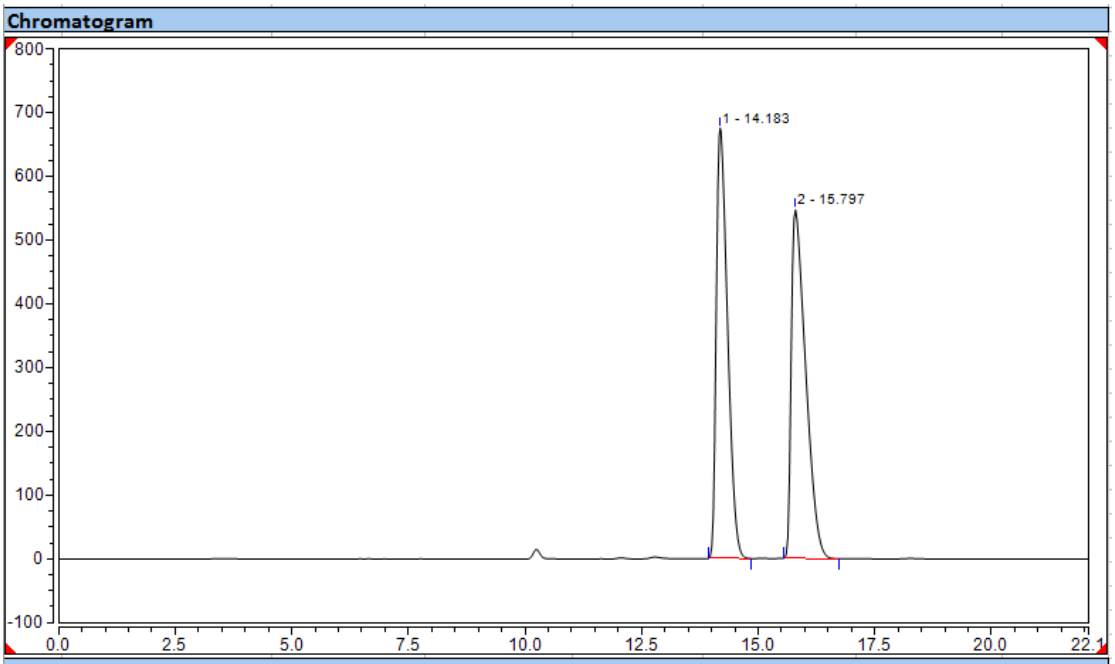

Integration Results

No.	Peak Name	Retention Time min	Area mAU*min	Height mAU	Relative Area %	Relative Height %	Amount n.a.
1		14.183	188.338	675.278	49.06	55.23	n.a.
2		15.797	195.542	547.307	50.94	44.77	n.a.
Total:			**383.880**	**1222.585**	**100.00**	**100.00**	

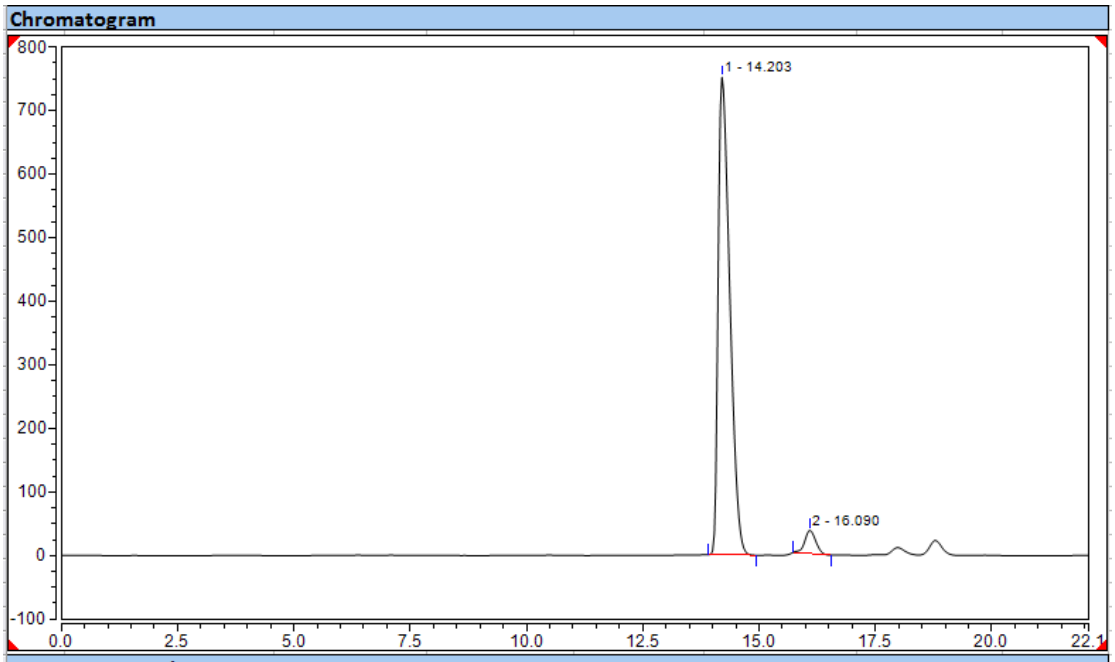

Integration Results

No.	Peak Name	Retention Time min	Area mAU*min	Height mAU	Relative Area %	Relative Height %	Amount n.a.
1		14.203	217.266	751.465	95.59	95.34	n.a.
2		16.090	10.027	36.734	4.41	4.66	n.a.
Total:			**227.293**	**788.199**	**100.00**	**100.00**	

Figure S113 HPLC Data and Chromatograms of 3p, related to Scheme 2

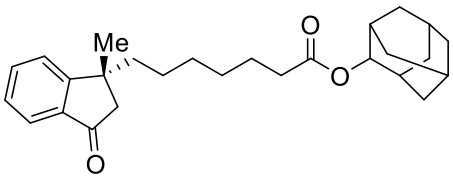

HPLC (Chiralpak IB): t_R= 14.8 (minor), 13.2 (major)
Condition: 95:5 n-Hexane: i-PrOH, flow rate 0.5 mL/min, 25℃.
254nm

3p

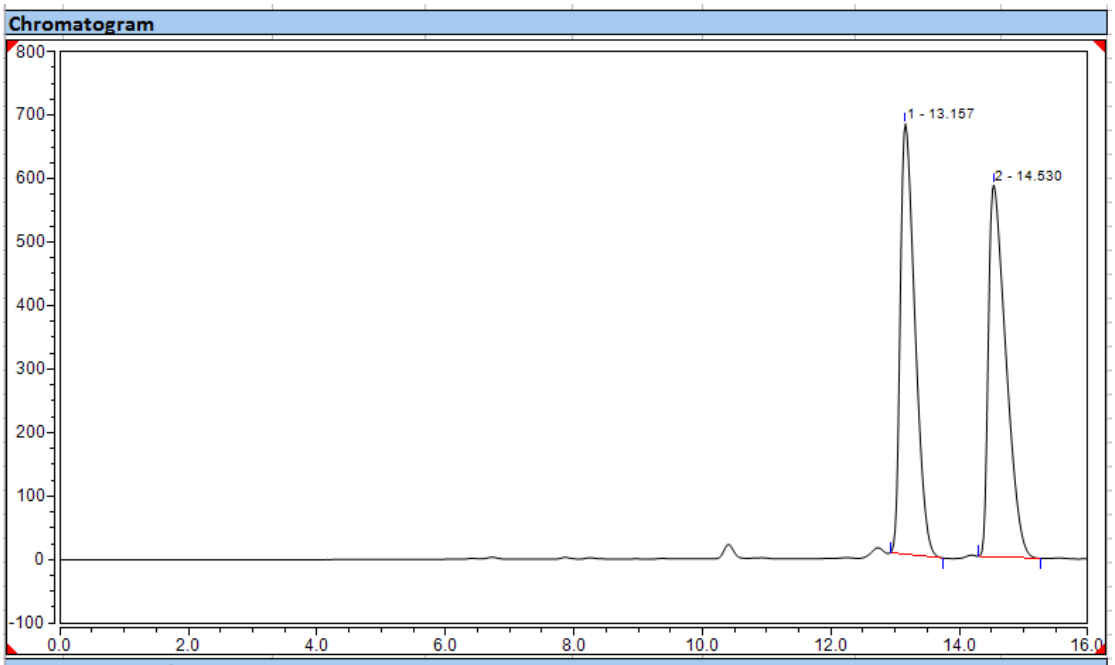

Integration Results

No.	Peak Name	Retention Time min	Area mAU*min	Height mAU	Relative Area %	Relative Height %	Amount n.a.
1		13.157	179.572	678.452	49.26	53.68	n.a.
2		14.530	184.943	585.504	50.74	46.32	n.a.
Total:			**364.515**	**1263.956**	**100.00**	**100.00**	

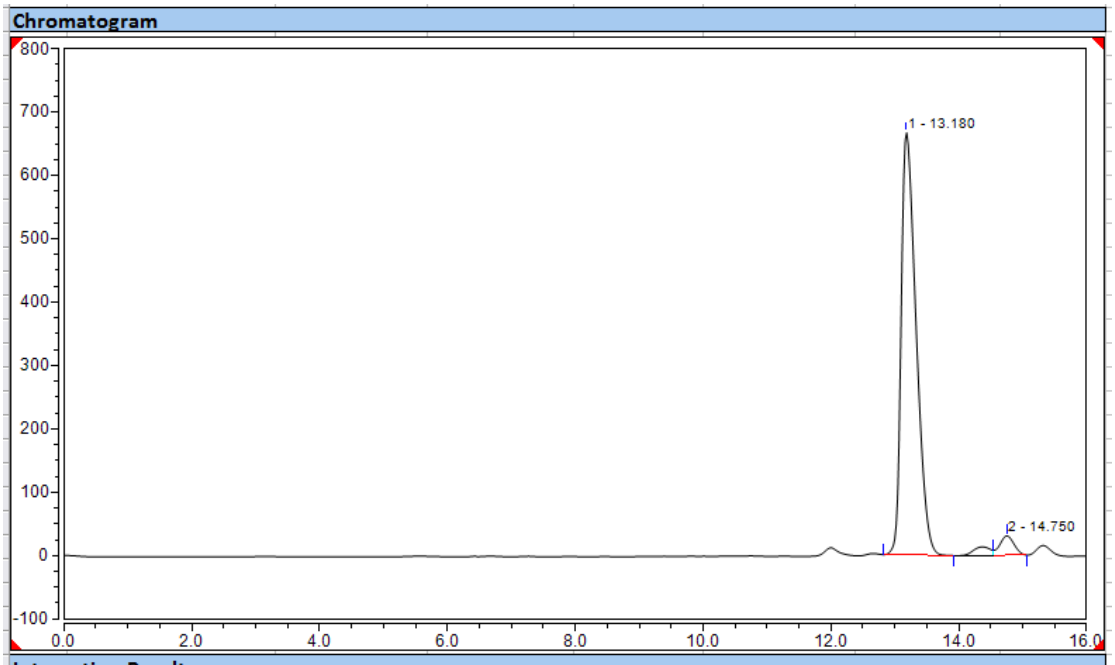

Integration Results

No.	Peak Name	Retention Time min	Area mAU*min	Height mAU	Relative Area %	Relative Height %	Amount n.a.
1		13.180	179.883	666.777	95.80	95.60	n.a.
2		14.750	7.889	30.670	4.20	4.40	n.a.
Total:			**187.772**	**697.447**	**100.00**	**100.00**	

Figure S114 HPLC Data and Chromatograms of 3q, related to Scheme 2

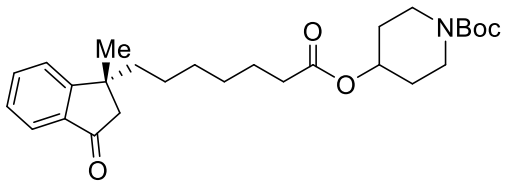

3q

HPLC (Chiralpak ADH): t_R= 28.7 (minor), 23.3 (major)
Condition: 90:10 n-Hexane: i-PrOH, flow rate 0.5 mL/min, 25°C. 254nm

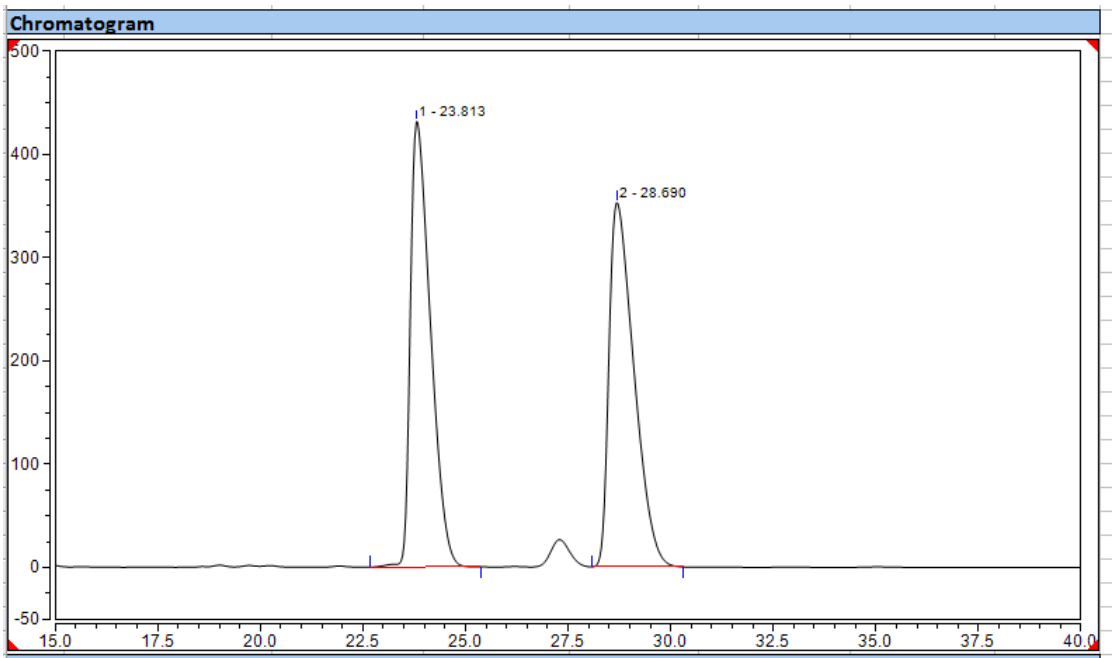

Integration Results

No.	Peak Name	Retention Time min	Area mAU*min	Height mAU	Relative Area %	Relative Height %	Amount n.a.
1		23.813	244.795	431.547	49.69	55.01	n.a.
2		28.690	247.818	352.928	50.31	44.99	n.a.
Total:			**492.614**	**784.475**	**100.00**	**100.00**	

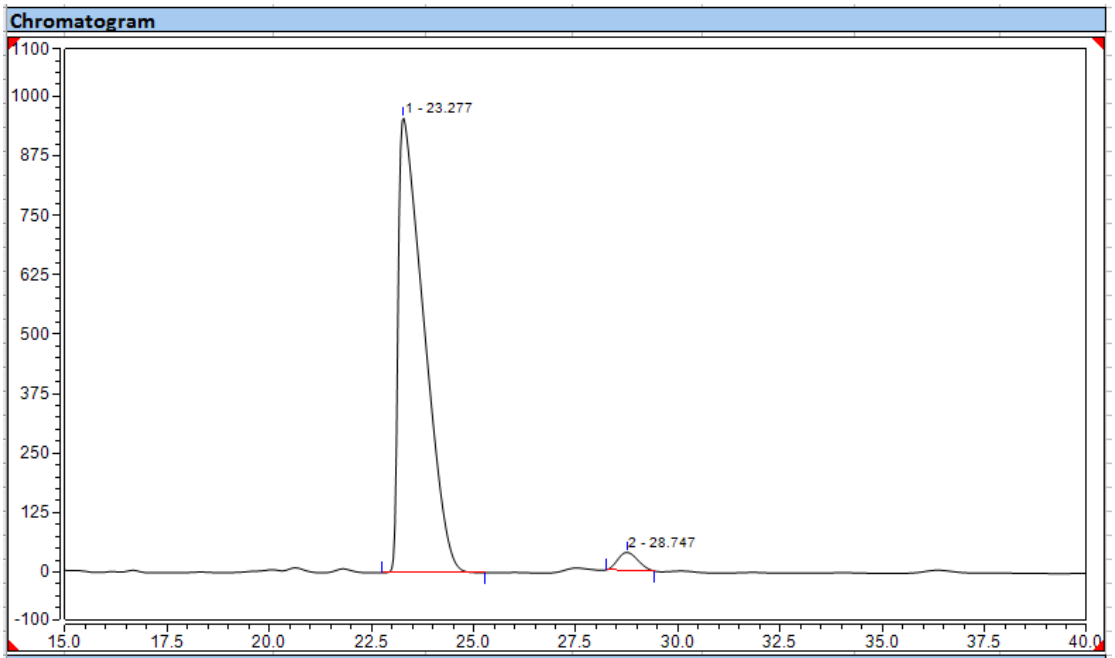

Integration Results

No.	Peak Name	Retention Time min	Area mAU*min	Height mAU	Relative Area %	Relative Height %	Amount n.a.
1		23.277	690.040	956.747	96.97	96.20	n.a.
2		28.747	21.598	37.761	3.03	3.80	n.a.
Total:			**711.638**	**994.508**	**100.00**	**100.00**	

Figure S115 HPLC Data and Chromatograms of 3r, related to Scheme 2

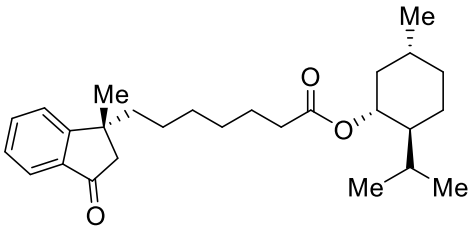

3r

HPLC (Chiralpak ADH): t_R= 21.2 (minor), 19.0 (major)
Condition: 95:5 n-Hexane: i-PrOH, flow rate 0.5 mL/min, 25°C.
254nm

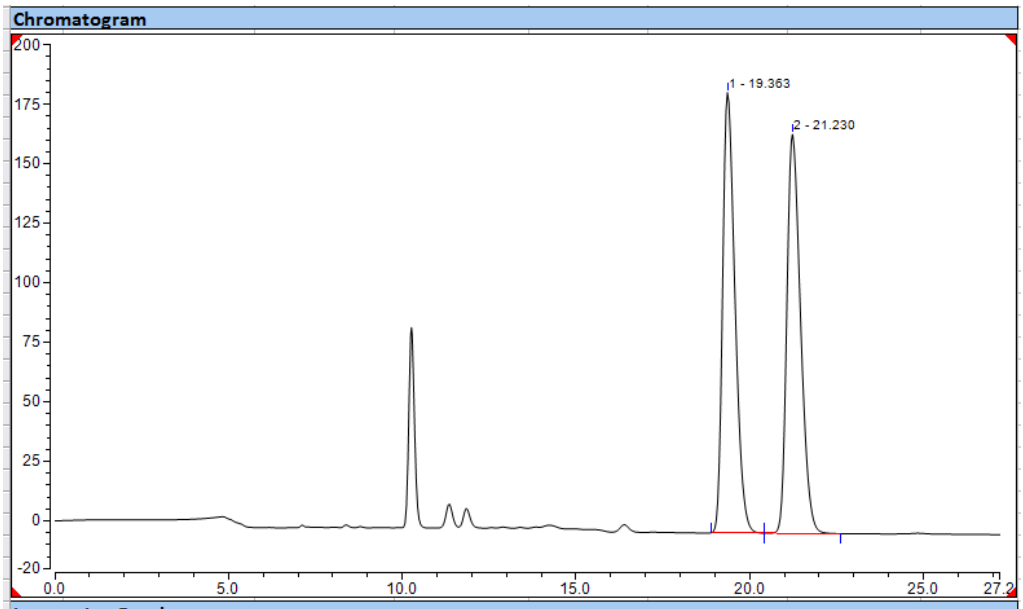

Integration Results

No.	Peak Name	Retention Time min	Area mAU*min	Height mAU	Relative Area %	Relative Height %	Amount n.a.
1		19.363	76.171	185.039	49.88	52.47	n.a.
2		21.230	76.533	167.623	50.12	47.53	n.a.
Total:			**152.705**	**352.662**	**100.00**	**100.00**	

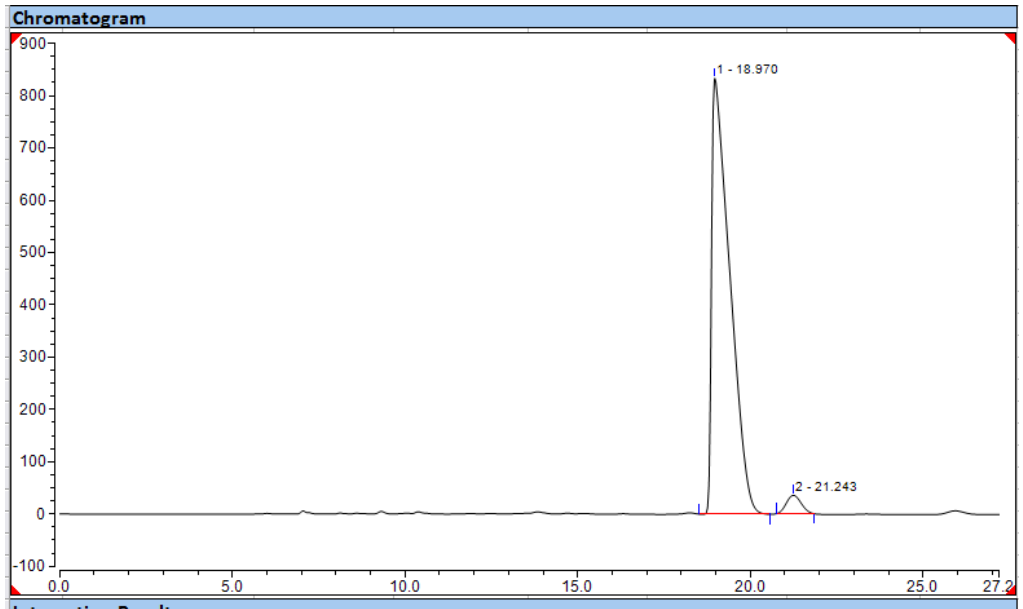

Integration Results

No.	Peak Name	Retention Time min	Area mAU*min	Height mAU	Relative Area %	Relative Height %	Amount n.a.
1		18.970	507.845	833.697	96.65	95.93	n.a.
2		21.243	17.600	35.355	3.35	4.07	n.a.
Total:			**525.444**	**869.053**	**100.00**	**100.00**	

Figure S116 HPLC Data and Chromatograms of 3s, related to Scheme 2

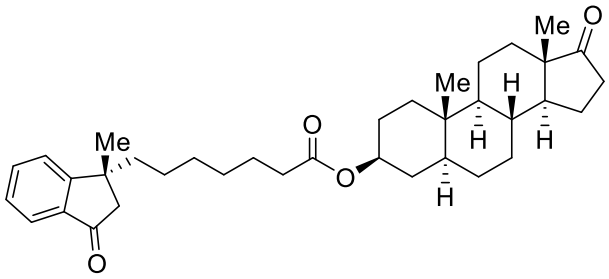

HPLC (Chiralpak IB): t_R= 25.7 (minor), 22.1 (major)
Condition: 85:15 n-Hexane: i-PrOH, flow rate 0.5 mL/min, 25℃. 254nm

3s

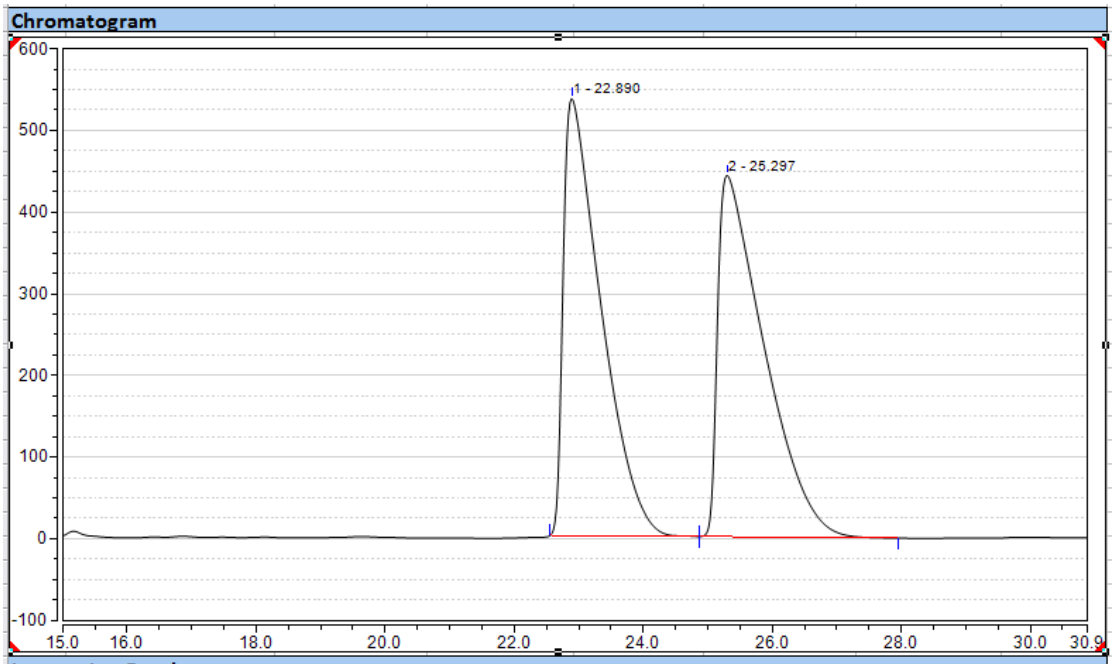

Integration Results

No.	Peak Name	Retention Time min	Area mAU*min	Height mAU	Relative Area %	Relative Height %	Amount n.a.
1		22.890	361.982	535.115	49.56	54.74	n.a.
2		25.297	368.450	442.517	50.44	45.26	n.a.
Total:			**730.432**	**977.633**	**100.00**	**100.00**	

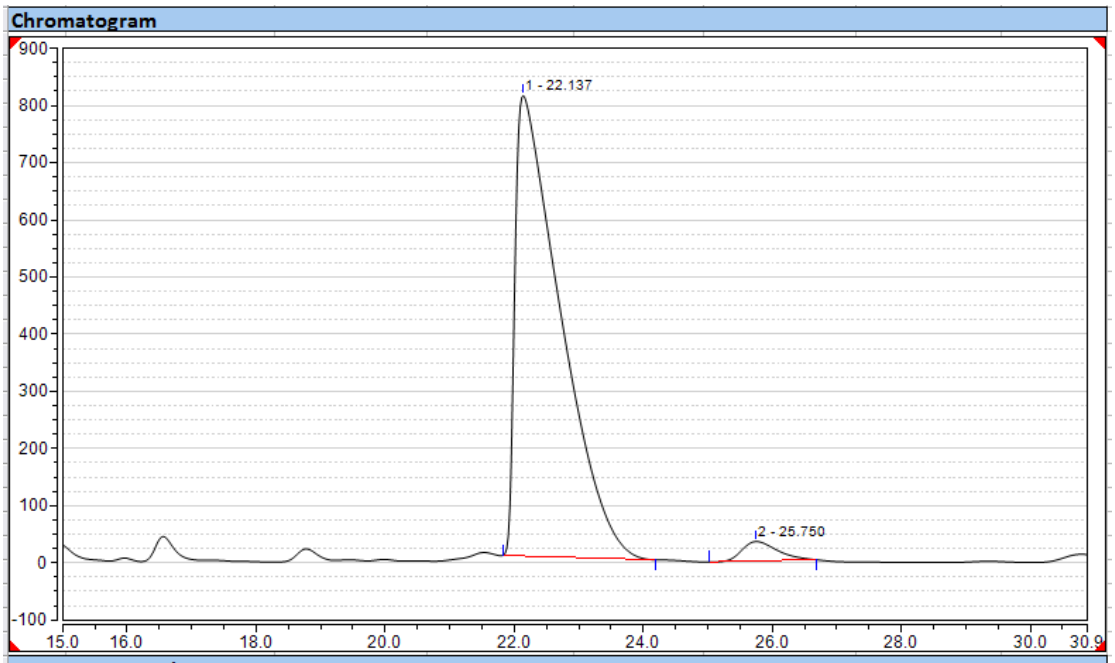

Integration Results

No.	Peak Name	Retention Time min	Area mAU*min	Height mAU	Relative Area %	Relative Height %	Amount n.a.
1		22.137	657.099	805.854	96.81	95.93	n.a.
2		25.750	21.681	34.214	3.19	4.07	n.a.
Total:			**678.781**	**840.068**	**100.00**	**100.00**	

Figure S117 HPLC Data and Chromatograms of 3t, related to Scheme 2

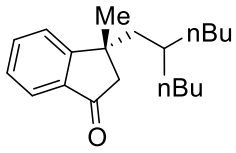

HPLC (Chiralpak IC): t_R= 12.7 (minor), 11.4 (major)
Condition: 95:5 n-Hexane: i-PrOH, flow rate 0.5 mL/min, 25°C.
254nm

3t

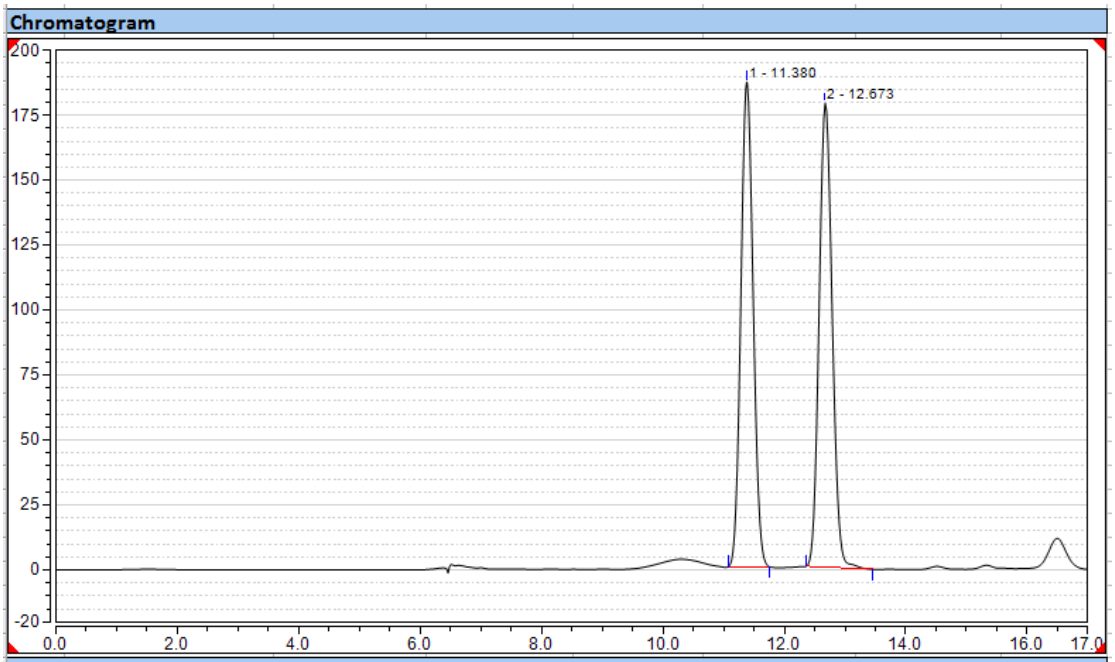

Integration Results

No.	Peak Name	Retention Time min	Area mAU*min	Height mAU	Relative Area %	Relative Height %	Amount n.a.
1		11.380	43.730	186.559	49.61	51.10	n.a.
2		12.673	44.410	178.517	50.39	48.90	n.a.
Total:			**88.140**	**365.075**	**100.00**	**100.00**	

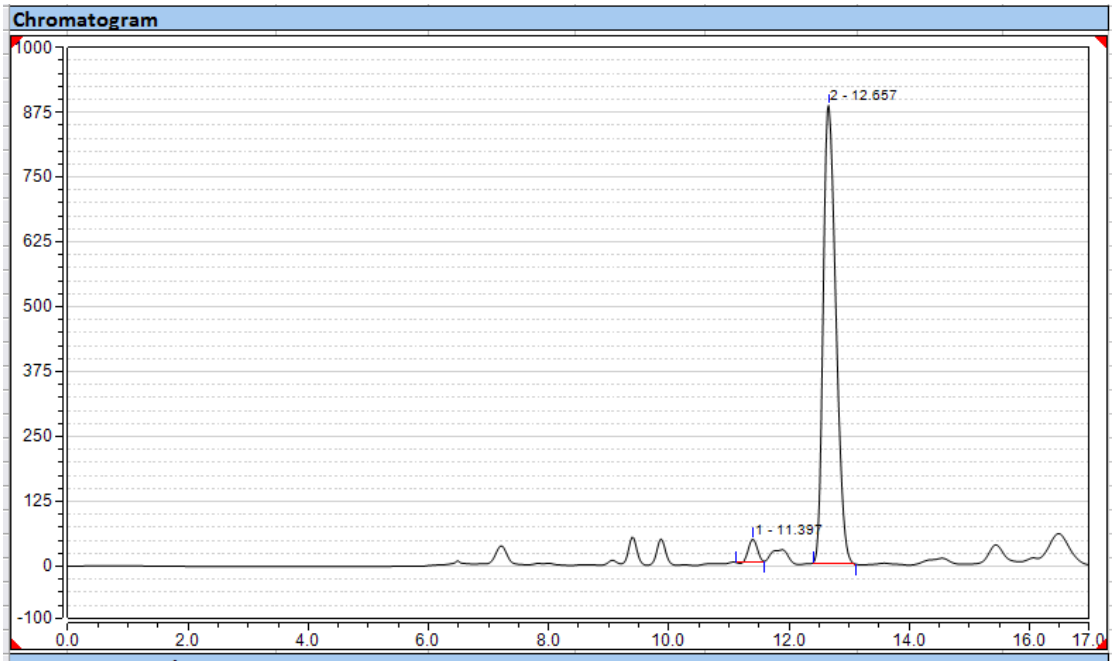

Integration Results

No.	Peak Name	Retention Time min	Area mAU*min	Height mAU	Relative Area %	Relative Height %	Amount n.a.
1		11.397	7.217	43.837	3.23	4.73	n.a.
2		12.657	216.324	883.098	96.77	95.27	n.a.
Total:			**223.541**	**926.934**	**100.00**	**100.00**	

Figure S118 HPLC Data and Chromatograms of 3u, related to Scheme 2

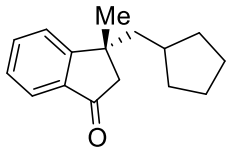

3u

HPLC (Chiralpak IC): t_R= 17.4 (minor), 19.7 (major)
Condition: 95:5 n-Hexane: i-PrOH, flow rate 0.5 mL/min, 25℃.
254nm

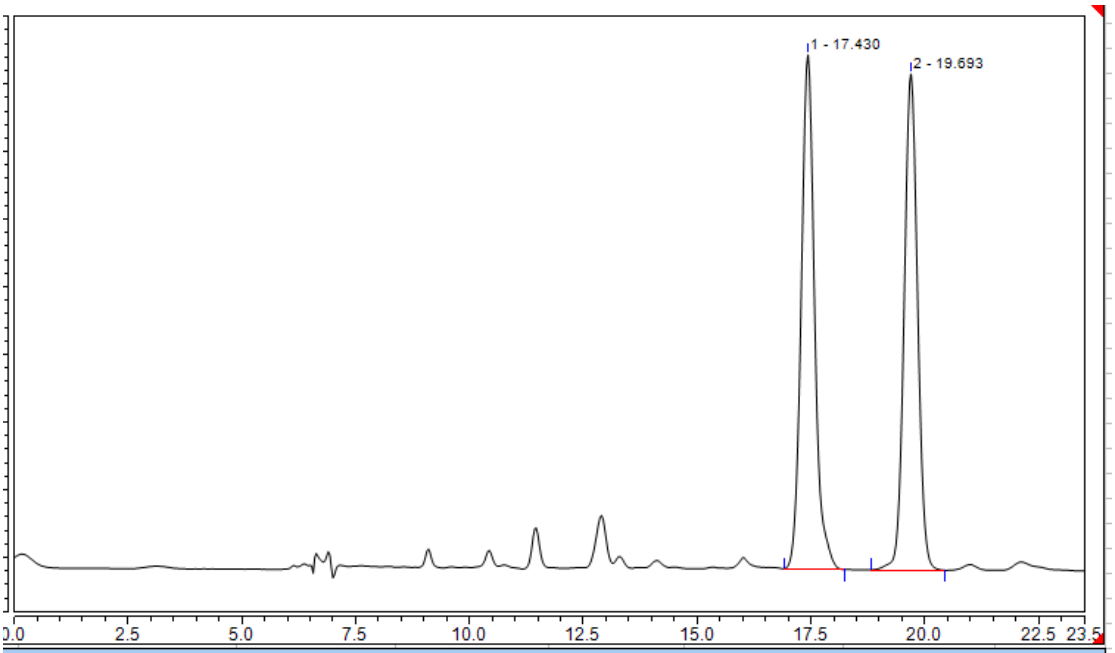

gration Results

Peak Name	Retention Time min	Area mAU*min	Height mAU	Relative Area %	Relative Height %	Amount n.a.
	17.430	6.474	19.021	50.81	50.90	n.a.
	19.693	6.269	18.348	49.19	49.10	n.a.
l:		**12.744**	**37.369**	**100.00**	**100.00**	

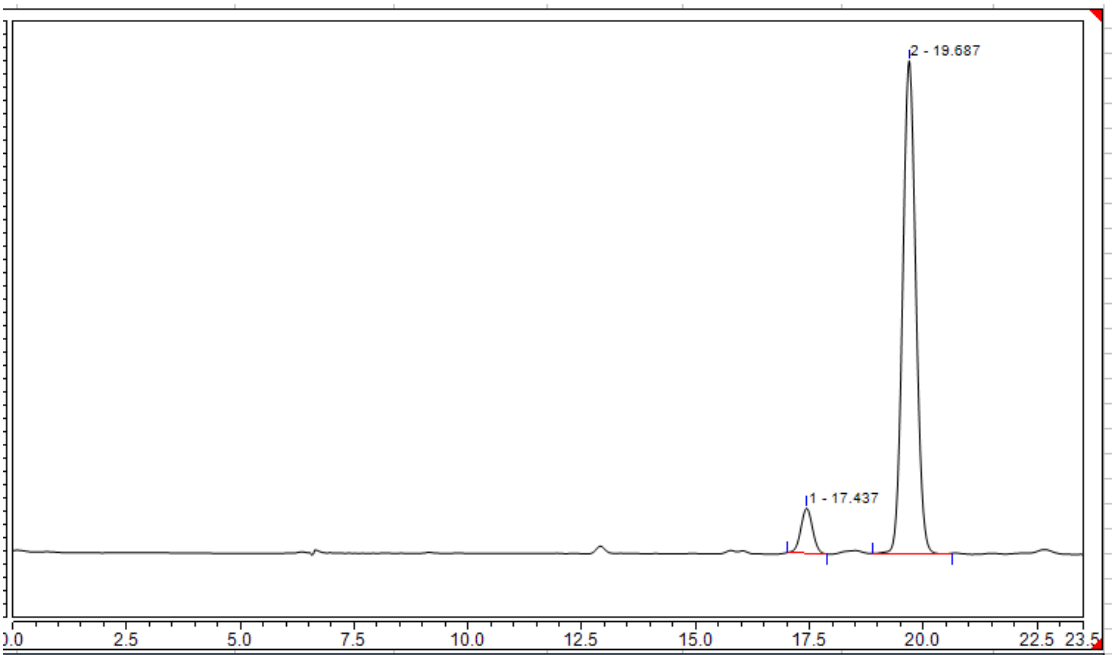

gration Results

Peak Name	Retention Time min	Area mAU*min	Height mAU	Relative Area %	Relative Height %	Amount n.a.
	17.437	1.016	3.410	7.58	8.39	n.a.
	19.687	12.383	37.226	92.42	91.61	n.a.
l:		**13.399**	**40.636**	**100.00**	**100.00**	

Figure S119 HPLC Data and Chromatograms of 3v, related to Scheme 2

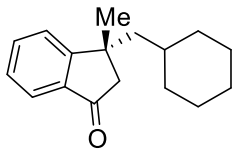

3v

HPLC (Chiralpak IC): t_R= 15.9 (minor), 18.0 (major)
Condition: 95:5 n-Hexane: i-PrOH, flow rate 0.5 mL/min, 25℃.
254nm.

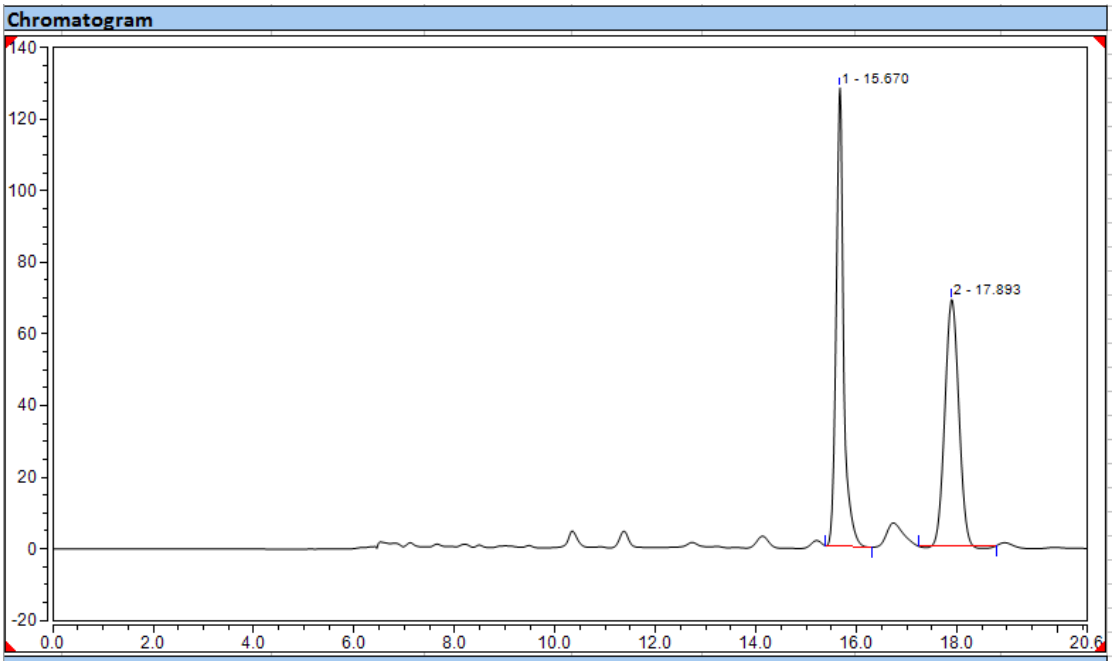

Integration Results

No.	Peak Name	Retention Time min	Area mAU*min	Height mAU	Relative Area %	Relative Height %	Amount n.a.
1		15.670	21.951	127.989	50.14	65.01	n.a.
2		17.893	21.830	68.882	49.86	34.99	n.a.
Total:			**43.781**	**196.871**	**100.00**	**100.00**	

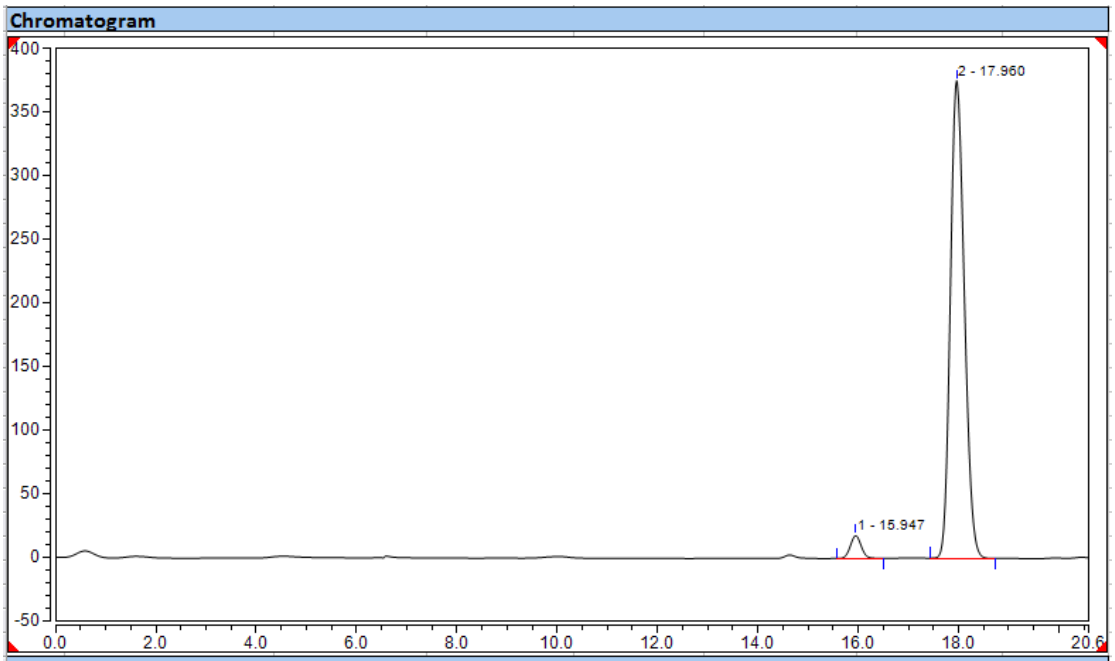

Integration Results

No.	Peak Name	Retention Time min	Area mAU*min	Height mAU	Relative Area %	Relative Height %	Amount n.a.
1		15.947	4.540	17.990	3.61	4.57	n.a.
2		17.960	121.213	375.657	96.39	95.43	n.a.
Total:			**125.753**	**393.647**	**100.00**	**100.00**	

Figure S120 HPLC Data and Chromatograms of 3w, related to Scheme 2

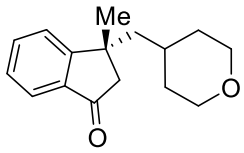

3w

HPLC (Chiralpak IB): t_R= 12.7 (minor), 13.8 (major)
Condition: 85:15 n-Hexane: i-PrOH, flow rate 0.5 mL/min, 25℃.
254nm

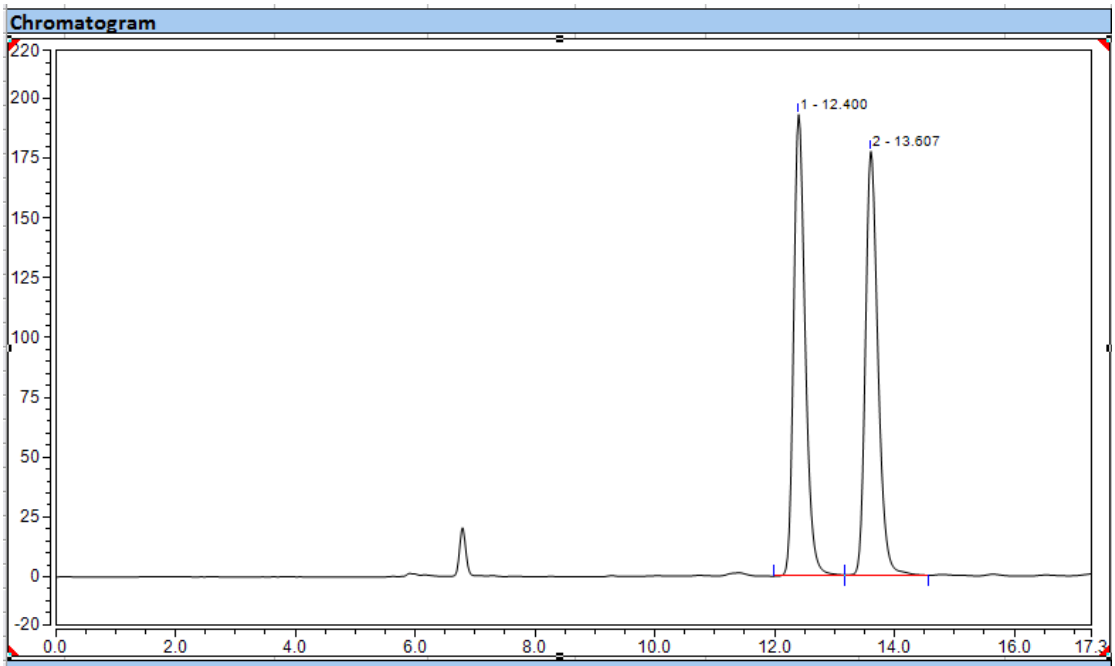

Integration Results

No.	Peak Name	Retention Time min	Area mAU*min	Height mAU	Relative Area %	Relative Height %	Amount n.a.
1		12.400	43.210	192.916	50.00	52.10	n.a.
2		13.607	43.218	177.382	50.00	47.90	n.a.
Total:			**86.427**	**370.298**	**100.00**	**100.00**	

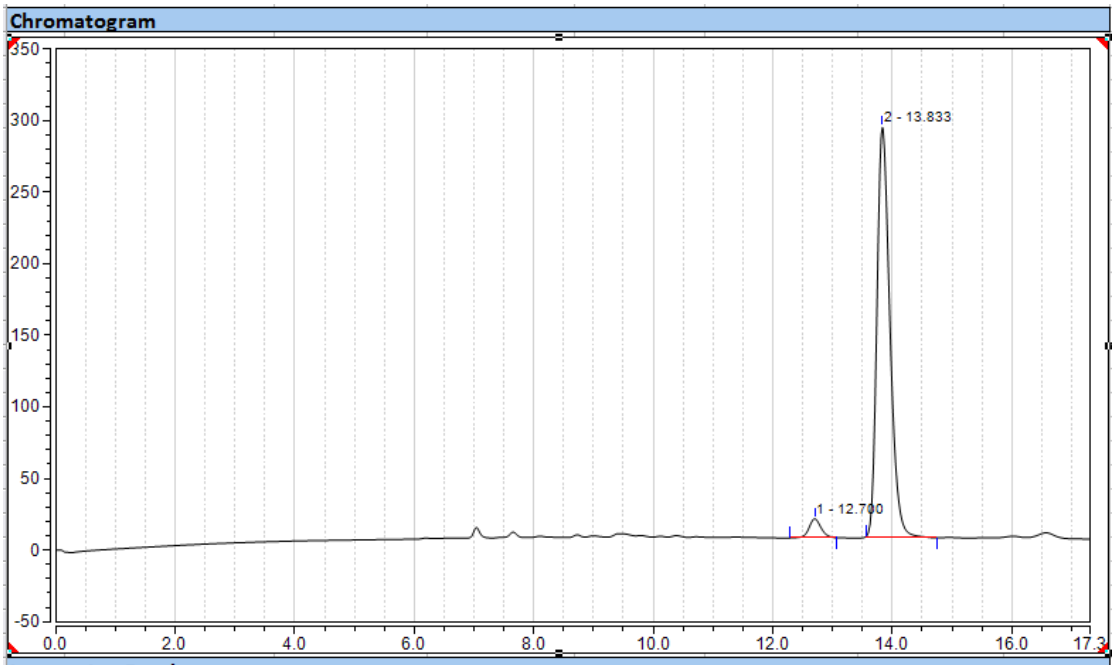

Integration Results

No.	Peak Name	Retention Time min	Area mAU*min	Height mAU	Relative Area %	Relative Height %	Amount n.a.
1		12.700	3.114	13.339	4.17	4.45	n.a.
2		13.833	71.621	286.091	95.83	95.55	n.a.
Total:			**74.735**	**299.430**	**100.00**	**100.00**	

Figure S121 HPLC Data and Chromatograms of 3x, related to Scheme 2

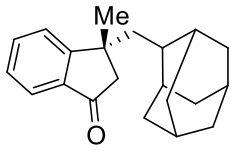

3x

HPLC (Chiralpak IC): t_R= 15.9 (minor), 18.1 (major)
Condition: 95:5 n-Hexane: i-PrOH, flow rate 0.5 mL/min, 25℃.
254nm

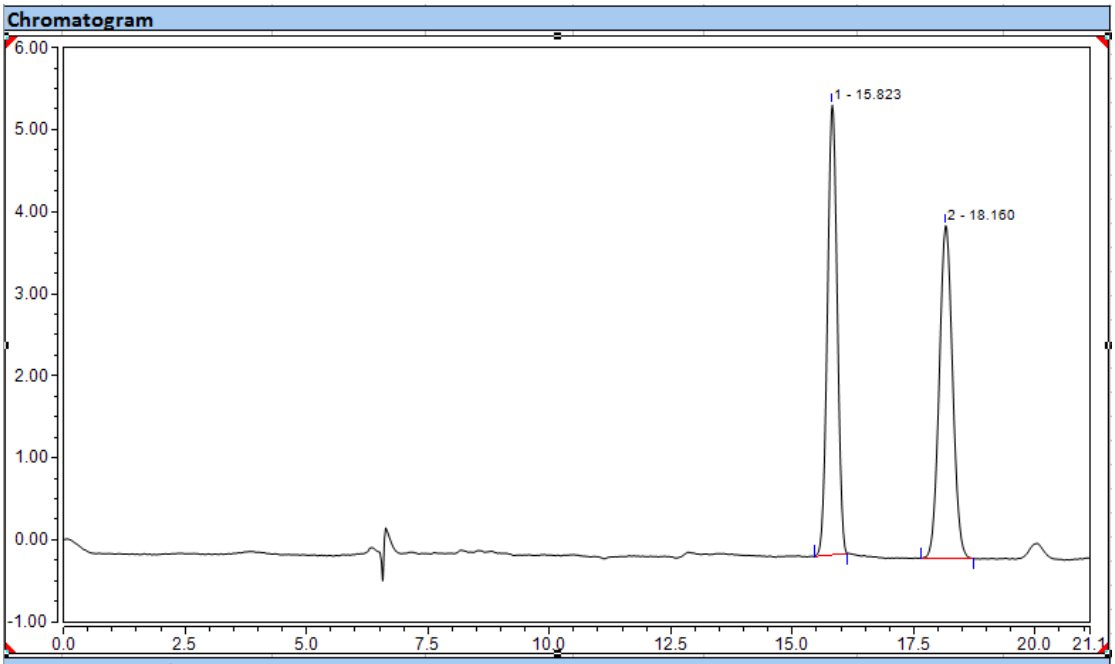

Integration Results

No.	Peak Name	Retention Time min	Area mAU*min	Height mAU	Relative Area %	Relative Height %	Amount n.a.
1		15.823	1.276	5.485	49.67	57.46	n.a.
2		18.160	1.293	4.061	50.33	42.54	n.a.
Total:			**2.569**	**9.545**	**100.00**	**100.00**	

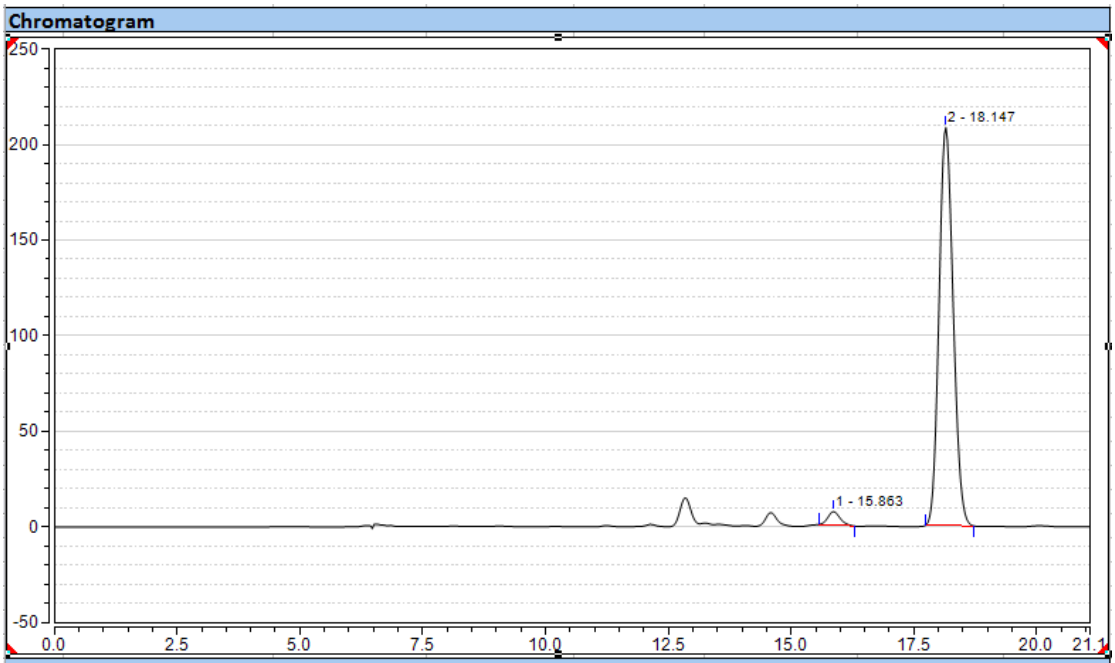

Integration Results

No.	Peak Name	Retention Time min	Area mAU*min	Height mAU	Relative Area %	Relative Height %	Amount n.a.
1		15.863	2.062	7.115	2.89	3.30	n.a.
2		18.147	69.425	208.538	97.11	96.70	n.a.
Total:			**71.487**	**215.653**	**100.00**	**100.00**	

Figure S122 HPLC Data and Chromatograms of 3y, related to Scheme 2

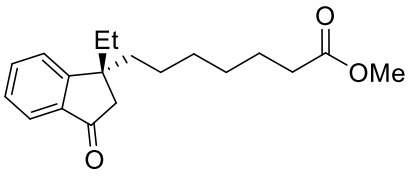

3y

HPLC (Chiralpak IB): t_R= 12.8 (minor), 11.7 (major)
Condition: 90:10 n-Hexane: i-PrOH, flow rate 0.5 mL/min, 25℃.
254nm

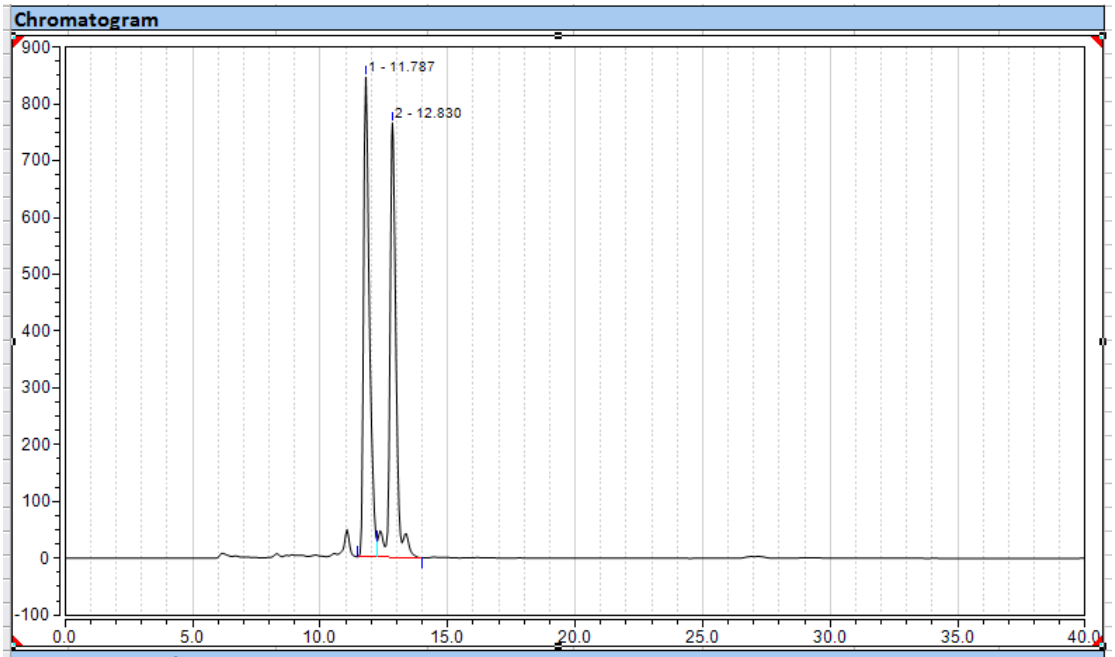

Integration Results

No.	Peak Name	Retention Time min	Area mAU*min	Height mAU	Relative Area %	Relative Height %	Amount n.a.
1		11.787	225.758	844.925	51.08	52.48	n.a.
2		12.830	216.174	765.062	48.92	47.52	n.a.
Total:			**441.932**	**1609.987**	**100.00**	**100.00**	

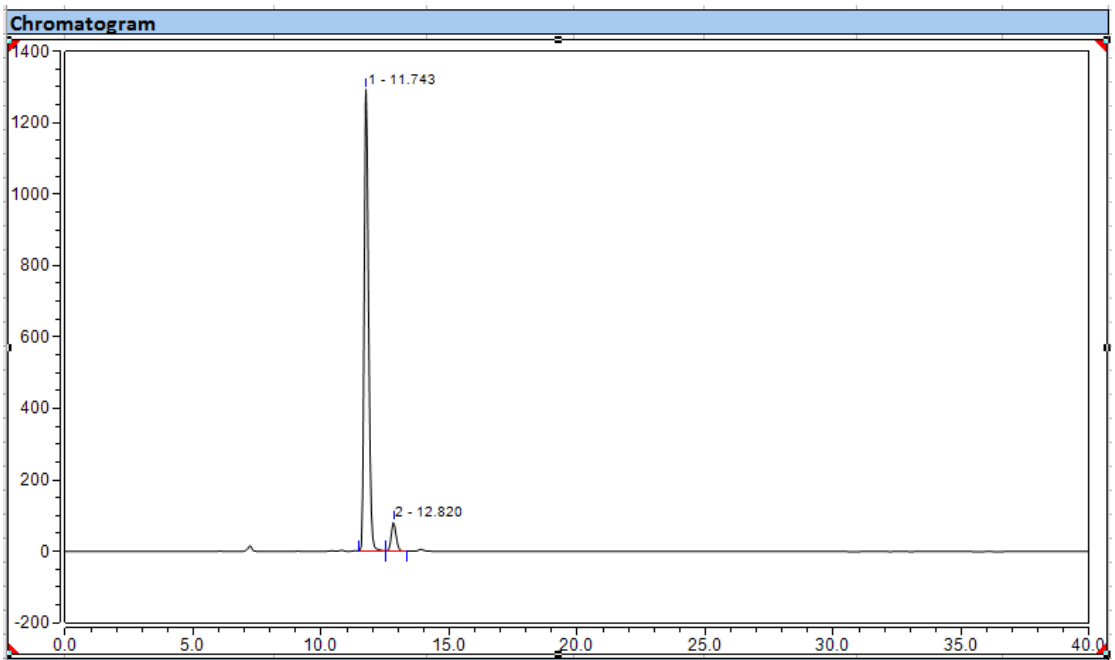

Integration Results

No.	Peak Name	Retention Time min	Area mAU*min	Height mAU	Relative Area %	Relative Height %	Amount n.a.
1		11.743	253.468	1292.680	93.43	94.10	n.a.
2		12.820	17.827	81.109	6.57	5.90	n.a.
Total:			**271.296**	**1373.789**	**100.00**	**100.00**	

Figure S123 HPLC Data and Chromatograms of 3z, related to Scheme 2

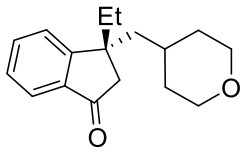

3z

HPLC (Chiralpak IB): t_R= 11.6 (minor), 12.4 (major)
Condition: 85:15 n-Hexane: i-PrOH, flow rate 0.5 mL/min, 25℃.
254nm

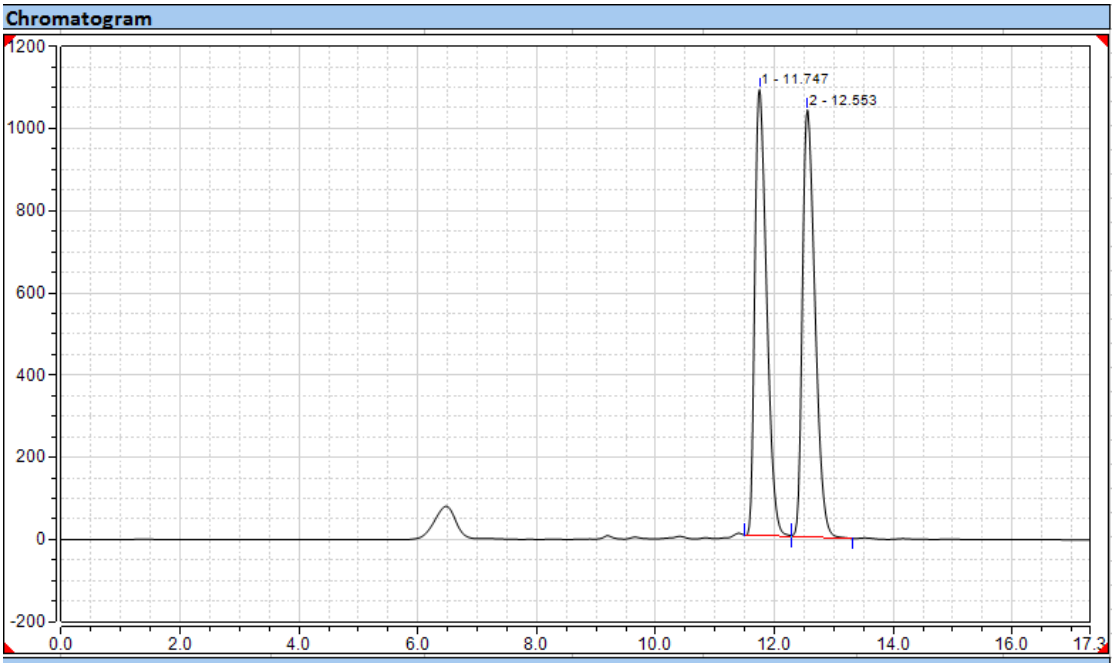

Integration Results

No.	Peak Name	Retention Time min	Area mAU*min	Height mAU	Relative Area %	Relative Height %	Amount n.a.
1		11.747	250.066	1085.799	49.47	51.09	n.a.
2		12.553	255.423	1039.517	50.53	48.91	n.a.
Total:			**505.489**	**2125.315**	**100.00**	**100.00**	

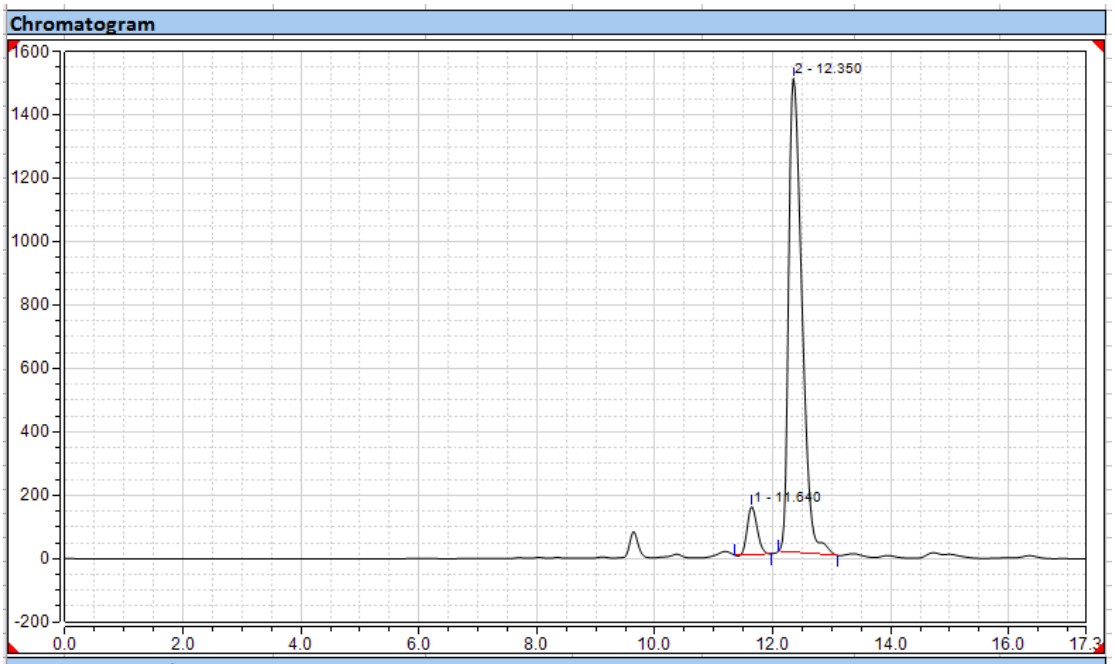

Integration Results

No.	Peak Name	Retention Time min	Area mAU*min	Height mAU	Relative Area %	Relative Height %	Amount n.a.
1		11.640	29.455	152.031	7.01	9.23	n.a.
2		12.350	390.918	1495.609	92.99	90.77	n.a.
Total:			**420.372**	**1647.641**	**100.00**	**100.00**	

Figure S124 HPLC Data and Chromatograms of 3aa, related to Scheme 2

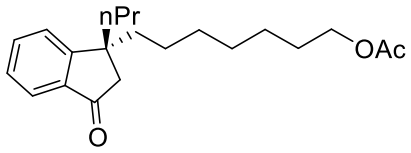

3aa

HPLC (Chiralcel OJH): t_R= 9.8 (minor), 10.8 (major)
Condition: 95:5 n-Hexane: i-PrOH, flow rate 1.0 mL/min, 25°C.
254nm

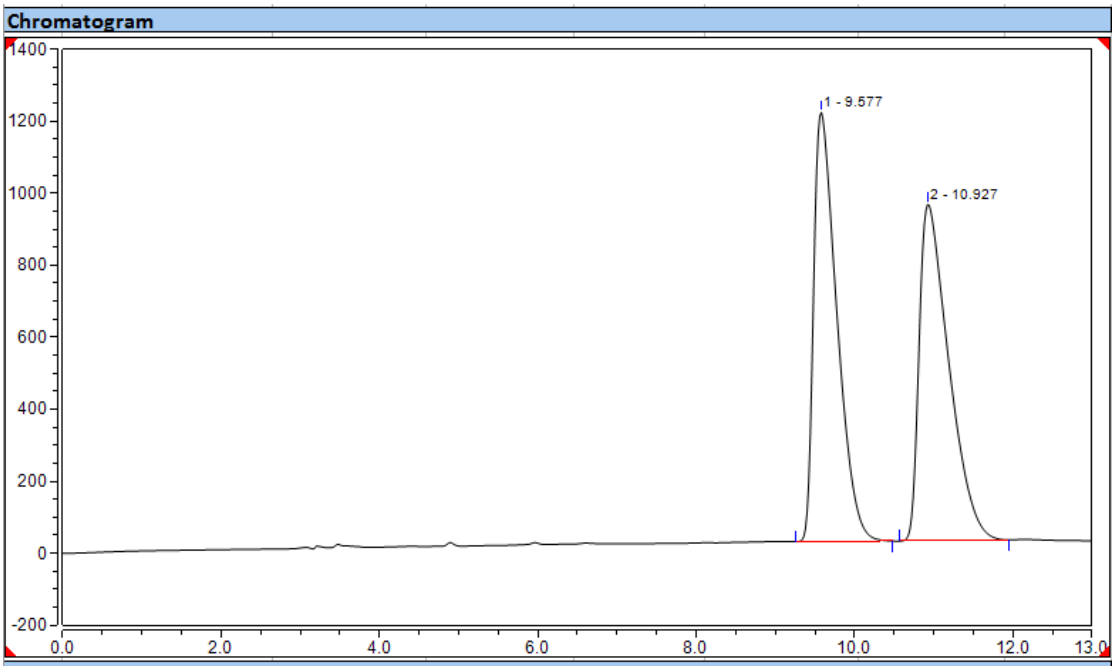

Integration Results

No.	Peak Name	Retention Time min	Area mAU*min	Height mAU	Relative Area %	Relative Height %	Amount n.a.
1		9.577	405.444	1192.717	50.06	56.05	n.a.
2		10.927	404.551	935.081	49.94	43.95	n.a.
Total:			**809.995**	**2127.799**	**100.00**	**100.00**	

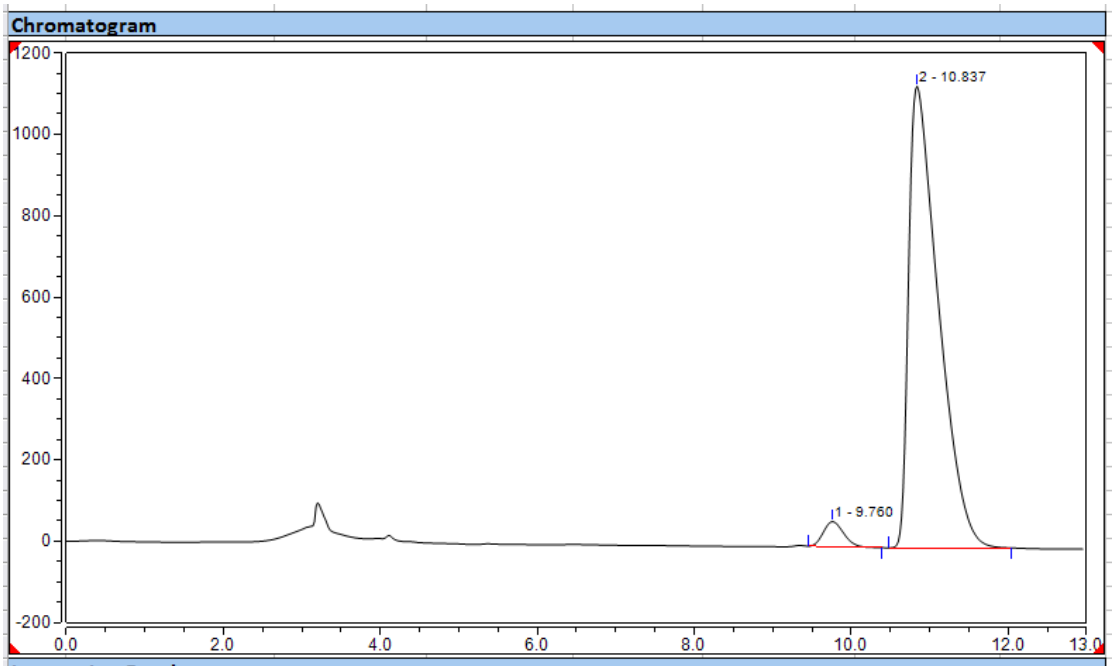

Integration Results

No.	Peak Name	Retention Time min	Area mAU*min	Height mAU	Relative Area %	Relative Height %	Amount n.a.
1		9.760	18.431	61.509	3.57	5.14	n.a.
2		10.837	498.291	1134.913	96.43	94.86	n.a.
Total:			**516.723**	**1196.421**	**100.00**	**100.00**	

Figure S125 HPLC Data and Chromatograms of 3ab, related to Scheme 2

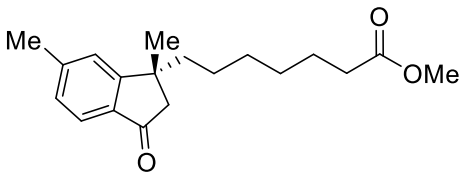

3ab

HPLC (Chiralpak IB): t_R= 16.2 (minor), 15.3 (major)
Condition: 92.5:7.5 n-Hexane: i-PrOH, flow rate 0.4 mL/min, 25℃. 254nm

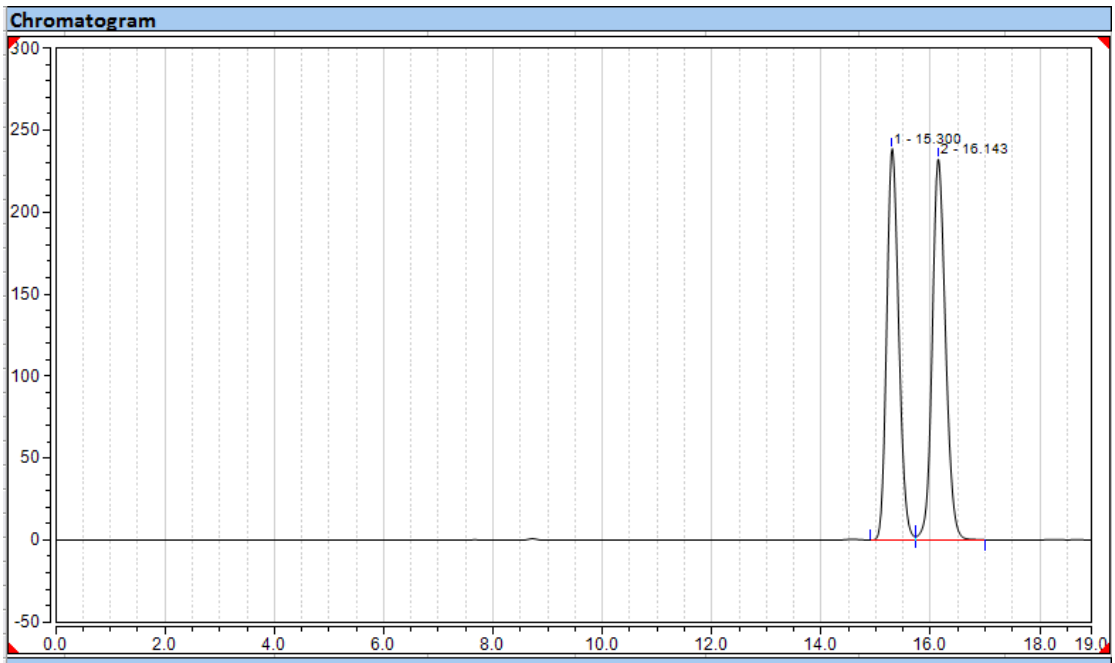

Integration Results

No.	Peak Name	Retention Time min	Area mAU*min	Height mAU	Relative Area %	Relative Height %	Amount n.a.
1		15.300	60.854	238.738	48.20	50.69	n.a.
2		16.143	65.388	232.250	51.80	49.31	n.a.
Total:			**126.242**	**470.988**	**100.00**	**100.00**	

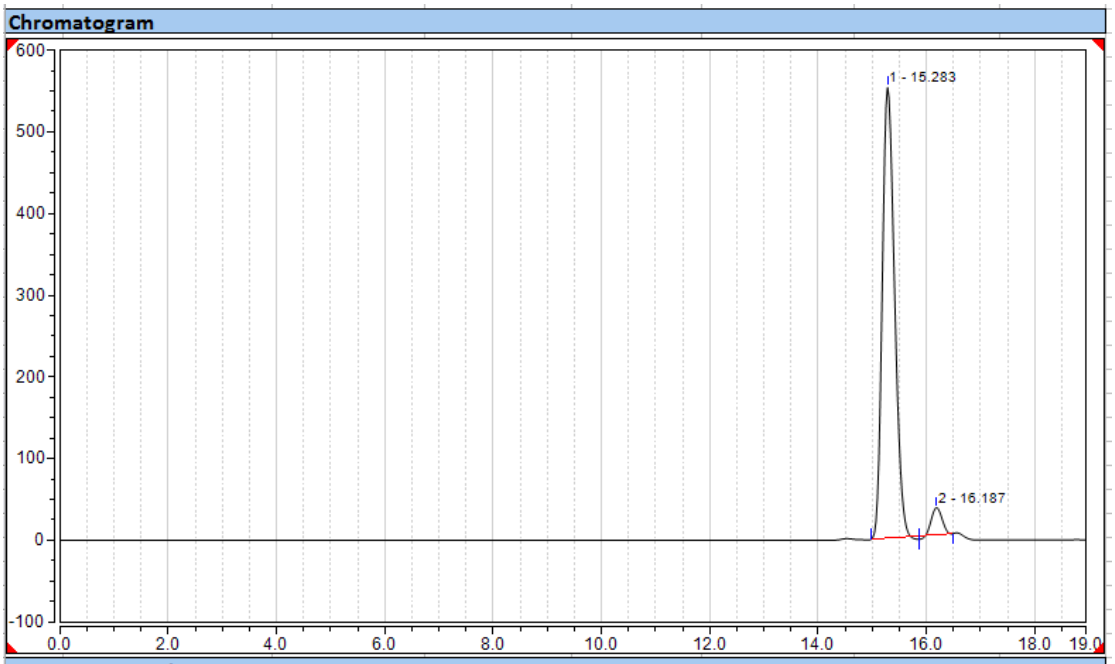

Integration Results

No.	Peak Name	Retention Time min	Area mAU*min	Height mAU	Relative Area %	Relative Height %	Amount n.a.
1		15.283	143.968	551.851	95.29	94.30	n.a.
2		16.187	7.123	33.328	4.71	5.70	n.a.
Total:			**151.091**	**585.179**	**100.00**	**100.00**	

Figure S126 HPLC Data and Chromatograms of 3ac, related to Scheme 2

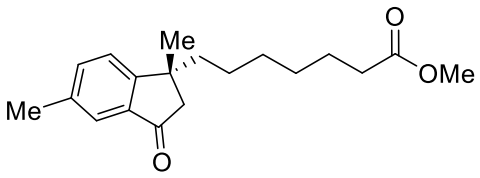

3ac

HPLC (Chiralpak IB): t_R= 17.5 (minor), 15.6 (major)
Condition: 92.5:7.5 n-Hexane: i-PrOH, flow rate 0.4 mL/min, 25℃.
254nm

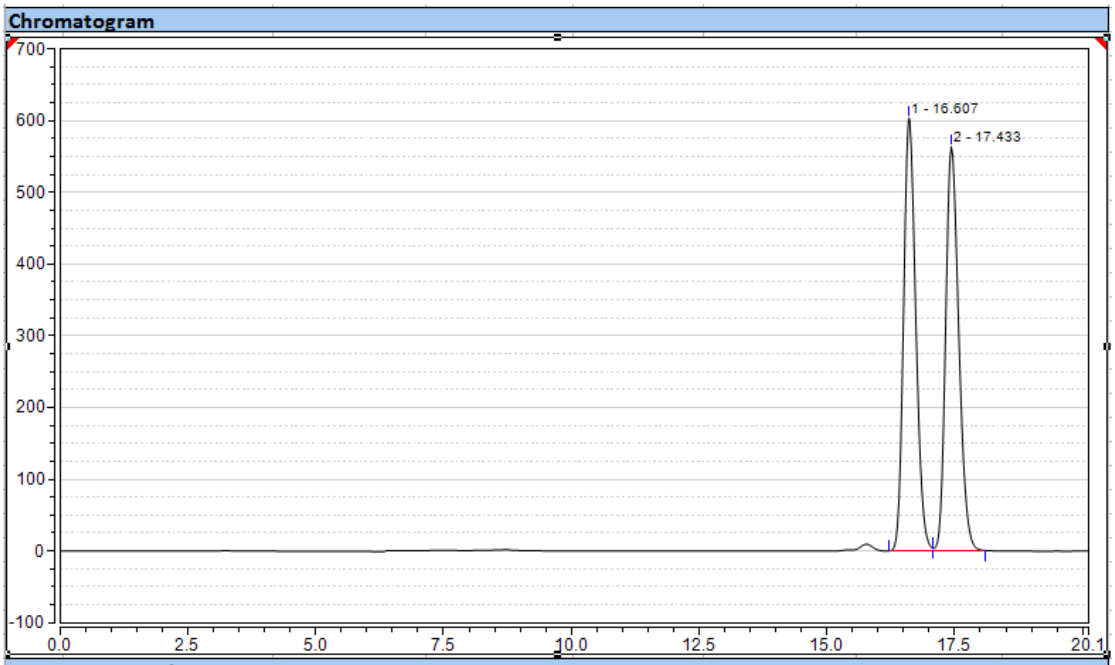

Integration Results

No.	Peak Name	Retention Time min	Area mAU*min	Height mAU	Relative Area %	Relative Height %	Amount n.a.
1		16.607	166.728	603.656	49.96	51.70	n.a.
2		17.433	166.966	563.969	50.04	48.30	n.a.
Total:			**333.694**	**1167.625**	**100.00**	**100.00**	

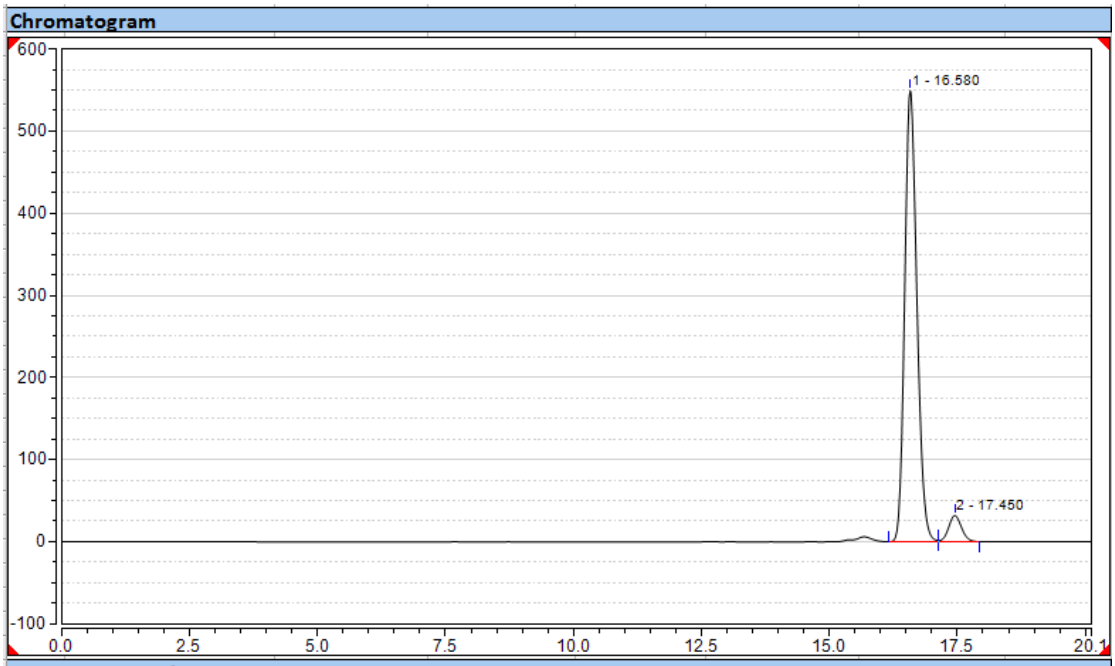

Integration Results

No.	Peak Name	Retention Time min	Area mAU*min	Height mAU	Relative Area %	Relative Height %	Amount n.a.
1		16.580	151.528	549.361	94.21	94.49	n.a.
2		17.450	9.315	32.061	5.79	5.51	n.a.
Total:			**160.843**	**581.422**	**100.00**	**100.00**	

Figure S127 HPLC Data and Chromatograms of 3ad, related to Scheme 2

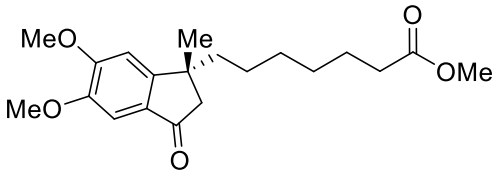

3ad

HPLC (Chiralpak ADH): t_R= 17.1 (minor), 19.9 (major)
Condition: 80:20 n-Hexane: i-PrOH, flow rate 0.5 mL/min, 25℃. 254nm

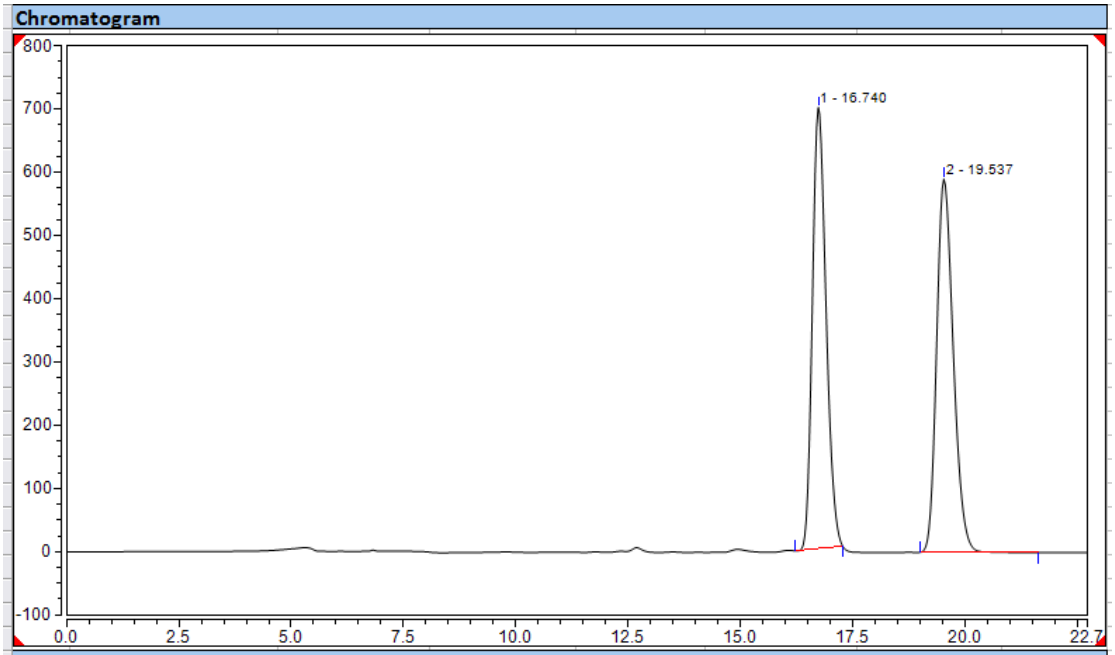

Integration Results

No.	Peak Name	Retention Time min	Area mAU*min	Height mAU	Relative Area %	Relative Height %	Amount n.a.
1		16.740	245.873	697.902	49.27	54.17	n.a.
2		19.537	253.208	590.546	50.73	45.83	n.a.
Total:			**499.082**	**1288.448**	**100.00**	**100.00**	

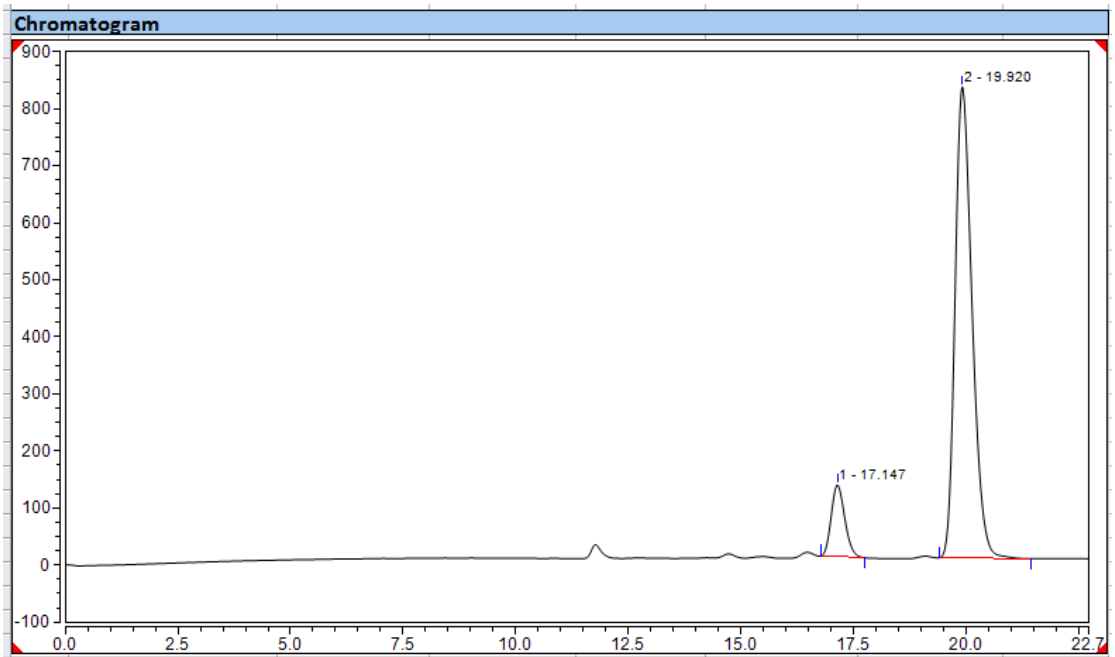

Integration Results

No.	Peak Name	Retention Time min	Area mAU*min	Height mAU	Relative Area %	Relative Height %	Amount n.a.
1		17.147	43.601	125.836	10.75	13.22	n.a.
2		19.920	361.876	826.181	89.25	86.78	n.a.
Total:			**405.476**	**952.018**	**100.00**	**100.00**	

Figure S128 HPLC Data and Chromatograms of 3ae, related to Scheme 2

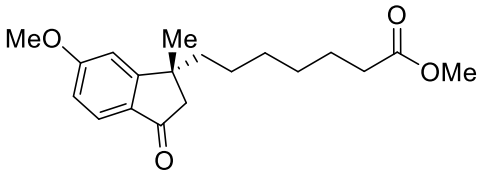

3ae

HPLC (Chiralpak IB): t_R= 10.8 (minor), 10.3 (major)
Condition: 80:20 n-Hexane: i-PrOH, flow rate 0.5 mL/min, 25℃.
254nm

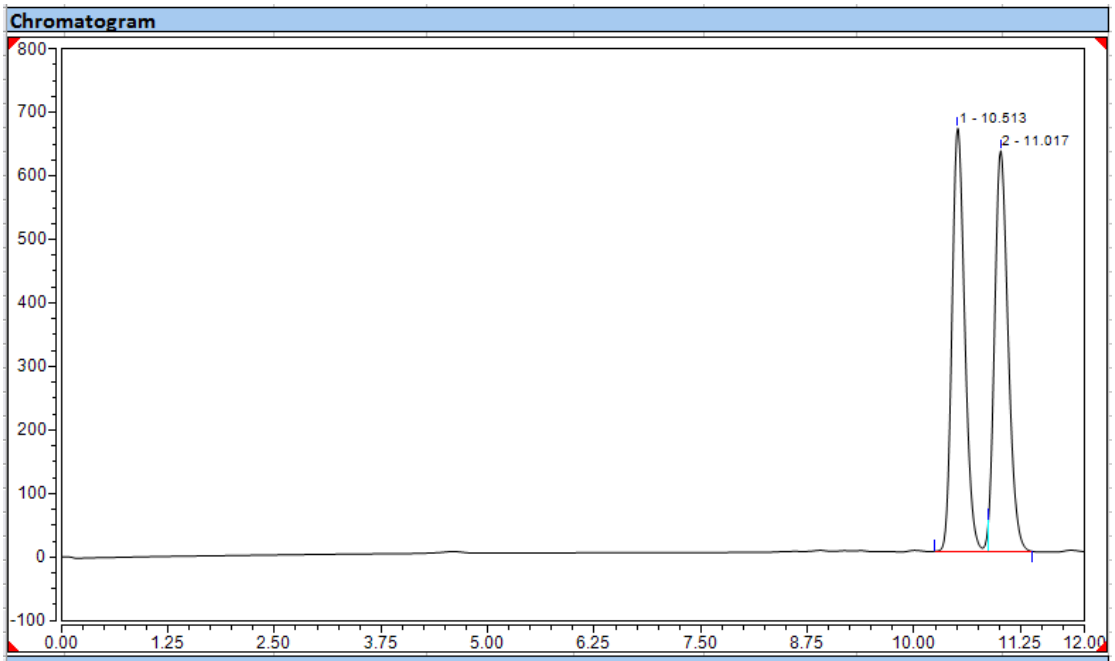

Integration Results

No.	Peak Name	Retention Time min	Area mAU*min	Height mAU	Relative Area %	Relative Height %	Amount n.a.
1		10.513	116.230	666.373	50.24	51.37	n.a.
2		11.017	115.140	630.760	49.76	48.63	n.a.
Total:			**231.369**	**1297.133**	**100.00**	**100.00**	

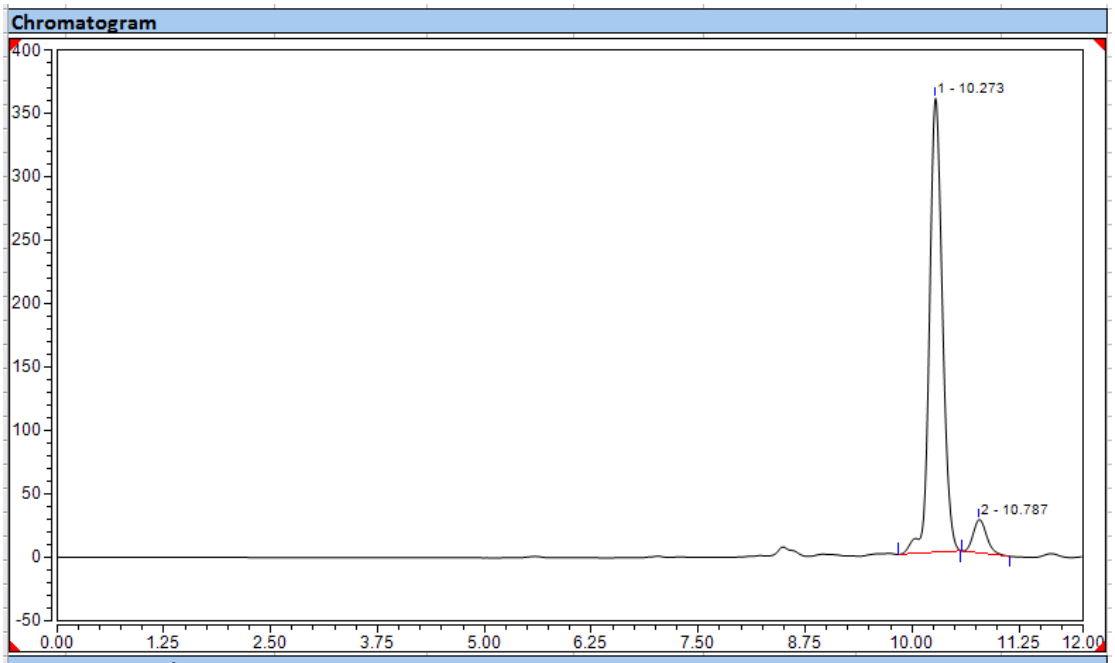

Integration Results

No.	Peak Name	Retention Time min	Area mAU*min	Height mAU	Relative Area %	Relative Height %	Amount n.a.
1		10.273	63.069	358.436	92.88	93.12	n.a.
2		10.787	4.838	26.494	7.12	6.88	n.a.
Total:			**67.907**	**384.931**	**100.00**	**100.00**	

Figure S129 HPLC Data and Chromatograms of 3af, related to Scheme 2

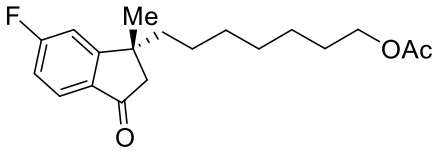

3af

HPLC (Chiralpak ADH): t_R= 22.2 (minor), 23.1 (major)
Condition: 97:3 n-Hexane: i-PrOH, flow rate 0.5 mL/min, 25℃.
254nm

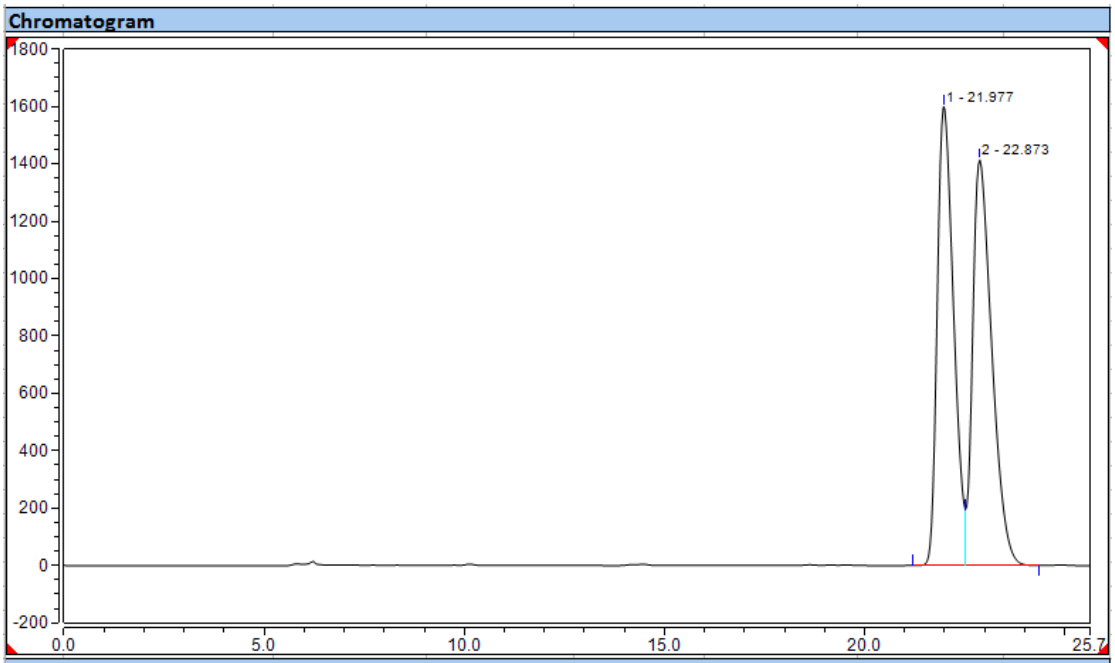

Integration Results

No.	Peak Name	Retention Time min	Area mAU*min	Height mAU	Relative Area %	Relative Height %	Amount n.a.
1		21.977	754.599	1599.881	48.99	53.07	n.a.
2		22.873	785.726	1414.625	51.01	46.93	n.a.
Total:			**1540.326**	**3014.506**	**100.00**	**100.00**	

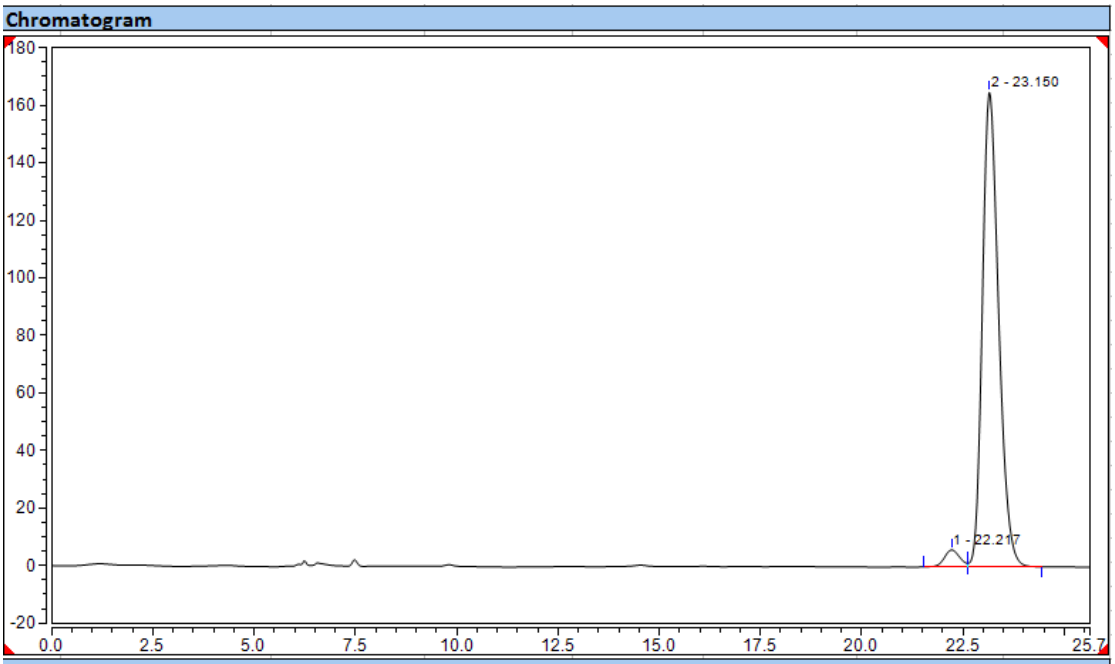

Integration Results

No.	Peak Name	Retention Time min	Area mAU*min	Height mAU	Relative Area %	Relative Height %	Amount n.a.
1		22.217	2.615	5.933	3.29	3.47	n.a.
2		23.150	76.855	164.956	96.71	96.53	n.a.
Total:			**79.470**	**170.889**	**100.00**	**100.00**	

Figure S130 HPLC Data and Chromatograms of 3ag, related to Scheme 2

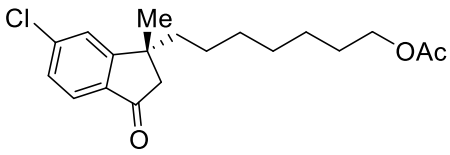

HPLC (Chiralpak ADH): t_R= 23.7 (minor), 25.3 (major)
Condition: 97:3 n-Hexane: i-PrOH, flow rate 0.5 mL/min, 25℃.
254nm

3ag

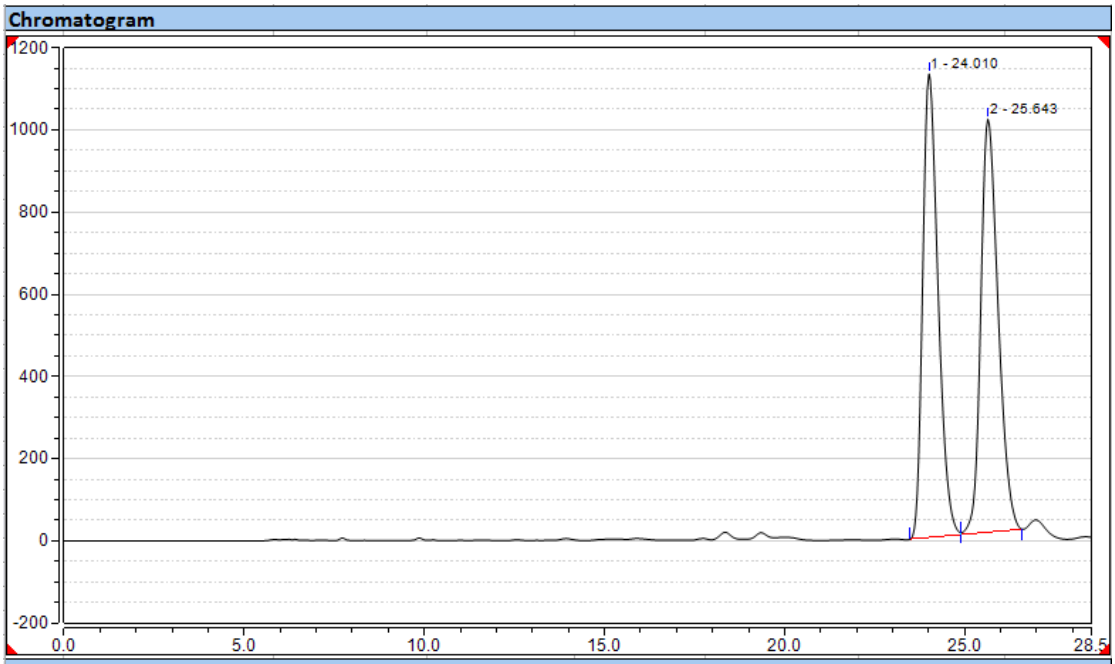

Integration Results

No.	Peak Name	Retention Time min	Area mAU*min	Height mAU	Relative Area %	Relative Height %	Amount n.a.
1		24.010	556.787	1128.157	49.77	52.86	n.a.
2		25.643	561.836	1006.154	50.23	47.14	n.a.
Total:			**1118.624**	**2134.310**	**100.00**	**100.00**	

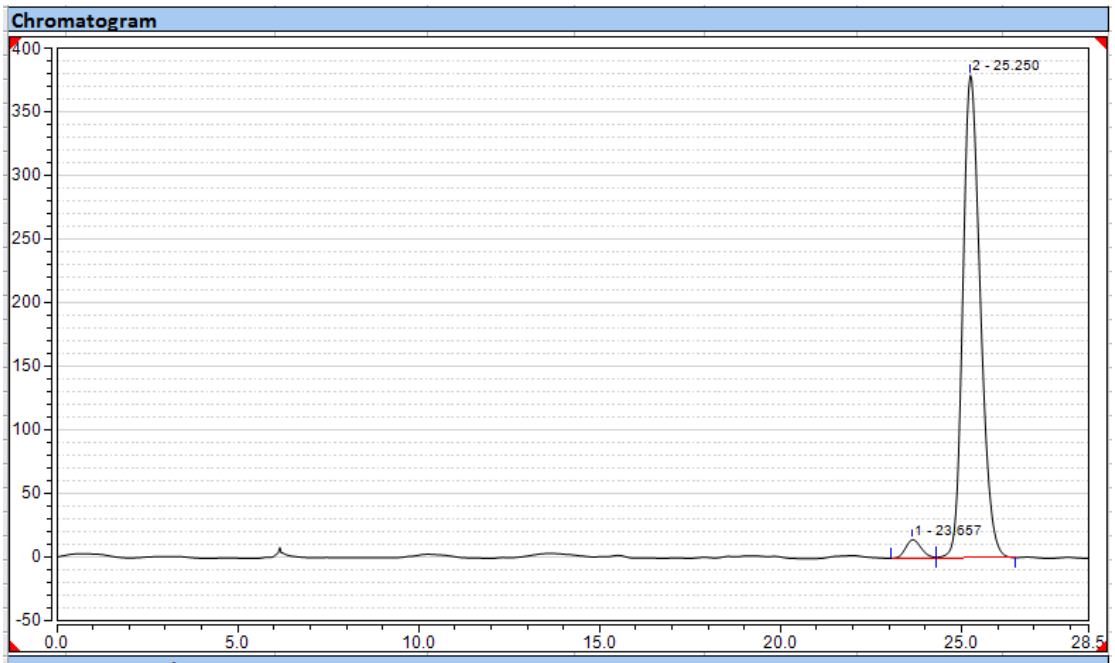

Integration Results

No.	Peak Name	Retention Time min	Area mAU*min	Height mAU	Relative Area %	Relative Height %	Amount n.a.
1		23.657	7.388	14.627	3.35	3.71	n.a.
2		25.250	213.183	379.829	96.65	96.29	n.a.
Total:			**220.571**	**394.456**	**100.00**	**100.00**	

Figure S131 HPLC Data and Chromatograms of 4, related to Scheme 3

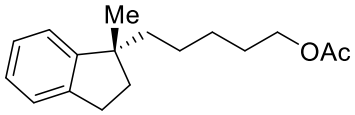

4

HPLC (ChiralpakIB): t_R= 11.6 (minor), 13.2 (major)
Condition: 98:2 n-Hexane:*i*-PrOH, flow rate 0.5 mL/min, 25°C.
254 nm

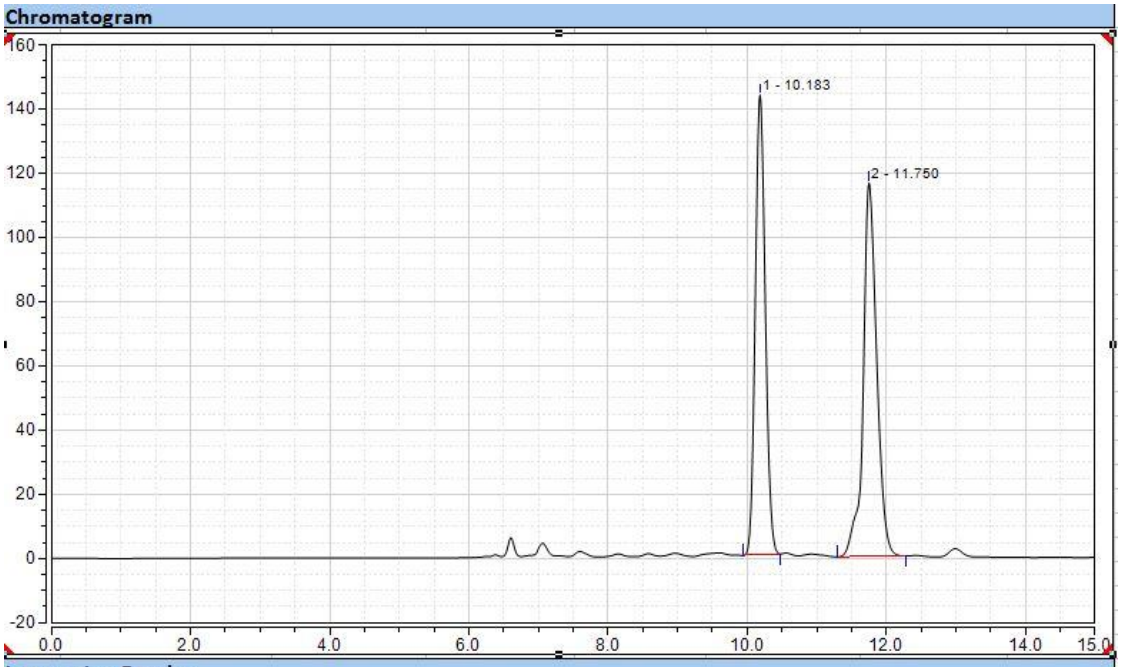

Integration Results

No.	Peak Name	Retention Time min	Area mAU*min	Height mAU	Relative Area %	Relative Height %	Amount n.a.
1		10.183	23.874	143.321	47.71	55.18	n.a.
2		11.750	26.162	116.403	52.29	44.82	n.a.
Total:			**50.036**	**259.724**	**100.00**	**100.00**	

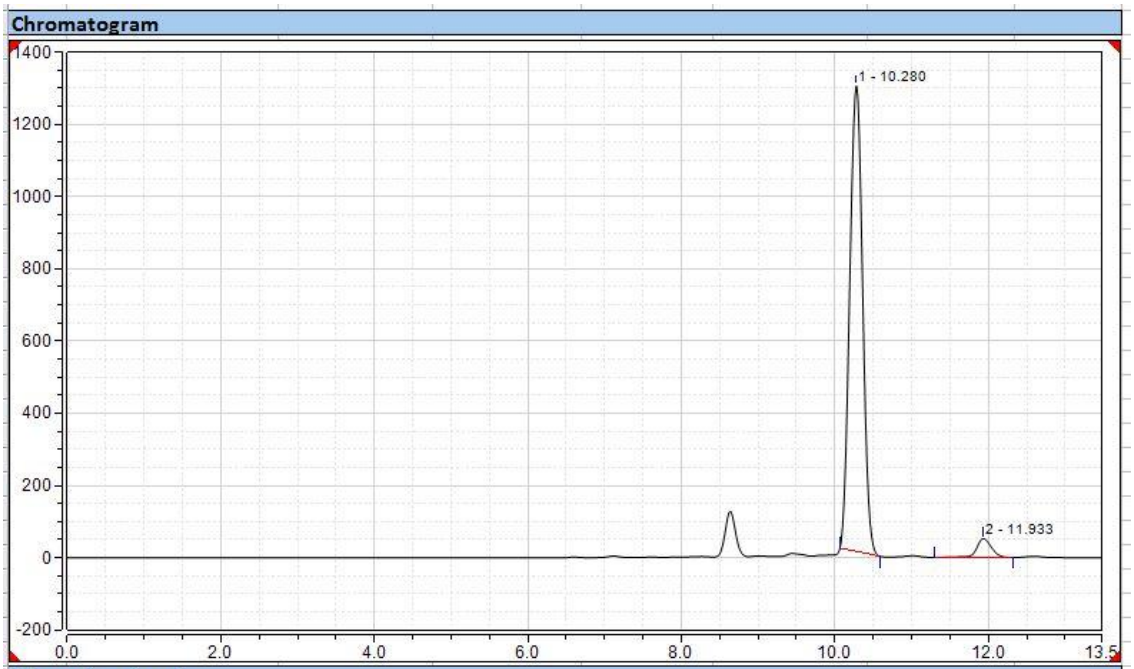

Integration Results

No.	Peak Name	Retention Time min	Area mAU*min	Height mAU	Relative Area %	Relative Height %	Amount n.a.
1		10.280	250.085	1289.300	95.49	96.09	n.a.
2		11.933	11.823	52.438	4.51	3.91	n.a.
Total:			**261.907**	**1341.738**	**100.00**	**100.00**	

Transparent Method

General Methods and Materials

^{1}H NMR and ^{13}C NMR spectra were recorded on a Bruker Advance 400M and 500M NMR spectrometers at ambient temperature in $CDCl_3$ at 400 and 101 MHz. The chemical shifts are given in ppm relative to tetramethylsilane [^{1}H: δ= ($SiMe_4$)= 0.00 ppm] as an internal standard or relative to the resonance of the solvent [^{1}H: δ=($CDCl_3$)= 7.26,^{13}C: δ= ($CDCl_3$)= 77.16 ppm].Multiplicities were given as: s (singlet); d (doublet); t (triplet); q (quartet); dd (doublet of doublets); dt (doublet of triplets); m (multiplets), etc. Coupling constants are reported as *J* values in Hz. High resolution mass spectral analysis (HRMS) was performed on Waters XEVO G2 Q-TOF. HPLC was performed on ThermoUltiMate 3000. Flash chromatography was performed using 300-400 mesh silica gel with the indicated solvent system.

All reagents and starting materials, unless otherwise noted, were purchased from commercial vendors and used without further purification.

Preparation of Cyclobutanones

Scheme S1. Cyclobutanones Employed, Related to Scheme 2

Successful Substrates for the Ni-Catalyzed Reactions:

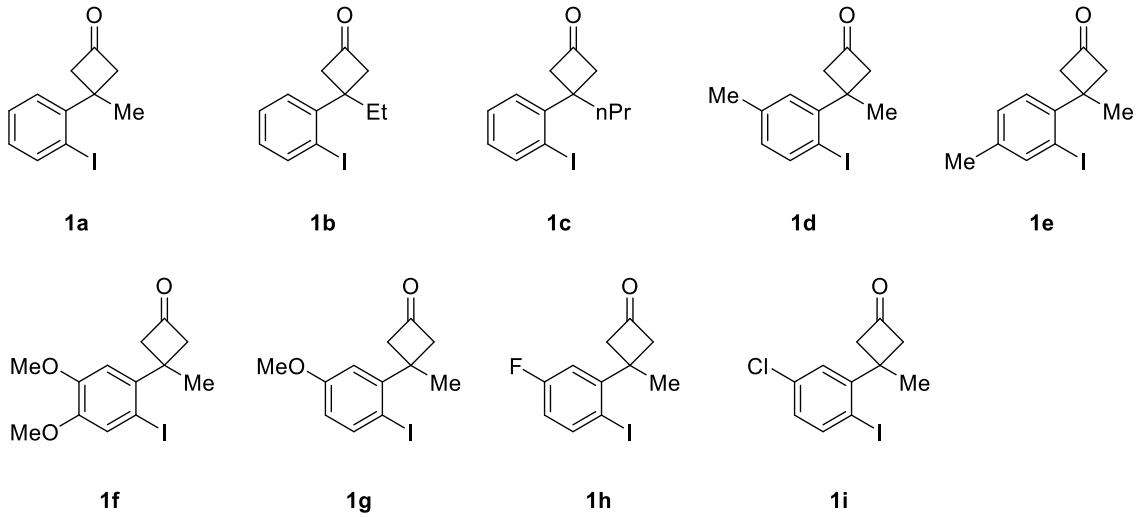

Unsuccessful Substrates for the Ni-Catalyzed Reactions:

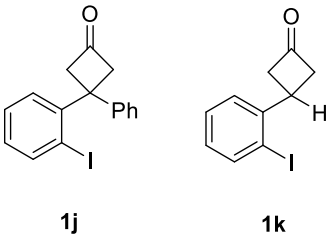

Cyclobutanones **1a**, **1b** and **1d-k** are known compounds in the literature procedures (Sun et al., 2019).

Scheme S2. Preparation of Cyclobutanone 1c (Guo et al., 2018), Related to Scheme 2

Triflic anhydride (3.95 g, 14 mmol, 1.4 equiv) was added dropwise to a solution of *N*,*N*-dimethylacetamide (1.05 g, 12 mmol, 1.2 equiv) in 14 mL of 1,2-dichloroethane under stirring at 5 ˚C. The mixture was stirred at 5℃ for 30 min, and then a mixture of 1-iodo-2-(pent-1-en-2-yl)benzene (2.72 g, 10 mmol, 1.0 equiv) and 2,4,6-collidine (1.69 g, 14 mmol, 1.4 equiv) in 2 mL of 1,2-dichloroethane was added dropwise. After the reaction mixture was refluxed for 18 h, 1,2 dichloromethane was removed in vacuum and the residue was treated with 4 mL H_2O and CCl_4 (1:1). The obtained mixture was refluxed for 18 h, and then the aqueous layer was extracted with CCl_4 (3 × 50 mL). The combined organic layers were dried over Na_2SO_4 and filtered. Concentration of the solution by rotary evaporation under reduced pressure gave a residue, which was purified by silica gel (petroleum ether: EtOAc= 25:1) to afford *3-(2-iodophenyl)-3-propylcyclobutan-1-one* (**1c**) as yellow solid (2.13g, 68% yield). ^{1}H NMR (500 MHz, Chloroform-*d*) δ= 7.92 (dd, *J*= 7.9, 1.3 Hz, 1H), 7.34 (td, *J*= 7.5, 1.4 Hz, 1H), 7.20 (dd, *J*= 7.8, 1.7 Hz, 1H), 6.93 (td, *J*= 7.6, 1.6 Hz, 1H), 3.61-3.16 (m, 4H), 2.39-1.56 (m, 2H), 1.18-0.96 (m, 2H), 0.84 (t, *J*= 7.2 Hz, 3H) ppm. ^{13}C NMR (126 MHz, Chloroform-*d*) δ= 206.2, 146.8, 141.6, 129.5, 128.3, 127.7, 95.4, 57.6, 41.4, 40.9 (2C), 18.9, 14.2 ppm. HRMS (ESI): calcd. for $C_{13}H_{15}IONa$ $[M+Na]^+$: 337.0060, found: 337.0065.

Preparation of Alkyl Bromides

Scheme S3. Alkyl Bromides Employed, Related to Scheme 2

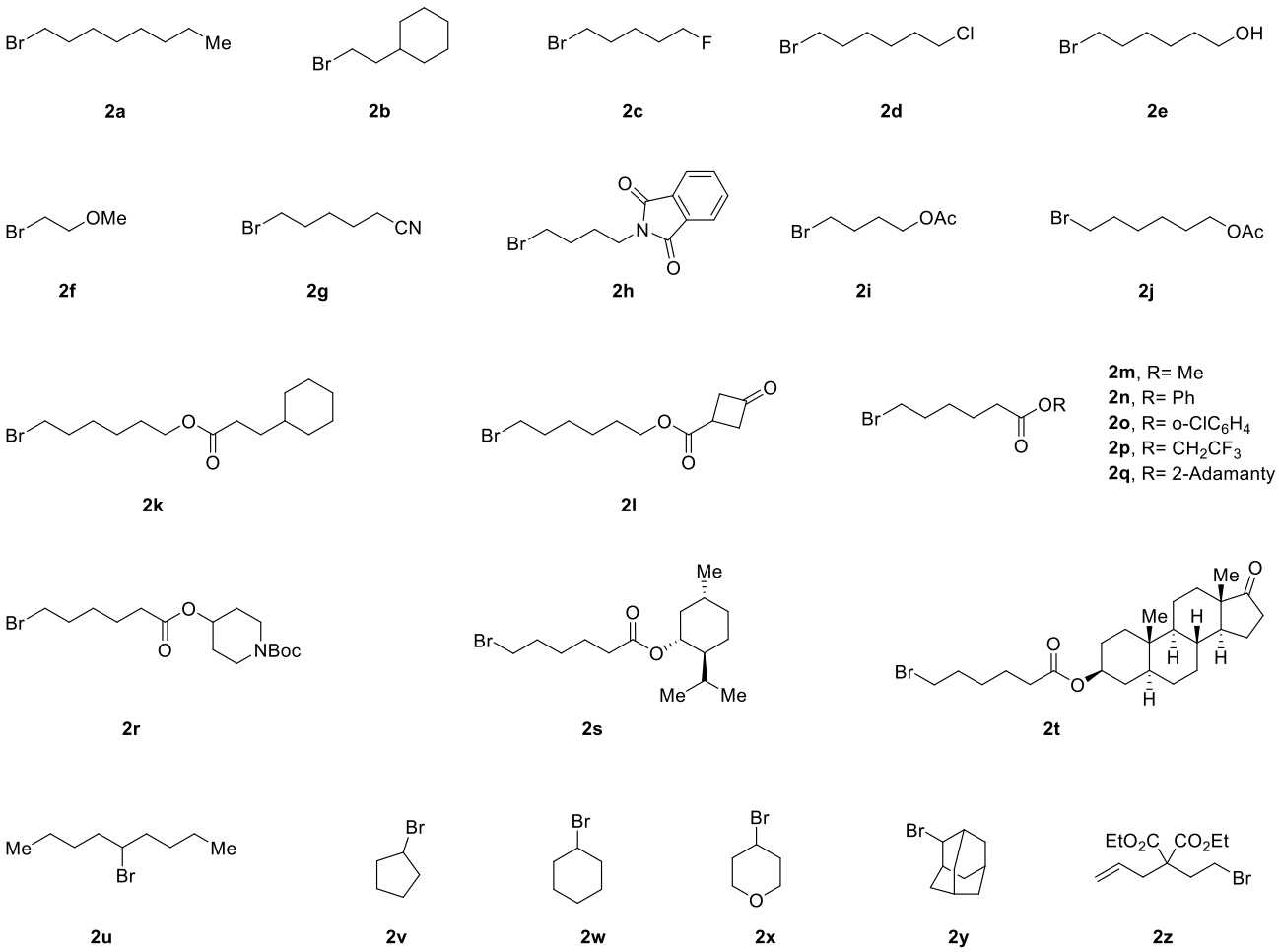

2a-j, **2m** and **2u-y** are commercially available. **2n**, **2p**, **2s** and **2z** are known compounds in the literature (Nicotrat et al., 1990; Zhang et al., 2004; Narayan et al., 2015; Burkhart et al., 2012).
2k, **2l**, **2o**, **2q**, **2r** and **2t** were prepared according to the following general procedure.

Scheme S4. Preparation of Alkyl Bromides 2k, 2l, 2o, 2q, 2r and 2t, Related to Scheme 2

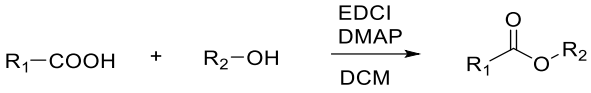

A mixture of acids (12 mmol, 1.2 equiv), 1-(3-dimethylaminopropyl)-3-ethylcarbodiimide hydrochloride (2.16 g, 12 mmol, 1.2 equiv), 4-dimethylaminopyridine (0.25g, 2 mmol, 0.2 equiv) and alcohols (10 mmol, 1.0 equiv) in DCM (0.2 M, 50 mL) was stirred at room temperature for 12 hours, before it was quenched by adding water. The aqueous phase was then extracted with DCM (3 × 25 mL). The combined organic phases were washed with water and brine, dried over $MgSO_4$, filtered, and concentrated under reduced pressure. The residue was subjected to column chromatography on silica gel with EtOAc–petroleum ether as an eluent to give the corresponding esters.

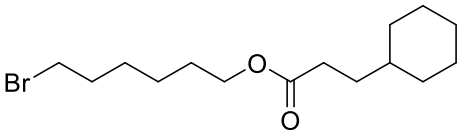

2k

6-Bromohexyl 3-cyclohexylpropanoate (**2k**) was isolated through column chromatography on silica gel (petroleum ether: EtOAc= 25:1) as a colorless oil (3.02g, 95%). ^{1}H NMR (500 MHz, Chloroform-*d*) δ= 4.00 (t, *J*= 6.6, 2H), 3.34 (t, *J*= 6.9, 2H), 2.27-2.18 (m, 2H), 1.85-1.76 (m, 2H), 1.67-1.54 (m, 7H), 1.51-1.38 (m, 4H), 1.36-1.28 (m, 2H), 1.22-1.01 (m, 4H), 0.89-0.76 (m, 2H) ppm. ^{13}C NMR (126 MHz, Chloroform-d) δ= 173.1, 63.1, 36.2, 32.6, 32.0 (2C), 31.6, 31.4, 30.9, 27.5, 26.8, 25.5, 25.2 (2C), 24.2 ppm. HRMS (ESI): calcd. for $C_{15}H_{27}BrO_2Na$ $[M+Na]^+$: 341.1087, found: 341.1082.

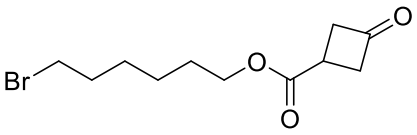

2l

6-Bromohexyl 3-oxocyclobutane-1-carboxylate (**2l**) was isolated through column chromatography on silica gel (petroleum ether: EtOAc= 15:1) as a colorless oil (2.62g, 95%). ^{1}H NMR (500 MHz, Chloroform-d) δ= 4.16 (t, J= 6.7 Hz, 2H), 3.46-3.37 (m, 4H), 3.34-3.16 (m, 3H), 1.87 (dt, J= 8.3, 6.8 Hz, 2H), 1.74-1.62 (m, 2H), 1.56-1.34 (m, 4H) ppm. ^{13}C NMR (126 MHz, Chloroform-*d*) δ= 203.7, 174.1, 65.2, 51.6 (2C), 33.7, 32.5, 28.4, 27.7, 27.4, 25.1 ppm. HRMS (ESI): calcd. for $C_{11}H_{17}BrO_3Na$ $[M+Na]^+$: 299.0253, found: 299.0256.

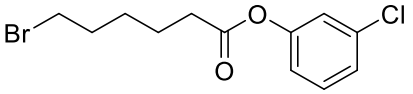

2o

3-Chlorophenyl 6-bromohexanoate (**2o**) was isolated through column chromatography on silica gel (petroleum ether: EtOAc= 25:1) as a colorless oil (2.70g, 90%). ^{1}H NMR (400 MHz, Chloroform-*d*) δ= 7.28 (t, *J*= 8.1 Hz, 1H), 7.23-7.16 (m, 1H), 7.12 (t, *J*= 2.2 Hz, 1H), 7.02-6.95 (m, 1H), 3.41 (t, *J*= 6.7 Hz, 2H), 2.55 (t, *J*= 7.4 Hz, 2H), 1.96-1.84 (m, 2H), 1.79-1.70 (m, 2H), 1.60-1.49 (m, 2H) ppm. ^{13}C NMR (101 MHz, Chloroform-*d*) δ= 171.5, 151.2, 134.6, 130.2, 126.1, 122.3, 120.1, 34.0, 33.6, 32.4, 27.6, 24.0 ppm. HRMS (ESI): calcd. for $C_{12}H_{14}BrClO_2Na$ $[M+Na]^+$: 326.9761, found: 326.9761.

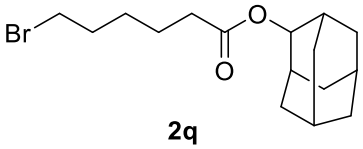

2q

Adamantan-2-yl 6-bromohexanoate (**2q**) was isolated through column chromatography on silica gel (petroleum ether: EtOAc= 25:1) as a colorless oil (2.79g, 85%). ^{1}H NMR (400 MHz, Chloroform-*d*) δ= 4.90 (t, *J*= 2.4 Hz, 1H), 3.41 (t, *J*= 6.8 Hz, 2H), 2.36 (t, *J*= 7.4 Hz, 2H), 2.04-1.96 (m, 4H), 1.94-1.81 (m, 6H), 1.80-1.72 (m, 4H), 1.71-1.63 (m, 2H), 1.59-1.44 (m, 4H) ppm. ^{13}C NMR (101 MHz, Chloroform-*d*) δ= 172.9, 76.9, 37.4, 36.3 (2C), 34.6, 33.6, 32.5, 31.9 (2C), 31.8 (2C), 27.7, 27.2, 27.0, 24.3 ppm. HRMS (ESI): calcd. for $C_{16}H_{25}BrO_2Na$ $[M+Na]^+$: 351.0930, found: 351.0935.

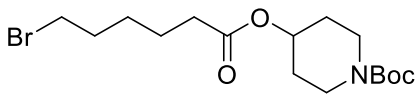

2r

Tert-butyl 4-((6-bromohexanoyl)oxy)piperidine-1-carboxylate (**2r**) was isolated through column chromatography on silica gel (petroleum ether: EtOAc= 10:1) as a white solid (3.39g, 90%). ^{1}H NMR (400 MHz, Chloroform-*d*) δ= 4.99-4.86 (m, 1H), 3.79-3.65 (m, 2H), 3.48 (t, *J*= 6.7 Hz, 2H), 3.29-3.11 (m, 2H), 2.33 (t, *J*= 7.4 Hz, 2H), 1.99-1.75 (m, 4H), 1.70-1.55 (m, 4H), 1.53-1.47 (m, 2H), 1.46 (s, 9H) ppm. ^{13}C NMR (101 MHz, Chloroform-*d*) δ= 172.6, 154.6, 79.5, 69.6, 44.7, 40.9, 34.2, 33.4, 32.3, 30.5, 28.4 (3C), 27.5, 26.2, 24.1 ppm. HRMS (ESI): calcd. for $C_{16}H_{29}BrO_2$ $[M+H]^+$: 378.1274, found: 378.1283.

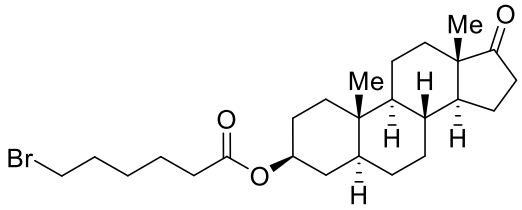

2t

(3S,5S,8R,9S,10S,13S,14S)-10,13-Dimethyl-17-oxohexadecahydro-1H-cyclopenta[a]phenanthren-3-yl 6-bromohexanoate (**2t**) was isolated through column chromatography on silica gel (petroleum ether: EtOAc= 10:1) as a white solid (3.7g, 80%). ^{1}H NMR (400 MHz, Chloroform-*d*) δ= 4.70 (tt, *J*= 10.8, 4.6 Hz, 1H), 3.4 (t, *J*= 6.7, 2H), 2.43 (dd, *J*= 19.2, 8.8 Hz, 1H), 2.29 (t, *J*= 7.4 Hz, 2H), 2.06 (dt, *J*= 18.8, 9.0 Hz, 1H), 1.99-1.73 (m, 7H), 1.70-1.57 (m, 4H), 1.59-1.43 (m, 5H), 1.41-1.15 (m, 7H), 1.10-0.92 (m, 2H), 0.86 (s, 6H), 0.72 (td, *J*= 11.1, 3.9 Hz, 1H) ppm. ^{13}C NMR (101 MHz, Chloroform-*d*) δ= 73.3, 54.3, 51.3, 47.7, 44.6, 36.7, 35.8, 35.6, 35.0, 34.4, 34.0, 33.6, 32.4, 32.2, 31.5, 30.8, 28.3, 27.6, 27.4, 26.3, 24.2, 21.8, 20.5, 13.8, 12.2 ppm. HRMS (ESI): calcd. for $C_{25}H_{39}BrO_2Na$ $[M+Na]^+$: 489.1975, found: 489.1980.

Experimental Procedures for Nickel-Catalyzed Asymmetric Domino Ring Opening/Cross-Coupling Reaction

Scheme S5. Nickel-Catalyzed Asymmetric Domino Ring Opening/Cross-Coupling Reaction, Related to Scheme 2

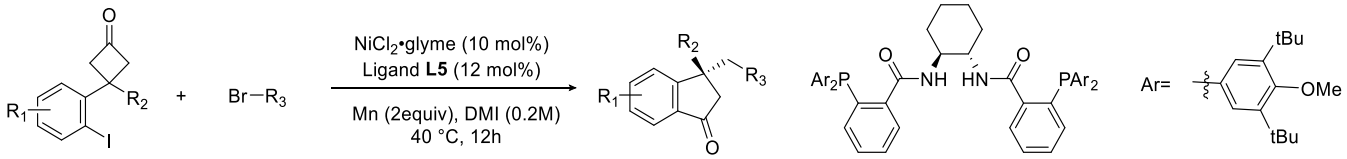

1 2 3 L5

A dry test tube equipped with a stirring bar was charged with $NiCl_2$•glyme (4.4 mg, 0.02 mmol, 10 mol%), ligand **L5** (30.2 mg, 0.024 mmol, 12 mol %), Mn (22 mg, 0.4 mmol, 2.0 equiv) and anhydrous 1,3-dimethyl-2-imidazolidinone (1 mL) under N_2. The mixture was heated to 40°C, before cyclobutanones **1** (0.2 mmol, 1.0 equiv) and alkyl bromides **2** (0.4 mmol, 2.0 equiv) were added. After stirring for 12 h at 40 ˚C, the reaction mixture was cooled to room temperature. The mixture was purified through column chromatography on silica gel, affording the corresponding products **3**.

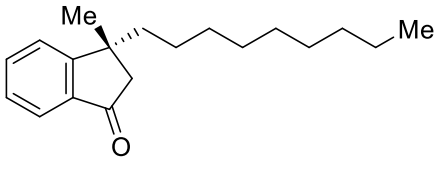

3a

(R)-3-Methyl-3-nonyl-2,3-dihydro-1H-inden-1-one (**3a**) was isolated through column chromatography on silica gel (petroleum ether: EtOAc= 25:1) as a yellow oil (45 mg, 83%, 93% *ee*). ^{1}H NMR (400 MHz, Chloroform-*d*) δ= 7.70 (d, *J*= 7.7 Hz, 1H), 7.60 (td, *J*= 7.5, 1.3 Hz, 1H), 7.45 (d, *J*= 7.7 Hz, 1H), 7.35 (t, *J*= 7.4 Hz, 1H), 2.67 (d, *J*= 18.8 Hz, 1H), 2.44 (d, *J*= 18.8 Hz, 1H), 1.79-1.57 (m, 2H), 1.40 (s, 3H), 1.30-1.17 (m, 14H), 0.86 (t, *J* = 6.9 Hz, 3H). ^{13}C

NMR (101 MHz, Chloroform-*d*) δ= 206.0, 163.0, 136.0, 134.8, 127.3, 123.8, 123.2, 50.2, 42.3, 42.0, 31.8, 30.0, 29.5, 29.4, 29.3, 28.4, 25.0, 22.6, 14.1 ppm. HRMS (ESI): calcd. for $C_{19}H_{29}O$ $[M+H]^+$: 273.2213, found: 273.2214. The *ee* was determined by HPLC analysis (Chiralpak IC column, λ = 254 nm, hexane/isopropanol = 95/5, flow rate = 0.5 mL/min): t_R(minor) = 13.7 min, t_R(major) = 15.3 min.

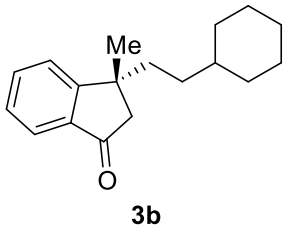

3b

(R)-3-(2-Cyclohexylethyl)-3-methyl-2,3-dihydro-1H-inden-1-one (**3b**) was isolated through column chromatography on silica gel (petroleum ether: EtOAc= 25:1) as a yellow oil (43 mg, 83%, 94% *ee*). ^{1}H NMR (400 MHz, Chloroform-*d*) δ= 7.70 (dt, *J* = 7.7, 1.1 Hz, 1H), 7.63-7.58 (m, 1H), 7.44 (dt, *J*= 7.8, 0.9 Hz, 1H), 7.36 (td, *J*= 7.3, 1.0 Hz, 1H), 2.66 (d, *J*= 18.9 Hz, 1H), 2.43 (d, *J*= 18.9 Hz, 1H), 1.79-1.57 (m, 7H), 1.40 (s, 3H), 1.20-1.04 (m, 5H), 0.88-0.72 (m, 3H) ppm. ^{13}C NMR (101 MHz, Chloroform-*d*) δ= 206.2, 163.0, 136.0, 134.8, 127.4, 123.8, 123.3, 50.1, 41.9, 39.5, 38.1, 33.0 (2C), 32.6, 28.5, 26.6, 26.31, 26.30 ppm. HRMS (ESI): calcd. for $C_{18}H_{24}ONa$ $[M+Na]^+$: 279.1719, found: 279.1711. The *ee* was determined by HPLC analysis (Chiralpak IC column, λ = 254 nm, hexane/isopropanol = 95/5, flow rate = 0.5 mL/min): t_R(minor) = 15.9 min, t_R(major) = 18.4 min.

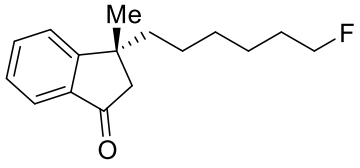

3c

(R)-3-(6-Fluorohexyl)-3-methyl-2,3-dihydro-1H-inden-1-one (**3c**) was isolated through column chromatography on silica gel (petroleum ether: EtOAc= 25:1) as a yellow oil (39 mg, 79%, 94% *ee*). ^{1}H NMR (400 MHz, Chloroform-*d*) δ= 7.70 (dt, *J*= 7.6, 1.0 Hz, 1H), 7.61 (td, *J*= 7.5, 1.2 Hz, 1H), 7.45 (dt, *J*= 7.8, 0.9 Hz, 1H), 7.37 (td, *J*= 7.4, 1.0 Hz, 1H), 4.39 (dt, *J*= 47.3, 6.1 Hz, 2H), 2.66 (d, *J*= 18.8 Hz, 1H), 2.45 (d, *J*= 18.8 Hz, 1H), 1.82-1.53 (m, 4H), 1.41 (s, 3H), 1.38-1.16 (m, 6H) ppm. ^{13}C NMR (101 MHz, Chloroform-*d*) δ= 206.1, 162.8, 136.0, 134.9, 127.4, 123.8, 123.3, 84.1 (d, *J*= 164.2 Hz), 50.2, 42.2, 42.0, 30.3 (d, *J*= 19.4 Hz), 29.6, 28.4, 25.0 (d, *J*= 5.3 Hz), 24.9 ppm. ^{19}F NMR (471 MHz, Chloroform-*d*) δ= -218.19 (s, 1F) ppm.HRMS (ESI): calcd. for $C_{16}H_{21}FONa$ $[M+Na]^+$:271.1469, found: 271.1473. The *ee* was determined by HPLC analysis (Chiralpak IC column, λ = 254 nm, hexane/isopropanol = 95/5, flow rate = 0.5 mL/min): t_R(minor) = 32.0 min, t_R(major) = 32.6 min.

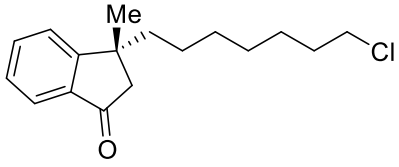

3d

(R)-3-(7-Chloroheptyl)-3-methyl-2,3-dihydro-1H-inden-1-one (**3d**) was isolated through column chromatography on silica gel (petroleum ether: EtOAc= 25:1) as a yellow oil (45 mg, 81%, 92% *ee*). ^{1}H NMR (400 MHz, Chloroform-*d*) δ= 7.63 (dt, *J*= 7.6, 1.0 Hz, 1H), 7.54 (td, *J*= 7.5, 1.2 Hz, 1H), 7.38 (dt, *J*= 7.8, 0.9 Hz, 1H), 7.29 (td, *J*= 7.4, 1.0 Hz, 1H), 3.42 (t, *J*= 6.7 Hz, 2H), 2.59 (d, *J*= 18.8 Hz, 1H), 2.37 (d, *J*= 18.8 Hz, 1H), 1.71-1.48 (m, 4H), 1.34 (s, 3H), 1.34-1.22 (m, 2H), 1.21-1.09 (m, 6H) ppm. ^{13}C NMR (101 MHz, Chloroform-*d*) δ= 206.2, 162.9, 136.0, 134.9, 127.4, 123.8, 123.3, 50.2, 45.1, 42.2, 42.0, 32.5, 29.8, 28.7, 28.4, 26.8, 24.9 ppm. HRMS (ESI): calcd. for $C_{17}H_{23}FClONa$ $[M+Na]^+$:301.1330, found: 301.1327. The *ee* was determined by HPLC analysis (Chiralpak IC column, λ = 254 nm, hexane/isopropanol = 95/5, flow rate = 0.5 mL/min): t_R(minor) = 29.0 min, t_R(major) = 30.2 min.

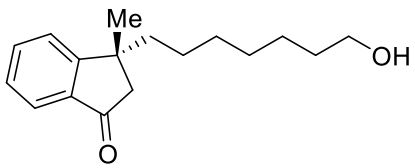

3e

(R)-3-(7-Hydroxyheptyl)-3-methyl-2,3-dihydro-1H-inden-1-one (**3e**) was isolated through column chromatography on silica gel (petroleum ether: EtOAc= 25:1) as a yellow oil (41 mg, 78%, 90% *ee*). ^{1}H NMR (400 MHz, Chloroform-*d*) δ= 7.70 (dt, *J*= 7.7, 1.0 Hz, 1H), 7.61 (td, *J*= 7.5, 1.3 Hz, 1H), 7.45 (dd, *J*= 7.8, 1.0 Hz, 1H), 7.36 (td, *J*= 7.5, 1.0 Hz, 1H), 3.60 (t, *J*= 6.6 Hz, 2H), 2.67 (d, *J*= 18.8 Hz, 1H), 2.44 (d, *J*= 18.8 Hz, 1H), 1.81 (s, 1H), 1.77-1.58 (m, 2H), 1.57-1.47 (m, 2H), 1.41 (s, 3H), 1.35-1.16 (m, 8H) ppm. ^{13}C NMR (101 MHz, Chloroform-*d*) δ= 206.3, 162.9, 136.0, 134.9, 127.4, 123.8, 123.3, 62.9, 50.2, 42.3, 42.0, 32.7, 30.0, 29.2, 28.4, 25.7, 25.0 ppm. HRMS (ESI): calcd.

for $C_{17}H_{24}O_2Na$ $[M+Na]^+$: 283.1669, found: 283.1666. The *ee* was determined by HPLC analysis (Chiralpak AD-H column, λ = 254 nm, hexane/isopropanol = 80/20, flow rate = 0.5 mL/min): t_R(minor) = 12.6 min, t_R(major) = 11.7 min.

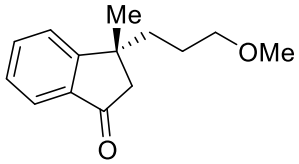

3f

(R)-3-(3-Methoxypropyl)-3-methyl-2,3-dihydro-1H-inden-1-one (**3f**) was isolated through column chromatography on silica gel (petroleum ether: EtOAc= 15:1) as a yellow oil (30 mg, 68%, 90% *ee*). ^{1}H NMR (400 MHz, Chloroform-*d*) δ= 7.63 (d, *J*= 7.7 Hz, 1H), 7.53 (d, *J*= 7.5 Hz, 1H), 7.40 (d, *J*= 7.8 Hz, 1H), 7.30 (t, *J*= 7.5 Hz, 1H), 3.24 (t, *J*= 6.7 Hz, 2H), 3.20 (s, 3H), 2.60 (d, *J*= 18.7 Hz, 1H), 2.40 (d, *J*= 18.8 Hz, 1H), 1.79-1.61 (m, 2H), 1.51-1.38 (m, 2H), 1.36 (s, 3H) ppm. ^{13}C NMR (101 MHz, Chloroform-*d*) δ= 204.9, 161.5, 135.0, 133.9, 126.5, 122.8, 122.3, 71.7, 57.5, 49.1, 40.7, 37.6, 27.3, 24.4 ppm. HRMS (ESI): calcd. for $C_{14}H_{18}O_2Na$ $[M+Na]^+$: 241.1199, found: 241.1196. The *ee* was determined by HPLC analysis (Chiralcel OJ-H column, λ = 254 nm, hexane/isopropanol = 90/10, flow rate = 0.5 mL/min): t_R(minor) = 12.7 min, t_R(major) = 12.0 min.

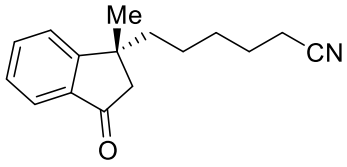

3g

(R)-6-(1-Methyl-3-oxo-2,3-dihydro-1H-inden-1-yl)hexanenitrile (**3g**) was isolated through column chromatography on silica gel (petroleum ether: EtOAc= 10:1) as a yellow oil (34 mg, 71%, 92% *ee*). ^{1}H NMR (400 MHz, Chloroform-*d*) δ= 7.62 (d, *J*= 7.6 Hz, 1H), 7.55 (t, *J*= 7.5 Hz, 1H), 7.38 (d, *J*= 7.7 Hz, 1H), 7.30 (t, *J*= 7.5 Hz, 1H), 2.57 (d, *J*= 18.8 Hz, 1H), 2.38 (d, *J*= 18.9 Hz, 1H), 2.20 (t, *J*= 7.1 Hz, 2H), 1.71-1.54 (m, 2H), 1.73-1.43 (m, 2H), 1.34 (s, 3H), 1.32-1.24 (m, 2H), 1.24-1.09 (m, 2H) ppm. ^{13}C NMR (101 MHz, Chloroform-*d*) δ= 205.9, 162.4, 136.0, 135.0, 127.6, 123.8, 123.3, 119.7, 50.1, 41.92, 41.89, 29.0, 28.4, 25.2, 24.3, 17.1 ppm. HRMS (ESI): calcd. for $C_{16}H_{19}NONa$ $[M+Na]^+$: 264.1359, found: 264.1363. The *ee* was determined by HPLC analysis (Chiralcel OD-H column, λ = 254 nm, hexane/isopropanol = 85/15, flow rate = 0.5 mL/min): t_R(minor) = 27.6 min, t_R(major) = 25.4 min.

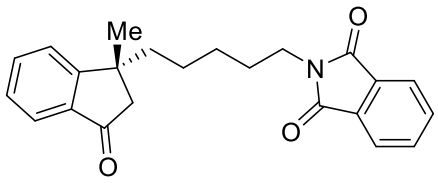

3h

(R)-2-(5-(1-Methyl-3-oxo-2,3-dihydro-1H-inden-1-yl)pentyl)isoindoline-1,3-dione (**3h**) was isolated through column chromatography on silica gel (petroleum ether: EtOAc= 3:1) as a yellow oil (60mg, 84%, 92% *ee*). ^{1}H NMR (400 MHz, Chloroform-*d*) δ= 7.87-7.79 (m, 2H), 7.74-7.65 (m, 3H), 7.60 (t, *J*= 7.5 Hz, 1H), 7.45 (d, *J*= 7.7 Hz, 1H), 7.35 (t, *J*= 7.4 Hz, 1H), 3.62 (t, *J*= 7.1 Hz, 2H), 2.66 (d, *J*= 18.9 Hz, 1H), 2.45 (d, *J*= 18.9 Hz, 1H), 1.79-1.54 (m, 4H), 1.40 (s, 3H), 1.36-1.15 (m, 4H) ppm. ^{13}C NMR (101 MHz, Chloroform-*d*) δ= 206.0, 168.4 (2C), 162.7, 135.9, 134.9 (2C), 133.9 (2C), 132.1, 127.4, 123.8, 123.3, 123.1 (2C), 50.1, 42.0, 41.9, 37.8, 28.4, 28.3, 27.2, 24.6 ppm. HRMS (ESI): calcd. for $C_{23}H_{23}NO_3Na$ $[M+Na]^+$: 384.1570, found: 384.1571. The *ee* was determined by HPLC analysis (Chiralpak AD-H column, λ = 254 nm, hexane/isopropanol = 85/15, flow rate = 0.5 mL/min): t_R(minor) = 30.2 min, t_R(major) = 31.4 min.

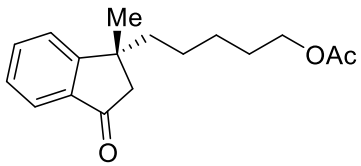

3i

(R)-5-(1-methyl-3-oxo-2,3-dihydro-1H-inden-1-yl)pentyl acetate (**3i**) was isolated through column chromatography on silica gel (petroleum ether: EtOAc= 10:1) as a yellow oil (38 mg, 70%, 90% *ee*). ^{1}H NMR (400 MHz, Chloroform-*d*) δ= 7.63 (d, *J* = 7.6 Hz, 1H), 7.54 (t, *J*= 7.5 Hz, 1H), 7.38 (d, *J*= 7.7 Hz, 1H), 7.31 (t, 1H), 3.92 (t, *J*= 6.7 Hz, 2H), 2.59 (d, *J*= 18.9 Hz, 1H), 2.39 (d, *J*= 18.8 Hz, 1H), 1.95 (s, 3H), 1.73-1.42 (m, 4H), 1.34 (s, 3H), 1.25-1.13 (m, 4H) ppm. ^{13}C NMR (101 MHz, Chloroform-*d*) δ= 206.1, 171.2, 162.7, 136.0, 135.0, 127.5, 123.8, 123.4, 64.4, 50.2, 42.2, 42.0, 28.44, 28.39, 26.4, 24.8, 21.0 ppm. HRMS (ESI): calcd. for $C_{17}H_{22}O_3Na$ $[M+Na]^+$: 297.1461, found: 397.1460. The *ee* was determined by HPLC analysis (Chiralpak IB column, λ = 254 nm,

hexane/isopropanol = 95/5, flow rate = 0.5 mL/min): t_R(minor) = 17.8 min, t_R(major) = 15.1 min.

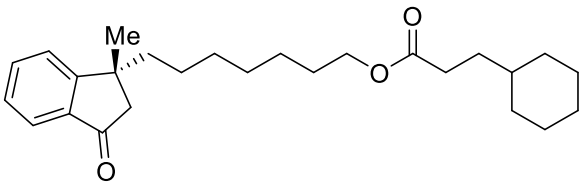

3j

(R)-7-(1-Methyl-3-oxo-2,3-dihydro-1H-inden-1-yl)heptyl 3-cyclohexylpropanoate (**3j**) was isolated through column chromatography on silica gel (petroleum ether: EtOAc= 10:1) as a yellow oil (60mg, 76%, 91% *ee*). ^{1}H NMR (400 MHz, Chloroform-*d*) δ= 7.63 (d, *J*= 7.7 Hz, 1H), 7.54 (t, *J*= 7.6 Hz, 1H), 7.38 (d, *J*= 7.8 Hz, 1H), 7.30 (t, *J*= 7.5 Hz, 1H), 3.94 (t, *J*= 6.8 Hz, 2H), 2.59 (d, *J*= 18.8 Hz, 1H), 2.37 (d, *J*= 18.8 Hz, 1H), 2.22 (t, *J*= 7.9 Hz, 2H), 1.75-1.39 (m, 13H), 1.34 (s, 3H), 1.24-1.05 (m, 12H) ppm. ^{13}C NMR (101 MHz, Chloroform-*d*) δ= 206.2, 174.3, 162.9, 136.0, 134.9, 127.4, 123.8, 123.3, 64.3, 50.2, 42.3, 42.0, 37.2, 33.0 (2C), 32.4, 32.0, 29.9, 29.1, 28.6, 28.4, 26.5, 26.2 (2C), 25.9, 25.0 ppm. HRMS (ESI): calcd. for $C_{26}H_{38}O_3Na$ $[M+Na]^+$: 421.2713, found: 421.2713. The *ee* was determined by HPLC analysis (Chiralpak AD-H column, λ = 254 nm, hexane/isopropanol = 95/5, flow rate = 0.5 mL/min): t_R(minor) = 19.8 min, t_R(major) = 18.4 min.

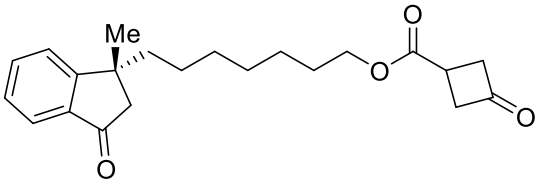

3K

(R)-7-(1-methyl-3-oxo-2,3-dihydro-1H-inden-1-yl)heptyl 3-oxocyclobutane-1-carboxylate (**3k**) was isolated through column chromatography on silica gel (petroleum ether: EtOAc= 5:1) as a yellow oil (56mg, 78%, 94% *ee*). ^{1}H NMR (400 MHz, Chloroform-*d*) δ= 7.76-7.67 (m, 1H), 7.61 (t, *J*= 7.5 Hz, 1H), 7.45 (d, *J*= 7.4 Hz, 1H), 7.37 (t, *J*= 7.4 Hz, 1H), 4.11 (t, *J*= 6.7 Hz, 2H), 3.46-3.34 (m, 2H), 3.33-3.16 (m, 3H), 2.64 (d, *J*= 18.8 Hz, 1H), 2.47 (d, *J*= 18.8 Hz, 1H), 1.79-1.53 (m, 4H), 1.41 (s, 3H), 1.34-1.18 (m, 8H). ^{13}C NMR (101 MHz, Chloroform-*d*) δ= 206.1, 203.8, 174.1, 162.8, 136.0, 134.9, 127.4, 123.8, 123.3, 65.4, 51.6 (2C), 50.2, 42.3, 42.0, 29.9, 29.0, 28.5, 28.4, 27.4, 25.8, 24.9 ppm. HRMS (ESI): calcd. for $C_{22}H_{28}O_4Na$ $[M+Na]^+$: 379.1880, found: 379.1883. The *ee* was determined by HPLC analysis (Chiralpak AD-H column, λ = 254 nm, hexane/isopropanol = 90/10, flow rate = 0.5 mL/min): t_R(minor) = 31.7 min, t_R(major) = 29.3 min.

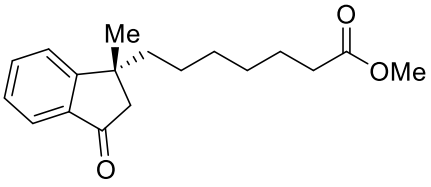

3l

Methyl (R)-7-(1-methyl-3-oxo-2,3-dihydro-1H-inden-1-yl)heptanoate (**3l**) was isolated through column chromatography on silica gel (petroleum ether: EtOAc= 10:1) as a yellow oil (49mg, 85%, 89% *ee*). ^{1}H NMR (400 MHz, Chloroform-*d*) δ= 7.70 (dt, *J*= 7.7, 1.0 Hz, 1H), 7.61 (ddd, *J*= 7.7, 7.2, 1.2 Hz, 1H), 7.45 (dt, *J*= 7.7, 0.9 Hz, 1H), 7.37 (td, *J*= 7.4, 1.0 Hz, 1H), 3.65 (s, 3H), 2.66 (d, *J*= 18.8 Hz, 1H), 2.45 (d, *J*= 18.9 Hz, 1H), 2.26 (t, *J* = 7.5 Hz, 2H), 1.73-1.61 (m, 2H), 1.60-1.52 (m, 2H), 1.41 (s, 3H), 1.31-1.22 (m, 6H) ppm. ^{13}C NMR (101 MHz, Chloroform-*d*) δ= 206.1, 174.2, 162.8, 136.0, 134.9, 127.4, 123.8, 123.3, 51.5, 50.2, 42.2, 42.0, 34.0, 29.7, 28.9, 28.4, 24.9, 24.8 ppm. HRMS (ESI): calcd. for $C_{18}H_{24}O_3Na$ $[M+Na]^+$: 311.1618, found: 311.1616. The *ee* was determined by HPLC analysis (Chiralpak AD-H column, λ = 254 nm, hexane/isopropanol = 90/10, flow rate = 0.5 mL/min): t_R(minor) = 24.4 min, t_R(major) = 21.2 min.

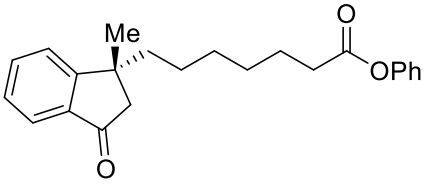

3m

Phenyl (R)-7-(1-methyl-3-oxo-2,3-dihydro-1H-inden-1-yl)heptanoate (**3m**) was isolated through column chromatography on silica gel (petroleum ether: EtOAc= 10:1) as a yellow oil (54mg, 77%, 84% *ee*). ^{1}H NMR (500 MHz, Chloroform-*d*) δ= 7.70 (dt, *J*= 7.7, 1.0 Hz, 1H), 7.61 (td, *J*= 7.5, 1.2 Hz, 1H), 7.45 (dt, *J*= 7.8, 0.9 Hz, 1H), 7.40-7.34 (m, 3H), 7.24-7.19 (m, 1H), 7.08-7.04 (m, 2H), 2.67 (d, *J*= 18.8 Hz, 1H), 2.51 (t, *J*= 7.5 Hz, 2H), 2.45 (d, *J*= 18.8 Hz, 1H), 1.79-1.61 (m, 4H), 1.41 (s, 3H), 1.37-1.26 (m, 6H) ppm. ^{13}C NMR (126

MHz, Chloroform-*d*) δ= 206.1, 172.2, 162.8, 150.7, 136.0, 134.9, 129.4 (2C), 127.5, 125.7, 123.8, 123.3, 121.6 (2C), 50.2, 42.2, 42.0, 34.3, 29.7, 28.9, 28.4, 24.9, 24.8 ppm. HRMS (ESI): calcd. for $C_{23}H_{26}O_3Na$ $[M+Na]^+$: 373.1774, found: 373.1772. The *ee* was determined by HPLC analysis (Chiralpak AD-H column, λ = 254 nm, hexane/isopropanol = 90/10, flow rate = 0.5 mL/min): t_R(minor) = 24.4 min, t_R(major) = 21.2 min.

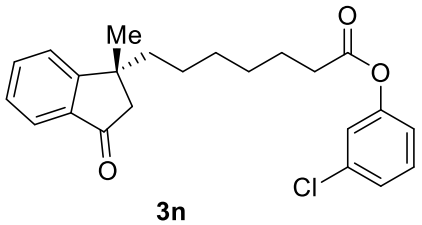

3n

3-Chlorophenyl (R)-7-(1-methyl-3-oxo-2,3-dihydro-1H-inden-1-yl)heptanoate (**3n**) was isolated through column chromatography on silica gel (petroleum ether: EtOAc= 10:1) as a yellow oil (53mg, 69%, 94% *ee*). ^{1}H NMR (400 MHz, Chloroform-*d*) δ= 7.71 (d, *J*= 7.7 Hz, 1H), 7.61 (t, *J*= 7.5 Hz, 1H), 7.46 (d, *J*= 7.7 Hz, 1H), 7.37 (t, *J*= 7.4 Hz, 1H), 7.29 (t, *J*= 8.2 Hz, 1H), 7.20 (d, *J*= 8.4 Hz, 1H), 7.10 (d, *J*= 2.3 Hz, 1H), 6.97 (d, *J*= 8.0 Hz, 1H), 2.67 (d, *J*= 18.9 Hz, 1H), 2.55-2.41 (m, 3H), 1.81-1.60 (m, 4H), 1.41 (s, 3H), 1.38-1.23 (m, 6H) ppm. ^{13}C NMR (101 MHz, Chloroform-*d*) δ= 206.3, 171.8, 162.8, 151.2, 136.0, 135.0, 134.6, 130.2, 127.5, 126.1, 123.8, 123.4, 122.3, 120.0, 50.2, 42.2, 42.0, 34.2, 29.7, 28.9, 28.4, 24.9, 24.7 ppm. HRMS (ESI): calcd. for $C_{23}H_{25}ClO_3Na$ $[M+Na]^+$: 407.1384, found: 407.1396. The *ee* was determined by HPLC analysis (Chiralpak AD-H column, λ = 254 nm, hexane/isopropanol = 90/10, flow rate = 0.5 mL/min): t_R(minor) = 23.0 min, t_R(major) = 20.5 min.

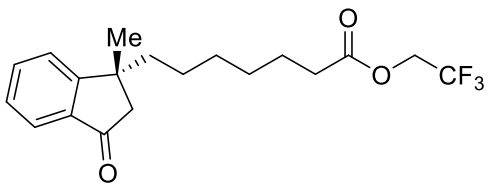

3o

2,2,2-Trifluoroethyl (R)-7-(1-methyl-3-oxo-2,3-dihydro-1H-inden-1-yl)heptanoate (**3o**) was isolated through column chromatography on silica gel (petroleum ether: EtOAc= 10:1) as a yellow oil (58mg, 82%, 89% *ee*). ^{1}H NMR (400 MHz, Chloroform-*d*) δ= 7.70 (ddd, *J*= 7.7, 1.3, 0.8 Hz, 1H), 7.61 (ddd, *J*= 7.7, 7.1, 1.2 Hz, 1H), 7.45 (dt, *J*= 7.7, 0.9 Hz, 1H), 7.37 (td, *J*= 7.5, 1.0 Hz, 1H), 4.45 (q, *J*= 8.5 Hz, 2H), 2.66 (d, *J*= 18.8 Hz, 1H), 2.45 (d, *J*= 18.8 Hz, 1H), 2.37 (t, *J*= 7.4 Hz, 2H), 1.78-1.52 (m, 4H), 1.41 (s, 3H), 1.33-1.21 (m, 6H) ppm. ^{13}C NMR (101 MHz, Chloroform-*d*) δ= 206.1, 172.0, 162.8, 136.0, 134.9, 127.4, 123.8, 123.3, 123.0 (q, *J* = 277.2 Hz), 60.1 (q, *J* = 36.4 Hz), 50.2, 42.1, 42.0, 33.5, 29.6, 28.7, 28.4, 24.8, 24.5 ppm. ^{19}F NMR (376 MHz, Chloroform-*d*) δ= -73.85 (s, 3F) ppm. HRMS (ESI): calcd. for $C_{19}H_{23}F_3O_3Na$ $[M+Na]^+$: 379.1492, found: 379.1498. The *ee* was determined by HPLC analysis (Chiralpak IB column, λ = 254 nm, hexane/isopropanol = 95/5, flow rate = 0.5 mL/min): t_R(minor) = 16.1 min, t_R(major) = 14.2 min.

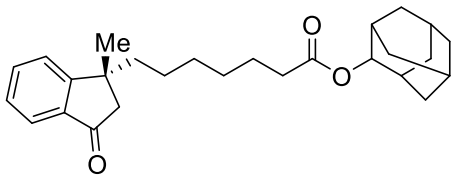

3p

Adamantan-2-yl (R)-7-(1-methyl-3-oxo-2,3-dihydro-1H-inden-1-yl)heptanoate (**3p**) was isolated through column chromatography on silica gel (petroleum ether: EtOAc= 15:1) as a yellow oil (60mg, 73%, 91% *ee*). ^{1}H NMR (400 MHz, Chloroform-*d*) δ= 7.70 (d, *J*= 7.7 Hz, 1H), 7.61 (t, *J*= 7.5 Hz, 1H), 7.45 (d, *J*= 7.7 Hz, 1H), 7.37 (t, *J*= 7.4 Hz, 1H), 4.91 (d, *J*= 3.4 Hz, 1H), 2.66 (d, *J*= 18.9 Hz, 1H), 2.44 (d, *J*= 18.9 Hz, 1H), 2.28 (t, *J*= 7.4 Hz, 2H), 2.03-1.94 (m, 5H), 1.85-1.79 (m, 4H), 1.77-1.71 (m, 4H), 1.62-1.53 (m, 6H), 1.40 (s, 3H), 1.31-1.22 (m, 5H). ppm. ^{13}C NMR (101 MHz, Chloroform-*d*) δ= 206.2, 173.2, 162.9, 136.0, 134.9, 127.4, 123.8, 123.3, 50.2, 42.2, 42.0, 37.4, 36.3 (3C), 34.8, 31.9 (2C), 31.8 (2C), 29.7, 29.0, 28.4, 27.2, 27.0, 25.1, 24.9 ppm. HRMS (ESI): calcd. for $C_{27}H_{36}O_3Na$ $[M+Na]^+$: 431.2557, found: 431.2562. The *ee* was determined by HPLC analysis (Chiralpak IB column, λ = 254 nm, hexane/isopropanol = 95/5, flow rate = 0.5 mL/min): t_R(minor) = 14.8 min, t_R(major) = 13.2 min.

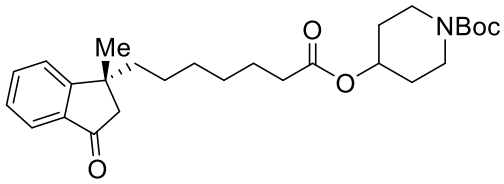

3q

Tert-butyl (R)-4-((7-(1-methyl-3-oxo-2,3-dihydro-1H-inden-1-yl)heptanoyl)oxy)piperidine-1-carboxylate (**3q**) was isolated through column chromatography on silica gel (petroleum ether: EtOAc= 10:1) as a yellow oil (73mg, 85%, 94% *ee*). ^{1}H NMR (400 MHz, Chloroform-*d*) δ= 7.70 (dd, *J*= 7.7 Hz, 1H), 7.61 (td, *J*= 7.5, 1.2 Hz, 1H), 7.45 (dd, *J*= 7.8, 1.0 Hz, 1H), 7.37 (td, *J*= 7.4, 0.9 Hz, 1H), 4.98-4.86 (m, 1H), 3.75-3.63 (m, 2H), 3.27-3.16 (m, 2H), 2.66 (d, *J*= 18.8 Hz, 1H), 2.45 (d, *J*= 18.8 Hz, 1H), 2.25 (t, *J*= 7.5 Hz, 2H), 1.86-1.77 (m, 3H), 1.62-1.55 (m, 5H), 1.46 (s, 9H), 1.41 (s, 3H), 1.29-1.26 (m, 6H) ppm. ^{13}C NMR (101 MHz, Chloroform-*d*) δ (mixture of two rotamers)= 206.1, 173.0, 162.8, 154.7, 136.0, 134.9, 127.4, 123.8, 123.3, 79.7, 69.5, 50.2, 42.2, 42.0, 41.0, 34.6, 34.5, 30.6, 29.4, 29.2, 29.1, 28.9, 28.4, 25.0, 24.9. ppm. HRMS (ESI): calcd. for $C_{27}H_{39}NO_5Na$ $[M+Na]^+$: 480.2720, found: 480.2726. The *ee* was determined by HPLC analysis (Chiralpak AD-H column, λ = 254 nm, hexane/isopropanol = 90/10, flow rate = 0.5 mL/min): t_R(minor) = 28.7 min, t_R(major) = 23.3 min.

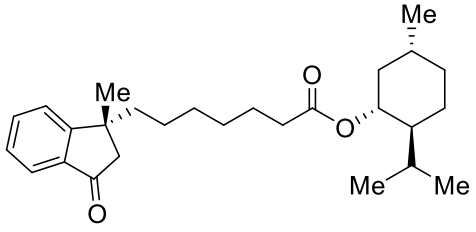

3r

(1R,2S,5R)-2-Isopropyl-5-methylcyclohexyl 7-((R)-1-methyl-3-oxo-2,3-dihydro-1H-inden-1-yl)heptanoate (**3r**) was isolated through column chromatography on silica gel (petroleum ether: EtOAc= 10:1) as a yellow oil (66mg, 80%, 93% *de*). ^{1}H NMR (400 MHz, Chloroform-*d*) δ= 7.70 (d, *J*= 7.6 Hz, 1H), 7.61 (td, *J*= 7.5, 1.3 Hz, 1H), 7.45 (d, *J*= 7.7 Hz, 1H), 7.36 (t, *J*= 7.4 Hz, 1H), 4.66 (td, *J*= 10.9, 4.4 Hz, 1H), 2.66 (d, *J*= 18.8 Hz, 1H), 2.45 (d, *J*= 18.8 Hz, 1H), 2.23 (t, *J*= 7.4 Hz, 2H), 2.02-1.91 (m, 1H), 1.89-1.76 (m, 1H), 1.76-1.61 (m, 5H), 1.60-1.49 (m, 3H), 1.40 (s, 3H), 1.38-1.29 (m, 2H), 1.26-1.20 (m, 5H), 1.12-0.97 (m, 2H), 0.89 (d, *J*= 6.6 Hz, 3H), 0.87 (d, *J*= 7.7 Hz, 3H), 0.73 (d, *J*= 6.9 Hz, 3H). ^{13}C NMR (101 MHz, Chloroform-*d*) δ= 203.6, 170.8, 160.3, 133.5, 132.3, 124.9, 121.3, 120.8, 71.4, 47.7, 44.5, 39.7, 39.4, 38.4, 32.1, 31.7, 28.8, 27.2, 26.4, 25.8, 23.7, 22.5, 22.4, 20.9, 19.5, 18.2, 13.8 ppm. HRMS (ESI): calcd. for $C_{27}H_{40}O_3Na$ $[M+Na]^+$: 435.2870, found: 435.2769. The *de* was determined by HPLC analysis (Chiralpak AD-H column, λ = 254 nm, hexane/isopropanol = 95/5, flow rate = 0.5 mL/min): t_R(minor) = 21.2 min, t_R(major) = 19.0 min.

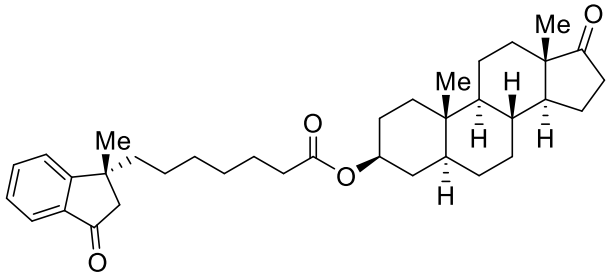

3s

(3S,5S,8R,9S,10S,13S,14S)-10,13-Dimethyl-17-oxohexadecahydro-1H-cyclopenta[a]phenanthren-3-yl 7-((R)-1-methyl-3-oxo-2,3-dihydro-1H-inden-1-yl)heptanoate (**3s**) was isolated through column chromatography on silica gel (petroleum ether: EtOAc= 5:1) as a yellow oil (78mg, 71%, 94% *de*). ^{1}H NMR (400 MHz, Chloroform-*d*) δ= 7.62 (dd, *J*= 7.8, 1.1 Hz, 1H), 7.54 (td, *J*= 7.5, 1.2 Hz, 1H), 7.38 (d, *J*= 7.7 Hz, 1H), 7.29 (t, *J*= 7.4 Hz, 1H), 4.67-4.52 (m, 1H), 2.59 (d, *J*= 18.8 Hz, 1H), 2.37 (d, *J*= 18.8 Hz, 1H), 2.31 (t, *J*= 17.1 Hz, 1H), 2.14 (t, *J*= 7.5 Hz, 2H), 2.06-1.93 (m, 1H), 1.91-1.80 (m, 1H), 1.78-1.36 (m, 15H), 1.33 (s, 3H), 1.29-1.08 (m, 14H), 0.78 (s, 3H), 0.77 (s, 3H) ppm. ^{13}C NMR (101 MHz, Chloroform-*d*) δ= 221.3, 206.2, 173.3, 162.9, 136.0, 134.9, 127.4, 123.8, 123.3, 73.2, 54.3, 51.4, 50.2, 47.8, 44.6, 42.2, 42.0, 36.7, 35.9, 35.7, 35.0, 34.6, 34.0, 31.5, 30.8, 29.7, 28.9, 28.4, 28.3, 27.5, 25.0, 24.9, 21.8, 20.5, 13.8, 12.2 ppm. HRMS (ESI): calcd. for $C_{36}H_{50}O_4Na$ $[M+Na]^+$: 569.3601, found: 569.3600. The *de* was determined by HPLC analysis (Chiralpak IB column, λ = 254 nm, hexane/isopropanol = 85/15, flow rate = 0.5 mL/min): t_R(minor) = 25.7 min, t_R(major) = 22.1 min.

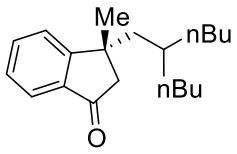

3t

(R)-3-(2-Butylhexyl)-3-methyl-2,3-dihydro-1H-inden-1-one (**3t**) was isolated through column chromatography on silica gel (petroleum ether: EtOAc= 25:1) as a yellow oil (34mg, 60%, 93% *ee*). ^{1}H NMR (400 MHz, Chloroform-*d*) δ= 7.70 (dt, *J*= 7.6, 1.0 Hz, 1H), 7.60 (td, *J*= 7.5, 1.2 Hz, 1H), 7.49 (d, *J*= 7.8 Hz, 1H), 7.36 (td, *J*= 7.4, 1.0 Hz, 1H), 2.72 (d, *J*= 18.8 Hz, 1H), 2.46 (d, *J*= 18.8 Hz, 1H), 1.75-1.56 (m, 4H), 1.41 (s, 3H), 1.25-1.13 (m, 7H), 1.09-0.99 (m, 4H), 0.88 (t, *J*= 6.8 Hz, 3H), 0.75 (t, *J*= 6.9 Hz, 3H) ppm. ^{13}C NMR (126 MHz, Chloroform-*d*) δ= 206.3, 163.3, 136.1, 134.7, 127.4, 124.3, 123.3, 50.7, 46.5, 42.3, 35.2, 34.5, 34.3, 29.1, 28.9, 28.4, 23.1, 22.9, 14.1, 14.0 ppm. HRMS (ESI): calcd. for $C_{20}H_{30}ONa$ $[M+Na]^+$: 309.2189, found: 309.2193. The *ee* was determined by HPLC analysis (Chiralpak IC column, λ = 254 nm, hexane/isopropanol = 95/5, flow rate = 0.5 mL/min): t_R(minor) = 12.7 min, t_R(major) = 11.4 min.

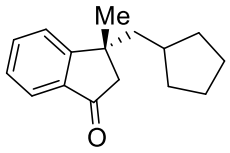

3u

(R)-3-(Cyclopentylmethyl)-3-methyl-2,3-dihydro-1H-inden-1-one (**3u**) was isolated through column chromatography on silica gel (petroleum ether: EtOAc= 25:1) as a yellow oil (31mg, 68%, 84% *ee*). ^{1}H NMR (400 MHz, Chloroform-d) δ= 7.70 (dt, J= 7.7, 1.1 Hz, 1H), 7.60 (td, J= 7.9, 1.2 Hz, 1H), 7.48 (dt, J= 7.8, 0.9 Hz, 1H), 7.37 (td, J= 7.3, 1.0 Hz, 1H), 2.77 (d, J= 18.9 Hz, 1H), 2.47 (d, J= 18.9 Hz, 1H), 1.92 (dd, J= 14.0, 5.3 Hz, 1H), 1.78-1.68 (m, 2H), 1.58-1.46 (m, 4H), 1.42 (s, 3H), 1.37-1.29 (m, 1H), 1.15-1.04 (m, 1H), 0.95-0.73 (m, 2H) ppm. ^{13}C NMR (101 MHz, Chloroform-*d*) δ= 206.4, 163.3, 136.0, 134.7, 127.4, 124.2, 123.3, 50.6, 48.3, 42.3, 37.5, 34.8, 34.1, 29.3, 25.1, 24.7 ppm. HRMS (ESI): calcd. for $C_{16}H_{20}ONa$ $[M+Na]^+$: 251.1406, found: 251.1410. The *ee* was determined by HPLC analysis (Chiralpak IC column, λ = 254 nm, hexane/isopropanol = 95/5, flow rate = 0.5 mL/min): t_R(minor) = 17.4 min, t_R(major) = 19.7 min.

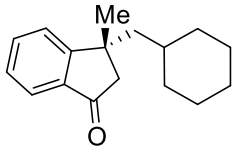

3v

(R)-3-(Cyclohexylmethyl)-3-methyl-2,3-dihydro-1H-inden-1-one (**3v**) was isolated through column chromatography on silica gel (petroleum ether: EtOAc= 25:1) as a yellow oil (31mg, 68%, 84% *ee*). ^{1}H NMR (400 MHz, Chloroform-*d*) δ= 7.70 (dt, *J*= 7.7, 1.1 Hz, 1H), 7.60 (ddd, *J*= 7.8, 7.2, 1.3 Hz, 1H), 7.48 (d, *J*= 7.8 Hz, 1H), 7.36 (ddd, *J*= 8.1, 7.2, 1.0 Hz, 1H), 2.74 (d, *J*= 18.9 Hz, 1H), 2.47 (d, *J*= 18.9 Hz, 1H), 1.70 (dd, *J*= 14.1, 4.3 Hz, 1H), 1.64-1.47 (m, 6H), 1.39 (s, 3H), 1.23-1.11 (m, 2H), 1.11-0.94 (m, 3H), 0.87- 0.69 (m, 1H) ppm. ^{13}C NMR (101 MHz, Chloroform-*d*) δ= 206.4, 163.6, 135.8, 134.7, 127.4, 124.1, 123.3, 50.7, 49.4, 42.0, 35.6, 34.9, 34.6, 29.3, 26.3, 26.2, 26.1 ppm. HRMS (ESI): calcd. for $C_{17}H_{22}ONa$ $[M+Na]^+$: 265.1563, found: 265.1566. The *ee* was determined by HPLC analysis (Chiralpak IC column, λ = 254 nm, hexane/isopropanol = 95/5, flow rate = 0.5 mL/min): t_R(minor) = 15.9 min, t_R(major) = 18.0 min.

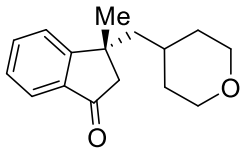

3w

(R)-3-Methyl-3-((tetrahydro-2H-pyran-4-yl)methyl)-2,3-dihydro-1H-inden-1-one (**3w**) was isolated through column chromatography on silica gel (petroleum ether: EtOAc= 5:1) as a yellow oil (40mg, 83%, 91% *ee*). ^{1}H NMR (500 MHz, Chloroform-*d*) δ= 7.71 (d, *J*= 7.6 Hz, 1H), 7.62 (t, *J*= 7.4 Hz, 1H), 7.49 (d, *J*= 7.8 Hz, 1H), 7.38 (t, *J*= 7.1 Hz, 1H), 3.94-3.61 (m, 2H), 3.36-3.09 (m, 2H)., 2.73 (d, *J*= 18.9 Hz, 1H), 2.50 (d, *J*= 18.9 Hz, 1H), 1.77 (dd, *J*= 14.3, 4.1 Hz, 1H), 1.67 (dd, *J*= 14.2, 6.7 Hz, 1H), 1.54-1.46 (m, 1H), 1.42 (s, 3H), 1.41-1.32 (m, 2H), 1.17-1.05 (m, 1H), 1.03-0.95 (m, 1H) ppm. ^{13}C NMR (126 MHz, Chloroform-*d*) δ= 205.9, 162.9, 135.9, 134.9, 127.6, 124.1, 123.4, 67.9, 67.7, 50.6, 49.0, 41.8, 34.9, 34.3, 32.3, 29.6 ppm. HRMS (ESI): calcd. for $C_{16}H_{20}O_2Na$ $[M+Na]^+$: 267.1356, found: 267.1355. The *ee* was determined by HPLC analysis (Chiralpak IB column, λ = 254 nm, hexane/isopropanol = 85/15, flow rate = 0.5 mL/min): t_R(minor) = 12.7 min, t_R(major) = 13.8 min.

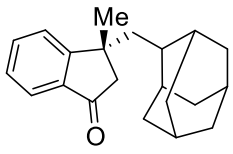

3x

(R)-3-(Adamantan-2-ylmethyl)-3-methyl-2,3-dihydro-1H-inden-1-one (**3x**) was isolated through column chromatography on silica gel (petroleum ether: EtOAc= 5:1) as a yellow oil (35mg, 59%, 92% *ee*). ^{1}H NMR (400 MHz, Chloroform-*d*) δ= 7.71 (dt, *J*= 7.6, 1.0 Hz, 1H), 7.60 (td, *J*= 7.5, 1.3 Hz, 1H), 7.48 (dd, *J*= 7.8, 1.0 Hz, 1H), 7.36 (td, *J*= 7.4, 1.1 Hz, 1H), 2.66 (d, *J*= 18.9 Hz, 1H), 2.45 (d, *J*= 18.9 Hz, 1H), 1.88-1.72 (m, 8H), 1.68-1.50 (m, 9H), 1.41 (s, 3H) ppm. ^{13}C NMR (101 MHz, Chloroform-*d*) δ= 206.4, 163.2, 136.1, 134.7, 127.4, 124.0, 123.3, 50.1, 45.5, 42.6, 41.3, 39.03, 38.95, 38.0, 34.4, 33.2, 32.0, 31.8, 28.8, 27.5 (2C). HRMS (ESI): calcd. for $C_{21}H_{26}ONa$ $[M+Na]^+$: 317.1876, found: 317.1875. The *ee* was determined by HPLC analysis (Chiralpak IC column, λ = 254 nm, hexane/isopropanol = 95/5, flow rate = 0.5 mL/min): t_R(minor) = 15.9 min, t_R(major) = 18.1 min.

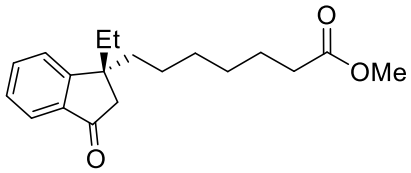

3y

Methyl (R)-7-(1-ethyl-3-oxo-2,3-dihydro-1H-inden-1-yl)heptanoate (**3y**) was isolated through column chromatography on silica gel (petroleum ether: EtOAc= 5:1) as a yellow oil (43mg, 71%, 87% *ee*). ^{1}H NMR (400 MHz, Chloroform-*d*) δ= 7.70 (ddd, *J*= 7.6, 1.3, 0.7 Hz, 1H), 7.60 (ddd, *J*= 7.8, 7.2, 1.3 Hz, 1H), 7.40 (dt, *J*= 7.8, 0.9 Hz, 1H), 7.36 (ddd, *J*= 7.7, 7.2, 1.0 Hz, 1H), 3.65 (s, 3H), 2.52 (s, 2H), 2.25 (t, *J*= 7.5 Hz, 2H), 1.84-1.65 (m, 3H), 1.59-1.47 (m, 2H), 1.31-1.17 (m, 6H), 0.97-0.82 (m, 1H), 0.70 (t, *J*= 7.4 Hz, 3H) ppm. ^{13}C NMR (126 MHz, Chloroform-*d*) δ= 206.4, 174.2, 161.2, 137.1, 134.7, 127.4, 124.2, 123.3, 51.5, 47.0, 46.0, 40.4, 34.0, 33.2, 29.8, 29.0, 24.9, 24.5, 8.9 ppm. HRMS (ESI): calcd. for $C_{19}H_{26}O_3Na$ $[M+Na]^+$: 325.1774, found: 325.1777. The *ee* was determined by HPLC analysis (Chiralpak IB column, λ = 254 nm, hexane/isopropanol = 90/10, flow rate = 0.5 mL/min): t_R(minor) = 12.8 min, t_R(major) = 11.7 min.

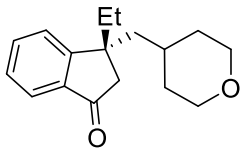

3z

(R)-3-Ethyl-3-((tetrahydro-2H-pyran-4-yl)methyl)-2,3-dihydro-1H-inden-1-one (**3z**) was isolated through column chromatography on silica gel (petroleum ether: EtOAc= 5:1) as a yellow oil (38mg, 74%, 85% *ee*). ^{1}H NMR (400 MHz, Chloroform-*d*) δ= 7.71 (dt, *J*= 7.6, 1.1 Hz, 1H), 7.61 (td, *J*= 7.5, 1.3 Hz, 1H), 7.44 (dd, *J*= 7.8, 0.9 Hz, 1H), 7.38 (td, *J*= 7.5, 1.0 Hz, 1H), 3.91-3.65 (m, 2H), 3.35-3.03 (m, 2H), 2.58 (s, 2H), 1.86-1.61 (m, 4H), 1.51-1.31 (m, 3H), 1.18-1.03 (m, 1H), 1.00-0.90 (m, 1H), 0.66 (t, *J*= 7.4 Hz, 3H) ppm. ^{13}C NMR (126 MHz, Chloroform-*d*) δ= 206.1, 161.1, 137.0, 134.8, 127.6, 124.4, 123.4, 67.9, 67.7, 47.6, 47.2, 45.7, 35.0, 34.5, 34.2, 31.9, 8.7 ppm. HRMS (ESI): calcd. for $C_{17}H_{22}O_2Na$ $[M+Na]^+$: 281.1512, found: 285.1516. The *ee* was determined by HPLC analysis (Chiralpak IB column, λ = 254 nm, hexane/isopropanol = 85/15, flow rate = 0.5 mL/min): t_R(minor) = 11.6 min, t_R(major) = 12.4 min.

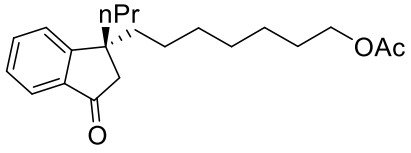

3aa

(R)-7-(3-Oxo-1-propyl-2,3-dihydro-1H-inden-1-yl)heptyl acetate (**3aa**) was isolated through column chromatography on silica gel (petroleum ether: EtOAc= 5:1) as a yellow oil (42mg, 64%, 93% *ee*). ^{1}H NMR (500 MHz, Chloroform-*d*) δ= 7.70 (d, *J*= 7.6 Hz, 1H), 7.60 (t, *J*= 7.5 Hz, 1H), 7.42 (d, *J*= 7.7 Hz, 1H), 7.36 (t, *J*= 7.4 Hz, 1H), 4.02 (t, *J*= 6.8 Hz, 2H), 2.54 (s, 2H), 2.03 (s, 3H), 1.81-1.50 (m, 7H), 1.30-1.14 (m, 7H), 0.97-0.87 (m, 2H), 0.84 (t, *J*= 7.0 Hz, 3H) ppm. ^{13}C NMR (126 MHz, Chloroform-*d*) δ= 206.4, 171.2, 161.6, 136.9, 134.7, 127.4, 124.1, 123.3, 64.5, 47.6, 45.7, 43.2, 40.8, 30.0, 29.0, 28.5, 25.8, 24.5, 21.0, 17.9, 14.6. HRMS (ESI): calcd. for $C_{21}H_{30}O_3Na$ $[M+Na]^+$: 353.2087, found: 353.2083. The *ee* was determined by HPLC analysis (Chiralcel OJ-H column, λ = 254 nm, hexane/isopropanol = 95/5, flow rate = 1.0 mL/min): t_R(minor) = 9.8 min, t_R(major) = 10.8 min.

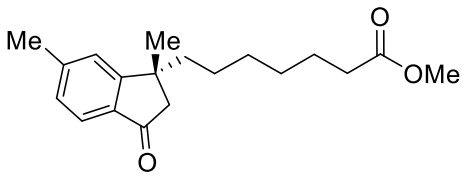

3ab

Methyl (R)-7-(1,6-dimethyl-3-oxo-2,3-dihydro-1H-inden-1-yl)heptanoate (**3ab**) was isolated through column chromatography on silica gel (petroleum ether: EtOAc= 5:1) as a yellow oil (50mg, 84%, 90% *ee*). ^{1}H NMR (500 MHz, Chloroform-*d*) δ= 7.49 (s, 1H), 7.43 (dd, *J*= 7.9, 1.7 Hz, 1H), 7.33 (d, *J*= 7.8 Hz, 1H), 3.65 (s, 3H), 2.64 (d, *J*= 18.8 Hz, 1H), 2.43 (d, *J*= 18.8 Hz, 1H), 2.40 (s, 3H), 2.26 (t, *J*= 7.5 Hz, 2H), 1.79-1.48 (m, 5H), 1.38 (s, 3H), 1.30-1.17 (m, 5H) ppm. ^{13}C NMR (126 MHz, Chloroform-*d*) δ= 206.2, 174.2, 160.3, 137.3, 136.2, 136.1, 123.5, 123.2, 51.5, 50.5, 42.2, 41.6, 34.0, 29.7, 29.0, 28.5, 24.9, 24.9, 21.1 ppm. HRMS (ESI): calcd. for $C_{19}H_{26}O_3Na$ $[M+Na]^+$: 325.1774, found: 325.1776. The *ee* was determined by HPLC analysis (Chiralpak IB column, λ = 254 nm, hexane/isopropanol = 92.5/7.5, flow rate = 0.4 mL/min): t_R(minor) = 16.2 min, t_R(major) = 15.3 min.

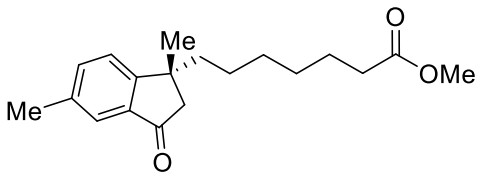

3ac

Methyl (R)-7-(1,5-dimethyl-3-oxo-2,3-dihydro-1H-inden-1-yl)heptanoate (**3ac**) was isolated through column chromatography on silica gel (petroleum ether: EtOAc= 5:1) as a yellow oil (47mg, 79%, 89% *ee*). ^{1}H NMR (500 MHz, Chloroform-*d*) δ= 7.59 (d, *J*= 7.8 Hz, 1H), 7.23 (s, 1H), 7.17 (dd, *J*= 7.7, 1.4 Hz, 1H), 3.65 (s, 3H), 2.64 (d, *J*= 18.7 Hz, 1H), 2.46 (s, 3H), 2.42 (d, *J*= 18.7 Hz, 1H), 2.26 (t, *J*= 7.5 Hz, 2H), 1.78-1.52 (m, 5H), 1.38 (s, 3H), 1.34-1.14 (m, 5H) ppm. ^{13}C NMR (126 MHz, Chloroform-*d*) δ= 205.6, 174.2, 163.4, 146.0, 133.8, 128.7, 124.1, 123.2, 51.5, 50.4, 42.2, 41.8, 34.0, 29.7, 29.0, 28.4, 24.88, 24.85, 22.3 ppm. HRMS (ESI): calcd. for $C_{19}H_{26}O_3Na$ $[M+Na]^+$: 325.1774, found: 325.1773. The *ee* was determined by HPLC analysis (Chiralpak IB column, λ = 254 nm, hexane/isopropanol = 92.5/7.5, flow rate = 0.4 mL/min): t_R(minor) = 17.5 min, t_R(major) = 15.6 min.

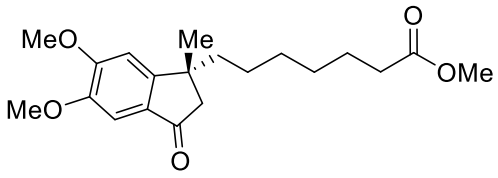

3ad

Methyl (R)-7-(5,6-dimethoxy-1-methyl-3-oxo-2,3-dihydro-1H-inden-1-yl)heptanoate (**3ad**) was isolated through column chromatography on silica gel (petroleum ether: EtOAc= 3:1) as a yellow oil (48mg, 69%, 78% *ee*). ^{1}H NMR (400 MHz, Chloroform-*d*) δ= 7.13 (s, 1H), 6.82 (s, 1H), 4.00 (s, 3H), 3.91 (s, 3H), 3.65 (s, 3H), 2.63 (d, *J*= 18.7 Hz, 1H), 2.42 (d, *J*= 18.7 Hz, 1H), 2.27 (t, *J*= 7.5 Hz, 2H), 1.78-1.51 (m, 5H), 1.39 (s, 3H), 1.30-1.20 (m, 5H) ppm. ^{13}C NMR (126 MHz, Chloroform-*d*) δ= 204.5, 174.2, 158.1, 155.6, 149.4, 128.9, 104.5, 103.7, 56.2, 56.1, 51.4, 50.1, 42.0, 41.6, 33.9, 29.6, 28.9, 28.4, 24.84, 24.80 ppm. HRMS (ESI): calcd. for $C_{20}H_{28}O_5Na$ $[M+Na]^+$: 371.1829, found: 370.1833. The *ee* was determined by HPLC analysis (Chiralpak AD-H column, λ = 254 nm, hexane/isopropanol = 80/20, flow rate = 0.5 mL/min): t_R(minor) = 17.1 min, t_R(major) = 19.9 min.

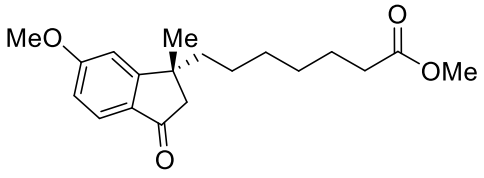

3ae

Methyl (R)-7-(6-methoxy-1-methyl-3-oxo-2,3-dihydro-1H-inden-1-yl)heptanoate (**3ae**) was isolated through column chromatography on silica gel (petroleum ether: EtOAc= 5:1) as a yellow oil (48mg, 70%, 84% *ee*). ^{1}H NMR (400 MHz, Chloroform-*d*) δ= 7.34 (dd, *J*= 8.4, 0.6 Hz, 1H), 7.20 (dd, *J*= 8.4, 2.6 Hz, 1H), 7.13 (dd, *J*= 2.6, 0.6 Hz, 1H), 3.84 (s, 3H), 3.65 (s, 3H), 2.67 (d, *J*= 18.8 Hz, 1H), 2.46 (d, *J*= 18.8 Hz, 1H), 2.26 (t, *J*= 7.5 Hz, 2H), 1.76-1.49 (m, 4H), 1.38 (s, 3H), 1.31-1.12 (m, 6H) ppm. ^{13}C NMR (101 MHz, Chloroform-*d*) δ= 205.9, 174.1, 159.4, 155.7, 137.2, 124.6, 124.1, 104.4, 55.6, 51.4, 50.7, 42.2, 41.4, 33.9, 29.6, 28.9, 28.4, 24.9, 24.8 ppm. HRMS (ESI): calcd. for $C_{19}H_{26}O_4Na$ $[M+Na]^+$: 341.1723, found: 341.1726. The *ee* was determined by HPLC analysis (Chiralpak IB column, λ = 254 nm, hexane/isopropanol = 80/20, flow rate = 0.5 mL/min): t_R(minor) = 10.8 min, t_R(major) = 10.3 min.

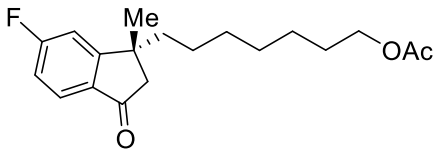

3af

(R)-7-(6-fluoro-1-methyl-3-oxo-2,3-dihydro-1H-inden-1-yl)heptyl acetate (**3af**) was isolated through column chromatography on silica gel (petroleum ether: EtOAc= 5:1) as a yellow oil (49mg, 76%, 93% *ee*). ^{1}H NMR (500 MHz, Chloroform-*d*) δ= 7.45-7.38 (m, 1H), 7.36-7.30 (m, 2H), 4.02 (t, *J*= 6.5 Hz, 2H), 2.70 (d, *J*= 18.9 Hz, 1H), 2.49 (d, *J*= 18.9 Hz, 1H), 2.04 (s, 3H), 1.76-1.51 (m, 5H), 1.40 (s, 3H), 1.33-1.13 (m, 7H) ppm. ^{13}C NMR (126 MHz, Chloroform-*d*) δ= 204.9, 171.2, 162.3 (d, *J*= 247.8 Hz), 158.3 (d, *J*= 2.2 Hz), 137.8 (d, *J*= 7.1 Hz), 125.4 (d, *J*= 8.0 Hz), 122.5 (d, *J*= 23.8 Hz), 109.1 (d, *J*= 21.6 Hz), 64.5, 50.6, 42.3, 41.7, 29.9, 29.0, 28.51, 28.46, 25.8, 25.0, 21.0 ppm. ^{19}F NMR (471 MHz, Chloroform-*d*) δ= -114.7 (s, 1F) ppm. HRMS (ESI): calcd. for $C_{19}H_{25}FO_3Na$ $[M+Na]^+$: 343.1680, found: 343.1675. The *ee* was determined by HPLC analysis (Chiralpak AD-H column, λ = 254 nm, hexane/isopropanol = 97/3, flow rate = 0.5 mL/min): t_R(minor) = 22.2 min, t_R(major) = 23.1 min.

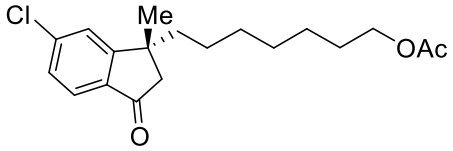

3ag

(R)-7-(6-chloro-1-methyl-3-oxo-2,3-dihydro-1H-inden-1-yl)heptyl acetate (**3ag**) was isolated through column chromatography on silica gel (petroleum ether: EtOAc= 5:1) as a yellow oil (49mg, 73%, 93% *ee*). 1H NMR (500 MHz, Chloroform-*d*) δ= 7.65 (s, 1H), 7.56 (d, *J*= 8.3 Hz, 1H), 7.39 (d, *J*= 8.3 Hz, 1H), 4.02 (td, *J*= 6.8, 1.4 Hz, 2H), 2.68 (d, *J*= 18.9 Hz, 1H), 2.47 (d, *J*= 18.9 Hz, 1H), 2.04 (s, 3H), 1.74-1.52 (m, 5H), 1.40 (s, 3H), 1.36-1.18 (m, 7H). ^{13}C NMR (126 MHz, Chloroform-*d*) δ= 204.6, 171.2, 160.9, 137.6, 134.9, 133.8, 125.2, 123.2, 64.5, 50.4, 42.2, 41.9, 29.9, 29.0, 28.5, 28.3, 25.8, 25.0, 21.0 ppm. HRMS (ESI): calcd. for $C_{19}H_{25}ClO_3Na$ $[M+Na]^+$: 359.1384, found: 359.1386. The *ee* was determined by HPLC analysis (Chiralpak AD-H column, λ = 254 nm, hexane/isopropanol = 97/3, flow rate = 0.5 mL/min): t_R(minor) = 23.7 min, t_R(major) = 25.3 min.

Scheme S6. Procedure for the 10-mmol-Scale Reaction for the Synthesis of 3i, Related to Scheme 2

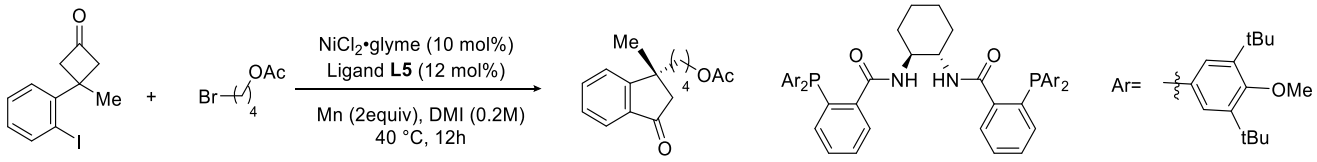

1a **2i** **3i** 74%, 90% *ee* **L5**

A dry flask equipped with a stirring bar was charged with $NiCl_2$•glyme (220 mg, 1.0 mmol, 10 mol%), ligand **L5** (1.51 g, 1.2 mmol, 12 mol %), Mn (1.10 g, 20 mmol, 2.0 equiv) and anhydrous 1,3-dimethyl-2-imidazolidinone (50 mL) under N_2. The mixture was heated to 40°C, before the cyclobutanone **1a** (2.86 g, 10 mmol, 1.0 equiv) and the alkyl bromides **2i** (3.90 g, 20 mmol, 2.0 equiv) were added. After stirring for 12 h at 40 ˚C, the reaction mixture was cooled to room temperature and quenched by adding water. The aqueous phase were extracted by EtOAc 3 times, and the combined organic phases were washed with brine, dried out over $MgSO_4$, filtered and removed under reduced pressure. The residue was purified through column chromatography on silica gel (petroleum ether: EtOAc= 10:1), affording the corresponding product **3i** as a yellow oil (2.02 g, 74%, 90%*ee*).

Control Experiments

Scheme S7. Stoichiometric Reaction of 1a with $Ni(COD)_2$, Related to Scheme 4

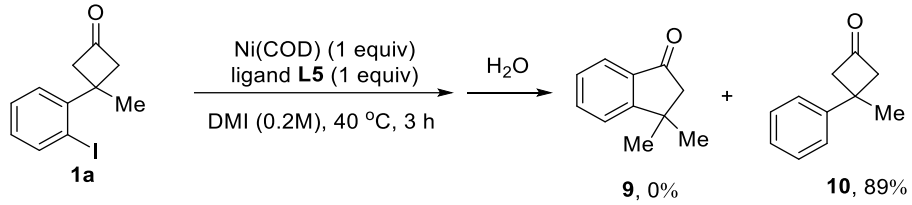

A dry test tube equipped with a stirring bar was charged with $Ni(COD)_2$ (55 mg, 0.2 mmol, 1.0 equiv), ligand **L5** (250 mg, 0.2 mmol, 1.0 equiv), and anhydrous 1,3-dimethyl-2-imidazolidinone (1 mL) under N_2. The mixture was heated to 40 ˚C, and then the cyclobutanone **1a** (57 mg, 0.2 mmol, 1.0 equiv) was added. After stirring for 3 h at 40 ˚C, the reaction mixture was cooled to room temperature and then quenched with H_2O. The aqueous phase was then extracted with EtOAc (3 × 10 mL). The combined organic layers were dried over Na_2SO_4, filtered and concentrated in vacuum. The residue was purified through column chromatography on silica gel (petroleum ether: EtOAc= 25:1) affording *3-methyl-3-phenylcyclobutan-1-one* (**10**) as a yellow oil (28 mg, 89%). ^{1}H NMR (400 MHz, Chloroform-*d*) δ= 7.29-7.16 (m, 4H), 7.16-7.08 (m, 1H), 3.38-3.27 (m, 2H), 3.04-2.90 (m, 2H), 1.48 (s, 3H) ppm. ^{13}C NMR (126 MHz, Chloroform-*d*) δ= 206.7, 148.3, 128.6 (2C), 126.3, 125.7 (2C), 59.3 (2C), 34.0, 31.1 ppm.

Scheme S8. Stoichiometric Reaction of 1a with $Ni(COD)_2$ in the Presence of MnI_2, Related to Scheme 4

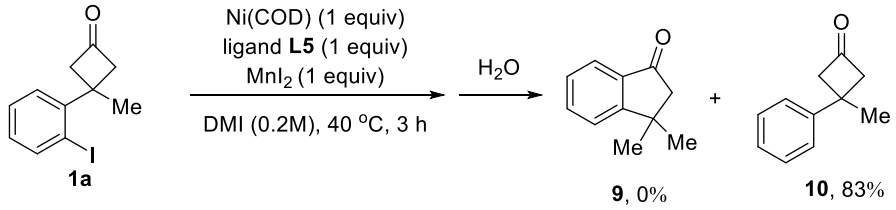

A dry test tube equipped with a stirring bar was charged with $Ni(COD)_2$ (55 mg, 0.2 mmol, 1.0 equiv), ligand **L5** (250 mg, 0.2 mmol, 1.0 equiv), MnI_2 (62 mg, 0.2 mmol, 1.0 equiv) and anhydrous 1,3-dimethyl-2-imidazolidinone (1 mL) under N_2. The mixture was heated to 40 ˚C, and then the cyclobutanone **1a** (57 mg, 0.2 mmol, 1.0 equiv) was added. After stirring for 3 h at 40 ˚C, the reaction mixture was cooled to room temperature and then quenched with H_2O. The aqueous phase was then extracted with EtOAc (3 × 10 mL). The combined organic layers were dried over Na_2SO_4, filtered and concentrated in vacuum. The residue was purified through column chromatography on silica gel (petroleum ether: EtOAc= 25:1) affording *3-methyl-3-phenylcyclobutan-1-one* (**10**) as a yellow oil (26 mg, 83%).

Scheme S9. Stoichiometric Reaction of 1a with $Ni(COD)_2$ in the Presence of Mn, Related to Scheme 4

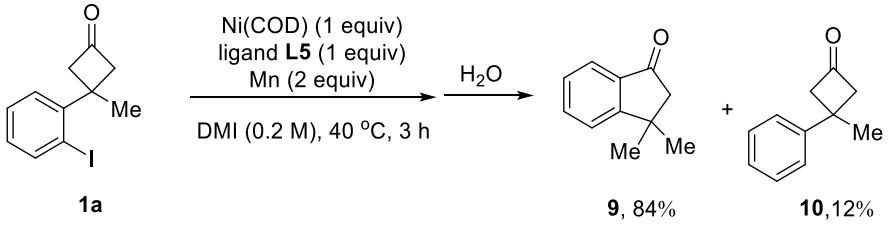

A dry test tube equipped with a stirring bar was charged with $Ni(COD)_2$ (55 mg, 0.2 mmol, 1.0 equiv), ligand

L5 (250 mg, 0.2 mmol, 1.0 equiv), Mn (22 mg, 0.4 mmol, 2.0 equiv) and anhydrous 1,3-dimethyl-2-imidazolidinone (1 mL) under N_2. The mixture was heated to 40 ˚C, and then the cyclobutanone **1a** (57 mg, 0.2 mmol, 1.0 equiv) was added. After stirring for 3 h at 40 ˚C, the reaction mixture was cooled to room temperature, and then quenched with H_2O. The aqueous phase was then extracted with EtOAc (3 × 10 mL). The combined organic layers were dried over Na_2SO_4, filtered and concentrated in vacuum. The residue was purified through column chromatography on silica gel (petroleum ether: EtOAc= 25:1) affording *3,3-dimethyl-2,3-dihydro-1H-inden-1-one* (**9**) as a yellow oil (27 mg, 84%). ^{1}H NMR (500 MHz, Chloroform-*d*) δ= 7.70 (dt, *J*= 7.7, 1.0 Hz, 1H), 7.62 (td, *J*= 7.5, 1.2 Hz, 1H), 7.51 (dd, *J*= 7.8, 0.9 Hz, 1H), 7.37 (td, *J*= 7.5, 1.0 Hz, 1H), 2.60 (s, 2H), 1.43 (s, 6H) ppm. ^{13}C NMR (126 MHz, Chloroform-*d*) δ= 206.0, 163.9, 135.3, 135.0, 127.4, 123.5, 123.4, 53.0, 38.6, 30.0 (2C).

Scheme S10. Stoichiometric Reaction of 16 with Ni(COD)$_2$ in the Presence of Mn, Related to Scheme 4

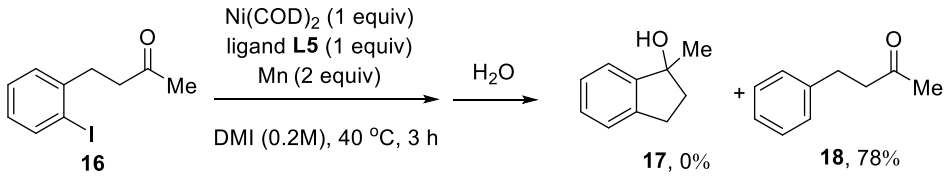

A dry test tube equipped with a stirring bar was charged with Ni(COD)$_2$ (55 mg, 0.2 mmol, 1.0 equiv), ligand **L5** (250 mg, 0.2 mmol, 1.0 equiv), Mn (22 mg, 0.4 mmol, 2.0 equiv) and anhydrous 1,3-dimethyl-2-imidazolidinone (1 mL) under N_2. The mixture was heated to 40°C, before the *4-(2-iodophenyl)butan-2-one* (**16**) (55 mg, 0.2 mmol, 1.0 equiv) was added. After stirring for 3 h at 40 ˚C, the reaction mixture was cooled to room temperature. The mixture was purified through column chromatography on silica gel (petroleum ether: EtOAc= 5:1) affording *3-(3-oxobutyl)benzene-1-ylium* (**18**) as a yellow oil (23 mg, 78%).^{1}H NMR (500 MHz, Chloroform-*d*) δ= 7.27 (dd, *J*= 8.6, 6.6 Hz, 2H), 7.20-7.15 (m, 3H), 2.88 (t, *J*= 7.7 Hz, 2H), 2.75 (dd, *J*= 8.4, 6.9 Hz, 2H), 2.12 (s, 3H) ppm. ^{13}C NMR (126 MHz, Chloroform-*d*) δ= 208.1, 141.0, 128.6 (2C), 128.4, 126.2 (2C), 45.2, 30.2, 29.7 ppm.

Scheme S11. Sequential Stoichiometric Reaction, Related to Scheme 4

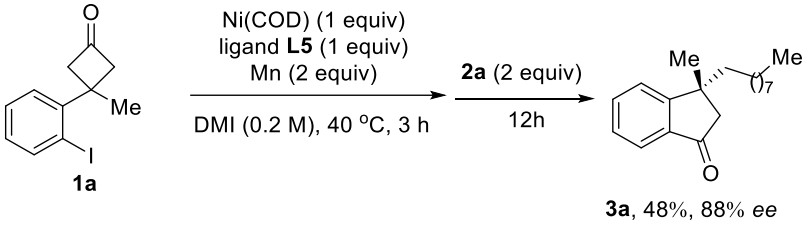

A dry test tube equipped with a stirring bar was charged with Ni(COD)$_2$ (55 mg, 0.2 mmol, 1.0 equiv), ligand **L5** (250 mg, 0.2 mmol, 1.0 equiv), Mn (22 mg, 0.4 mmol, 2 equiv) and anhydrous 1,3-dimethyl-2-imidazolidinone (1 mL) under N_2. The mixture was heated to 40 ˚C, and then the cyclobutanone **1a** (57 mg, 0.2 mmol, 1.0 equiv) was added. After stirring for 3 h at 40 ˚C, *n*-octyl bromide **2a** (77 mg, 0.4 mmol, 2.0 equiv) was added to the reaction mixture. The mixture was stirred for 12h at 40 ˚C and then quenched with H_2O. The aqueous phase was extracted with EtOAc (3 × 10 mL). The combined organic layers were dried over Na_2SO_4, filtered and concentrated in vacuum. The residue was purified through column chromatography on silica gel (petroleum ether: EtOAc= 25:1) affording **3a** as a yellow oil (26 mg, 48%).

Scheme S12. Radical Clock Experiment, Related to Scheme 4

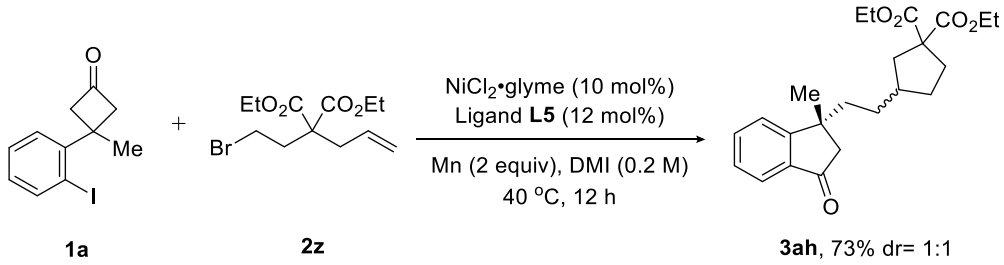

A dry test tube equipped with a stirring bar was charged with $NiCl_2$(dme) (4.4 mg, 0.02 mmol, 10 mol %), ligand **L5** (30.1 mg, 0.024 mmol, 12 mol %), Mn (22 mg, 0.4 mmol, 2.0 equiv) and anhydrous 1,3-dimethyl-2-imidazolidinone (1 mL) under N_2. The mixture was heated to 40°C, before the cycloketone **1a** (57 mg, 0.2 mmol, 1 equiv) and the alkyl bromide **2z** (130 mg, 0.4 mmol, 2equiv) were added. After stirring for 12 h at 40 ˚C, the reaction mixture was cooled to room temperature. The mixture was purified through column chromatography on silica gel (petroleum ether: EtOAc= 5:1) affording **3ah** as a yellow oil (56 mg, 73%). ^{1}H NMR (400 MHz, Chloroform-*d*) δ= 7.70 (dt, *J*= 7.6, 1.0 Hz, 1H), 7.66-7.57 (m, 1H), 7.48-7.40 (m, 1H), 7.37 (td, *J*= 7.4, 0.9 Hz, 1H), 4.21-4.09 (m, 4H), 2.65 (d, *J*= 18.9 Hz, 1H), 2.44 (d, *J*= 18.9 Hz, 1H), 2.43-2.33 (m, 1H), 2.31-2.19 (m, 1H), 2.13-2.04 (m, 1H), 1.88-1.52 (m, 6H), 1.40 (s, 3H), 1.31-1.13 (m, 8H) ppm. ^{13}C NMR (101 MHz, Chloroform-*d*) δ (mixture of two diastereomers)= 205.9, 172.64, 172.58, 162.62, 162.57, 136.0, 134.9, 127.5, 123.8, 123.7, 123.3, 61.3, 59.87, 59.85, 50.1, 50.0, 41.9, 41.1, 41.0, 40.60, 40.58, 40.1, 40.0, 33.63, 33.61, 32.0, 30.49, 30.48, 28.41, 28.43, 14.0 ppm. HRMS (ESI): calcd. for $C_{23}H_{30}O_5Na$ $[M+Na]^+$: 409.1958, found: 409.1988.

Derivatization of the Cross-Coupling Product

Scheme S13. Clemmensen Reduction of the Indanone 3i, Related to Scheme 3

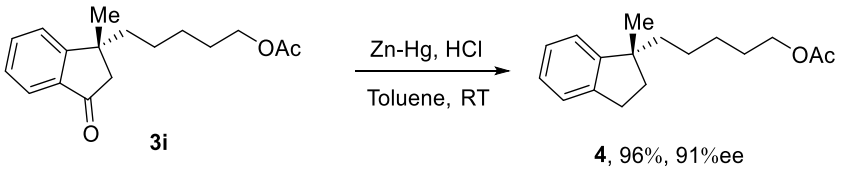

5 g of zinc powder was washed with HCl (6 M in water, 2 × 4.45 mL). Then $HgCl_2$ (214.5 mg, 0.79 mmol, 4.0 equiv), water (3.4 mL), and concentrated HCl (0.6 mL) were added to the washed Zn dust, and the resulting mixture was stirred vigorously for 1 h at room temperature. To this mixture was added the indanone **3i** (55 mg, 0.2 mmol, 1.0 equiv) in toluene (2.0 mL) followed by addition of concentrated HCl (3.2 mL). After stirring overnight at room temperature, it was filtered through a pad of Celite to remove the solid and washed with EtOAc. The organic layer was sperated, dried over Na_2SO_4, filtered and concentrated under reduced pressure. The residue was purified by flash column chromatography on silica gel (petroleum ether) to *(R)-5-(1-methyl-2,3-dihydro-1H-inden-1-yl)pentyl acetate* (**4**) afford as a colorless oil (50 mg, 96%, 91% *ee*). ^{1}H NMR: (400 MHz, Chloroform-*d*) δ= 7.23-7.00 (m, 4H), 4.02 (t, *J*= 6.7 Hz, 2H), 2.96-2.79 (m, 2H), 2.10-1.94 (m, 1H), 2.03 (s, 3H),1.87-1.76(m, 1H), 1.66-1.54 (m, 3H), 1.53-1.42 (m, 1H), 1.39-1.15 (m, 4H), 1.23 (s, 3H) ppm. ^{13}CNMR (101MHz, Chloroform-*d*): δ= 171.3, 151.5, 143.2, 126.2, 126.1, 124.5, 122.6, 64.7, 47.3, 41.3, 38.6, 30.3, 28.6, 26.8, 26.7, 24.6, 21.0 ppm.

Scheme S14. Wittig Olefination of the Indanone 3i, Related to Scheme 3

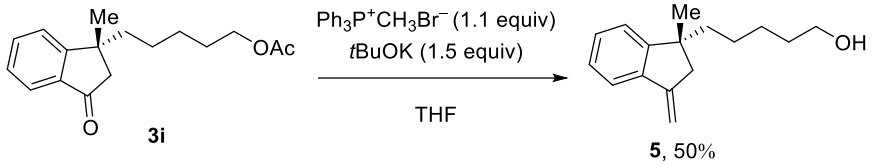

To a 10-mL flame-dried flask charged with $Ph_3P^+CH_3Br^-$ (79 mg, 0.22 mmol, 1.1 equiv) and dry THF (1 mL), *t*BuOK (33 mg, 0.3 mmol, 1.5 equiv) was added slowly at 0 ˚C over 10 minutes. After stirring at room temperature for 2 h, the indanone **3i** (32 mg, 0.2 mmol, 1.0 equiv) was added. Then the mixture was stirred at room temperature overnight, before water (5.0 mL) was added. The aqueous layer was extracted with ethyl acetate (3 × 5mL). The combined organic phases were dried over anhydrous Na_2SO_4, filtered and concentrated under vacuum. The residue was then purified by flash column chromatography (petroleum ether:EtOAc= 5:1) to give product *(R)-5-(1-methyl-3-methylene-2,3-dihydro-1H-inden-1-yl)pentan-1-ol* (**5)** as colorless oil (23 mg, 50% yield). ^{1}H NMR (400 MHz, Chloroform-*d*) δ= 7.48-7.42 (m, 1H), 7.26-7.13 (m, 3H), 5.43 (t, *J*= 2.5 Hz, 1H), 5.01 (t, *J*= 2.1 Hz, 1H), 3.57 (t, *J*= 6.6 Hz, 2H), 2.72 (dt, *J*= 16.2, 2.2 Hz, 1H), 2.53 (dt, *J*= 16.3, 2.4 Hz, 1H), 1.61-1.46 (m, 4H), 1.33-1.27 (m, 4H), 1.25 (s, 3H) ppm. ^{13}C NMR (126 MHz, Chloroform-*d*) δ= 154.1, 148.8, 140.1, 128.4, 126.7, 123.2, 120.5, 102.8, 63.0, 45.7, 45.2, 42.4, 32.7, 28.0, 26.3, 24.7 ppm. HRMS (ESI): calcd. for $C_{16}H_{23}O$ $[M+H]^+$: 231.1743, found: 231.1749.

Scheme S15. Beckmann Rearrangement of the Indanone 3i, Related to Scheme 3

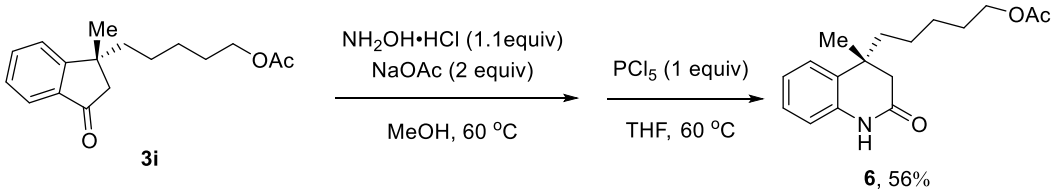

Step 1: To a 10-mL flame-dried flask charged with **3i** (137 mg, 0.5 mmol, 1.0 equiv), hydroxylaminium chloride (39.0 mg, 0.55 mmol, 1.1 equiv) and dry EtOH (1.0 mL), sodium acetate (82.0 mg, 1.0 mmol, 2.0 equiv) was added slowly at 0 ˚C. Then the mixture was heated to 60 ˚C and stirred at this temperature for 2 h, before water (5.0 mL) was added. The aqueous layer was extracted with ethyl acetate (3 × 5 mL). The combined organic phases were dried over anhydrous Na_2SO_4, filtered and concentrated under vacuum. The residue was then used without further purification.

Step 2: Phosphorus pentachloride (105 mg, 0.5 mmol, 1.0 equiv) was added in one portion to the residue in THF (4 mL). The reaction mixture was then heated to 60 ˚C and stirred at this temperature for 1.5 h, before it was quenched with sat. aq. NH_4Cl solution (10mL). The aqueous phase was extracted with EtOAc (2×10 mL) and the combined organic extracts were washed with brine (10 mL), dried over $NaSO_4$, filtered, and concentrated under reduced pressure. The residue was purified by column chromatography on silica gel (petroleum ether:EtOAc= 1:1) to give *(R)-5-(4-methyl-2-oxo-1,2,3,4-tetrahydroquinolin-4-yl)pentyl acetate* (**6)** as a colorless oil (81 mg, 56 % yield). ^{1}H NMR (500 MHz, Chloroform-*d*) δ= 8.79 (s, 1H), 7.17-7.07 (m, 2H), 6.97 (td, *J*= 7.6, 1.3 Hz, 1H), 6.76 (dd, *J*= 7.8, 1.3 Hz, 1H), 3.92 (t, *J*= 6.6 Hz, 2H), 2.51-2.37 (m, 2H), 1.95 (s, 3H), 1.57-1.45 (m, 4H), 1.26 (s, 3H), 1.24-1.18 (m, 4H). ^{13}C NMR (126 MHz, Chloroform-*d*) δ= 171.28, 171.31, 136.2, 131.0, 127.5, 125.5, 123.4, 116.0, 64.5, 43.4, 39.7, 36.9, 28.5, 26.4, 25.4, 23.9, 21.0 ppm. HRMS (ESI): calcd. for $C_{17}H_{23}NO_3$ $[M+H]^+$: 290.1751, found: 290.1748.

Determination of the Absolute Configuration

Scheme S16. Preparation the Indane 4 with a Known Absolute Configuration, Related to Scheme 2

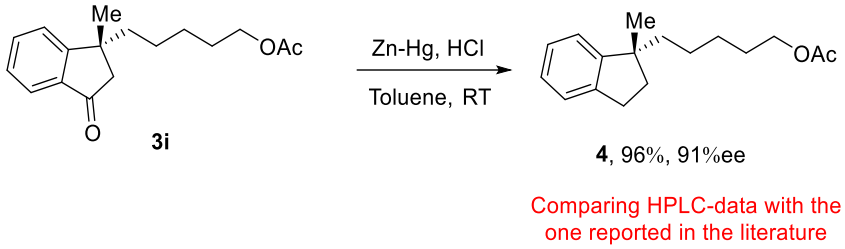

The *ee* of **4** (91%) was determined by HPLC analysis: Chiralpak IB column, λ = 254 nm, hexane/isopropanol = 97/3, flow rate = 0.5 mL/min): t_R(major) = 11.6 min, t_R(minor) = 13.2 min. (For HPLC-chromatograms, see: Page S152)

The HPLC data for *ent*-**4** (*(S)-5-(1-methyl-2,3-dihydro-1H-inden-1-yl)pentyl acetate*) reported in the literature (Jin and Wang, 2019): Chiralpak IB column, λ = 254 nm, hexane/isopropanol = 97/3, flow rate = 0.5 mL/min): t_R(minor) = 11.6 min, t_R(major) = 13.2 min.

Relying on the comparison of the HPLC data, the absolute configuration of **4** was determined to be *R*. Accordingly, the stereochemistry of **3i** was determined to be *R*. The absolute configuration of all the other ring opening/cross-coupling products was assigned to be *R* assuming a common reaction pathway.

Supplementary References

Sun, Y.-L., Wang, X.-B., Sun, F.-N., Chen, Q.-Q., Cao, J., Xu, Z., and Xu, L.-W. (2019). Enantioselective cross-exchange between C-I and C-C σ bonds. Angew. Chem. Int. Ed. *58*, 6747-6751.

Guo, J.-W., Xu, X.-M., Xing, Q.-Z., Gao, Z.-W., Gou, J., and Yu, B.-X. (2018). Furfuryl cation induced cascade formal [3 + 2] cycloaddition/double ring-opening/chlorination: an approach to chlorine-containing complex triazoles. Org. Lett. *20*, 7410-7414.

Nicotrat, F., Riva, S., Secundo, F., and Zucchelli, L. ω-Functionalized esters by enzymatic acylation. (1990). Synth. Commun. *20*, 679-685.

Zhang, M.-J., Vedantham, P., Flynn, D. L., and Hanson, P. R. (2004). High-load, soluble oligomeric carbodiimide: synthesis and application in coupling reactions. J. Org. Chem. *69*, 8340-8344.

Narayan, A., Jiménez-Osés, G., Liu, P., Negretti, S., Zhao, W.-X., Gilbert, M., Ramabhadran, R., Yang, Y., Furan, L., Li, Z., Podust, L., Montgomery, J., Houk, K., and Sherman, D. (2015). Enzymatic hydroxylation of an unactivated methylene C–H bond guided by molecular dynamics simulations. Nature Chem. *7*, 653-660.

Burkhart, B., Khlyabich, P., and Thompson, B. (2012). Solar cells based on semi-random P3HT analogues containing dithienopyrrole: influence of incorporating a strong donor. J. Photon. Energy *2*, 021002.

Jin, Y., and Wang, C. Nickel-catalyzed asymmetric reductive arylalkylationof unactivated alkenes. (2019). Angew. Chem. Int. Ed. *58*, 6722-6726.